A PENTON PUBLICATION SEPTEMBER 2000

FOR DESIGNERS AT HIGHER FREQUENCIES

Microwaves & RF

Dual-Use Technology Issue

NEWS
NRL's efforts advance vacuum electronics

DESIGN FEATURE
FBAR technology shrinks duplexers

PRODUCT TECHNOLOGY
Speedy VNAs drive on PC power

Aluminum nitride forges high-power resistive components

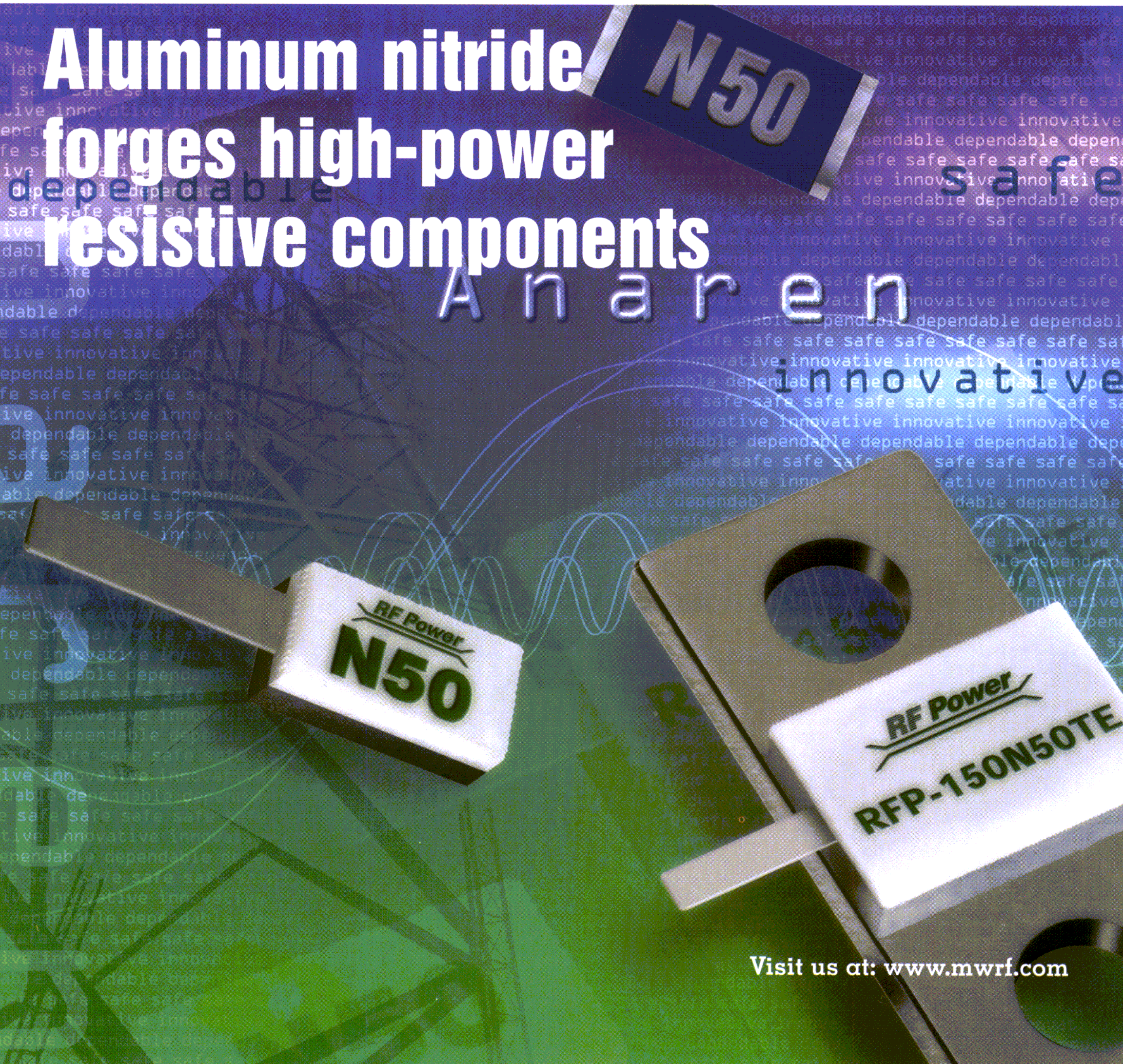

Visit us at: www.mwrf.com

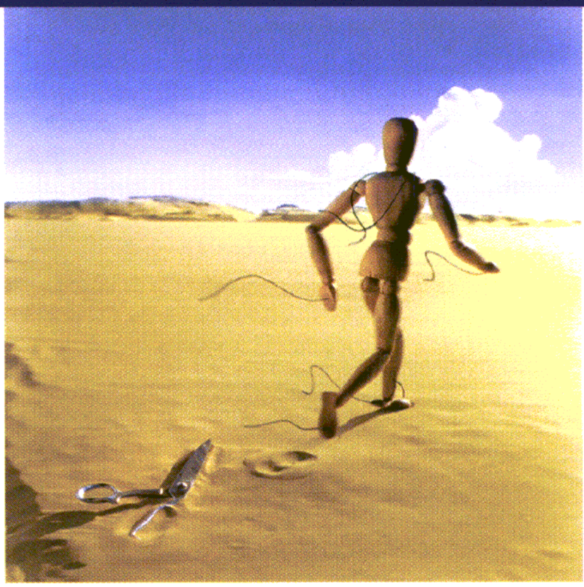

LOW SPURIOUS SPACEBORNE MIXERS

FEATURES:

- Broadband operation
- Minimal variation in conversion loss
- High IP3 and 1 dB compression versus LO power

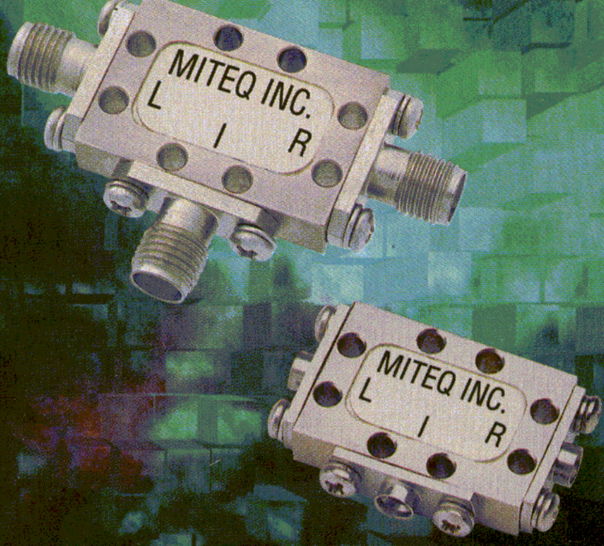

CONVERSION LOSS/SPURIOUS

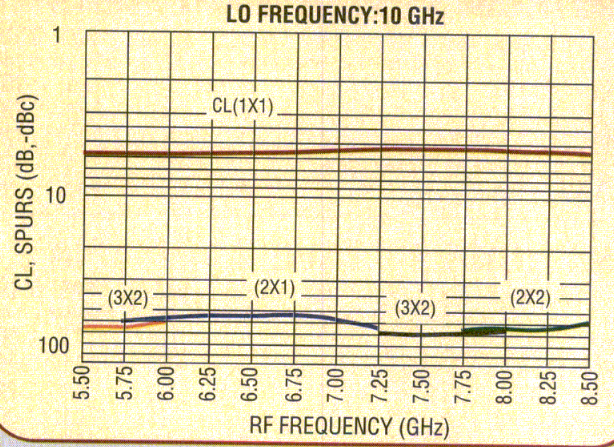

TYPICAL OPERATING BANDS

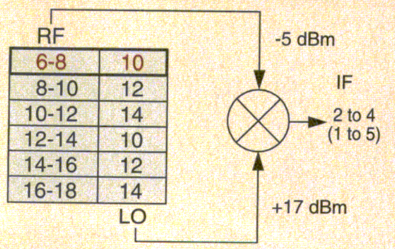

SPECIFICATIONS - Model TBR0618HA1/TBR0618HA1-S

RF/LO Input Frequency Range	6 to 18 GHz
IF Output Frequency Range	0.05 to 5 GHz
Conversion Loss	6 dB Typical
Spurious	-55 dBc
Third Order Intercept Point	+23 dBm Typical
1 dB Compression Point	+13 dBm Typical

For further information, please contact Mary Becker at (631) 439-9423 or e-mail mbecker@miteq.com

NQA ISO 9001 REGISTERED COMPANY

MITEQ

100 Davids Drive • Hauppauge, NY 11788
TEL.: (631) 436-7400 • FAX: (631) 436-7430
www.miteq.com

CIRCLE NO. 248

Worth switching to...

UPG158TB
Shown actual size, these low voltage L-Band SPDT switches are available now in low cost 6-pin 2.0 x 1.25 x 0.9 mm "super minimold" package.

Want to save more real estate in your cordless phone, PCS, and digital cellular handset designs? Our ultraminiature GaAs SPDT switches deliver wide bandwidth, low insertion loss and high P_{1dB}, plus the quality and consistency you've come to expect from NEC.

Best of all is the price. At less than 50 cents each in production quantities, they're switches worth switching to!

Ultraminiature GaAs Switches, from 49¢.

Want more information? You can download data sheets for our NEC switches directly from our website.

	UPG158TB	UPG137GV
Frequency Range	100 MHz to 2.5 GHz	100 MHz to 2.5 GHz
Insertion Loss	0.4 dB @ 2 GHz	0.55 dB @ 1 GHz 0.65 dB @ 2 GHz
P_{1dB}	+27 dBm	up to +35 dBm
Control Voltage	+3V to +5V	+3V to +5V
Package	6-pin super minimold	8 Pin SSOP
Price*	49¢	95¢

*100K Piece Qty.

They can all be found in our *RFIC Selection Guide* under GaAs RFICs at:
www.cel.com/prod/prod_rfics.asp

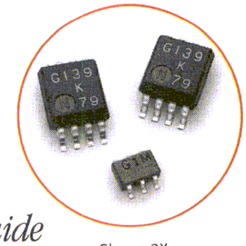

Shown 3X actual size.

www.cel.com

CEL California Eastern Laboratories

NEC

4590 Patrick Henry Drive ▪ Santa Clara, CA 95054 ▪ 408 988-3500
DISTRIBUTORS: Arrow (800) 525-6666 Reptron Electronics (888) REPTRON
Mouser Electronics (800) 346-6873 Electro Sonic (800) 567-6642 (CANADA)

CIRCLE NO. 220

A Penton Publication

Microwaves & RF

SEPTEMBER 2000 VOL. 39, NO. 9

Visit us at www.mwrf.com

COVER FEATURE

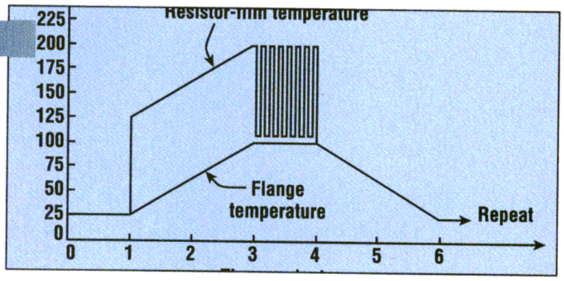

DEPARTMENTS

NEWS

DESIGN FEATURES

PRODUCT TECHNOLOGY

Penton

BPA

SUBSCRIPTION ASSISTANCE AND INFORMATION POSTMASTER: Please send change of address to *Microwaves & RF*, Penton Media, Inc., 1100 Superior Ave., Cleveland, OH 44114-2543. For other subscription information or assistance, please call (216) 696-7000 and have a copy of your mailing label handy.

Microwaves & RF (ISSN 0745-2993) is published monthly, except semi-monthly in December. Subscription rates for US are $80 for 1 year ($105 in Canada, $140 for International). Published by Penton Media, Inc., 1100 Superior Ave., Cleveland, OH 44114-2543. Periodicals Postage Paid at Cleveland, OH and at additional mailing offices.

Canada Post International Publications Mail (Canadian Distribution Sales Agreement Number 344311). CAN. GST #R126431964.

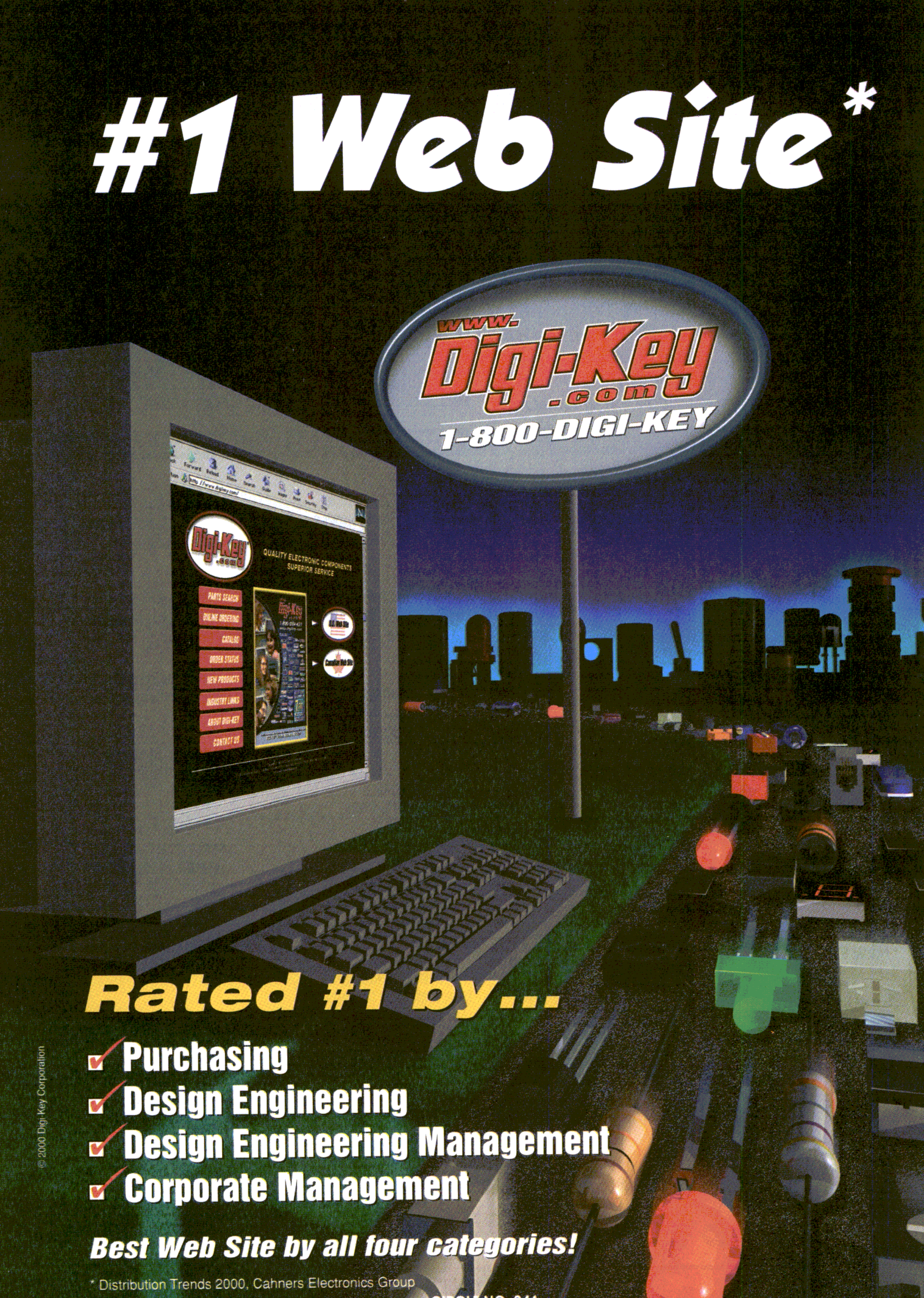

CIRCLE NO. 241

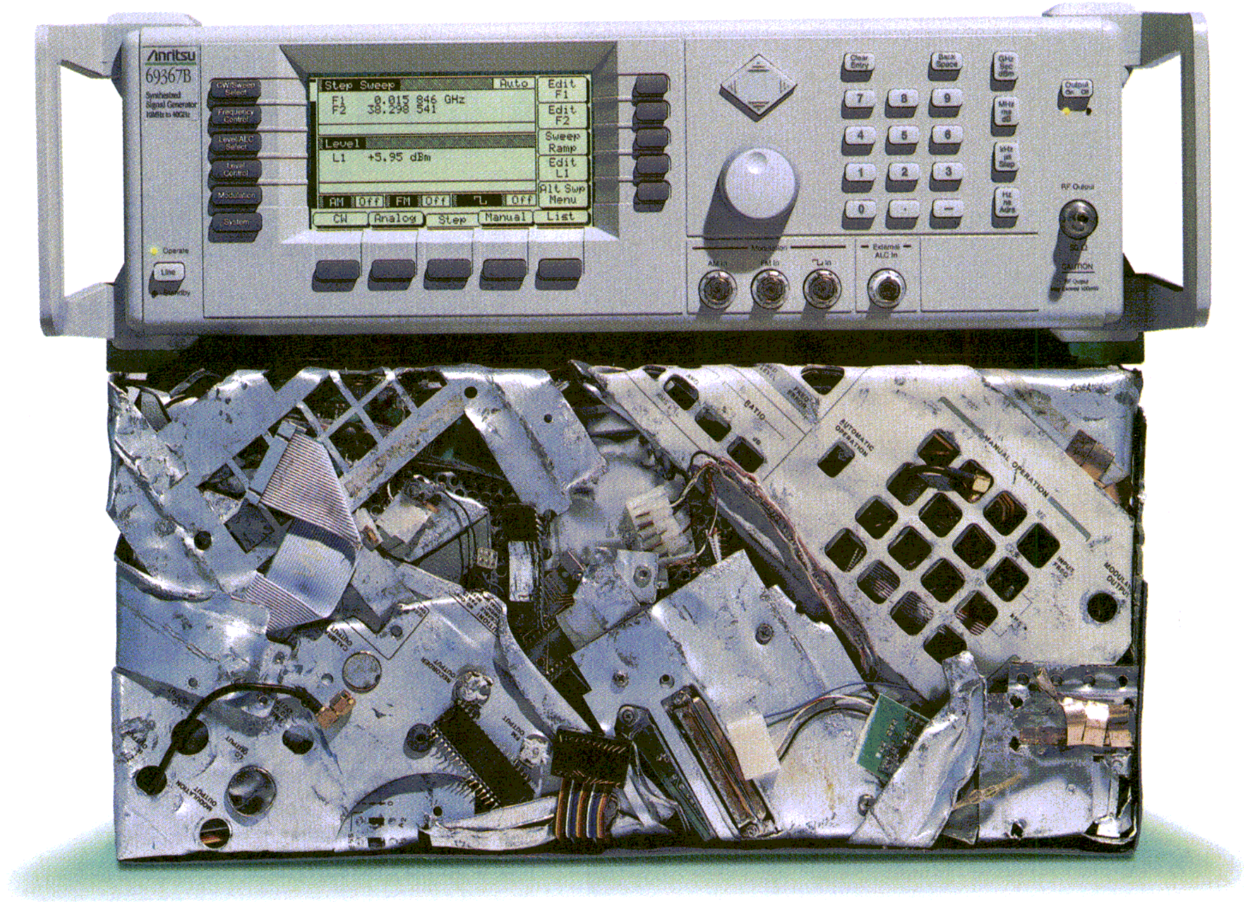

Waste Not. Want Not.

If you're throwing out your old technology every time you upgrade, perhaps what you're really scrapping is your productivity. Introducing the fully-upgradeable El Toro™ Microwave Synthesizers from Anritsu: the 68C and 69B. With 42 levels of technology to choose from, you can upgrade to a higher-performing model at anytime without buying a completely new synthesizer.

Choose from the widest frequency coverage and the lowest phase noise available today. Whether you want CW signals to 8 GHz, fully modulated signals to 65 GHz, or anything in between, Anritsu can configure the right signal generator for you. And because you're buying an Anritsu, you'll also enjoy the peace of mind that comes with owning one of the hardest working and longest lasting synthesizers on the market.

For more information call 1-800-ANRITSU or check out our website at www.global.anritsu.com. The El Toro from Anritsu. The end to disposable technology.

Linking the World

Anritsu

El Toro 68C/69B Microwave Synthesizer

One world. One name. Anritsu.

 Sales Offices: United States and Canada, 1-800-ANRITSU, Europe 44(01582)433200, Japan 81(03)3446-1111, Asia-Pacific 65-2822400, South America 55(21)527-6922, http://www.anritsu.com

CIRCLE NO. 381

Motorola & Richardson— Keeping Worldwide RF Customers in Balance

Motorola and Richardson Electronics offer the perfect balance of exceptional products and services.

Motorola's broadcast, PCN and cellular components are incomparable in performance, and Richardson provides the stability of unrivaled global logistics and engineering support.

High power, low cost and small packages are just a few of the advantages of Motorola's RF components. When combined with Richardson's global, technical and logistical support, you get the perfect balance of exceptional products and services.

Motorola and Richardson Electronics — providing global solutions for all your RF component needs.

PCN PRODUCT

Device	Frequency	Voltage	Oper. Gain (Typ.)	Output Power
MRF18060A/AS	1805-1880 MHz	26 Volts	13.0 dB	60 Watts CW
MRF18060B/BS	1805-1880 MHz	26 Volts	13.0 dB	60 Watts CW
MRF18090A/AS	1930-1990 MHz	26 Volts	13.5 dB	90 Watts CW
MRF18090B/BS	1930-1990 MHz	26 Volts	13.5 dB	90 Watts CW
MRF19030/S	1930-1990 MHz	26 Volts	13.0 dB	30 Watts PEP
MRF19045/S	1930-1990 MHz	26 Volts	14.0 dB	45 Watts PEP
MRF19060/S	1930-1990 MHz	26 Volts	12.5 dB	60 Watts PEP
MRF19085/S	1930-1990 MHz	26 Volts	12.5 dB	90 Watts PEP
MRF19125/S	1930-1990 MHz	26 Volts	12.5 dB	125 Watts PEP
MRF21125/S	1930-1990 MHz	28 Volts	12.0 dB	125 Watts PEP
MRF21180/S	1930-1990 MHz	28 Volts	11.3 dB	160 Watts PEP

CELLULAR

Device	Frequency	Voltage	Oper. Gain (Typ.)	Output Power
MRF9180	880 MHz	26 Volts	17.0 dB	180 Watts PEP
MRF9085/S	880 MHz	26 Volts	17.0 dB	85 Watts PEP
MRF9045/S	945 MHz	28 Volts	18.0 dB	45 Watts PEP
MRF9045M	945 MHz	28 Volts	16.0 dB	45 Watts PEP

BROADCAST

Device	Frequency	Voltage	Oper. Gain (Typ.)	Output Power
MRF372	470-860 MHz	28 Volts	14.0 dB	180 Watts PEP
MRF373A/AS*	470-860 MHz	28 Volts	11.2 dB	100 Watts PEP
MRF374A*	470-860 MHz	28 Volts	12.0 dB	100 Watts PEP

** Under development.*

MOTOROLA

Richardson Electronics
Engineered Solutions

RELL Online Catalog catalog.rell.com

Visit Richardson's online catalog at *catalog.rell.com*

More than 60 locations worldwide to serve you. E-mail: ssc@rell.com, **Internet:** www.rfpowernet.com/motorola.asp, **Toll Free:** 800-RF Power or 800-737-6937 (U.S. & Canada), **Australia:** Castle Hill, ACN 069 808 108, +61 (2) 9894-7288, Bayswater, ACN 069 808 108, +61 (3) 9738-0733, **Brazil:** São Paulo, +55 (11) 820-6199, **China:** Shanghai, +86 (21) 6440-0807, **Colombia:** Sante Fe de Bogota, DC, (57-1) 636-1028, **France:** Colombes Cedex, +33 (1) 55.66.00.30, **Germany:** Puchheim, +49 (89) 890 214-0, Hamburg, +49 (40) 555 88 410, **Italy:** Sesto Fiorentino (FI), +39 (055) 420831, Agrate Brianza (MI), +39 (039) 653145, Roma, +39 (06) 41.73.37.51, **Japan:** Osaka, +81 (6) 6314-5557, Tokyo, +81 (3) 5215-1577, **Korea:** Seoul, +82 (2) 539-4731, **Mexico:** Mexico City, +52 (5) 674-2228, Guadalajara, +52 (3) 645-4641, **Netherlands:** Amsterdam, +31 (20) 446 7070, **Philippines:** 63-2-633-9480, **Singapore:** +65 487-5995, **Spain:** Madrid, +34 (91) 528 3700, Barcelona, +34 (93) 415 8303, **Sweden:** Stockholm, +46 8 564 705 90, **Taiwan:** Taipei, +886 (2) 86915238, **Thailand:** Bangkok, +66 (2) 749-4402, **Turkey:** Içlevent Istanbul, +90 212 264 3721, **United Kingdom:** Lincoln, +44 (1522) 542631, Slough, +44 (1753) 733010, **Vietnam:** Ho Chi Minh City, +84 8.811.1919. For other international inquiries call **Corporate Headquarters:** LaFox, IL (630) 208-2200, Fax (630) 208-2550. MK0518

1-800-RF-POWER • www.rfpowernet.com/motorola.asp • ssc@rell.com

CIRCLE NO. 333

Lorch Microwave: Multi-product Solutions for Commercial Wireless Applications

With over 35 years experience designing and manufacturing microwave components, Lorch Microwave provides filtering solutions to the commercial market

- from base station to microwave radio links
- from less than 1MHz to 40GHz
- from high volume to small custom runs

Diverse engineering and manufacturing capabilities allow Lorch Microwave to quickly respond to customer needs and provide custom tailored solutions, all with trademark service and satisfaction.

LORCH MICROWAVE

1725 North Salisbury Blvd. · PO Box 2828
Salisbury, Maryland 21802
Tel: 800.780.2169 · Fax: 410.860.1949
E-mail: lorchsales@lorch.com
Web: http://www.lorch.com

CIRCLE NO. 229

Commercial, High Performance & Custom-Design Products

WIRELESS FILTERS AND DUPLEXERS

- cellular and PCS base stations filters, duplexers and assemblies
- delay assemblies for feed forward amplifier applicat

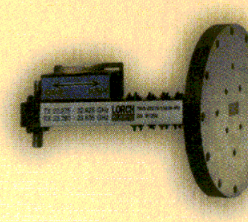

WAVEGUIDE DIPLEXERS

- point-to-point microwave radio links to 40GHz
- terrestrial communication networks

CERAMIC FILTERS

- filters and diplexers to 5.8
- specialized cellular and PCS applications
- diplexers and finite pole placed topologies availab

OTHER COMMERCIAL MILITARY APPLICATIO

- cavity filters
- discrete filters
- tunable filters
- other signal processing products

RADIATION EFFECTS

To the editor:

I have read Professor Bansal's letter that appeared in June's Feedback (p. 13). Professor Bansal must have seen the report on mobile phones and health by the Independent Expert Group on Mobile Phones (IEGMP) of the U.K. The report confirms that there is now scientific evidence, however, that suggests there may be biological effects occurring at exposures below the guidelines of the International Commission of Non-Ionizing Radiation Protection (ICNIRP). This does not necessarily mean that these effects lead to disease or injury but it is not possible to say that exposure to RF radiation, even below national (ICNIRP) guidelines, is totally without potential adverse health effects. In light of these findings, the IEGMP recommends a precautionary approach to the use of mobile-phone technologies until more detailed and scientifically robust information on any health effects becomes available. The Group also recommends that radiation exposure from different mobile phones be stated on the box in the U.K.

Readers can find my explanation on Dr. J.M. Osepchuk's statement in the April 2000 issue of the *IEEE AP-S* magazine (Vol. 42, No. 2, pp. 127-128). The Expert Group recommends that the ICNIRP public exposure guidelines (for example: power density = f(MHz)/200 W/m^2 for the frequency range of 400 to 2000 MHz) are adopted for use in the U.K. For the base-station emission, exposure of the general population will be to the whole body but normally at levels of intensity many times less than those from handsets.

A. Kumar
AK Electromagnetique, Inc.
Les Coteaux, Quebec, Canada

NF METERS

To the editor:

In July's Feedback (p. 13), I read about the noise-figure (NF) meters and the role that Swedish companies have had on them. I have a Sievers Lab SL 5825. On the inside of the lid are the instructions, dated February 1957. Maybe it qualifies as an early NF meter?

The function is that of a thermally limited diode. The filament current is varied from the front panel and the plate current is monitored with an analog meter, calibrated in "dB BRUSFAKTOR." The current is set so the output reading from the device under test, as measured with an RMS voltmeter, doubles compared to no noise signal on the input. The meter is good for 2 ~ 350 MHz. A 1-dB NF is readable and there are two ranges—0 to 10 and 0 to 20 dB. The plate is grounded with 50 Ω and the output is taken from across this resistance.

With L.M. Ericsson as an important maker of radar and AGA of communication radios, there was probably a satisfying domestic market.

Carl Lodstrom
Carlsbad, CA

AFS SERIES...

MORE THAN JUST LOW NOISE AMPLIFIERS

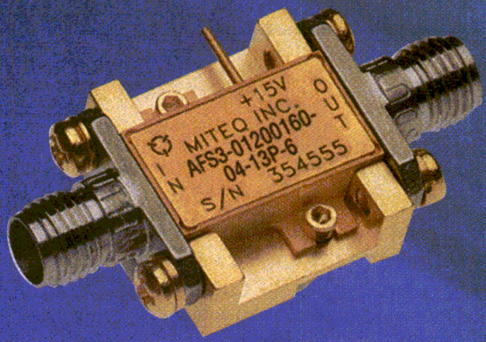

Model Number	Frequency Range (GHz)	Gain (Min./Max.) (dB)	Gain Flatness (±dB, Max.)	Noise Figure (dB, Max.)	VSWR Input (Max.)	VSWR Output (Max.)	Output Power @ 1 dB Comp. (dBm, Min.)	Nom. DC Power (+15 V, mA)
TEMPERATURE COMPENSATED AMPLIFIERS								
AFS3-01000200-15-TC-6	1–2	36-40	1.00	1.5	2.0:1	2.0:1	+5	125
AFS2-02000400-15-TC-6	2–4	22-26	1.00	1.5	2.0:1	2.0:1	+5	125
AFS3-02000400-15-TC-6	2–4	22-26	1.00	1.5	2.0:1	2.0:1	+5	125
AFS2-04000800-20-TC-2	4–8	18-22	1.00	2.0	2.0:1	2.0:1	+5	100
AFS3-04000800-18-TC-4	4–8	26-30	1.00	1.8	2.0:1	2.0:1	+8	150
AFS2-02000800-40-TC-2	2–8	14-19	1.50	4.0	2.0:1	2.0:1	+5	100
AFS3-02000800-30-TC-4	2–8	22-27	1.50	3.0	2.0:1	2.2:1	+8	150
AFS2-08001200-30-TC-2	8–12	12-16	1.00	3.0	2.0:1	2.0:1	+5	100
AFS3-08001200-22-TC-4	8–12	24-28	1.00	2.2	2.0:1	2.0:1	+8	150
AFS4-12001800-30-TC-8	12–18	22-26	1.00	3.0	2.0:1	2.0:1	+8	250
AFS4-06001800-35-TC-6	6–18	22-26	1.00	3.5	2.0:1	2.0:1	+8	250
AFS6-06001800-35-TC-8	6–18	30-34	1.00	3.5	2.0:1	2.0:1	+8	400
AFS4-02001800-45-TC-5	2–18	18-24	1.50	4.5	2.2:1	2.2:1	+8	175

Note: All specifications guaranteed -54 to +85°C.
Many other frequencies, noise figures and gain windows are available.

Model Number	Frequency Range (GHz)	Gain (Min./Max.) (dB)	Gain Flatness (±dB, Max.)	Noise Figure (dB, Max.)	VSWR Input (Max.)	VSWR Output (Max.)	Output Power @ 1 dB Comp. (dBm, Min.)	Nom. DC Power (+15 V, mA)
HIGHER POWER AMPLIFIERS								
AFS4-00050100-25-25P-6	0.5–2	36	1.50	2.5*	2.0:1	2.5:1	+25	325
AFS3-00100100-23-25P-6	.1–1	38	2.00	2.3	2.5:1	2.5:1	+25	280
AFS3-00100200-25-27P-6	.1–2	33	1.50	2.5	2.0:1	2.5:1	+27	300
AFS3-00100300-25-23P-6	.1–3	25	1.50	2.5	2.0:1	2.5:1	+23	300
AFS3-00100400-26-20P-4	.1–4	26	1.50	2.6	2.0:1	2.0:1	+20	250
AFS4-00100600-25-20P-4	.1–6	32	1.50	2.5	2.0:1	2.0:1	+20	300
AFS4-00100800-28-20P-4	.1–8	30	1.50	2.8	2.0:1	2.0:1	+20	300
AFS4-00101200-40-20P-4	.1–12	20	1.50	4.0	2.0:1	2.0:1	+20	300
AFS4-00501800-60-20P-6	.5–18	25	2.75	6.0	2.5:1	2.5:1	+20	350
AFS5-00102000-60-18P-6	.1–20	25	3.00	6.0	2.5:1	2.5:1	+18	360
AFS3-01000200-20-27P-6	1–2	33	1.50	2.0	2.0:1	2.0:1	+27	350
AFS3-02000400-30-25P-6	2–4	28	1.50	3.0	2.0:1	2.0:1	+25	250
AFS3-04000800-40-20P-4	4–8	20	1.00	4.0	2.0:1	2.0:1	+20	200
AFS4-08001200-50-20P-4	8–12	22	1.25	5.0	2.0:1	2.0:1	+20	200
AFS6-12001800-40-20P-6	12–18	28	2.00	4.0	2.0:1	2.0:1	+20	375
AFS6-06001800-50-20P-6	6–18	23	2.00	5.0	2.0:1	2.0:1	+20	365
AFS4-02001800-60-20P-6	2–18	23	2.50	6.0	2.5:1	2.0:1	+20	350

*Noise figure degrades below 100 MHz. Please consult factory for details.
Note: Noise figures increase below 500 MHz in bands wider than .1-10 GHz.

OPTIONS:

- CRYOGENIC
- LIMITING
- VARIABLE GAIN
- LIMITER INPUT
- TTL CONTROLLED
- HIGH DYNAMIC RANGE
- EQUALIZED GAIN
- BUILT-IN TEST
- DETECTED OUTPUT
- MILITARY VERSIONS
- SPACE QUALIFIED

This is only a small sample of our extensive list of standard catalog items. Please contact Dave Krautheimer at (631) 439-9413 or e-mail dkrautheimer@miteq.com for additional information or to discuss your custom requirements.

MITEQ

100 Davids Drive, Hauppauge, NY 11788
TEL.: (631) 436-7400 • FAX: (631) 436-7430
www.miteq.com

Model Number	Frequency Range (GHz)	Gain (Min.) (dB)	Gain Flatness (±dB)	Noise Figure (dB, Max.)	VSWR Input (Max.)	VSWR Output (Max.)	Output Power @ 1 dB Comp. (dBm, Min.)	Nom. DC Power (+15 V, mA)
MODERATE BAND AMPLIFIERS								
AFS2-00700080-05-10P-4	.7–.8	30	0.50	0.45	1.5:1	1.5:1	+10	90
AFS2-00800100-05-10P-4	.8–1	30	0.50	0.45	1.5:1	1.5:1	+10	90
AFS3-01200160-05-13P-6	1.2–1.6	40	0.50	0.45	1.5:1	1.5:1	+13	150
AFS3-01400170-05-13P-6	1.4–1.7	40	0.50	0.45	1.5:1	1.5:1	+13	150
AFS3-01500180-04-13P-6	1.5–1.8	40	0.50	0.40	1.5:1	1.5:1	+13	150
AFS3-01500250-06-13P-6	1.5–2.5	36	0.50	0.60	2.0:1	2.0:1	+13	150
AFS3-01700190-04-13P-6	1.7–1.9	36	0.50	0.40	1.5:1	1.5:1	+13	150
AFS3-01800220-05-13P-6	1.8–2.2	36	0.50	0.50	1.5:1	1.5:1	+13	150
AFS3-02200230-04-13P-6	2.2–2.3	36	0.50	0.40	1.5:1	1.5:1	+13	150
AFS3-02300270-05-13P-6	2.3–2.7	34	0.50	0.45	1.5:1	1.5:1	+13	150
AFS3-02700290-05-13P-6	2.7–2.9	32	0.50	0.50	1.5:1	1.5:1	+13	150
AFS3-02900310-05-13P-6	2.9–3.1	32	0.50	0.45	1.5:1	1.5:1	+13	150
AFS3-03100350-06-10P-4	3.1–3.5	29	0.50	0.6	1.5:1	1.5:1	+10	150
AFS4-03400420-06-13P-6	3.4–4.2	40	0.50	0.60	1.5:1	1.5:1	+13	225
AFS3-04400510-07-5P-4	4.4–5.1	30	0.50	0.70	1.5:1	1.5:1	+5	100
AFS3-04500480-07-5P-4	4.5–4.8	30	0.50	0.70	1.5:1	1.5:1	+5	100
AFS3-05200600-07-5P-4	5.2–6	30	0.50	0.70	1.5:1	1.5:1	+5	100
AFS3-05400590-07-5P-4	5.4–5.9	30	0.50	0.70	1.5:1	1.5:1	+5	100
AFS3-05800670-07-5P-4	5.8–6.7	30	0.50	0.70	1.5:1	1.5:1	+5	100
AFS3-07250775-06-5P-4	7.25–7.75	30	0.50	0.60	1.5:1	1.5:1	+5	100
AFS3-07900840-07-5P-4	7.9–8.4	30	0.50	0.70	1.5:1	1.5:1	+5	100
AFS4-08500960-08-5P-4	8.5–9.6	32	0.75	0.80	1.5:1	1.5:1	+5	125
AFS3-09001100-09-5P-4	9–11	26	0.50	0.90	1.5:1	1.5:1	+5	100
AFS4-09001100-09-5P-4	9–11	32	0.75	0.90	1.5:1	1.5:1	+5	125
AFS4-10951175-09-5P-4	10.95–11.75	32	0.75	0.90	1.5:1	1.5:1	+5	125
AFS4-11701220-09-5P-4	11.7–12.2	32	0.75	0.90	1.5:1	1.5:1	+5	125
AFS2-12201280-10-8P-4	12.2–12.8	14	0.75	1.00	1.5:1	1.5:1	+8	80
AFS4-12201280-10-12P-4	12.2–12.8	27	0.75	1.00	1.5:1	1.5:1	+12	200
AFS4-12701330-13-10P-4	12.7–13.3	27	0.75	1.30	1.5:1	1.5:1	+10	175
AFS4-13201400-14-10P-4	13.2–14	24	0.75	1.40	1.5:1	1.5:1	+10	175
AFS4-14001450-14-10P-4	14–14.5	24	0.75	1.40	1.5:1	1.5:1	+10	175
AFS4-20202120-20-8P-4	20.2–21.2	20	1.00	2.00	1.5:1	1.5:1	+8	175
AFS4-21202400-22-10P-4	21.2–24	18	1.00	2.2	2.0:1	2.0:1	+10	100
OCTAVE BAND AMPLIFIERS								
AFS3-00120025-09-10P-4	.12–.25	38	0.50	0.9	2.0:1	2.0:1	+10	175
AFS3-00250050-08-10P-4	.25–.5	38	0.50	0.8	2.0:1	2.0:1	+10	125
AFS3-00500100-05-10P-6	.5–1	38	0.75	0.5	2.0:1	2.0:1	+10	150
AFS3-01000200-05-10P-6	1–2	38	1.00	0.5	2.0:1	2.0:1	+10	150
AFS3-01200240-05-10P-6	1.2–2.4	34	1.00	0.5	2.0:1	2.0:1	+10	175
AFS3-02000400-06-10P-4	2–4	30	1.00	0.6	2.0:1	2.0:1	+10	125
AFS3-02600520-10-10P-4	2.6–5.2	28	1.00	1.0	2.0:1	2.0:1	+10	150
AFS3-04000800-07-10P-4	4–8	30	1.00	0.7	2.0:1	2.0:1	+10	125
AFS3-08001200-09-10P-4	8–12	26	1.00	0.9	2.0:1	2.0:1	+10	125
AFS3-08001600-15-8P-4	8–16	26	1.00	1.5	2.0:1	2.0:1	+8	80
AFS4-12002400-25-10P-4	12–24	20	2.00	2.5	2.0:1	2.0:1	+10	85
AFS4-12001800-18-10P-4	12–18	26	1.00	1.8	2.0:1	2.0:1	+10	125
AFS4-18002650-28-8P-4	18–26.5	18	1.75	2.8	2.5:1	2.2:1	+8	150
MULTIOCTAVE BAND AMPLIFIERS								
AFS1-00040200-12-10P-4	.04–2	15	1.50	1.2	2.5:1	2.0:1	+10	75
AFS3-00300140-08-10P-4	.3–1.4	33	1.00	0.8	2.0:1	2.0:1	+10	150
AFS2-00400350-12-10P-4	.4–3.5	22	1.50	1.2	2.0:1	2.0:1	+10	80
AFS3-00500200-08-15P-4	.5–2	38	1.00	0.8	2.0:1	2.0:1	+15	125
AFS3-01000400-09-10P-4	1–4	30	1.50	0.9	2.0:1	2.0:1	+10	125
AFS3-02000800-09-10P-4	2–8	26	1.00	0.9	2.0:1	2.0:1	+10	125
AFS4-02001800-23-10P-4	2–18	25	2.00	2.3	2.0:1	2.0:1	+10	175
AFS4-06001800-22-10P-4	6–18	24	2.00	2.2	2.0:1	2.0:1	+10	150
AFS4-08001800-22-10P-4	8–18	26	2.00	2.2	2.0:1	2.0:1	+10	150
ULTRA WIDEBAND AMPLIFIERS								
AFS3-00100100-09-10P-4	.1–1	38	1.00	0.9	2.0:1	2.0:1	+10	150
AFS3-00100200-10-15P-4	.1–2	38	1.00	1.0	2.0:1	2.0:1	+15	150
AFS3-00100300-11-10P-4	.1–3	32	1.00	1.1	2.0:1	2.0:1	+10	150
AFS3-00100400-13-10P-4	.1–4	28	1.00	1.3	2.0:1	2.0:1	+10	150
AFS3-00100600-13-10P-4	.1–6	28	1.25	1.3	2.0:1	2.0:1	+10	125
AFS3-00100800-14-10P-4	.1–8	25	1.50	1.4	2.0:1	2.0:1	+10	125
AFS4-00101200-22-10P-4	.1–12	28	1.50	2.2	2.0:1	2.0:1	+10	175
AFS4-00101400-23-10P-4	.1–14	24	2.00	2.3	2.5:1	2.5:1	+10	200
AFS4-00101800-25-10P-4	.1–18	25	2.00	2.5	2.5:1	2.5:1	+10	175
AFS4-00102000-30-10P-4	.1–20	20	2.50	3.0	2.5:1	2.5:1	+10	175
AFS4-00102650-40-8P-4	.1–26.5	18	2.50	4.0	2.5:1	2.5:1	+8	175

Note: Noise figure increases below 500 MHz in bands greater than 0.1-10 GHz.

3 YEAR WARRANTY

NQA ISO 9001 REGISTERED COMPANY

tyco | Electronics M/A-COM

Shaping the future of wireless.

OpenSky™

Wireless Private Networks

M/A-COM provides an integrated digital voice and data communications network solution to the Public Safety, Transportation, Transit and Utilities Markets.

Semiconductors

Portables and Infrastructure

Today the cellular telephone is used primarily as a mode of voice based communication. M/A-COM provides semiconductor products which will help transform today's mobile phones into tomorrow's wireless voice and data terminals.

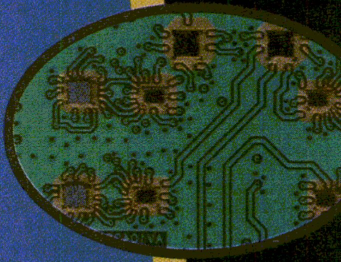

Fixed Wireless

Local Multipoint Distribution Systems

LMDS uses high-powered radio signals to transmit voice, video and data communications.It offers full two-way symmetric and asymmetric communications between a single base station point to various customer premise location within a clear line-of-sight.

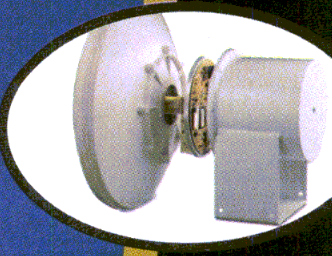

Automotive

Sensors and Telematics

M/A-COM is a leader in the development of wireless products designed to enhance automotive information and safety. Applications include autonomous cruise control, collision avoidance radar and GPS.

M/A-COM 50 Years in the making

CIRCLE NO. 230

www.macom.com

WELCOME TO PLANET EE

Today, Penton Media's Electronics Group is proud to announce PlanetEE, your new website. Notice I didn't say our new website. When we conceived the idea to build *PlanetEE* (www.PlanetEE.com), we were determined to make it your site—a site built specifically for electronics engineers. And we think we have succeeded in bringing to you a content- and feature-rich portal site that will help you do your job better—from concept to completion.

That's our mission. And I, along with my web staff, look forward to working with you in the future.

PlanetEE
Penton Electronics Group

The site is supported by the PlanetEE staff plus more than 50 technical editors from the Electronics Group's stable of five leading technical publications: *Electronic Design*, *EE Product News*, *Microwaves & RF*, *Wireless Systems Design*, and *Embedded Systems Development*. In addition, we've partnered with a number of leading companies to bring you a wide variety of resources that will assist you in your job and career. We've partnered in areas of commerce, education, directories, and career services.

Moreover, we've constructed two exclusive directories that empower you to intelligently and quickly search out the best products for your new designs. Initially, you'll be able to locate products from some 63 categories of electronic components. Once you've pinpointed the products you need, you can then latch onto data sheets, app notes, and other technical information quickly and efficiently directly from the vendors' websites. Our exclusive, vendor-neutral directories will provide you with the most complete, accurate, and up-to-date product information available from manufacturers.

And there's more. We will deliver news and analysis from our worldwide network of editors and correspondents. You will have searchable archives to all of our magazines, an Ideas For Design library, discussion rooms, career information, and as much information and data from vendors that we can pull together to serve you.

To make it easy for you to cut right to the chase, we've launched 10 specialized Communities within PlanetEE that aggregate content in a number of key technologies: Analog/Mixed-Signal, Communications/Networking, Components & Assemblies, Computing & Information Appliances, Digital ICs & ASICs, Electronic Design Automation, Embedded Systems, Interconnects/Packaging & Materials, Power Control & Supplies, and Test & Measurement. Look for more Communities to roll out in the months ahead.

As the former Editor-In-Chief of *Electronic Design* magazine, I understand your world, that's why we named the site PlanetEE. Our intention from day one has been to build a site specifically to assist electronics engineers in their professional careers. It's your site. I welcome you to log-on, "kick the tires," and let me know what you think. I'll listen to you and we'll act on your comments to make PlanetEE a better place to assist you in achieving your goals.

Tom Halligan, Group Web Director

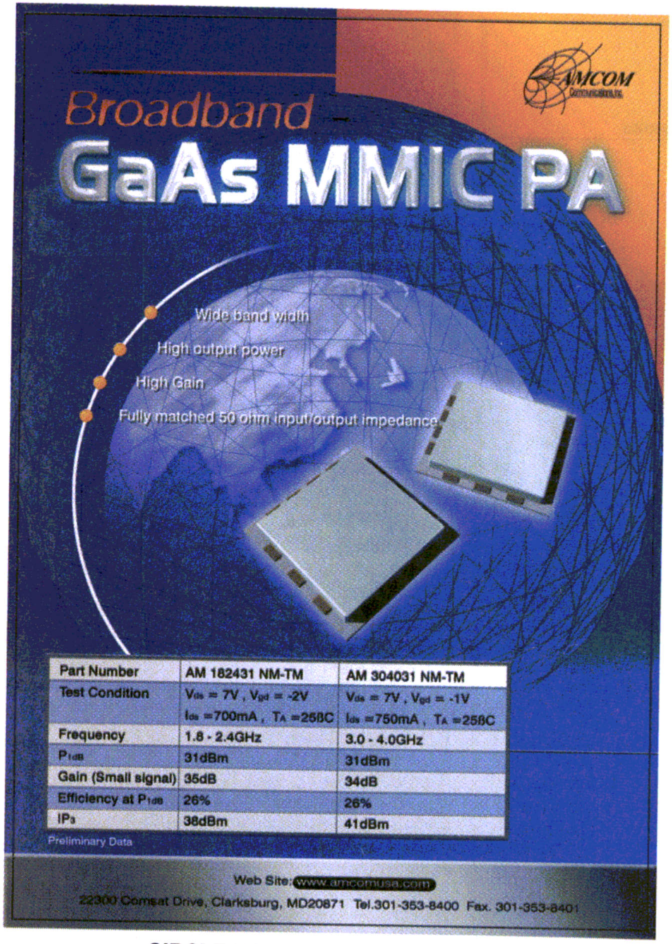

Microwaves & RF

A Penton Publication

Group Publisher Craig Roth—(201) 393-6225
Publisher/Editor Jack Browne—(201) 393-6293
Managing Editor Peter Stavenick—(201) 393-6028
Senior Editor Gene Heftman—(201) 393-6251
Senior Editor Don Keller—(201) 393-6295
Special Projects Editor Alan ("Pete") Conrad
Copy Editors John Curley ▪ Mitchell Gang
Editorial Assistant Dawn Prior
Contributing Editors Andrew Laundrie ▪ Allen Podell

MANUFACTURING GROUP

Director Of Manufacturing Ilene Weiner
Group Production Director Mike McCabe
Customer Service Representative
Dorothy Sowa—(201) 393-6083 or FAX: (201) 393-0410
Production Coordinators Lu Hlavaty, Judy Osborn, Eileen Slavinsky
Digital Production Coordinators Mike Turro, Leilani Locket, Pat Boselli

ART DEPARTMENT

Group Art Director Peter K. Jeziorski
Associate Group Art Director Anthony Vitolo
Staff Artists Linda Gravell ▪ James Miller ▪ Michael Descul
Art Coordinator Wayne M. Morris

Reprints Reprint Services (651) 582-3800
Circulation Manager Nancy Graham—(216) 696-7000
Vice President/Group Director John G. French

Penton
Penton Media, Inc.

Chief Executive Officer Thomas L. Kemp
President/Chief Operating Officer Daniel J. Ramella
Chief Financial Officer Joseph G. NeCastro
Chief Technology Officer Gary W. Hargreaves
Executive Vice President/Group President David B. Nussbaum
Executive Vice President/Group President James W. Zaremba
Senior Vice President/Human Resources Katherine P. Torgerson
Vice President/Investor Relations Mary E. Abood

Editorial Office
Penton Media, Inc.
611 Route #46 West, Hasbrouck Heights, NJ 07604
Phone: (201) 393-6286, FAX: (201) 393-6297

International editions are shipped via several entry points, including: Editeur Responsable (Belgique), Vuurgatstraat 92, 3090 Overijse, Belgique.

Microwaves & RF is sent free to individuals actively engaged in high-frequency electronics engineering. In addition, paid subscriptions are available by writing to: Penton Media, *Microwaves & RF*, c/o Bank of America, Subscription Lockbox, P.O. Box 96732, Chicago, IL 60693; Tel.: (216) 931-9188, FAX: (216) 696-6413. Prices for non-qualified subscribers are:

	1 Yr. (Surface)	1 Yr. (Air Mail)	Single Copies: Regular Issues	Single Copies: PDD Only
U.S.	$ 75.00	—	$10.00	$100.00
Canada	$100.00	$135.00	$12.00	$125.00
Mexico	$120.00	$174.00	$14.00	$125.00
All other countries	$135.00	$243.00	$16.00	$125.00

Reprints can be ordered from Reprints Services at (651) 582-3800.

Back issues of *MicroWaves* and *Microwaves & RF* are available on microfilm, microfiche, 16-mm, or 35-mm roll film. They can be ordered from Xerox University Microfilms, 300 North Zeeb Rd., Ann Arbor, MI 48106. For immediate information, call (313) 761-4700. Copying: Permission is granted to users registered with the Copyright Clearance Center, Inc. (CCC) to photocopy any article, with the exception of those for which separate copyright ownership is indicated on the first page of the article, provided that a base fee of $1.25 per copy of the article plus 60 cents per page is paid directly to the CCC, 222 Rosewood Dr., Danvers, MA 01923. (Code 0745–2993/00 $1.25+.60) Copying done for other than personal or internal reference use without the expressed permission of Penton Media, Inc., is prohibited. Requests for special permission or bulk orders should be addressed in writing to the publisher.

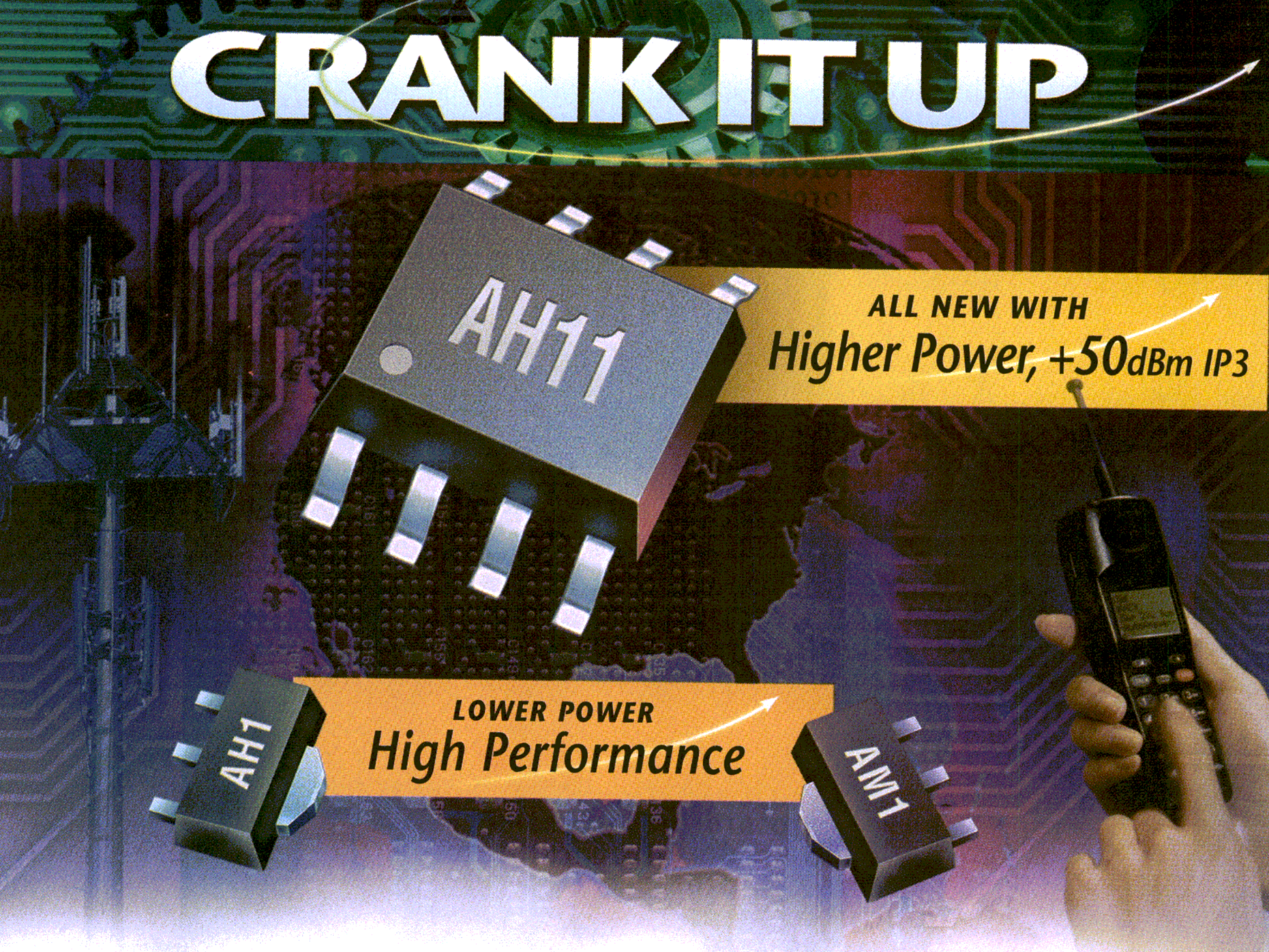

Need Higher Power? You need Watkins-Johnson's new AH11 amplifier.

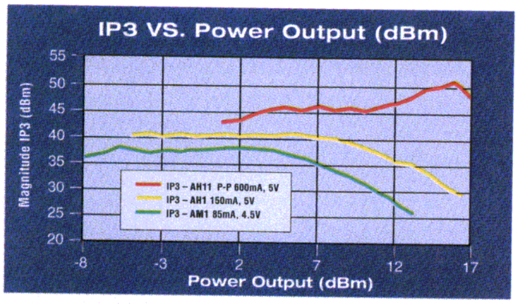

WJ High Dynamic Range Amplifiers

Product	Frequency (MHz)	IP3 (dBm, typ.)	P1dB (dBm, typ.)	NF (dB, typ.)	Bias current (mA, typ.)
AH11	250-3000	47	27	3.7	600
AH1	250-3000	41	21	2.9	150
AM1	250-3000	36	18	2.6	75

Ultra high IP3 is what our new **AH11** is all about. Combined with a very low noise figure, it's the perfect choice for today's multichannel wireless systems. Drawing only 600mA, the AH11 delivers 17dBm of linear output power with an IP3 of 50dBm. A great price combined with the outstanding linear efficiency makes this versatile amplifier perfect for multiple sockets, reducing overall part count.

Need Lower Power? Both the **AH1** and **AM1** offer low noise figures which, together with their inherent high IP3, deliver superior performance at the best price in the industry.

For more details, call our toll free number or fax us at 650-813-2447. Email us at wireless.info@wj.com to request data sheets and a complete catalog.

The Communications Edge™

ISO 9001 WATKINS-JOHNSON WIRELESS PRODUCTS GROUP

Visit us on the web at www.wj.com

1-800-WJ1-4401

WATKINS-JOHNSON

Distributed In U.S.A. by Nu Horizons Electronics: 888-747-6846; **Richardson Electronics:** 800-348-5580
In Europe call WJ: +44-1252-661761 or your local Richardson Electronics Office: **France:** (01) 55 66 00 30; **Germany:** (089) 890 214 0; **Italy:** (055) 420 10 30 **UK:** (01753) 733010

CIRCLE NO. 308

3G Design In Build Out

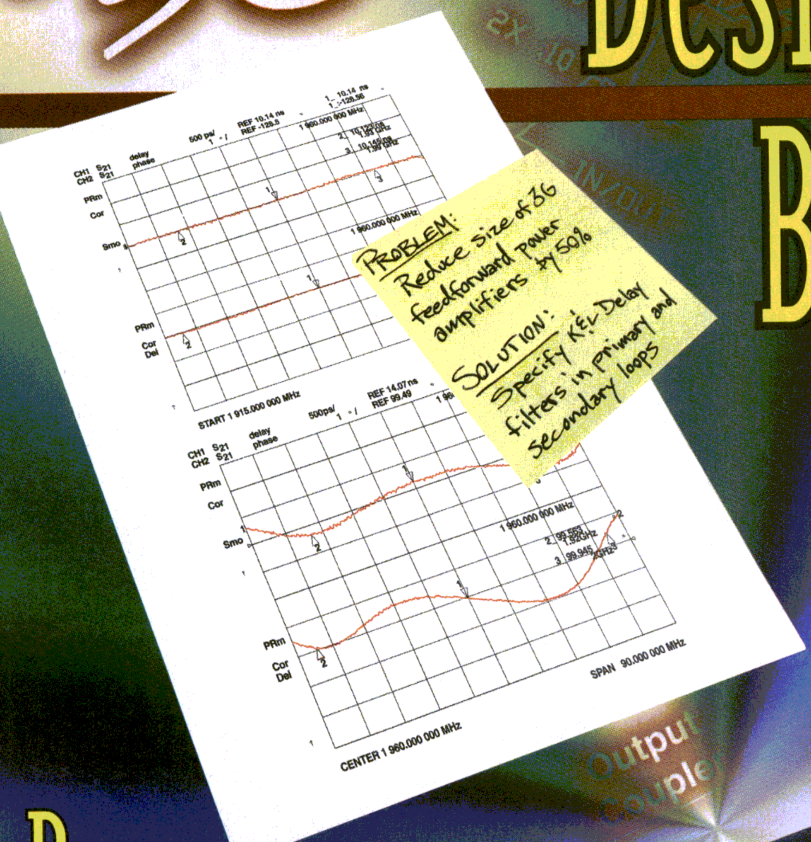

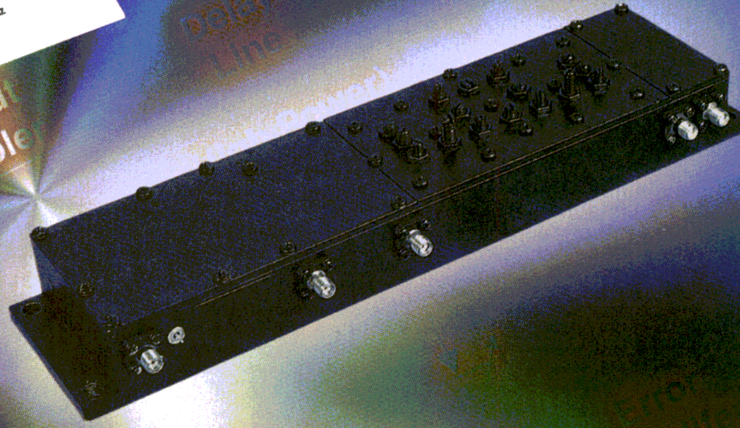

Primary loop delay filter assemblies integrate high power cavity delay filters, couplers and isolators into a single compact module for performance improvement, space savings and cost reduction.

Secondary loop miniature delay filters utilize a Patent Pending topology to provide delay equalization. The filters exhibit excellent delay and phase flatness in a miniature surface mount package. The 3G model measures a mere 1.5"L x 0.60"W x 0.4"H and can be mounted directly onto your PWB with pick and place machinery.

Order On-Line

New! Buy K&L Filters over the web
www.klmicrowave.com

K&L MICROWAVE INCORPORATED®
A DOVER TECHNOLOGIES COMPANY

USA
Phone: 410-749-2424
FAX: 410-749-2788

EUROPE
Phone: 44-(0)-1262 605500
FAX: 44-(0)-1262 605504

www.klmicrowave.com • E-mail: wireless@klmicrowave.com

CIRCLE NO. 262


Broadband Wireless Solutions
Look to Stellex for your
Application Requirements
Mini and Micro YIGs
YIG Filters / Oscillators
YIG Synthesizers
YIG Synthesizers
Millimeter Wave
Transceivers/Receivers
Transceivers, Subassemblies
28GHz LMDS and
Millimeter Wave ODUs
ODU's
Broadband Products, Pricing & Performance
in Volume Production....Today!
Questions, Specifications, Literature, Quotes...
Contact Us at
www.stellexms.com or 1-800-321-8075
Stellex
5300 Hellyer Avenue, San Jose, CA 95138-1005 • Tel (408) 624-3000 • Fax (408) 624-3911
CIRCLE NO. 247

Shipments Of GPS And Smart Antennas Are Up

OYSTER BAY, NY—The continued growth of wireless users worldwide and the increasing integration of Global Positioning Systems (GPS) applications into every day life will raise the value of the antenna market substantially over the next five years, according to a report from Allied Business Intelligence (ABI).

Smart Antennas, which will help to satisfy a wireless operator's capacity crunch, will be one of the largest growth areas for antennas. Smart-antenna technology will become especially important as actual and truncated Internet access and other data applications continue to be deployed on mobile wireless systems worldwide. "Interference limits the amount of data that can be transmitted over a wireless system, so many wireless operators are turning to smart-antenna systems to reduce interference, and to squeeze more capacity out of existing networks," says ABI analyst Frank Viqez, the report's author. Smart-antenna manufacturers are boasting capacity gains from 50 to 100 percent in digital networks, depending on the air interface. Shipments for smart-antenna base stations will rise at a compound-average-annual-growth (CAAG) rate of 44 percent from 2000 to 2005.

The GPS antenna industry is experiencing tremendous growth as well, driven by many factors including sales of in-vehicle navigation systems (IVNS), a synthesis of wireless and GPS technologies. US telematics-services providers General Motors (GM) and ATX Technologies, which have close to 300,000 subscribers collectively, are aggressively drawing in new subscribers with navigation and information services for one's car. LoJack Corp. and the Automobile Club of America will offer services in 2001, adding to the market potential. Most automobile manufacturers will have telematics as a standard option in many models during the next few years. GM already offers the option in over 30 vehicle models.

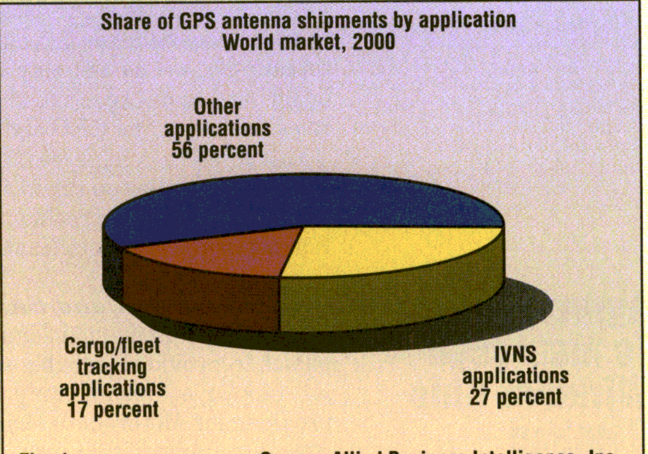

Fig. 1

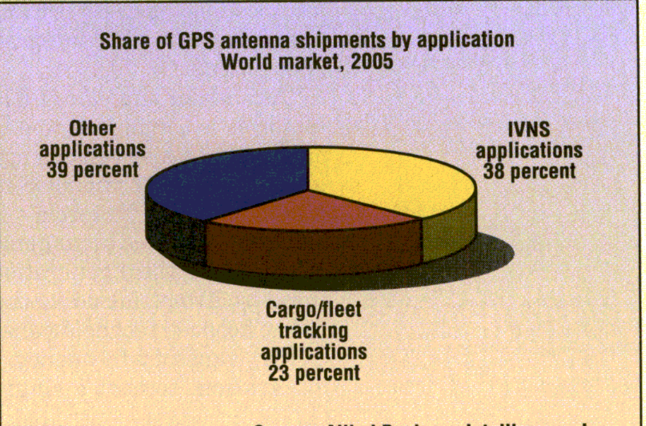

Fig. 2

IVNS will account for 27 percent of total worldwide GPS antenna shipments for this year—the highest percentage of any category. Between 2000 and 2005, the rise in worldwide antenna shipments for IVNS will represent a CAAG of 35 percent. Cargo/fleet-tracking applications will account for 17 percent of shipments in 2000 and 23 percent of shipments by year-end 2005 (Figs. 1 and 2).

"Antennas 2000, Global Technologies and Strategies for Cellular/PCS, GPS, and Smart Base Station Antennas" covers the antenna market in detail for the US and the rest of the world. ABI publishes strategic research on the broadband, wireless, electronics, automation, energy, and transportation industries.

E-Commerce To Become A Major Market Force

CLEVELAND, OH—This year, technology and the Internet continue to drive businesses across all industries, according to the fifth annual Hot & Not-So-Hot Executive Jobs Report compiled by Christian & Timbers, a CEO executive search firm. The report shows that virtually every job on the list is related not only to technology or the Web, but specifically to e-commerce. "Industry experts agree that any company not doing business over the Web in the next two years will be out of business," says Jeffery E. Christian, chairman and CEO of Christian & Timbers. "The race is on for survival in an e-commerce world and the winners are assembling executive teams that focus on Web-enabling companies and creating brands to establish market leadership."

According to Christian, the intensity in securing top talent increased throughout 1999 as more of the firm's executive searches centered around e-commerce. "The forces characterizing the executive market include demand, compensation, quality of the talent pool, timing issues, and industry pressures. Therefore, we tracked demand across all of our industry practices through personal telephone interviews, client and website surveys, and new search requests," Christian says.

"In our analysis of the data collected and our own industry expertise, we are seeing the e-commerce fever drive the pace of business change with increasing urgency. Interestingly, we see not only some new positions emerging, like 'entrepreneur in residence' and 'non-executive chairman' but also some significant changes in traditional roles, including the CEO and chairman of the board," Christian continues.

Adversely, e-commerce is also turning traditional roles into not-so-hot jobs for 2000. With most of the top talent flocking to e-commerce, the demand for traditional positions, such as a vice president of retail operations and a CEO of a traditional distribution company, has significantly declined.

Agreement Aims To Meet High Wireless Chip Demand

PHOENIX, AZ and SAN JOSE, CA—The Semiconductor Products Sector of Motorola and Atmel have announced a licensing agreement that will enable the companies to provide a reliable supply of a popular technology for wireless applications, RF bipolar complementary metal-oxide semiconductor (BiCMOS). The agreement provides for Motorola to share its BiCMOS technology with Atmel. This will enable Atmel to immediately provide wireless original equipment manufacturers (OEMs) with products designed in a process that is fully mask-compatible with Motorola's advanced 0.35-μm RF BiCMOS technology. The result will help to meet demand for high integration RF integrated circuits (RF ICs), for low-voltage portable wireless applications.

"As a major supplier of RF/IF BiCMOS integrated circuits to the wireless market, Motorola is committed to a strategy that provides its customers with a viable alternate source. this licensing agreement allows our customers to source Motorola's 0.35-μm Advanced RF BiCMOS technology directly from Atmel," says Behrooz Abdi, general manager of Motorola's RF/IF Division. "We'll continue to pursue both foundry and second-source arrangements to our customers in this accelerating market."

This is the third generation (3G) of Motorola's BiCMOS technology to be manufactured by Atmel, including the 0.5-μm RF BiCMOS process.

The licensed technology has a 0.35-μm feature size and a negative-positive-negative (NPN) transition frequency (ft) of 28 GHz. BiCMOS technology enables high levels of integration, so that a single device can contain RF mixers, low-noise amplifiers (LNAs), voltage-controlled oscillators (VCOs), gain-controlled amplifiers, and frequency synthesizers, as well as baseband analog functions (signal-strength detectors and filters), and significant digital circuitry. It is suitable for portable wireless applications such as cellular phones, cordless phones, Global Positioning System (GPS) receivers, wireless local-area networks (WLANs), and transceivers for the unlicensed industrial-scientific-medical (ISM) bands up to 2400 GHz.

As a producer of embedded processors, Motorola's Semiconductor Products Sector offers multiple DigitalDNA™ technologies which enable its customers to create "smart" products and new business opportunities in the networking and computing, wireless communications, transportation, and imaging and entertainment markets. Motorola's worldwide semiconducter sales were $7.4 billion in 1999.

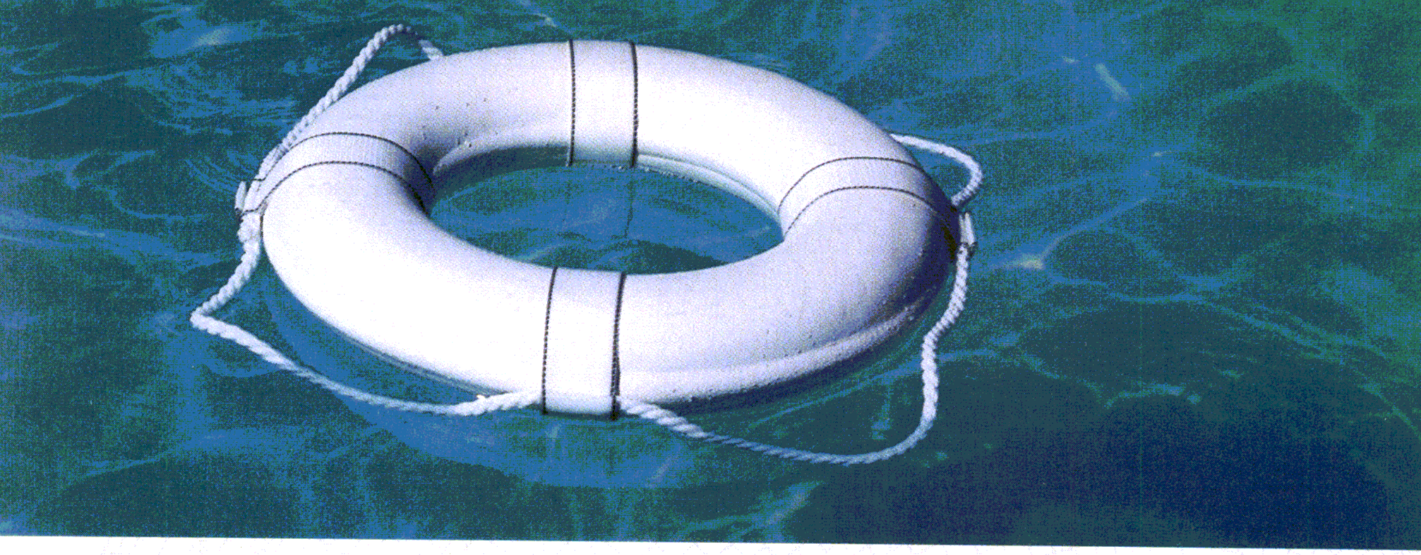

System Offers Protection Against Lightning Strikes

BOULDER, CO—Lightning strikes can incinerate trees, ignite fires, and knock out power and communications lines. Each year, lightning causes massive damage to business facilities across the US. The destructive power of lightning is so great that even structures equipped with traditional lightning rods can suffer extensive damage.

The danger of a lightning strike is often exacerbated by so-called "prevention" devices such as lightning rods and early-streamer emitters, which are designed to collect and channel the force of a strike to the ground. This 200-year-old technology was never intended for protection of modern high-tech automated facilities, but rather barns and other wood structures of the early 1800s.

One technology, the Dissipation Array System (DAS), is being touted as the ultimate solution for lightning protection. DAS is based on a natural phenomenon known to scientists for centuries as the "point-discharge" principle, or charge transfer. A sharp point in a strong electrostatic field will leak off electrons by ionizing the adjacent air molecules, providing that the point's potential is raised by +10,000 VDC above that of its surroundings. This principle is demonstrated by what scientists call natural dissipation. The ionization produced by trees, grass, towers, fences, and other structures can naturally dissipate up to 90 percent of the total energy generated by a storm, thereby preventing the formation of lightning.

The DAS employs the point-discharge principle by providing thousands of points with specific point separation which simultaneously produce ions over a large area, thus preventing the formation of a streamer, which is the precursor of a lightning strike.

This ionization process creates a flow of current from the point(s) into the surrounding air. Under storm conditions, this ionization current increases exponentially with the storm's electronic field, which can reach levels up to +30,000 VDC per meter of elevation above earth during a mature storm.

The charge induced on the site by the storm is removed from the protected area and transferred to the air molecules. These charged molecules then move away from the site.

Thus, DAS prevents strikes by continually lowering the voltage differential between the ground and the charged crowd to well-below the lightning potential, even in the midst of a worst-case storm. This differential has been measured at up to 6000 percent.

One company, Lightning Eliminators and Consultants, Inc. (LEC), based in Boulder, CO, has long been involved in DAS development. In the three decades since LEC introduced DAS into the US marketplace, it has been the only lightning-protection system proven to prevent lightning strikes to any protected facility. The system has accumulated over 20,000 system-years of history with a 99.7-percent reliability.

Ultraminiature Radio Component Is Produced

REDONDO BEACH, CA—TRW has produced a highly miniaturized radio component which improves the messaging capability of TRW communications-satellite payloads, while dramatically decreasing size and weight. Its first use will be in the payloads that TRW is building for the Astrolink global broadband-telecommunications system, slated to begin service in 2003.

The TRW low-noise-amplifier (LNA) downconverter detects and converts signals received by the satellite's antennas at frequencies of 30 billion cycles per second (30 GHz) to lower frequencies that are easier to process electronically. Astrolink's satellites receive signals from Earth at 30 GHz and transmit to Earth at 20 GHz, in a frequency range known as the K_a band.

The LNA downconverter is packaged as an integrated microwave assembly, housing a number of TRW gallium-arsenide (GaAs) integrated circuits (ICs) designed for K_a-band operation. Devices contained in the unit include low-noise amplifiers (LNAs), filters, voltage regulators, frequency converters, low-loss redundancy switches, and frequency multipliers.

"Our miniature package shows the advantages of TRW's advanced microelectronics for spacecraft use, where weight and size are always at a premium," says Paul Borzcik, vice president and program manager of the TRW Astrolink program. "Our unit is about the size of a matchbook and weighs little more than an ounce."

TALENT

DESIGNERS

National's New Multi-Carrier 14-Bit, 135 MSPS D/A Converter Simplifies Wireless Basestation Design

DAC14135 Combines Multiple Carriers, Reducing Basestation Cost and Size

- Wide dynamic range with:
  85dBc SFDR @ 1MHz
  70dBc SFDR @ 20MHz
- TTL/CMOS (+3.3V or +5V) Inputs
- 48-pin TSSOP provides small footprint
- Low 185mW power dissipation
- Costs less than $10

Ideal for Multi-Carrier and Multi-Standard Cellular Basestations, Wireless Local Loop Basestations, Direct Digital Synthesis (DDS), ADSL and HFC Modems, and Instrumentation

For More Information on DAC14135:
www.national.com/appinfo/wbp/
1-800-272-9959

Evaluation Board Available at:
www.national.com

Free CD-ROM Data Catalog
Available at freecd.national.com

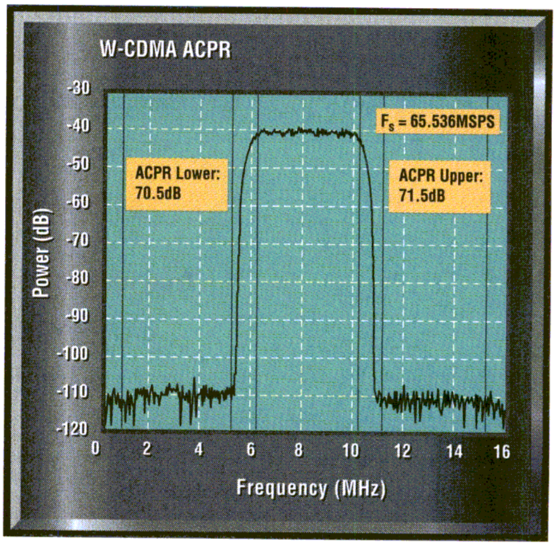

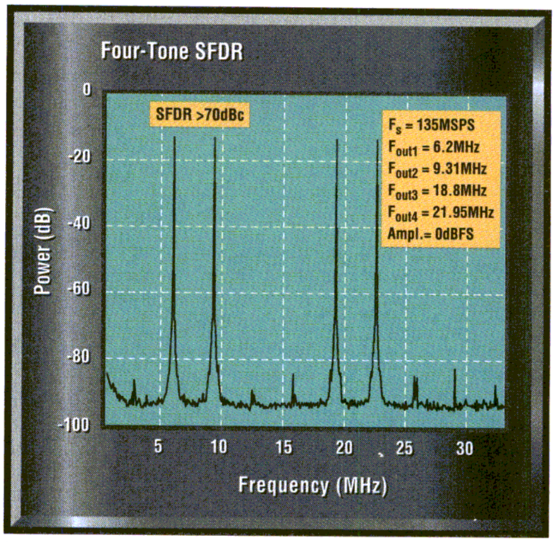

National Semiconductor®

CIRCLE NO. 293

The Naval Research Laboratory's impressive efforts in modeling and simulation, as well as their close ties within the industry, are pushing vacuum electronics to new levels of performance.

Vacuum Electronics Are Alive And Well At The NRL

JACK BROWNE
Publisher/Editor

TRADITION is strong at the Naval Research Laboratory (Washington, DC). Commissioned in 1923 by Congress to provide research for the Department of the Navy, the NRL is now an impressive intellectual group of more than 3000 personnel, with more than 1900 of these research staff, and nearly one-half of these researchers having achieved Ph.D. educational status. Known as the Navy's "corporate laboratory," the NRL is actually much more, providing leading-edge technology and engineering across a wide range of disciplines, including high-frequency vacuum electronics.

The NRL is headed jointly by Commanding Officer, Captain Douglas H. Rau of the US Navy, and Director of Research, Dr. Timothy Coffey. Five Associate Directors of Research work under the authority of the joint heads. The NRL's parent organization is the Office of Naval Research (Arlington, VA), which coordinates, executes, and promotes the science and technology programs of the US Navy and Marine Corps through universities, government laboratories, and non-profit and for-profit organizations. The NRL operates as a Navy Working Capital Fund (NWCF). Costs are charged to various research projects, with funding coming from such organizations as the Chief of Naval Research, the Naval Systems Commands, the US Air Force, the Defense Advanced Research Projects Agency (DARPA), and the National Aeronautics and Space Administration (NASA).

The Vacuum Electronics Branch of the Electronic Science and Technology Division is a relatively small part of the NRL, but a major contributor to the advancement of high-power vacuum devices. Headed by Robert Parker, the Vacuum Electronics Branch is involved in a wide range of vacuum electronics research and development (R&D), in such areas as microwave and millimeter-wave power amplifiers (PAs), field-emission arrays, enhanced cathodes, and thermionic energy conversion. Parker notes that current research concerns devices far removed from simple glass-encased vacuum tubes: "The microwave power module (MPM) is a good example of the advances that are still possible in vacuum electronics." In addition to MPMs, the Vacuum Electronics Branch has been involved in significant advances in multistage depressed collectors and improvements in traveling-wave-tube (TWT) helix structures in efforts to increase the operating bandwidths of vacuum electronic devices.

Parker credits the development of sophisticated computer-modeling codes with many of the NRL's recent advances in vacuum electronic devices. He also cites the NRL's close working relationships within the industry and individuals such as Carter Armstrong of Litton Industries (San Carlos, CA), formerly of Northrop Grumman (Baltimore, MD), for making the advances possible. "Carter Armstrong was one of the people who recognized the importance of simulation code for vacuum electronics," notes Parker.

A number of different vacuum electronic devices are used in high-frequency applications. They share the same basic features, including a source of accelerated electrons, an interaction circuit where electron energy is converted to radiation, a collector to absorb the spent electrons, an output coupler to couple the radiation out of the device, and structures to mechanically support the device and to help dissipate heat. Vacuum electronic devices are difficult to model due to the distributed nature of the interaction between the beam electrons and the device's electromagnetic (EM) fields, as well as the large number of charged particles present in the device.

A variety of computational codes is used in the analysis and simulation of vacuum electronic devices, including steady-state beam trajectory codes, computational EM codes, beam-wave interaction codes, and particle-in-cell (PIC) codes. Steady-state beam trajectory codes are also known as gun

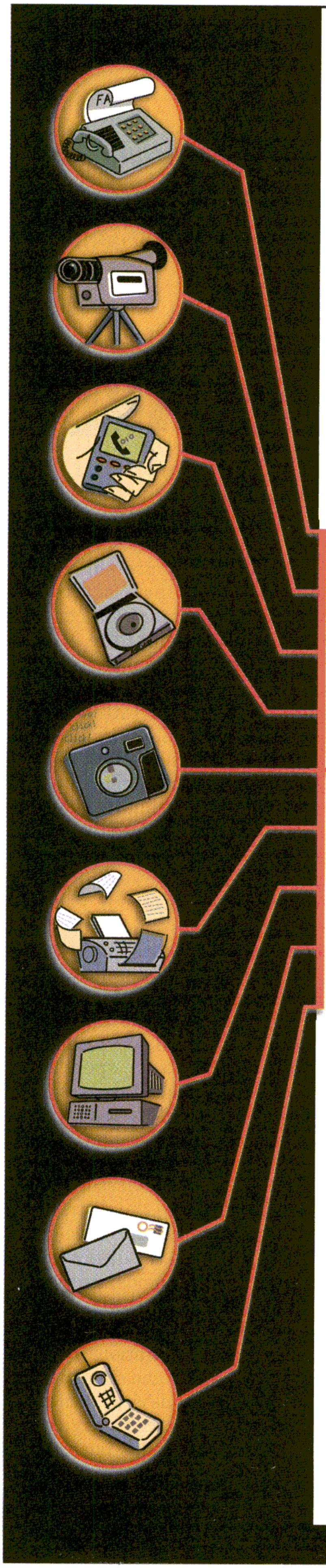

codes. This special class of iterative particle-simulation code converges to mutually consistent steady particle-flow fields and static electric and magnetic fields for time-independent problems.

Parker acknowledges the work of Baruch Levush, head of the Theory and Design Section of the Vacuum Electronics Branch, who came to the NRL from the University of Maryland (College Park, MD). Levush, who has co-authored numerous technical papers on modeling vacuum electronic devices, agrees that codes are critical to achieving advancements in vacuum electronics, but that "you must know the limitations of your models and their predictive capabilities, which can be verified through extensive testing."

Levush mentions the development of a 94-GHz gyro-klystron when citing the diversity of code needed for modeling. Involving a team comprised of Litton Electron Devices (San Carlos, CA), CPI (Palo Alto, CA), and the University of Maryland working with the NRL under the leadership of Bruce Danly, head of

CITING THE NRL'S HISTORICAL ACHIEVEMENTS

The US Naval Research Laboratory (NRL) deserves credit for many advances in electronics, such as the excimer laser, which is now commonly used for shaping the cornea in corrective eye surgery. The NRL has enjoyed a rich history of technological achievements in many different fields of science and engineering, including the development of the first modern radar system in the US. Based on observations of phase distortions in radio waves reflected from a steam ship in the Potomac River in 1922, the NRL's Robert Page was able to assemble and demonstrate the world's first pulsed radar system in 1934. In 1939, NRL installed the first operational radar aboard the battleship USS New York in time to contribute to victories at the battles of the Coral Sea, Midway, and Guadalcanal.

In 1939, as a complement to the radar system, the NRL also developed the plan-position indicator (PPI), a round display and plot which could be used to show the range and bearing of all targets detected by a radar. The PPI is now used throughout the world for target detection, navigation, air-traffic control, and object-identification radar systems.

IN THE 1970s, THE NRL DEVELOPED A METHOD FOR GROWING HIGH-PURITY SINGLE-CRYSTAL GALLIUM-ARSENIDE (GaAs) MATERIALS. THIS SPARKED THE GROWTH OF GaAs SEMICONDUCTORS.

In addition, the NRL's discovery of the principles behind the "skip distance effect" formed the basis for modern high-frequency (HF) wave propagation theory. This effect describes the reappearance of radio signals at a considerable distance varying with frequency, time of day, and season. Investigation of this phenomenon led to NRL's later invention of the magnetic-drum-radar equipment (MADRE) over-the-horizon radar system in 1961. This first HF over-the-horizon radar system was able to detect targets at distances and altitudes beyond the line of sight, and improved radar detection range by an order of magnitude compared to higher-frequency radar systems. The over-the-horizon radar formed the basis for the Air Force's continental air-defense radar and the Navy's relocatable over-the-horizon radar (ROTHR).

NRL's TIMe/navigATION (TIMATION) program was the progenitor of the NAVSTART Global Positioning System (GPS). The TIMATION concept led to NRL's invention and development of the first satellite prototypes of the proof-of-concept for a revolutionary navigation system which would use passive ranging techniques and highly accurate clocks to provide three-dimensional (3D) [longitude, latitude, and altitude] coverage throughout the world.

In a major advance in electronic intelligence gathering, NRL scientists discovered how to uniquely identify specific radar transmitters (Tx) by their particular signal fingerprint, catalog the radar's host platform, and handoff information about these emitters for tracking by other systems. The US National Security Agency (NSA) recognized NRL's concept and equipment in 1993 as the specific-emitter-identification (SEI) national standard. SEI systems are currently deployed on ships, aircraft, submarines, and ground sites throughout the armed forces.

In the 1970s, the NRL developed a method of growing high-purity single-crystal gallium-arsenide (GaAs) materials, thus sparking growth in the production and use of GaAs semiconductors. The high purity of the single-crystal materials enabled the ion implantation of the crystals to produce micrometer- and millimeter-wave devices and integrated circuits (ICs). NRL was also instrumental in transferring the technology to industry.

From 1988 to 1992, NRL developed the Navy Operational Global Atmospheric Prediction System (NOGAPS), a unified global weather analysis/forecast system which predicts the weather in areas of Department of Defense (DoD) operations worldwide. The system provides global atmospheric and oceanographic support, including cloud-cover prediction, estimation of weather effects on weapon systems, tropical cyclone formation and movement, and high seas warnings. The system is also used by the US Coast Guard, Department of Energy (DoE), and National Oceanic and Atmospheric Administration (NOAA). Recent work in NOGAPS has included the modeling and parameterization of mountain waves—oscillations in the wind passing over mountain ranges—to predict the resulting stratospheric effects.

the High Power Devices section of the Vacuum Electronics Branch, the device-development program was performed with three design tools. "The idea is to develop code for a particular device based on our knowledge of physics. By using optimized code, processing and computations can be greatly accelerated," says Levush. "In developing the circuitry for the W-band gyro-klystron, we needed to use three-dimensional codes to refine our designs for high peak-power levels," adds Levush. The fast-wave device employs ceramic loading to help dissipate heat, and a diamond waveguide window to handle the high output power. Modeling was instrumental in predicting the effects of the ceramic loading on the resonant cavity.

THE FAST-WAVE DEVICE EMPLOYS CERAMIC LOADING TO HELP DISSIPATE HEAT, AND A DIAMOND WAVEGUIDE WINDOW TO HANDLE THE HIGH OUTPUT POWER.

"For this 94-GHz gyro-klystron design," notes Levush, "we used the best technology available. We started with a four-cavity design but discovered that we needed more gain, so we developed a five-cavity device." For their efforts on the 94-GHz device, all members of the development team, including Litton Electron Devices, CPI, and the University of Maryland received the Department of Defense's (DoD's) prestigious Robert Wood award. Development of the high-power 94-GHz devices is critical to the success of the WARLOC program, a high-power W-band radar system.

An area of great pride within the Vacuum Electronics Branch is the MPM. The device essentially combines a low-noise solid-state monolithic-microwave-integrated-circuit (MMIC) driver amplifier with a high-efficiency miniature traveling-wave tube (TWT) and an integrated power conditioner. The NRL has worked extensively within the industry, including Northrop Grumman, Litton Electron Devices, and CPI, to miniaturize these high-power amplifiers through painstaking modeling and measurements. The devices have proven to be extremely reliable, and are counted upon by the Air Force in such critical applications as towed decoys.

According to Dick Abrams, who heads the NRL's MPM efforts, the devices are very durable: "The tubes themselves are very rugged; the high-voltage interfaces can be more of a problem than the tube itself," says Abrams. He notes that the NRL is working with the industry to increase the bandwidths of their MPMs: "We now have a family of MPMs capable of producing 100-W output power from 2 to 18 GHz, and we are looking to expand that to 100 W from 2 to 40 GHz."

Many of the advances in MPM technology can be traced back to the codes developed by Levush and his team. Codes, such as the "Christine" code (named after the daughter of Thomas Antonsen, the team's chief theoretician) for analyzing the behavior of a TWT helix, and the "Michelle" gun-collector code (named after Levush's daughter), will help to solve complex problems in the development of vacuum devices. The codes must predict not only first-order EM field effects, using finite-element-analysis (FEA) techniques, but also the effects of secondary electron emissions, which are difficult to predict and can greatly alter the performance of a vacuum electronics device. Levush notes that these codes are developed in stages: "The first version of Christine was one-dimensional; to make it more powerful, we needed to add an optimizer." The code was useful in optimizing helix efficiency by varying the helix pitch, using 11 points along the helix as optimization points. A three-dimensional (3D) version of the code is being developed to describe what happens to the beam and to achieve further refinement in the vacuum device. Levush adds that the code was validated through measurements at Northrop Grumman.

The NRL is also using the codes, combined with mathematical programs such as MATLAB, to model the performance of different modulation approaches in high-data-rate communications links. "Software codes are the key to advances in vacuum electronics in the next five years," states Levush, pointing to the NRL's many development programs for gyro-klystrons, gyro-TWTs, and free-electron lasers (FELs), which are useful at millimeter-wave through submillimeter-wave frequencies.

What has been reported here is a mere sampling of the work being performed at the NRL's Vacuum Electronics Branch, and of the NRL in general (see sidebar). It is hoped that future articles will explore some of the activity in various other branches of the NRL's Electronic Science and Technology Division. For more information on the NRL, contact: Naval Research Laboratory, 4555 Overlook Ave. SW, Washington, DC 20375-5320; Internet: http://www.nrl.navy.mil. ••

Acknowledgments
The author would like to acknowledge the efforts of Dick Thompson, the NRL's Public Affairs Officer, and the hospitality of the NRL's Robert Parker, Baruch Levush, Dick Abrams, and their associates for making this story possible.

For more information on this topic, visit us at **www.mwrf.com**

Reverse-path amp serves CATV

The model RF3320 reverse-path, programmable-gain, integrated-circuit (IC) amplifier is designed for use in cable modems, set-top boxes, and pay-per-view systems. Its 5-to-100-MHz operating range of covers current and proposed US and European cable-television (CATV) systems. The amplifier has a maximum output power of 63 dBmV and its programmable voltage gain spans a 50-dB range from −22 to +28 dB. The amplifier is serially programmable, and output control is selectable in 1-dB steps via a three-wire digital bus for compatibility with existing standard baseband chip sets. Other features include transient-switching characteristics that are compatible with DOCSIS and proprietary cable-modem standards, sleep and shutdown modes, and differential input and output. The amplifier operates from a single +5-VDC power supply and it typically draws 130-mA current at high gain, 90-mA current at low gain, 31 mA in transmit-disable mode, 3 mA in sleep mode, along with 0.05 mA in shut-down mode. It is housed in an SSOP16-EPP package. **RF Micro Devices, Inc., 7625 Thorndike Rd., Greensboro, NC 27409; (336) 664-1233, FAX: (336) 664-0454, Internet: http://www.rfmd.com.**

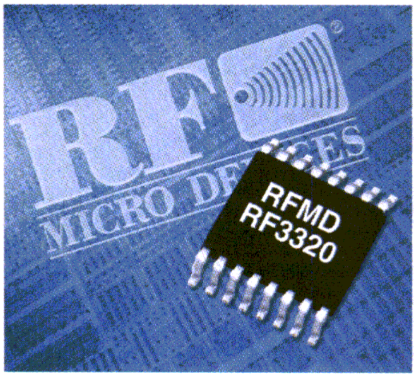

CIRCLE NO. 113 or visit www.mwrf.com

Mini OXCOs cover 4.9 to 90 MHz

The 270 series oven-controlled crystal oscillators (OCXOs) drop into a standard European CO-08 footprint and are available at frequencies from 4.9 to 90 MHz. Using a full-size TO-8 quartz resonator, the oscillators perform to the stability required for applications such as Stratum II and IIIe, Global Positioning System (GPS), and time-division-multiple-access (TDMA) personal communication services (PCS). The oscillators have a thermal-stability range of 2^{-10} to 5^{-9} over an ambient-temperature range of –30 to +70°C. Warm-up power consumption is typically 5.5 W, and steady-state power consumption is 1.7 W. After 1 second, stability is 2^{-12}. After a 10-minute warmup period, stability is typically 5^{-9}. Typical RF output is +9 dbm ±2-dB sinewave into a 50-Ω load with –30-dBc harmonics and –80-dBc spurious levels. Each oscillator operates from a +12-VDC power supply and is housed in a hermetically sealed package measuring 1.423 × 1.071 × 0.765 in. (3.614 × 2.720 × 1.943 cm). **Milliren Technologies, Inc., Two New Pasture Rd., Newburyport, MA 01950; (978) 465-6064, FAX: (978) 465-6637, Internet: http://www.mti-milliren.com.**

CIRCLE NO. 115 or visit www.mwrf.com

Software augments system analyzers

The Guided Scalar Measurement software allows unskilled operators to perform complex or repetitive measurements on the company's 6800-series scalar and system microwave analyzers. The software allows the instruments to be customized for specific applications, including short-run production measurements on components, assemblies, and subsystems, cable and waveguide installation measurements in ships and aircraft, and radio-link feeder testing. The software uses a series of screens to guide the operator through several tasks, including selecting pre-defined measurements or tests such as insertion loss, return loss, or fault location, setting relevant measurement options for accessories, calibrating the instrument, connecting the device under test, and carrying out the desired measurement(s). **IFR Systems, Inc., 10200 West York St., Wichita, KS 67215-8999; (316) 522-4981, FAX: (316) 524 2623, Internet: http://www.ifrsys.com.**

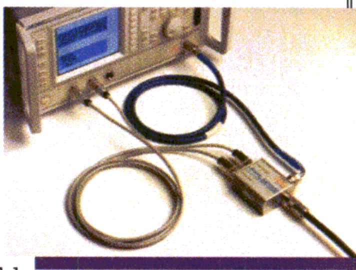

CIRCLE NO. 114 or visit www.mwrf.com

Test chamber boasts small size, low cost

The GTEM line of test cells for electromagnetic-compliance (EMC) testing claims to be an affordable alternative to larger, more expensive test chambers for testing pagers, mobile phones, and other commercial electronic products. The standard GTEM test cells can perform radiated (emissions) and immunity testing in a single, fixed, shielded environment at frequencies from DC to 18 GHz. The GTEM "Lite" version has a narrower test frequency range (DC to 5 GHz), but also is less costly, smaller, and requires less cabling. **Schaffner EMC, Inc., 52 Mayfield Ave., Edison, NJ 08837; (732) 225-9533, FAX: (732) 225-4789, Internet: http://www.schaffner.com.**

CIRCLE NO. 116 or visit www.mwrf.com.

Ericsson Stumbles In Wireless

Telecommunications giant LM Ericsson (Stockholm, Sweden) reported a mixed bag of business activity for the second quarter ending June 30. The upside was a quadrupling of net income to $1.1 billion (10.2 billion kroner) on sales of $7.4 billion, an increase of 28 percent over a year earlier. This was due mostly to rising sales in its wireless equipment group. But the good news was offset by disappointing performance in the consumer products division—20 percent of the business—which produces the company's handsets. While sales climbed to $1.5 billion, an increase of 29 percent, and 40 percent over the same period last year, the division posted an operating loss of more than $250 million. As the world's third-largest mobile-phone manufacturer, Ericsson is a major factor in this rapidly growing market.

According to company officials, the immediate problem in handsets stems from a parts shortage that resulted from a fire in a New Mexico factory run by Royal Philips Electronics, a major parts supplier to Ericsson. That factory supplies application-specific integrated circuits (ASICs), an important component of the wireless phone. The company also stated that they expect the shortfall to persist into the fourth quarter, continuing to affect deliveries, inventories, and profits. In the interim, the company will manufacture the ASICs in its own Ericsson Microelectronics facility.

A deeper problem for the consumer-products group is the changing product mix in the handset market. Currently, consumer sentiment is shifting toward less-expensive (entry-level) mobile phones as it moves away from more-sophisticated models. This has left Ericsson with an uncompetitive mix that will force it to close unprofitable product lines, focus on fewer products, and streamline manufacturing. News of the difficulties in the handset business rippled through the stock market where Ericsson shares fell by $2.75 to close at $19.813 on July 21.

Trying to regroup, the company has set up a special unit to develop cheaper mobile phones. An organization dedicated to entry-level phones has been established in Asia. Apparently the strategy is to produce higher volumes of less-expensive phones. Ericsson also wants to cut costs by moving production to low labor-cost countries. It has taken this step by opening new facilities in Mexico, Estonia, and Hungary.

The good news for the world's biggest supplier of mobile networks is that its second-quarter sales to network operators and service providers rose 29 percent to $5.1 billion. This is being driven by strong demand for new technology that allows mobile phones to access the Internet. ••

CIRCLE NO. 277

Contracts

Granada Media—Formed a joint venture company, Liverpool FC Broadband, with English soccer club Liverpool FC. Under terms of the agreement, Granada will acquire a 50-percent stake in the joint venture for 20 million pounds (approximately $30 million US) and will develop entertainment, e-commerce, education, and personalized services for the new company. The services will be delivered to home and personal devices such as wireless-application-protocol (WAP) phones, personal digital assistants (PDAs), digital set-top boxes, and personal computers (PCs).

RIFOCS Corp.—Was awarded a $14.1 million contract by the Space and Naval Warfare Systems (SPAWAR) Center in San Diego, CA (SSC San Diego). As prime contractor, RIFOCS will manufacture, test, and ship up to 270 units plus spares of the Global Positioning Fiber Optic Antenna Link (GPS FOAL) subsystem over a five-year period.

Harris Corp.—Has been awarded an $11 million contract from the Singapore Ministry of Defense (MOD) for its Falcon™ II family of tactical radio equipment. The Falcon II family will provide Singapore with a communications system that allows soldiers to communicate over greater range with optional frequency extensions down to the very-high-frequency (VHF) band which reduces the number of radios that a soldier is required to carry.

Sanders—Has received a $5.7 million firm fixed-price contract from the US Navy for five AIMS antenna-group systems and associated spares. Designated the OE-120/UPX, the AIMS antenna group is a part of the AIMS—an acronym for Air Traffic Control Radar Beacon System; Identification-friend or foe (IFF); MKXII; System.

Motorola, Inc.'s Network Solutions Sector (NSS)—Was awarded a $27 million expansion contract by Telkomsel, an Indonesian cellular network operator, to upgrade Indonesia's nationwide GSM-900 cellular network. The deal includes hardware, software, and services that are to be awarded in stages.

COMSAT Mobile Communications (CMC)—Signed a four-year agreement with Silversea Cruises Ltd. to provide global voice and data communications for Silversea's fleet of cruise ships.

EMS Technologies, Inc.—Announced that ASTRUM (formerly Matra Marconi Space) has selected EMS through its Space & Technology Group in Montreal, Quebec, Canada, for a contract valued at approximately $25 million US to supply three combined transmit/receive antenna feeds for the INMARSAT Broadband Global Area Network (B-GAN) program.

Fresh Starts

Interad Ltd.—Has moved from Gaithersburg, MD to its new facility in Melfa, VA. Interad manufactures RF antennas and receivers.

G.A.L.I.M. Wireless—Has launched its new website. The website's address is http://www.galimwireless.com. G.A.L.I.M. manufactures millimeter and microwave filter components.

Universal Microwave Corp.—Has named three firms to represent its voltage-controlled oscillators (VCOs) and synthesizers in the US. Trionic Associates will cover Long Island, Metro New York, and New Jersey. Youngewirth & Olenick will cover Arizona and New Mexico while dBm Technical Sales will cover Massachusetts, New Hampshire, Maine, Vermont, Connecticut, and Rhode Island.

Monitor Products Co., Inc.—Has been acquired by Zimmerman Holdings, Inc. (ZHI) of Pasadena, CA. ZHI is a private investment firm specializing in the acquisition, management, and growth of middle-market manufacturing companies.

RF Micro Devices, Inc.—Announced the opening of a new 6000-sq.-ft. engineering design center in the Phoenix, AZ area.

Harmonic, Inc.—Has completed its acquisition of the DiviCom business of C-Cube Microsystems, Inc. Harmonic, including the DiviCom business, will provide open-systems solutions for delivering video, voice, and data over cable, satellite, telco, and wireless networks.

Fujitsu Compound Semiconductor, Inc. (FCSI)—Has named S&S Technology, Inc. of Northridge, CA as its new sales representative to sell Fujitsu's microwave products in its southern California territory, which is south of and includes San Luis Obispo, Kern, and San Bernadino counties.

Tropian, Inc.—Has closed $25 million in third-round financing from two leading semiconductor companies and three venture-capital firms. Tropian received a $10 million strategic investment from two wireless industry semiconductor-system companies—Infineon Technologies AG and TriQuint Semiconductor, Inc. In addition, $15 million in financing was received from Tropian's Silicon Valley-based VC investor group.

Telcordia Technologies, Inc. and SignalSoft Corp.—Announced an agreement to integrate select software applications and platforms to enable wireless network operators worldwide to offer their subscribers personalized new m-commerce services that help capitalize on the revenue-generating potential of mobile location. The agreement will also help operators in the US meet Federal Communications Commission (FCC) mandates for 911 Phase I and II compliance.

Atmel Corp.—Announced that it is collaborating with RF Micro Devices, Inc. to provide reference designs based on the IEEE802.11b, 11-Mb/s wireless local-area-network (WLAN) standard. The reference designs use RF Micro Devices' 2.4-GHz chip set and Atmel's family of fast-Virtualnet™ ARM®-based media-access controllers (MACs), which run the network protocol and provide a variety of interfaces to the host platform.

Broadcom Corp.—Has signed a definitive agreement to acquire Innovent Systems, Inc., a firm involved in the development and commercial integration of RF integrated circuits (RF ICs) for short-range wireless data communications, including the world's first fully integrated RF transceiver in pure digital complementary metal-oxide semiconductor (CMOS).


High Performance
Fractional-N
SYNTHESIZER
100 to 3000 MHz
Very Small Step Sizes
Low Phase Noise
SMC
FN3000 810-830
Fastest
FN3000 series
SMC
FN4000 869
Faster
FN4000 Series
SMC
FJPLH-1710
Fast
FJPLL/FJPLH Series
For additional information,
contact Synergy's Sales and Application team.
201 McLean Blvd., Paterson, New Jersey 07504
Phone: (973) 881-8800 Fax: (973) 881-8361
E-mail: sales@synergymwave.com
Visit our web site at http://www.synergymwave.com
SYNERGY
MICROWAVE CORPORATION
CIRCLE NO. 237

Cidera, Inc.—Richard J. Hanna to chief executive officer (CEO); formerly president of Telligent International.

Calibre, Inc.—Dan McKay to director of system architecture; formerly software and wireless protocol architect and software-development manager for IBM's Wireless Communications Group (WCG).

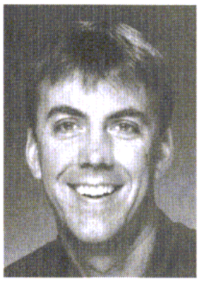
McKAY

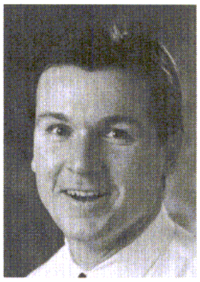
COMERFORD

Alpha Industries—Mark Comerford to general manager of the Discrete Semiconductor and Passive Integrated Circuit Division; formerly business unit director for Discrete Products.

Tropian, Inc.—Michael A. Kinser to vice president of sales and marketing; formerly senior vice president of marketing for Telular Corp.

Davidson Optronics—Tollis Deslis to vice president and chief operating officer (COO); formerly senior optical designer engineer at JPL.

SmartLynx, Inc.—Eugene (Skip) Vish to executive vice president of sales and marketing; formerly the director of worldwide sales for the alternate channel for selling hardware-description-language (HDL) tools. Also, Joe Gamache to vice president of engineering; formerly worked as an independent software-systems consultant.

BMI, Inc.—Jim Sturm to director of marketing for BMI and its two divisions—Metronic Shields and Metronic Contacts; formerly director of marketing at Essilor Lenses.

Monitor Products Co., Inc.—Dave Abrams to president and chief executive officer (CEO); formerly executive vice president of Zimmerman Holdings, Inc. (ZHI).

Sanders—Dr. Glenn Thoren to director of intellectual-property exploitation; formerly director of technology licensing.

Circuits Processing Technology (CPT)—Dr. Terry Brog to vice president of operations; formerly director of manufacturing at Coherent Technologies.

Paragon Innovations—Michael P. Caranfa to vice president of sales; formerly director of sales Digital Speech Systems, Inc.

Andrew Corp.—Alan Haase to group president for Communication Products; formerly vice president of Terrestrial Microwave (TMW) Products.

Richco, Inc.—Rick Streicher to president; formerly vice president of Sealing Systems, Visibility, and Systems Protection Products at Federal-Mogul.

appli-tec, Inc.—Thomas W. Campbell to sales representative for Northern California; formerly chief executive officer (CEO) and senior account manager at BC Marketing.

ShareWave, Inc.—Kevin Daroca to vice president of worldwide sales; formerly employed in executive positions with Allayer Technologies.

Microwave Instrumentation Technologies, LLC—Isaac A. (Ike) Prather to director of human resources; formerly worked as a human resources consultant.


PRATHER

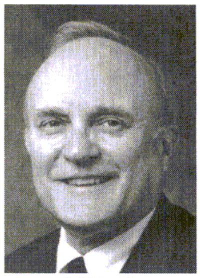
PETRINI

Communications & Power Industries (CPI)—Bart F. Petrini to president and chief executive officer (CEO); formerly employed as the executive vice president and general manager of the Electronic Device Group of Richardson Electronics.

ETL SEMKO, Americas Division of Intertek Testing Services (ITS)—Carl E. Felts to technical director for the West region; formerly employed as the director of compliance engineering and general manager for EMC Technology Services (EMC/TS).

RF LDMOS

Move Up to the Next Generation with Motorola

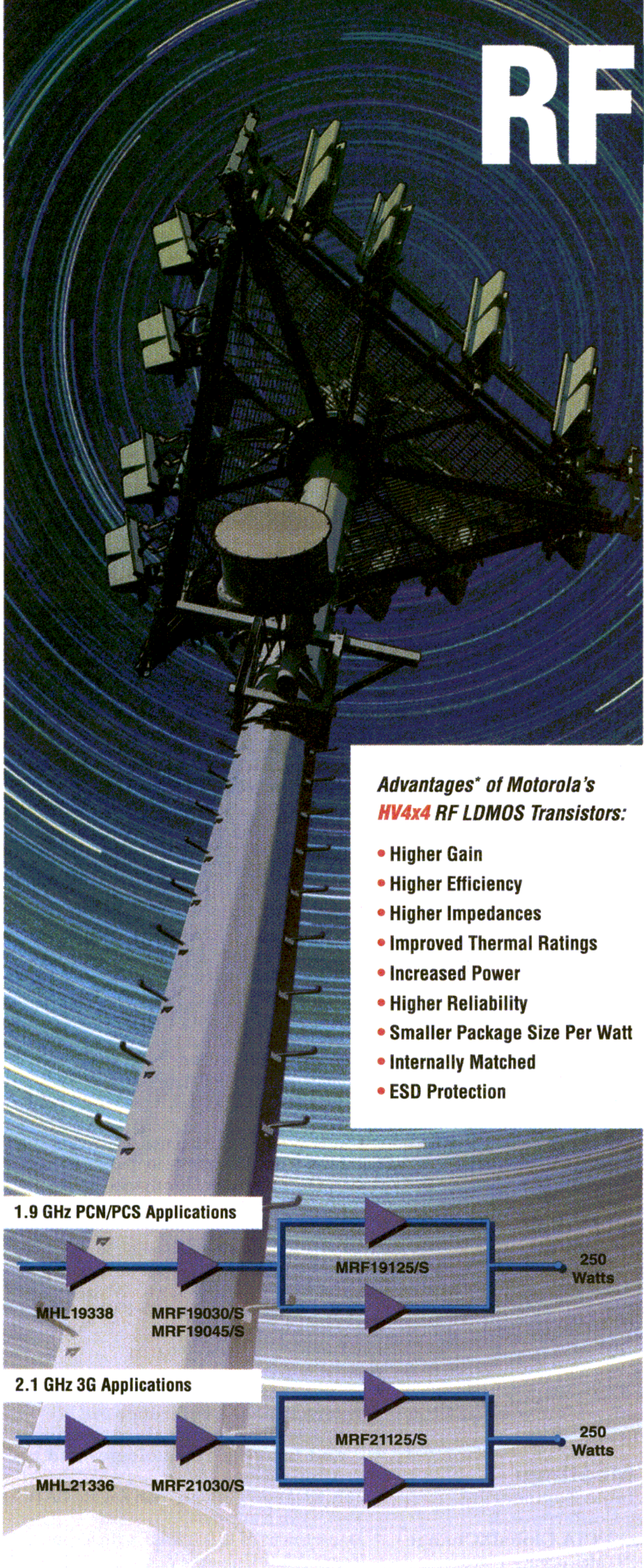

As digital standards increasingly dominate the wireless communication market, Motorola's RF LDMOS continues to be the industry's technology of choice. And, Motorola continues to develop and improve its patented RF LDMOS design and has recently extended performance on new 4th generation RF LDMOS products. The newest product introductions incorporate the latest process improvements and the most advanced technology. With a dedicated business group for RF & Microwave products and services, local market resources for support, plus one of the largest RF inventories in the world, Avnet Electronics Marketing is uniquely positioned to be your source for RF LDMOS products from Motorola.

DigitalDNA™ from Motorola

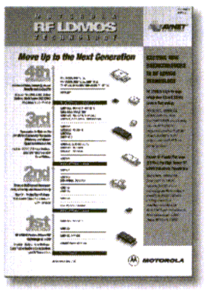

For a copy of Motorola's RF LDMOS Selector Guide, visit our Web site at www.em.avnet.com/rfm/motldmos.html or call **1-800-261-9602 ext. 302.**

IN STOCK AT

AVNET® electronics marketing

* Compared to previous generations of Motorola RF LDMOS

CIRCLE NO. 234

Short Courses

Fundamentals of Data Communication
October 2-4 (Madison, WI)
University of Wisconsin-Madison
Department of Engineering Professional Development
Madison, WI 53706
Katie Peterson
(800) 462-0876, FAX: (608) 263-3160
e-mail: custserv@epd.engr.wisc.edu.
Internet: http://epd.engr.wisc.edu/

Software Radio Design
October 9-11 (Los Angeles, CA)
UCLA Extension Department of Engineering, Information Systems and Technical Management—Short Courses
Los Angeles, CA 90024-2883
(310) 825-3344, FAX: (310) 206-2815
e-mail: mhenness@unex.ucla.edu.
Internet: http://www.uclaextension.org/shortcourses

Fiber Optic Training
October 10-12 (Pittsburgh, PA)
National Technology Training, Inc.
P.O. Box 4558
Englewood, CO 80155-4558
Alex Black
(800) 922-2820, FAX: (303) 649-9930
Internet: http://www.nttinc.com

Mobile Communications and Wireless Networks
October 10-13 (Washington, DC)
Learning Tree International
Reston, VA 20190-5630
(800) 843-8733
Internet: http://www.learningtree.com

Network Fundamentals
October 10-19 (Lisle, IL)
Telcordia Technologies
Lisle, IL 60532-3198
(800) 832-2463, FAX: (630) 960-6230
e-mail: www.800teachme.com
Internet: http://www.800teachme.com

Principles of Modern Radar
October 30-November 3 (Atlanta, GA)
Georgia Institute of Technology-Continuing Education
Atlanta, GA 30332
(404) 385-3502, FAX: (404) 894-7398
e-mail: conted@gatech.edu
Internet: http://www.conted.gatech.edu.

Fundamentals of Cellular and PCS Wireless Communications
November 13-15 (Madison, WI)
Department of Engineering Professional Development
University of Wisconsin-Madison
Madison, WI 53706
Katie Peterson
(800) 462-0876, FAX: (608) 263-3160
e-mail: custserv@epd.engr.wisc.edu/
Internet: http://epd.wisc.edu/

Meetings

Wireless/Portable Engineering Technology Conference & Showcase at PCIA GlobalXChange
September 26-29 (McCormick Place, Chicago, IL)
Penton Media, Inc.
611 Route 46 West
Hasbrouck Heights, NJ 07604
(888) 947-3734, FAX: (201) 393-6297
e-mail: wirelessreg@penton.com
Internet: http://www.WirelessPortable.com

IEEE Broadcast Technology Society 50th Annual Broadcast Symposium (Broadcasting for the New Millennium)
September 27-29 (Sheraton Premiere at Tyson's Corner, Vienna, VA)
IEEE Broadcast Technology Society
445 Hoes Lane
Piscataway, NJ 08855-1331
Mary Clemente
(732) 562-5350, FAX: (732) 981-1203
e-mail: m.e.clemente@ieee.org.

CTIA Wireless I.T. 20000
October 16-18 (Santa Clara Convention Center, Santa Clara, CA)
The Cellular Telecommunications Industry Association (CTIA) and the Wireless Data Forum
Internet: http://www.wirelessIT.com

ICSPAT 2000 (International Conference on Signal Processing Applications and Technology)
October 16-19 (Adam's Mark Hotel, Dallas, TX)
CMP Media, Inc.
Joan Watkins
(800) 789-2223
e-mail: dspworld@cmp.com
Internet: http://www.icspat.com

AMTA 2000—Antenna Measurement Techniques Association
October 16-19 (Philadelphia, PA)
AMTA c/o ORBIT/FR
Horsham, PA 19046
Irene Honeycutt
(215) 674-5100, FAX: (215) 674-1102
e-mail: irene@orbitfr.comn
Internet: http://www.amta.org.

Access Technologies 2000
October 24-26 (Hotel Fira Palace, Barcelona, Spain)
Vision in Business Ltd.
London WC2H 7BT, England
+44 (0)20 7839 8391, FAX: +44 (0)20 7839 3777
e-mail: booking 1@visionbusiness.com
Internet: http://www.visionbusiness.com

CDMA Americas Congress 2000
October 26-27 (Sheraton Harbor Island, San Diego, CA)
CDMA Development Group
575 Anton Blvd., Suite 560
Costa Mesa, CA 92626
(888) 888-CDMA, (714) 545-4601
e-mail: cdg@cdg.org
Internet: http://www.cdg.org

Call for Papers

International Conference on Subsurface and Surface Sensing and Imaging Technologies and Applications III
July 29-August 3, 2001 (San Diego, CA)
Prof. Cam Nguyen
Department of Electrical Engineering
Texas A&M University
College Station, TX 77843-3128
(979) 845-7469, FAX: (979) 845-6259
e-mail: cam@ee.tamu.edu
Abstract Deadline: December 18, 2000

GaAs attenuator processes microwave signals

A direct-analog method of processing microwave signals offers a simpler, faster, and lower-cost alternative to downconversion and digital-signal processing (DSP). To improve the analog method, Xu Tao, Sun Xiaowei, *et al.* of the Shanghai Institute of Metallurgy (Shanghai, People's Republic of China) have developed a new type of gallium-arsenide (GaAs) voltage-controlled vector attenuator and a vector attenuator, in monolithic-microwave-integrated-circuit (MMIC) form. The novel aspect of the voltage-controlled attenuator design is its ring structure, using metal-semiconductor-field-effect transistors (MESFETs) in place of the traditional PIN diodes. DC voltage levels are used to control the two pairs of opposing MESFETs in the ring (a bridge circuit), effectively determining the phase (in or out) of the output signal. The voltage-controlled attenuator (a biphase device) changes only the amplitude of a signal, so the authors have developed the vector-attenuator MMIC for applications which have a complex component in the signal. See "A Novel GaAs MMIC Vector Attenuator," *Microwave and Optical Technology Letters*, July 20, 2000, Vol. 26, No. 2, p. 96.

Fundamental grounding and shielding principles revisited

As most engineers know, one of the most difficult aspects of completing a design is getting it to work in a noisy environment (i.e., every environment) and building in features that ensure human safety. Solving these two problems is more often art than science, but they are based on sound engineering principles. A review of grounding and shielding techniques is offered by Kim Fowler of Stimsoft, Inc., (Baltimore, MD) in a two-part article which covers these subjects in straightforward, on-the-job language. Fowler will complete the series with a third article on electrostatic discharge (ESD), and a final article summarizing the series and providing basic design tips and techniques. The first article highlights the overall problem of electromagnetic interference (EMI) and the coupling mechanisms by which it disrupts circuit operation (conductive, capacitive, etc.). The second article examines grounding, including the problem of ground loops, which introduce noise into the signal circuit. See "Grounding and Shielding, Part 1—Noise," and "Grounding and Shielding, Part 2—Grounding and Return," *IEEE Instrumentation & Measurement Magazine*, June 2000, Vol. 3, No. 2, p. 41.

Moore's Law rides again—this time in communications

Every engineer who designs with digital integrated circuits (ICs) has probably heard of Moore's Law, first proposed by Gordon Moore, co-founder and former CEO of Intel. In 1965, Moore predicted that the number of transistors in an IC doubles every 12 months, and later revised this number to between 18 and 24 months. The Law has been remarkably accurate for semiconductor technology over the past 35 years, and it may have found a new application, according to Charles A. Eldering and Mouhamadou Lamine Sylla of Telecom Partners Ltd. (Washington, DC) and Jeffrey A. Eisenbach of the Progress and Freedom Foundation (Washington, DC). They believe that Moore's Law can be applied to communications bandwidth—the historical rate at which the bandwidth available to residential subscribers has grown. Using Moore's Law, they hypothesize that analog modem technology has exhibited a regular pattern of doubling throughput approximately every two years. Then they extrapolate, as Moore did, to estimate the rate at which digital-subscriber-line (DSL) and cable-modem will evolve and be deployed. See "Is There a Moore's Law for Bandwidth?," *IEEE Communications Magazine*, October 1999, Vol. 37, No. 10, p. 117.

Direct-conversion receiver aims at 3G CDMA systems

A prototype chip set for the third-generation (3G) wideband-code-division-multiple-access (WCDMA) wireless scheme to be used in Europe and Japan has been developed by Aarno Pärssinen, Jarrko Jussila, *et al.* at the Electronic Circuit Design Laboratory, Helsinki University of Technology (Helsinki, Finland). Architecturally, the design (four chips) is a direct-conversion receiver consisting of signal-processing circuitry [including analog-to-digital converters (ADCs)] which suppresses the adjacent channel and other interferers passing through the preselection filter before digital-signal processing. The receiver (Rx) achieves −114-dBm sensitivity for 128-kb/s data at a 4.096-Mc/s spreading rate. It is intended for use in mobile terminals and base stations. See "A 2-GHz Wide-Band Direct Conversion Receiver for WCDMA Applications," *IEEE Journal of Solid-State Circuits*, December 1999, Vol. 34, No. 12, p. 1893.

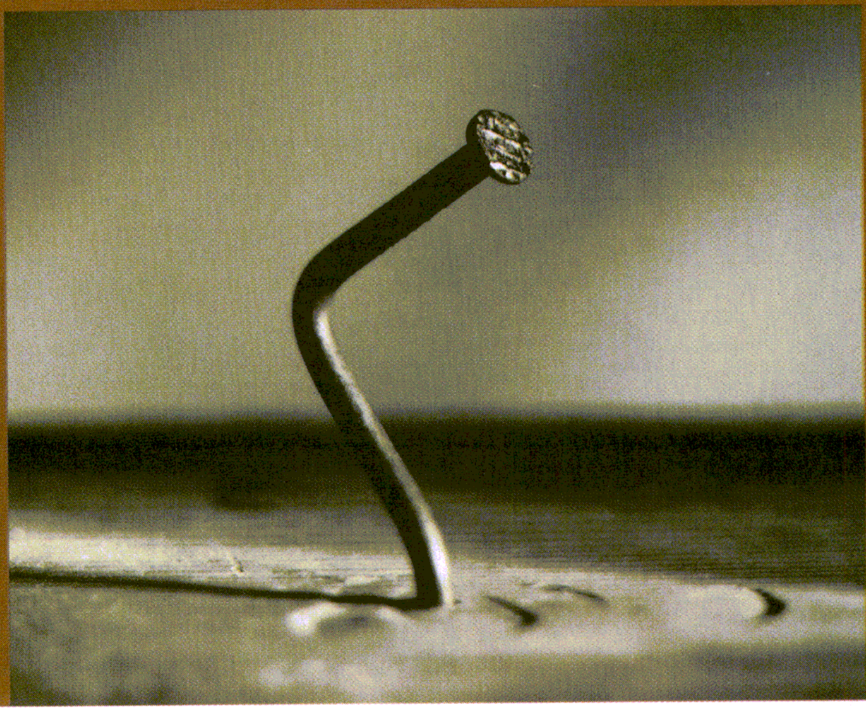

CIRCLE NO. 264

Mathematical Recipe Calculates The Response Of Dipole Antennas

A simplified method is presented for calculating the impulse performance of electrically long dipole antennas.

Dr. Dieter R. Lohrmann

Naval Research Laboratory, 4555 Overlook Ave. S.W., Washington, DC 20375-5339; (202) 767-0241, FAX: (202) 404-7690, e-mail: Lohrmann@nrl.navy.mil.

THERE has been recent interest in the pulse performance of dipole antennas. Traditionally, this problem is treated theoretically by using known steady-state periodic solutions in the frequency domain and calculating the real-time pulse response of the dipole by Laplace Transform. While this method provides technically useful solutions, it falls short in explaining certain effects observed in experiments. The reason for this is that the solutions in the frequency domain do not include the frequencies at zero and infinity. An example of this is a battery connected to a long dipole. "Long" in this context means that the rise time of the battery current is short compared to the time it takes the wave to travel to the end of the antenna, get reflected, and return to the source.

The work by O. Einarsson[1] and T.T. Wu[2] gives the exact solution, using Maxwell's Equations, for the current on a long cylinder-type dipole antenna resulting from a voltage step at the input.

Several features of these solutions are remarkable in that they are not intuitively obvious:

1. At the first moment after application of the voltage step, the antenna exhibits a zero-input impedance (i.e., the current is infinite).
2. The current decays with a time constant which depends only on the radius, a, of the antenna cylinder and, of course, not on the length of the antenna. The decay time decreases with decreasing diameter.
3. After a time which is large compared to a/c, where c is the speed of light, the current at the input decays proportional to 1/log(t).
4. The current waveform created at the input travels down the antenna with the speed of light, without any change of shape. This is remarkable because it might be expected that the current waveform would be attenuated due to radiation loss while traveling along the dipole, but this is not the case. Figure 1 depicts the current at the input of the antenna following the application of a +2-VDC step at the input 1. In Ref. 1, a detailed table of the current versus normalized time is also provided. The ordinate in Fig. 1 depicts the current at the input in Amperes[1], the abscissa depicts the normalized time,

$$v = (1/a) * \sqrt{(c*t)^2 - z^2} \qquad (1)$$

where:

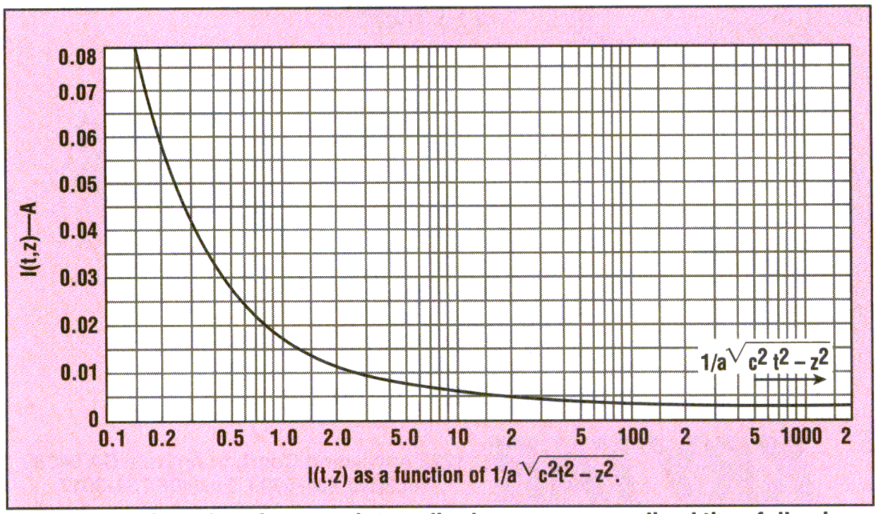

1. This graph is a plot of current into a dipole versus normalized time following a +2-VDC step input to the dipole.

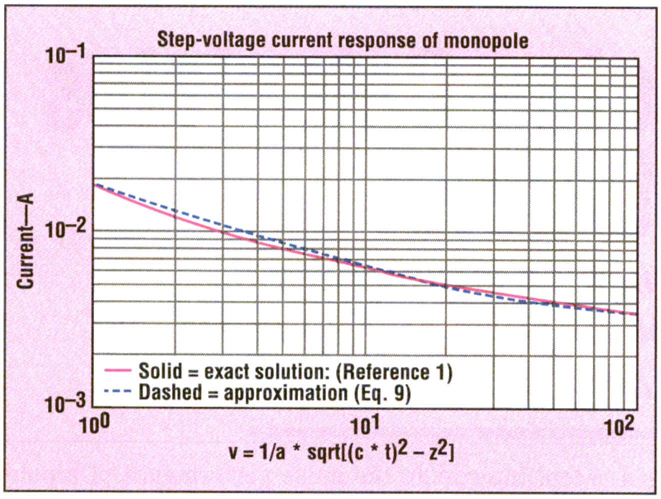

2. An input step of +1 VDC to a monopole antenna produces the current response illustrated here. The solid line is the exact solution according to Ref. 1, while the dashed line is an approximation according to Eq. 9.

a = radius of the dipole cylinder, c = speed of light , and z = length coordinate on the dipole, starting at the feed point. Note that at the feed point, z = 0 and v = c/a* t.

The exact solution for the current is very complicated and therefore not well-suited to solving practical problems, such as accounting for the impedance of the source. For this reason, an attempt was made to model the input impedance of the antenna, simulating the accurate performance as closely as possible.

The antenna acts as a transmission line. However, since for a voltage-step input with zero rise time the current is infinite at time t=0, the input impedance of the antenna must be zero for infinite frequency. A transmission line with distributed series R and L and shunt G and C has this property only if the distributed inductance is zero. Therefore, the input impedance is modeled :

$$Z(j\omega) = \sqrt{R/(G + j\omega C)} \qquad (2)$$

In the following, instead of a dipole, consider a monopole over a conducting plane.

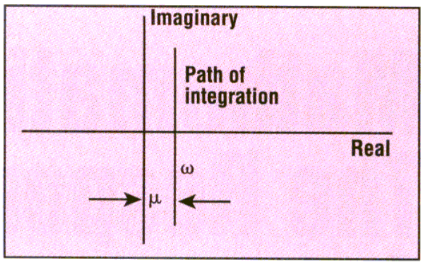

3. To calculate the current to a monopole, the integration path moves parallel to the imaginary axis at a distance μ from the axis with jω as the parameter.

Therefore, the input voltage is now a +1-VDC step instead of +2 VDC as in Ref. 1. The current is the same, and Z is the input impedance of the monopole. For a dipole, the input impedance is then 2Z.

The next step to investigate is how accurately the current resulting from a voltage step applied to Z will approximate the exact solution. For this purpose, the current versus time response is calculated by Inverse Laplace Transform and compared to the exact solution shown in Fig. 1, using the model of Eq. 2.

$$I(s) = V(s) / Z(s) \qquad (3)$$

V(s) = Vz/s is the voltage step in the frequency domain and Vz is the amplitude of the step. Then:

$$I(s) = Vz / s / Z(s) = Vz / (s * \sqrt{R / (G + s * C)}) \qquad (4)$$

And

$$I(t) = 1/(2*\pi j) \int_{s=-j\infty}^{s=j\infty} I(s)\, exp(s*t)\, ds \qquad (5)$$

The solution of this integral is:

$$I(t) = \sqrt{C/R}\{1/\sqrt{\pi * t} * exp(-b*t) + \sqrt{b} * erf(\sqrt{b*t})\} \qquad (6)$$

Here, b = G/C, and erf is the Gaussian error function:

$$erf(x) = 2/\sqrt{\pi} * \int_{\xi=0}^{\xi=x} exp(-\xi^2)\, d\xi \qquad (7a)$$

Replacing t by v and setting the length coordinate z = 0:
v = c/a*t , t = v*a/c.
Letting:

$$\text{Letting } p = \sqrt{(C*c)/(\pi * R * a)}, \quad q = a*b/c: \qquad (7b)$$

$$I(v) = p*\{1/\sqrt{v} * exp(-q*v) + \sqrt{\pi * q} * erf(\sqrt{q*v})\} \qquad (8)$$

The coefficients p and q are chosen so that I(v) resembles the exact function of the current shown in Fig. 1 as closely as possible. However, for practical purposes, it is sufficient to limit this range to 1≤v ≤ 100. Where v ≥ 1, consider only values of t which are greater than or equal to the time it takes an electromagnetic (EM) wave to travel the radius of the antenna tube. This appears to be a reasonable restriction because in practice, leads connecting the source to the antenna will not be shorter than the radius, a, of the antenna cylinder. Further, v≤ 100 means that only those times are considered which are less than or equal to the time it takes light to travel 100 radii. Depending on the particular application, the values of p and q can be chosen to emulate the curve for different regions of v. For the range chosen here it is found for 1≤ v ≤100 that:
p = 0.01799
q = 0.01094 .
With these values, the approximated curve and the exact curve are shown in Fig. 2. The error of the approximation is less than 10 percent.

Now Z(jω) can be expressed using the parameters of the dipole:

$$Z(j\omega) = 1/p * \sqrt{c/(a*\pi)} \sqrt{1/(q*c/a + j\omega)} \qquad (9a)$$

This can be re-written:

$$Z(j\omega) = 31.4\Omega * \sqrt{1/(0.01094 + a/c * j\omega)} \qquad (9b)$$

for the Monopole and

$$Z(j\omega) = 62.8\Omega * \sqrt{1/(0.01094 + a/c * j\omega)} \qquad (9c)$$

for the Dipole.

This is the approximated pulse input impedance of the dipole and the monopole, where 2a = diameter of the antenna cylinder and c = the speed of light. This is valid for the time a/c≤ t≤ 100a/c,

and until the wave is reflected at the end of the antenna reaches the feed point.

Now the current to the monopole can be calculated for any particular source impedance. However, since the source impedance can be a complicated function, the Inverse Laplace Transform correspondence may not be provided in any table, and therefore, numerical integration will be necessary. In order to show the procedure and the problems associated with that, I(t) will now be calculated by numerical integration of Eq. 5, using Eqs. 3 and 9b. The result must be the same as shown in Fig. 2, if everything goes according to plan.

Since it is not possible to numerically integrate to infinity, s = μ+jω must be terminated at some value, but at which value?

First, choose the path of integration in the right half of the complex plane, leaving all poles to the left of the integration path, (Fig. 3). The path is chosen to go parallel to the imaginary axis at distance μ, with jω the parameter.

It is a good idea to observe how the function of being integrated appears. It can be illustrated that the true

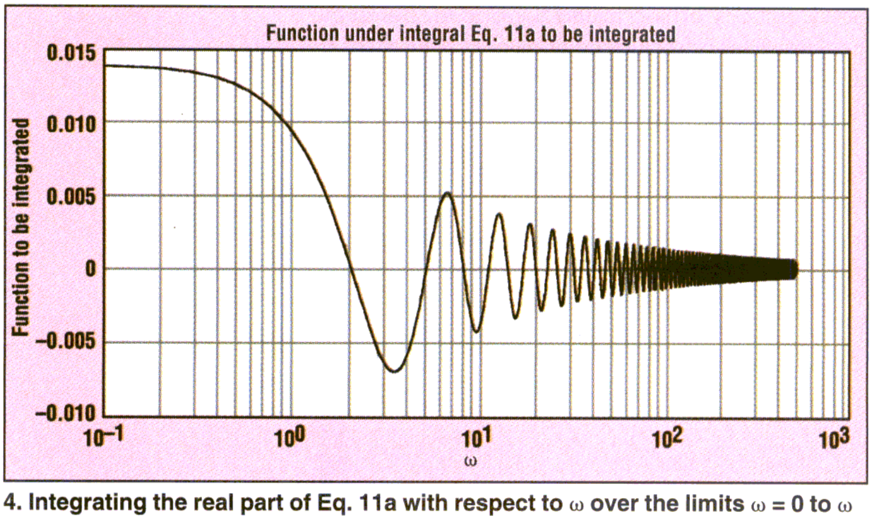

4. Integrating the real part of Eq. 11a with respect to ω over the limits ω = 0 to ω = ωmax yields this curve.

part of the function of ω under the integral is odd in regard to the integration parameter ω, and therefore, by integration from –ω to +ω, the imaginary portion of Eq. 5 is zero. This makes sense because the solution of the real-time current cannot be complex. Therefore, consider only the real portion of Eq. 5. Furthermore, because the real portion of the function under the integral is an even function of ω, integrate only from ω = 0 to ω = ωmax and multiply the result by a factor of two.

Replacing s in Eq. 4 and 5 by μ +jω, ds by jdω μ is constant on the path), and t by v*a/c,

$$I(t) = 4 * \sqrt{\pi} \,/\, p * exp(\mu * v) \int_{\omega=0}^{\omega=\omega max} ((\mu+q)^2 + \omega^2))^{1/4} / (\mu^2 + \omega^2)^{1/2} * cos(\omega * v + 1/2 * arctg(\omega / (\mu + q)) - arctg(\omega / \mu))\, d\omega \qquad (10)$$

The function under the integral of ω is plotted in Fig. 4 with μ=1/v. For large ω, the function oscillates with a period close to 2π, but the amplitude decays very slowly. Therefore, integration to very high values of ω would be required, which in turn would require excessive computation time. However, for large ω, the function is nearly periodic in:

ω*v = k *2π, with k being an integer.

A simple method of obtaining a good approximation is to evaluate the integral first to a multiple of kπ, then to (k+1) π, add both values and divide the result by two.

With μ=1/v , a value of k = 50....100 renders values which are accurate to a few percent.

Theoretically, μ can be chosen to be any real value greater than zero. However, because the factor exp(μ*v) appears in front of the integral in Eq. 10, that factor can become excessively large, which may cause problems in the numerical integration. Good values are obtained choosing μ so that 1/(μ*v) exp(μ*v) becomes a minimum , which is the case for μ*v=1 , or μ = 1/v.

In practice, the integral need not be programmed for integration by machine in the form of Eq. 10, but can be processed rather in the simpler form of Eq. 11a, provided that the machine can process complex arithmetic:

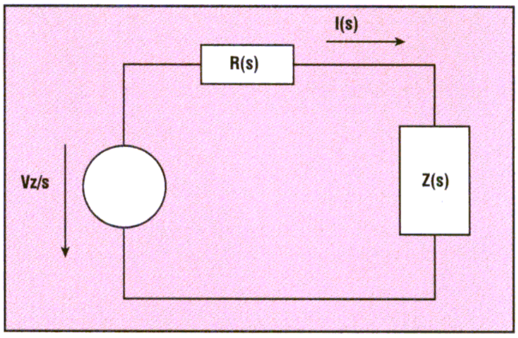

5. The circuit for determining the voltage response resulting from a current step depends upon the source impedance R(s) and the impedance of the monopole, Z(s).

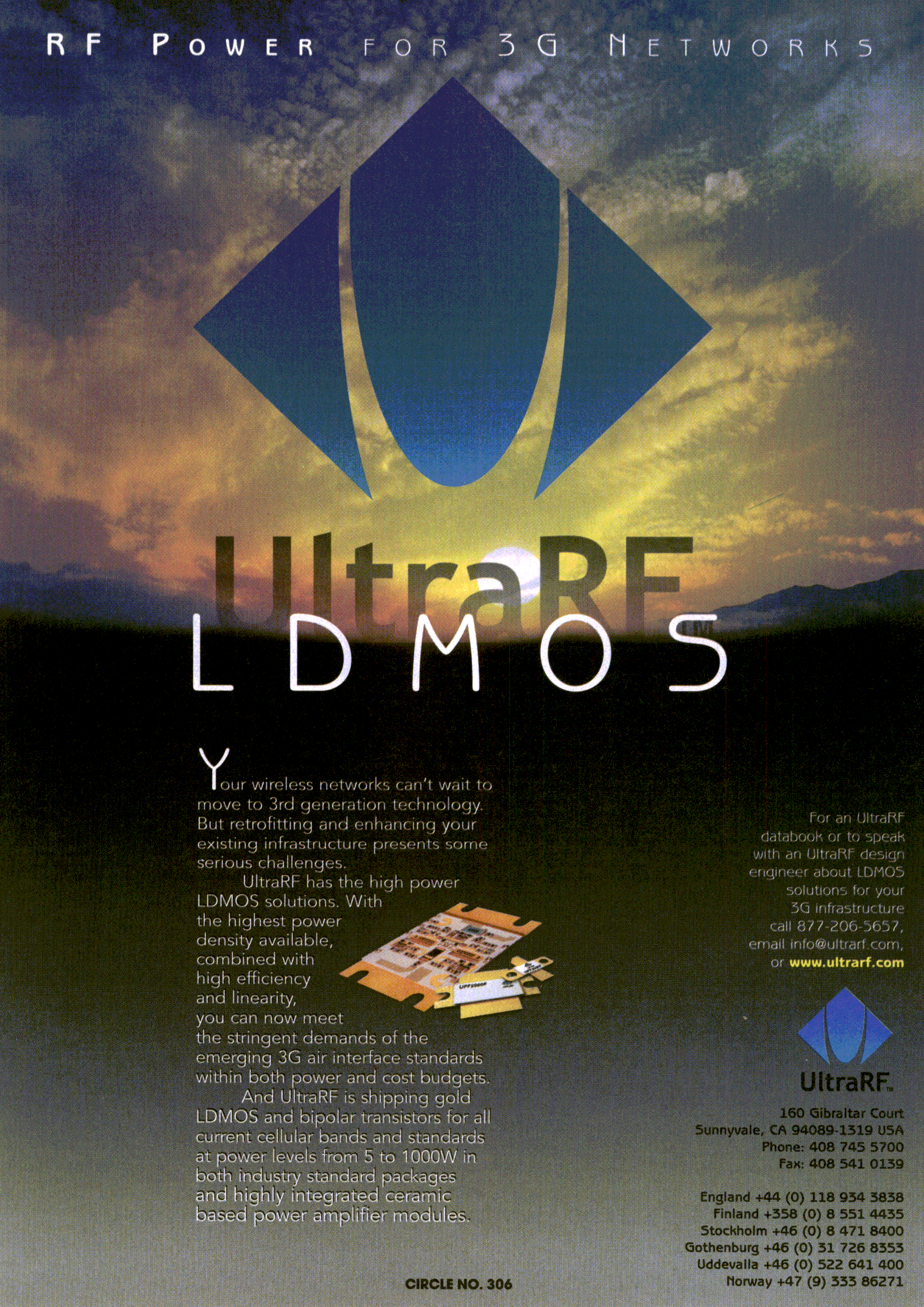
RF Power for 3G Networks
UltraRF™
LDMOS
Your wireless networks can't wait to move to 3rd generation technology. But retrofitting and enhancing your existing infrastructure presents some serious challenges.
UltraRF has the high power LDMOS solutions. With the highest power density available, combined with high efficiency and linearity, you can now meet the stringent demands of the emerging 3G air interface standards within both power and cost budgets.
And UltraRF is shipping gold LDMOS and bipolar transistors for all current cellular bands and standards at power levels from 5 to 1000W in both industry standard packages and highly integrated ceramic based power amplifier modules.
For an UltraRF databook or to speak with an UltraRF design engineer about LDMOS solutions for your 3G infrastructure call 877-206-5657, email info@ultrarf.com, or www.ultrarf.com
UltraRF™
160 Gibraltar Court
Sunnyvale, CA 94089-1319 USA
Phone: 408 745 5700
Fax: 408 541 0139
England +44 (0) 118 934 3838
Finland +358 (0) 8 551 4435
Stockholm +46 (0) 8 471 8400
Gothenburg +46 (0) 31 726 8353
Uddevalla +46 (0) 522 641 400
Norway +47 (9) 333 86271
CIRCLE NO. 306

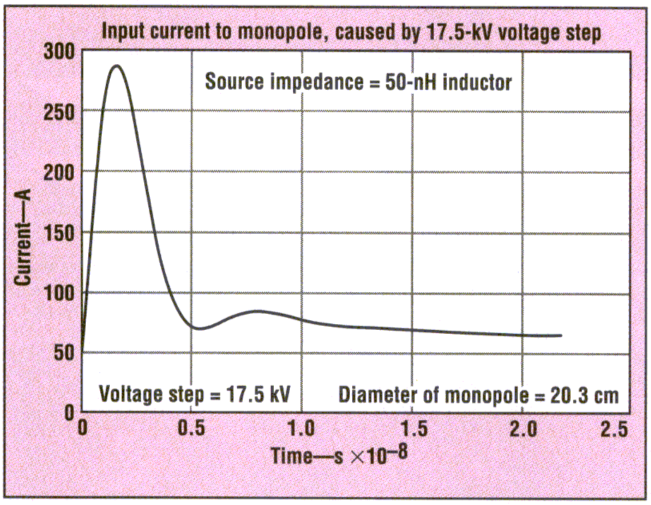

6. This curve illustrates the input current to a monopole when excited with a 17.5-kV voltage step having a source impedance of 50 nH.

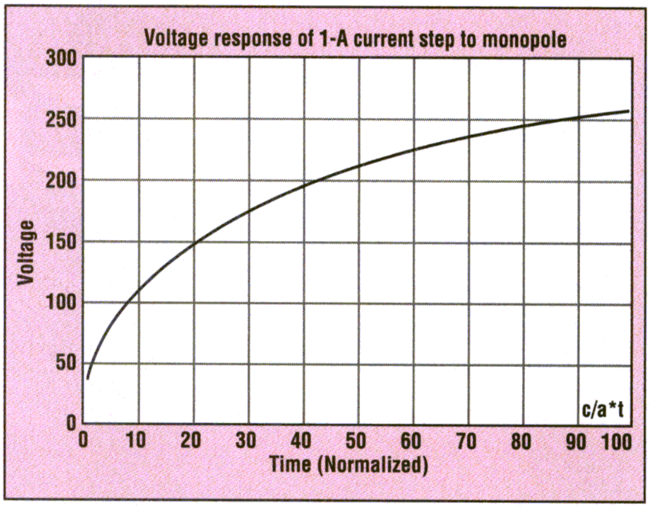

7. The voltage as a function of time (normalized) for a monople for a 1-A input current step is depicted by this curve.

$$I(t) = real\{1/\pi \int_{\omega=0}^{\omega=\omega max} I(\mu + j\omega) * exp$$
$$(\mu + j\omega) * t \; d\omega\} \qquad (11a)$$

with

$$with\; I(\mu + j\omega) = Vz / (\mu + j\omega) /$$
$$Z(\mu + j\omega), \qquad (11b)$$

and

$$Z(\mu + j\omega) = 1/\, p * \sqrt{c/(a*\pi)} *$$
$$\sqrt{1/(q*c/a + \mu + j\omega)} \qquad (11c)$$

Letting μ = 1/t , and

$$\omega max = k * \pi / t, \text{ with } k = 50...100 \quad (11d)$$

provides a satisfactory solution.

Taking the source impedance into account, Fig. 5 shows the arrangement.

$$I(s) = Vz / s / (\mathbf{R}(s) + Z(s)), \quad (12)$$

where:

$\mathbf{R}(s)$ = the impedance of the source, and Z(s) = the impedance of the monopole, as given in Eqs. 9a, 9b, and 9c.

Again, s is replaced in Eq. 12 by s = μ+jω and inserted into Eq. 11.

Figure 6 shows the calculated input current of a "long" monopole having a diameter of 20 cm, to which a source was connected which provided a 17-kV voltage step with 50-nH source impedance.

Next calculate the voltage response at the input to the monopole resulting from a current step. Let the current step Iz be: I(s) = Iz / s

Then,

$$V(s) = Iz / s * Z(s), \text{ and} \quad (13)$$

$$V(t) = real\{1/\pi * Iz * \int_{\omega=0}^{\omega=\omega max} Z(\mu + j\omega) * exp((\mu + j\omega) * t) / (\mu + j\omega)\, d\omega\} \quad (14)$$

The solution of this integral is given in closed form in Laplace Transform correspondence tables:

$$V(t) = Iz / (p * \sqrt{\pi * q}) * erf(\sqrt{q * v}), \text{ with } v = c / a * t \quad (15)$$

Figure 7 is a plot of V as function of the normalized time v=c/a *t for a current step of 1 A. Numerical integration (Eq. 11) provides the same result. The input impedance V/I at the first moment is 0 (the monopole is a short circuit at the beginning). The voltage then rises with a tangent perpendicular to the abscissa similar to the $\sqrt{t}$. The rise time is proportional to the diameter of the monopole cylinder. Going to infinity, the voltage also tends toward infinity (i.e., no finite asymptote).

It has been suggested that the current pole at t = 0 for a step voltage input results from capacitive effects at the feed point of the antenna. That is not the case, because calculation of the input voltage following a current step from Maxwell's Equations given in Ref. 3 yielded the same result as that of Ref. 4. There, it was assumed, a priori, that the current wave moves along the dipole unabated, with the speed of light. Since only the current appeared in the equations and not the electric fields between the dipole, it follows that this is not an effect caused by capacity at the feed point, but is inherent to the propagating magnetic field.

Additional comments on this problem were published in Ref. 5. ●●

References

1. Olov Einarsson, "The Step Voltage Current Response of an Infinite Conducting Cylinder," *Transactions of the Royal Institute of Technology*, No. 191, 1962, Stockholm, Sweden.
2. Tai Tsun Wu, "Transient Response of a Dipole Antenna," *Journal of Mathematical Physics*, Vol. 2, No. 6, November-December 1961, pp. 892-894.
3. Feynman, *Lectures on Physics, Electodynamics II*, pp. 21-1 and 21-5.
4. D. Lohrmann and D. Wu, *The Step Current Voltage Response of a Very Long Dipole*, October 1998, unpublished manuscript.
5. D. Lohrmann and J. Bernardes, "Recipe for Calculation of Pulse Response of Dipole Antennas," Naval Research Report NRL/FR/5740-00-9949.

DESIGN FEATURE

Safer Materials

New Materials Make Microwave Components Safer For Users

Concerns over toxic substance effects have spawned materials that offer performance benefits and environmental friendliness.

Joseph Mazzochette

EMC Technology, Inc., 1971 Old Culbert Rd., Cherry Hill, NJ 08034; (856) 429-7800, FAX: (856) 429-6814, e-mail: jbm@emct.com.

DESIGNING and manufacturing high-power microwave components such as transistors, terminations, and attenuators present challenging materials problems. They are fabricated on substrates which must be temperature and frequency stable, well-matched with other materials used in the construction, have high thermal conductivity (TC), and low parasitic reactance. For many years, beryllium-oxide (BeO) substrates have been used for applications that require such characteristics. While the electrical and thermal properties of BeO are attractive, the problem of the material toxicity has caused many users to search for alternatives. According to the Center for Disease Control, there are chronic and acute reactions which can result from exposure to Be, the base metal in BeO.[1]

Inhaling fine Be dust into the lungs causes both effects. Less is understood about the effects of ingesting Be because it is not present in large amounts in the food or water supply. For most people, the exposure to Be in the air results from the burning of coal and oil, or from tobacco smoke. The acute effects from the inhalation of large amounts of Be dust are lung damage and a disease that resembles pneumonia.[2] The acute effects may diminish if the exposure to Be ceases. Some people are hypersensitive to Be and may have an allergic reaction to the inhalation of low levels of dust.[2] It is estimated that between 5 and 15 percent of the population is allergic to Be.[3] People who are hypersensitive to Be may develop a condition known as chronic beryllium disease. The chronic and acute reactions to inhaling Be dust may cause death. Be is also a likely human carcinogen.

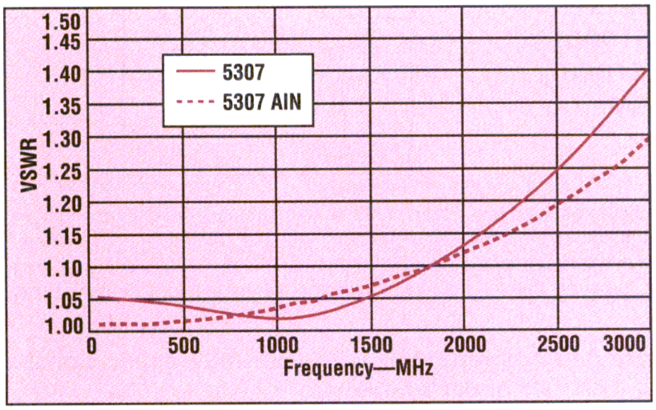

1. A graph of VSWR as a function of frequency comparing BeO and AlN shows the materials have similar VSWRs up to 1.5 GHz. Above 2 GHz, AlN has slightly better characteristics.

Although the effects of Be disease are severe, the risk of illness from Be appears to be quite low. In the US, 60 cases of Be disease were reported from 1973 to 1978. Over the past five years 10 to 12 new cases were reported annually. These cases are divided approximately 80 percent chronic and 20 percent acute.[4] In 90 percent of the cases, workers are employed in ore smelting, metal production, and metal reclaiming.[4,5] As a solid ceramic of the size used in most electronic applications there is no risk of inhalation. Be does not make the Environmental Protection Agency's (EPA's) list of Top 20 hazardous substances.[2] In fact, Be is number 39 on the EPA's complete list of priority hazardous substances after materials such as lead (Pb), mercury (Hg), chromium (Cr), and creosote.[2]

An important issue with the use of

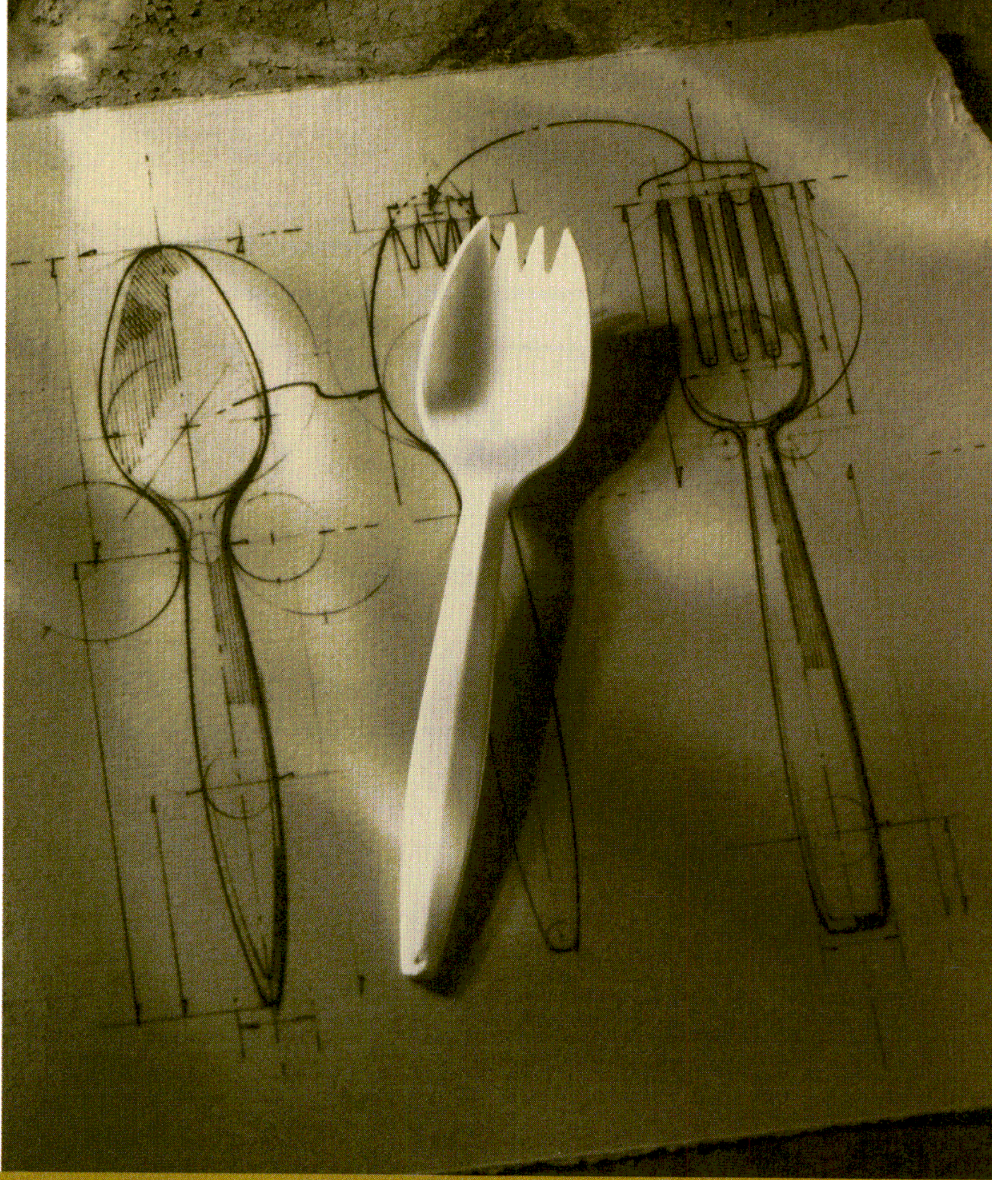

Table 1: BeO properties

Property	Value
Density	2.85 g/cc
Temperature coefficient of expansion	7.2 PPM/°C
Thermal conductivity	260 W/mK
Dielectric loss	0.0004
Bending strength	221 MPa
Relative dielectric constant	6.7

Table 2: AlN properties

Property	Value
Density	3.3 g/cc
Temperature coefficient of expansion	4.6 PPM/°C
Thermal conductivity	190 W/mK
Dielectric loss	0.0005
Bending strength	290 MPa
Relative dielectric constant	8.9

Be and Be compounds is the end-use responsibility. Increasingly, governments are requiring companies to be responsible for the entire "life" of the products that they produce. This includes the use of the product as it is intended and its proper disposal after the end product is obsolete. The concern over product responsibility has led many consumers of high-power RF and microwave components to search for alternative materials.

The TC of BeO is roughly half that of pure copper (Cu). TC is the property which makes BeO useful for electronic applications. Devices that are required to convert electrical energy into heat must be fabricated or mounted on a substrate that will carry the heat away in order to keep the device at a safe operating temperature. Electrical properties such as low dielectric constant ϵ, low loss-tangent, and high breakdown voltage are required for high-frequency applications. Fortunately, the electrical and thermal properties of BeO make it a good choice for high-power RF and microwave circuits and components (Table 1).[6]

ALTERNATIVES TO BeO

Some potential alternatives to BeO are boron nitride (BN), silicon carbide (SiC), and diamond. Each of these materials falls short in replacing BeO due to TC, relative permittivity ϵ, and price, respectively. One material which comes close to matching BeO performance is aluminum nitride (AlN). Table 2 lists some relevant AlN properties.[7]

The TC for AlN ceramics is clearly lower than BeO. Depending on the application, the lower TC for AlN may or may not be acceptable. Constructing film-type high-power resistors on a ceramic substrate demands some of the most comprehensive performance standards from a ceramic. The metal-resistive film requires

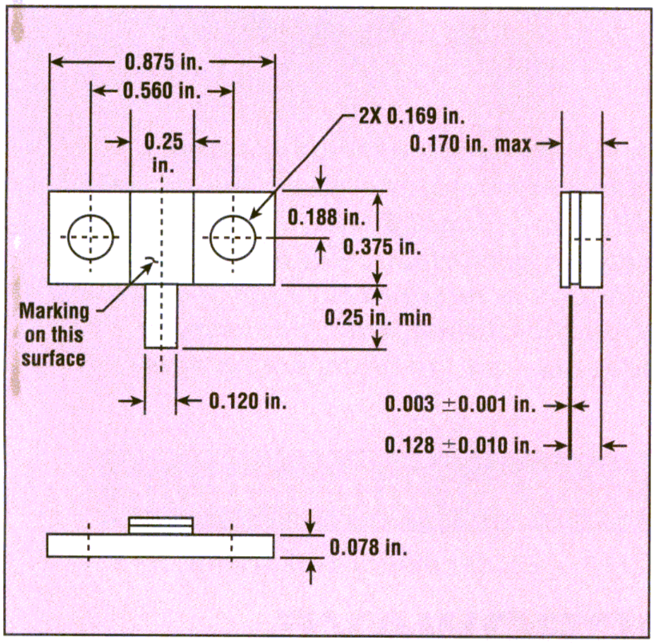

2. This 5307AIN package is a two-hole flange-mounted part for attachment to a large metal heatsink for ground and thermal connections with a center tab that is soldered to microstrip for the input power.

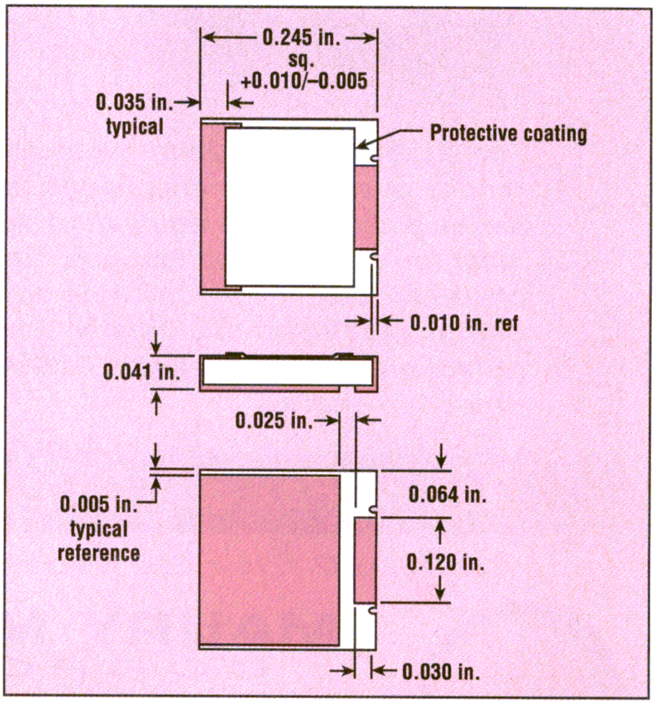

3. The SMT2525AIN is an SMT package designed to be soldered directly to a PCB.

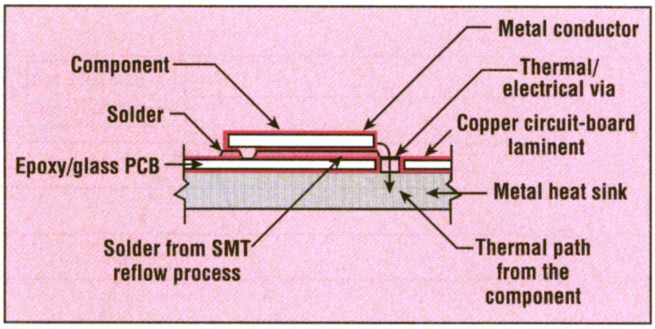

4. Surface mounting requires that the PCB layout provides vias to ensure proper heatsinking and a low-inductance ground connection.

excellent adhesion and closely matched temperature-coefficient-of-expansion (TCE) specifications in order to meet minimum reliability needs. Under normal operating conditions, the heat generated by the resistor creates a considerable temperature gradient through and along the surface of the ceramic. In other applications, such as packaged high-power transistors, where the devices are mounted on the ceramic, a mounting medium may be used to buffer any TCE mismatch. The buffer may be further optimized for good adhesion. The analysis and results presented in this article will focus on the more stressful power-resistor fabrications.

In side-by-side power-capability tests on high-power microwave terminations, parts built with BeO substrates outperformed similar AlN parts as detailed in Table 3. In the tests, the parts in each "family" are identical in size and have similar VSWR specifications. The higher ϵ_r of AlN, when compared to BeO, makes it difficult to achieve identical S-Parameters for the two parts. Figure 1 shows VSWR as a function of frequency for the 5307 and the 5307 AlN. Package drawings of the 5307 and SMT 2525 parts are illustrated in Figs. 2 and 3, respectively.

The 5307 is a two-hole flange-mounted part. It is normally mounted on a large metal heatsink for ground and thermal connections, while the center tab is soldered to a microstrip circuit for the input-power connection. The surface-mount (SMT) part is connected to a circuit by soldering it directly to a printed-circuit board (PCB), as shown in Fig. 4.

Care must be taken with the SMT part that adequate ground vias are added to the PCB layout to insure proper heat sinking and a low-inductance ground connection. Despite the reduction in power capability, the AlN-based components are functional for many applications. While the power margin on the part may be reduced, this is often justified by the benefit of using AlN to eliminate the toxic BeO from the circuit. The 5307AlN device was first developed in 1995. After the production of hun-

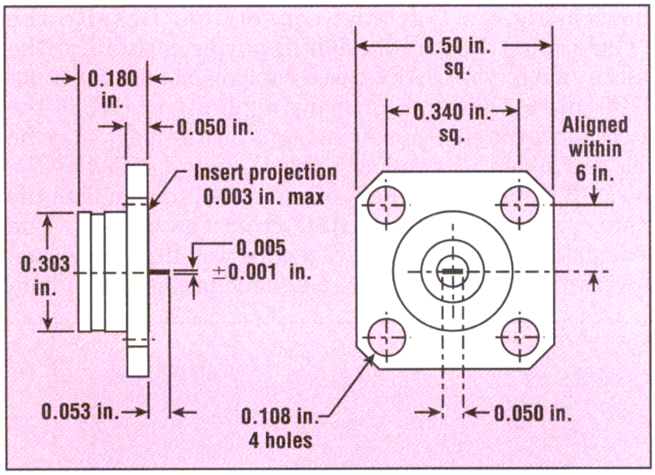

5. The 8475AIN package is a standard four-hole, 0.5-in. (1.27-cm) high-power termination that relies on the flexural strength of the internal rod resistor to survive normal mounting stress.

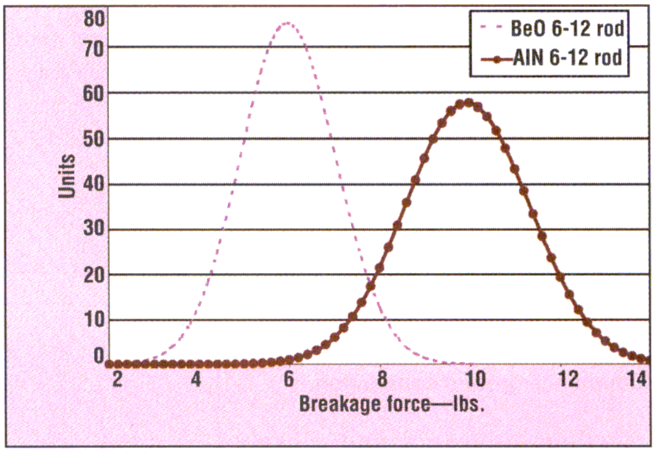

6. AIN has greater breaking force than BeO as illustrated by the curve comparing the materials when fabricated in 0.06-in. (1.52-cm) diameter rods. This characteristic of AIN gives it higher reliability than BeO.

dreds of thousands of devices over the past four years, it has proven to be as reliable as its BeO sister product.

MECHANICAL FEATURES

An important advantage of AlN ceramic over BeO is increased mechanical strength. The AlN ceramic provides 30-percent greater flexural strength than the BeO ceramic. Standard, four-hole, 0.5-in. (1.27-cm) high-power terminations, such as the type illustrated in Fig. 5, rely on the flexural strength of the internal-rod resistor to survive normal mounting stress.

In most applications, the center conductor of the load is soldered to the conductor of a stripline or microstrip circuit. The load case is then attached to the circuit housing with screws. Stress on the load is created during the soldering and screw-mounting operations. Since the rod resistor is supported on the load-housing end, much of the stress is placed on the rod resistor. Furthermore, the stress causes the rod resistor to flex. Since it is a ceramic, the rod resistor performs well in compression. However, cracks may propagate from small notches in the surface when the part is flexed. Figure 6 shows the distribution of flexural force required to break AlN and BeO, 0.06-in. (0.15-cm) diameter ceramic rods. This test was conducted on 200 specimens which were mounted in the same configuration as the device featured in Fig. 4. The resulting 60-percent improvement in breaking force adds considerably to the overall reliability of the product.

In the case of flat ceramic devices, such as the types featured in Figs. 2 and 3, the greater flexural strength helps the AlN parts to survive the stresses that result from the TCE mismatches between the ceramic and mounting surfaces. The most common mounting surfaces are Cu (TCE ≈ 18 PPM/°C) for the device in Fig. 2 and epoxy-based PCBs (TCE ≈ 12 PPM/°C) for the device in Fig. 3. Some of the TCE mismatch stress is absorbed by the solder connections between the ceramic and the mounting surface. However, AlN ceramics, with a higher flexural strength, provide additional insurance against failures due to thermal stress when compared to BeO.

Manufacturers of AlN substrates have struggled for years to produce consistent material. Variations in the AlN fabrication process such as temperature, grain size, and firing atmosphere can affect the properties of the finished product. Materials such as yttrium oxide, which melts at a lower temperature than AlN, are used as flux to aid in bonding the AlN grains during the sintering process. The TC of the material is significantly affected by the grain size, the integrity of the connection at the grain boundaries, and N vacancies which may form when the ceramic is sintered. The variation in the formation of the ceramic is demonstrated by the variation in color from part to part and from lot to lot.

The condition of the surface of the substrate is also quite critical to the performance of components produced using AlN. Surface contamination and physical defects can affect the adhesion of materials such as conductors, dielectrics, and even

(continued on p. 170)

Table 3: Power capability of BeO versus AIN substrates

Part number	5307	5307AIN	SMT2525	SMT2525AIN	SMT2010	SMT2010AIN
Ceramic substrate	BeO	AIN	BeO	AIN	BeO	AIN
Substrate area (square inches)	0.0938	0.0938	0.0625	0.0625	0.02	0.02
Absolute maximum power at 100°C (W)	180	150	23	20	13	10

FBAR Technology Shrinks CDMA Handset Duplexers

Refinements to film-bulk-acoustic-resonator (FBAR) technology have made tiny filters with performance rivaling much larger ceramic resonator designs.

Dan McNamara

CDMA Product Manager

Agilent Technologies, Semiconductor Products Group, 39201 Cherry St., Newark, CA 94560; (510) 505-5600, FAX: (510) 505-5730, e-mail: daniel_mcnamara@agilent.com, Internet: http://www.agilent.com.

DUPLEXERS are used in cellular telephones to separate transmit- and receive-frequency bands, enabling simultaneous transmission and reception. Duplexers for code-division-multiple-access (CDMA) systems at personal-communications-services (PCS) frequencies must meet demanding requirements, providing a 50-dB attenuation rolloff from a low-loss passband within a 20-MHz bandwidth (including variations with temperature), while handling transmit-power levels of approximately 1 W. The key parameters for the filter include quality factor (Q), which is roughly proportional to filter rolloff, temperature coefficient, power handling, and insertion loss. What follows is an examination of a technology—film bulk-acoustic resonator (FBAR)—well-suited for cellular/PCS handset duplexers.

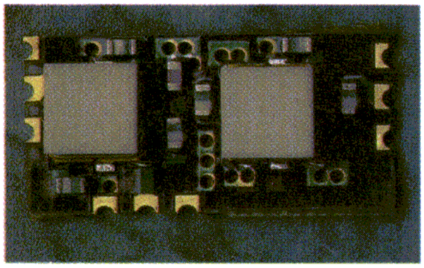

1. The first production FBAR duplexer for PCS-band CDMA handsets occupies a volume of only 126 mm³, versus 674 mm³ for current coaxial ceramic-filter-based duplexers.

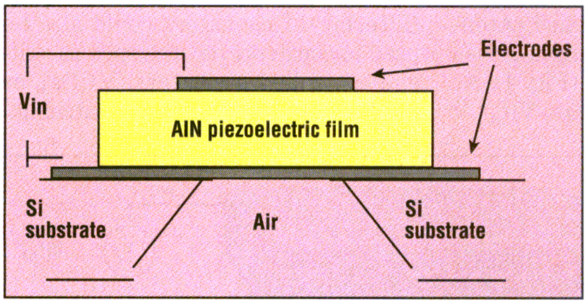

2. The basic FBAR structure consists of an AlN piezoelectric membrane with thin-film metallic electrodes. The "active" portion of the membrane is unsupported.

Until now, the only filters suitable for duplexer applications in the PCS band have been relatively bulky ceramic coaxial dielectric-resonator filters. However, FBAR technology can yield extremely compact filters with a combination of high Q, moderate temperature coefficients, and excellent power-handling capacity, to provide the first "semiconductor-sized" duplexer/filter solution. The long-term promise of FBAR technology includes the integration of filters with active circuits, supporting new high-performance radios ranging from small personal communicators, person-level networks, and any type of device which can operate on a wireless data link (Fig. 1).

When compared to ceramic filters, FBAR-based solutions offer significant advances in miniaturization. Ceramic duplexer products available from 1997 through 1998 were typically 1309 mm³ in volume, having been reduced to approximately 674 mm³ by 1999. The first FBAR duplexer product can be realized in less than 20 percent of the volume of these smaller ceramic filters, with a volume of only 126 mm³. Since FBAR duplexer filters can be made with a height of only 2 mm (compared to 5 mm for ceramic duplexers), the same handset housings can be used for CDMA units as for Global System for Mobile Communications/time-division-multiple-access (GSM/TDMA) units, which is not possible with bulky ceramic PCS duplexers.

The table summarizes important performance parameters for ceramic, surface-acoustic-wave (SAW), and FBAR filters. From the data, one difference is the high-Q value for the FBAR filter. The consequent steep rolloff compensates for variations in the filter's response curves over temperature, creating a structure comparable in electrical performance to the less steep, but temperature-stable results seen with ceramic filters.

When compared to SAW devices, the higher Q and lower temperature coefficient of FBAR resonators equips them with the potential for lower insertion loss and steeper filter "sidewalls." These advantages are derived from the lower parasitic-circuit elements associated with a bulk device, as well as the elimination of Bragg reflectors from the topology. Some of this performance margin can be traded for improvements in bandwidth, eliminating the need for split-band filters. The use of vibrating membranes, rather than fine-pitched interdigitated structures, provides intrinsically better power-handling capacity, and enables operation to higher frequencies. FBAR technology can readily handle continuous-wave (CW) signals in excess of 1 W with minimal added distortion. The technology readily extends to PCS frequencies and, in fact, can be used to create resonators which operate at frequencies above 10 GHz.

FBAR resonators are created using a thin-film semiconductor process to build a AlN-metal sandwich in air (Fig. 2). When an alternating electrical potential is applied across the metal AlN metal sandwich, the entire AlN layer expands and contracts, creating a vibration. This resonance is in the body (bulk) of the material, as opposed to being confined to the surface, which is the case for SAW devices (Fig. 3). One advantage of bulk resonators is the intrinsically better power-handling characteristics, opposed to the interdigitated structures which are used in SAW devices, especially at higher frequencies where the pitch of the interdigitated structures must be reduced.

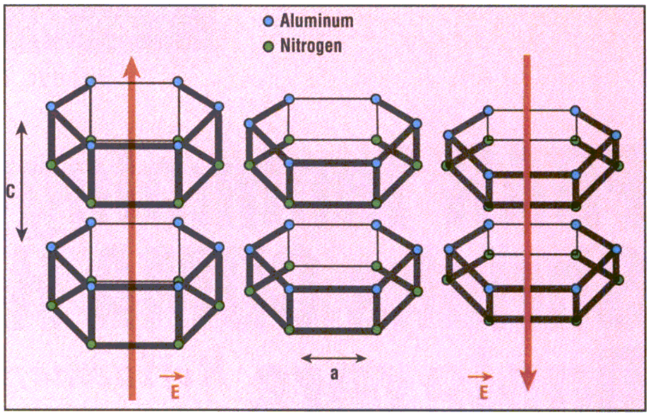

3. In operation, the entire AlN layer expands and contracts, creating an acoustic vibration. The resonance is in the bulk of the material, as opposed to being confined to the surface, which is the case with SAW devices.

The vibrating membrane creates a high-Q mechanical (acoustic) resonance. The dimensions for an acoustic resonator at a particular frequency are several orders of magnitude smaller than those of a coaxial resonator, enabling acoustic devices to fit easily on a semiconductor chip.

As alternating voltage is applied across the AlN stack, the polarization vector P of the stack will change in phase. At some voltage, $V(f_s)$, P will be in phase with the vector E created by the applied potential, creating a series resonance (Fig. 4). At some voltage, $V(f_p)$, P will be 180-deg. out of phase with E, creating a parallel resonance (Fig. 5). These resonances can be characterized (Fig. 6) by the following equations:

For series resonance:

$$f_s = (L_m C_m)^{-0.5}$$

$$R_s = R_{series} + R_m$$

For parallel resonance:

$$f_p = (L_m C_m)^{-0.5} (1 + C_m/C_p)^{0.5}$$

$$R_p = Z_{2plate}/(R_m + 1/G_{shunt}) - 1$$

where:

$V(f_s)$ = the voltage for conditions of series resonance,

$V(f_p)$ = the voltage for conditions of parallel resonance,

L_m = the equivalent-circuit inductance,

C_m = the equivalent-circuit capacitance,

R_m = the equivalent-circuit resistance,

Z_{2plate} = the plate capacitance of the AlN stack, and

G_{shunt} = the shunt transconductance of the AlN stack.

Piezoelectric coupling is used to access these acoustic resonances. Resonators can, in turn, be built into networks which provide signal shaping (filtering). Resonators could also be used to construct devices such as voltage-controlled oscillators (VCOs), or used to perform impedance matching.

Comparing filter performance at PCS frequencies

Parameter	Ceramic	SAW	FBAR
Q	~200	~200	800 to 1200
Temperature coefficient (all negative) [PPM/°C]	0 to 5	35 to 40	25 to 30
Frequency margin to fit in 20 MHz (MHz)	2 to 4	Exceeds 20 MHz	3 to 6
Power handling (dBm)	>+35	~+20	+32
Insertion loss (dB)	Excellent	Good	Excellent
Size (mm³)	675	140 (cellular band)	126

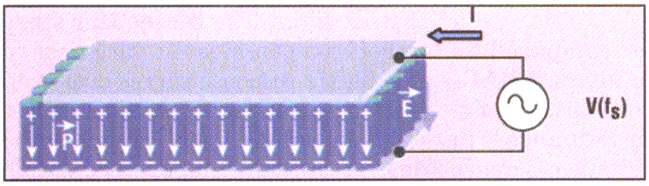

4. The series resonance in the bulk of the FBAR membrane is obtained from the equation: $f_s = (L_mC_m - 0.5$; $R_s = R_{series} + R_m$.

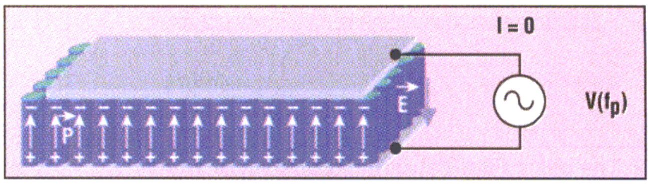

5. The parallel resonance in the bulk of the FBAR membrane is obtained from the equation: $f_p = (L_mC_m - 0.5(1 + C_m/C_p) - 0.5$; $R_p = Z_{2plate}/(R_m + 1/G_{shunt})$.

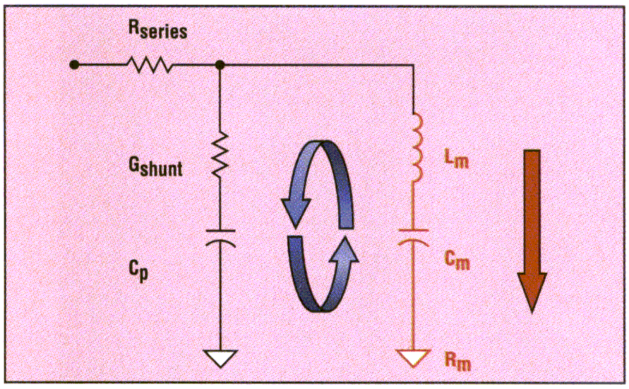

6. This equivalent circuit represents a BAW resonator.

To achieve practical success, bulk-acoustic-wave (BAW) devices must overcome several fundamental difficulties, including extreme demands in thin-film stack uniformity (for frequency control), acoustic-coupling constant, Q (electrical and mechanical), and relatively low thin-film stress to meet device-reliability requirements.[1]

As previously mentioned, the piezoelectric stack is comprised of an AlN film sandwiched between two metal layers that serve as electrical terminals. The crystalline quality of the AlN film determines the quality of the resonator, which determines how efficiently the electrical energy applied to the terminals is converted into mechanical energy (and vice versa)—this is referred to as the acoustic-coupling constant for the resonator. The basic electrical model for the resonator is represented by the classical Butterworth-Van Dyke circuit illustrated in Fig. 7, where C_0 is the equivalent parallel-plate capacitance of the piezoelectric sandwich and C_1, L_1, and R_1 represent the elements of the equivalent electrical circuit of the piezoelectric element.

A two-step modeling process was used for optimizing FBAR resonator

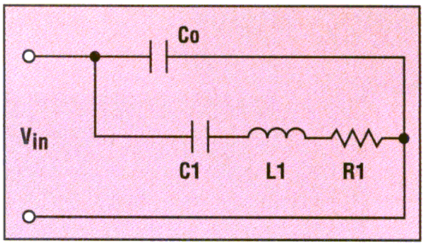

7. The FBAR device can be represented by the Butterworth-Van Dyke model, where C_O is the equivalent capacitance of the piezoelectric sandwich and C_1, L_1, and R_1 represent the piezoelectric element.

and filter performance. First, a physical simulator based on the Mason[2] model was used to determine the resonator-layer thickness. Optimization for FBAR filters and more "integrated" structures (such as a duplexer), including printed-circuit-board (PCB) and passive elements, have been performed using the EEsof Advanced Design System (ADS) simulation software from Agilent Technologies (Palo Alto, CA). The physical (Mason) and electrical (Butterworth-Van Dyke) models are relatively simple. Thus, good agreement between measured and predicted

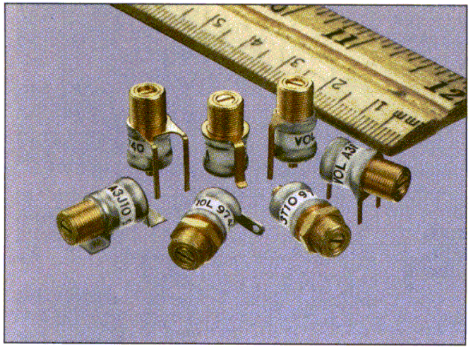

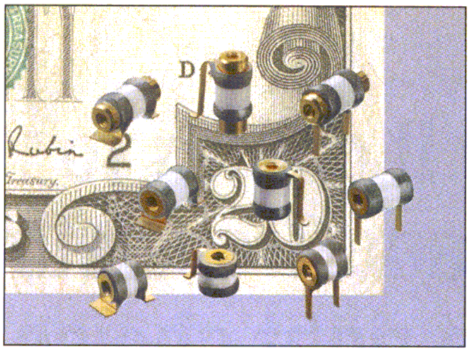

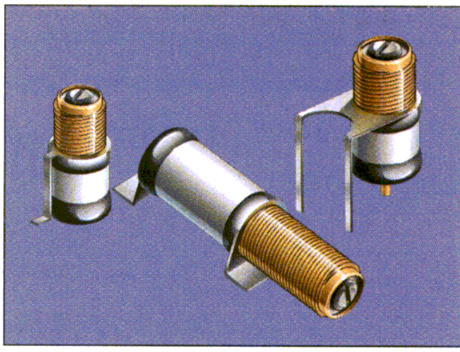

A_3 Series

- Capacitance range: 1 to 10 pF
- Self-resonance 2.3 GHz at 10 pF
- Working voltage up to 1000 VDC
- 10 turns of linear tuning
- Drop-in replacement for expensive air piston trimmers
- High reliability solid dielectric

A_4 Series

- 3 capacitance ranges from 0.45 to 5 pF
- Shortest length of any piston trimmer
- Size from 0.150" long x 0.155" diameter
- Up to 5 turns of linear tuning
- High reliability solid dielectric
- Replaces expensive sapphire trimmers

HV Series

- 7 capacitance ranges with max capacitance from 4 pF to 55 pF
- Working voltage up to 1000 VDC
- Frequency up to 1.5 GHz
- Up to 29 turns of linear tuning
- Sealed construction, 40 psi
- Various mounting styles
- Non-magnetic versions

What makes Voltronics trimmer capacitors the world's best? Just look inside...

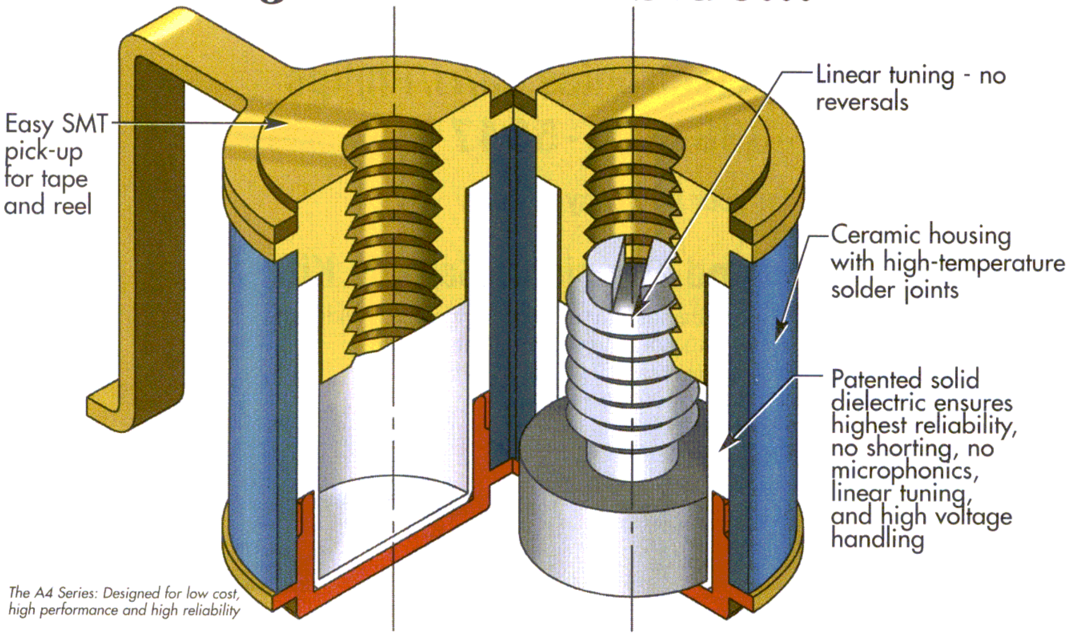

The A4 Series: Designed for low cost, high performance and high reliability

Voltronics trimmer capacitors provide:

- **Long-term reliability designed-in**
- **Low cost - under $1 in quantity**
- **Self-resonant frequency range to 5 GHz**
- **Lowest profile in the industry**
- **Available on tape-and-reel**
- **High-voltage options**
- **Capacitance ranges from 0.2-1.0pF to 1.5-55pF**

Only Voltronics trimmers give you all this... for less than $1

Voltronics CORPORATION

The Trimmer Capacitor Company

Call Voltronics today, or check out our complete catalog on-line at www.voltronicscorp.com

100 Ford Road • Denville, NJ 07834
973.586.8585 • FAX : 973.586.3404
e-mail: info@voltronicscorp.com

CIRCLE NO. 206

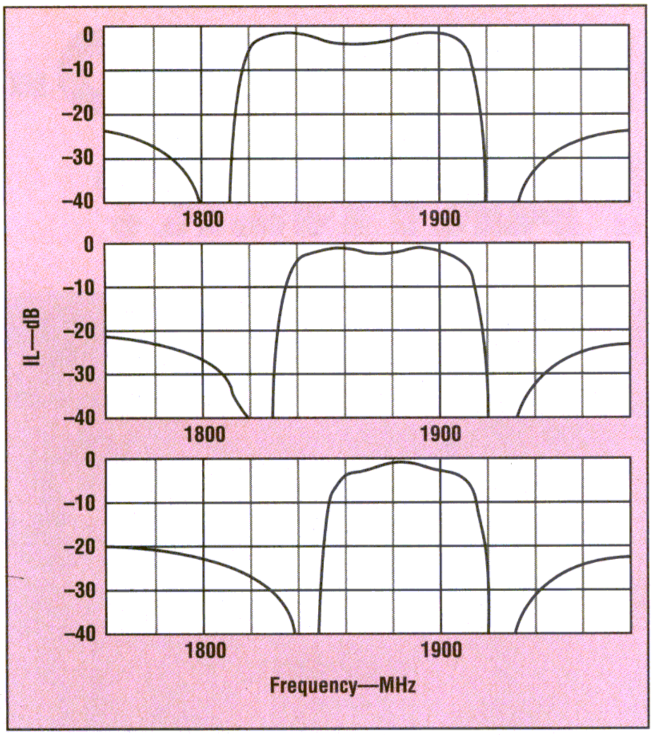

8. This simulation of the transmit filter was performed with kt² of approximately 5 percent and mass loading of (a) 4 percent, (b) 3 percent, and (c) 2 percent.

performance can be achieved.

Two additional variables are used in the design of filters and resonators. The mass loading determines the offset frequency between resonators and the effective acoustic constant (kt^2). The effects of these parameters on the performance of a typical PCS transmit filter are depicted in Fig. 8.

As a general rule, increasing the acoustic-coupling constant and mass loading (_f) will increase the filter bandwidth while the number of resonator stages and the Q will determine the rolloff characteristics (at the cost of insertion loss).

Figure 9 illustrates the measured and simulated performance of a 1900-MHz FBAR PCS duplexer. Small size, together with excellent electrical performance, are the key value propositions for this solution. The effects of the passives and the PCB are also included in the results depicted. This particular solution is a chip-on-board device (no filter package).

Environmental-chamber measurements have been used to determine an average temperature coefficient of 25 to −30 PPM/°C, which compares favorably to the −35 to −40 PPM/°C of lithium-tantalum-oxide ($LiTaO_3$) SAW duplexers. These numbers, taken together with the acoustic-coupling constant and the Q factor, are important for designing product applications where excellent performance over a wide temperature range is required.

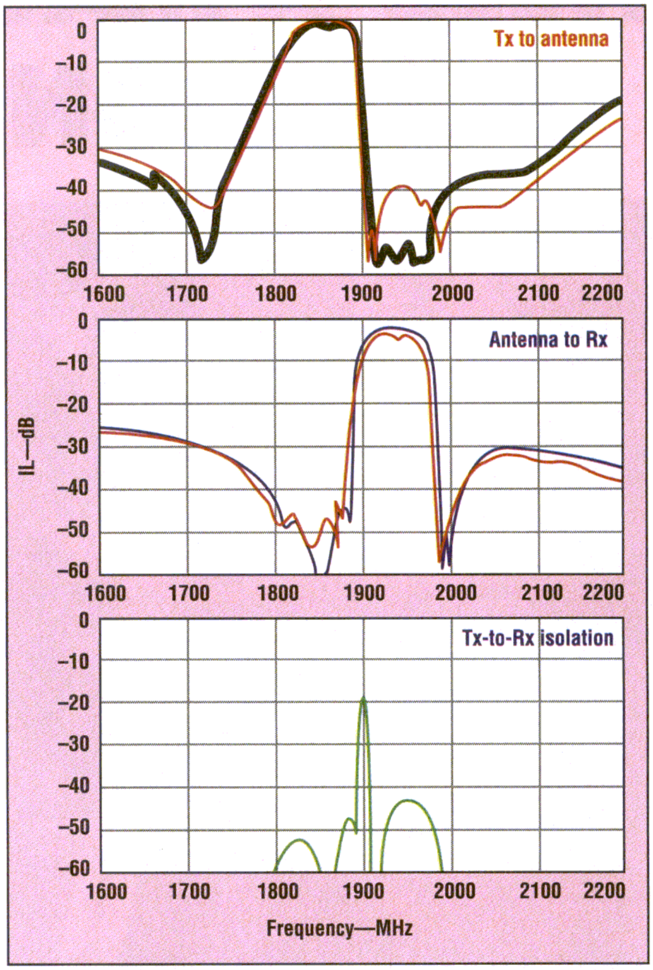

9. The measured (dotted line) and modeled (solid line) performances of an FBAR duplexer were plotted for (a) the Tx to antenna-filter response, (b) the receiver (Rx) to antenna-filter response, and (c) the Tx to receiver isolation.

Further details of FBAR duplexer performance (measured and simulated) have been published recently.[3,4]

The high Q and coupling coefficients achieved by FBAR technology allow structures to be created which rival present state-of-the-art ceramic and SAW resonators. Qs in excess of 1000 have been realized (Fig. 10). This translates into steep filter rolloff. More than 40-dB rejection in 8 MHz or 50-dB rejection in 12 MHz has been achieved.

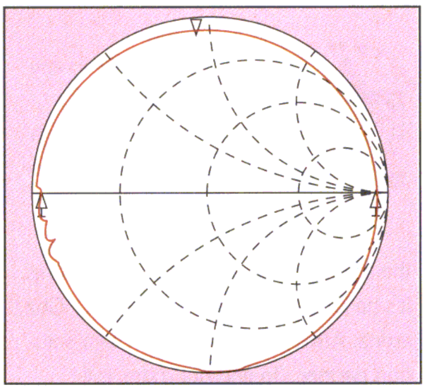

10. This Q circle was plotted for a representative FBAR filter

REACHING RELIABILITY

Rigorous testing has been performed to verify the ruggedness of the FBAR duplexer. Devices have been tested through thermal shock, high-temperature storage, autoclave, and thermal cycling without any observed failures. Mechanical shock tests have also been performed without failures.

In addition to the duplexer, FBAR-point filters designed for transmitter (Tx) applications have been subjected to various CW RF input-power levels. Input-power stresses of approximately +34 dBm for up to 200 hours show no

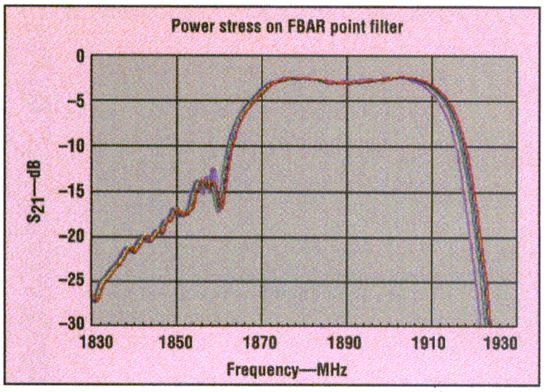

11. This plot shows the results of power stress on an FBAR point filter.

changes in filter response. During these tests, the temperature of the PCB that holds the ceramic filter carrier as well as the return and insertion losses of the filter are monitored to ensure that the device is operating under worst-case conditions [i.e., with maximum absorption of the incident RF power (Fig. 11)].

While FBAR is not a new technology,[1,5] it is only now being prepared for use in large-volume applications. The development of acoustic resonators has been ongoing for approximately 30 years and patents exist for this technology dating back to 1976. In the past, there had always been some substantial hurdle which limited the use of this technology to niche applications. It is only now that a robust process has been developed which can support the demands of a large-volume market.

The initial FBAR product for the mass market will be a PCS duplexer used in CDMA applications. Logically, this technology could be adopted for duplexers at the other CDMA frequencies, 800 MHz, and wideband-CDMA (WCDMA) applications.

Although the focus of this paper has been primarily on 1900-MHz PCS applications, filters and resonators covering frequencies from 800 MHz to more than 7.5 GHz have also been demonstrated. In addition to this, information on a multichip amplifier and filter module was published last year.[6] The concept of combining filters and active circuits could take many forms. One example of this is a low-noise amplifier (LNA) with a bypass switch followed by a bandpass filter, in a single small package.

There is also the potential for reduction in overall circuit size by integrating the various pieces of a radio. FBAR technology is compatible with silicon (Si) and gallium-arsenide (GaAs) wafer processing, opening the door for integrated radio solutions that include active elements and filtering in the same semiconductor package, and eventually on the same chip. ●●

References

1. K.M. Lakin, K.T. McCarron, and R.E. Rose, *Solidly Mounted Resonators and Filters*, 1995 IEEE Ultrasonics Symposium, pp. 905-908.
2. W.P. Mason, *Physical Acoustic Principles and Methods*, Vol. 1A, Academic Press, New York, 1964, pp. 239-247.
3. R. Ruby, P. Bradley, and J. Larson III, "PCS 1900 MHz Duplexer Using Thin Film Bulk Acoustic Resonators (FBARS)," *Electronic Letters*, Vol. 13, No. 10, May 1999, pp. 794-795.
4. J. Larson III, R. Ruby, P. Bradley, and Y. Oshmyansky, "A BAW Antenna Duplexer for the 1900 MHz PCS Band," *1999 IEEE International Ultrasonics Symposium*, October 17-20, 1999.
5. R. Ruby and P. Merchant, "Micromachined Thin Film Bulk Acoustic Resonators," *1994 IEEE International Frequency Control Symposium*, pp. 135-138.
6. H. Morkner, R. Ruby, M. Frank, and D. Figueredo, "An Integrated FBAR Filter and PHEMT Switched-Amp for Wireless Applications," *1999 IEEE MTT-S International Microwave Symposium*, Vol. 4, pp. 1393-1396.

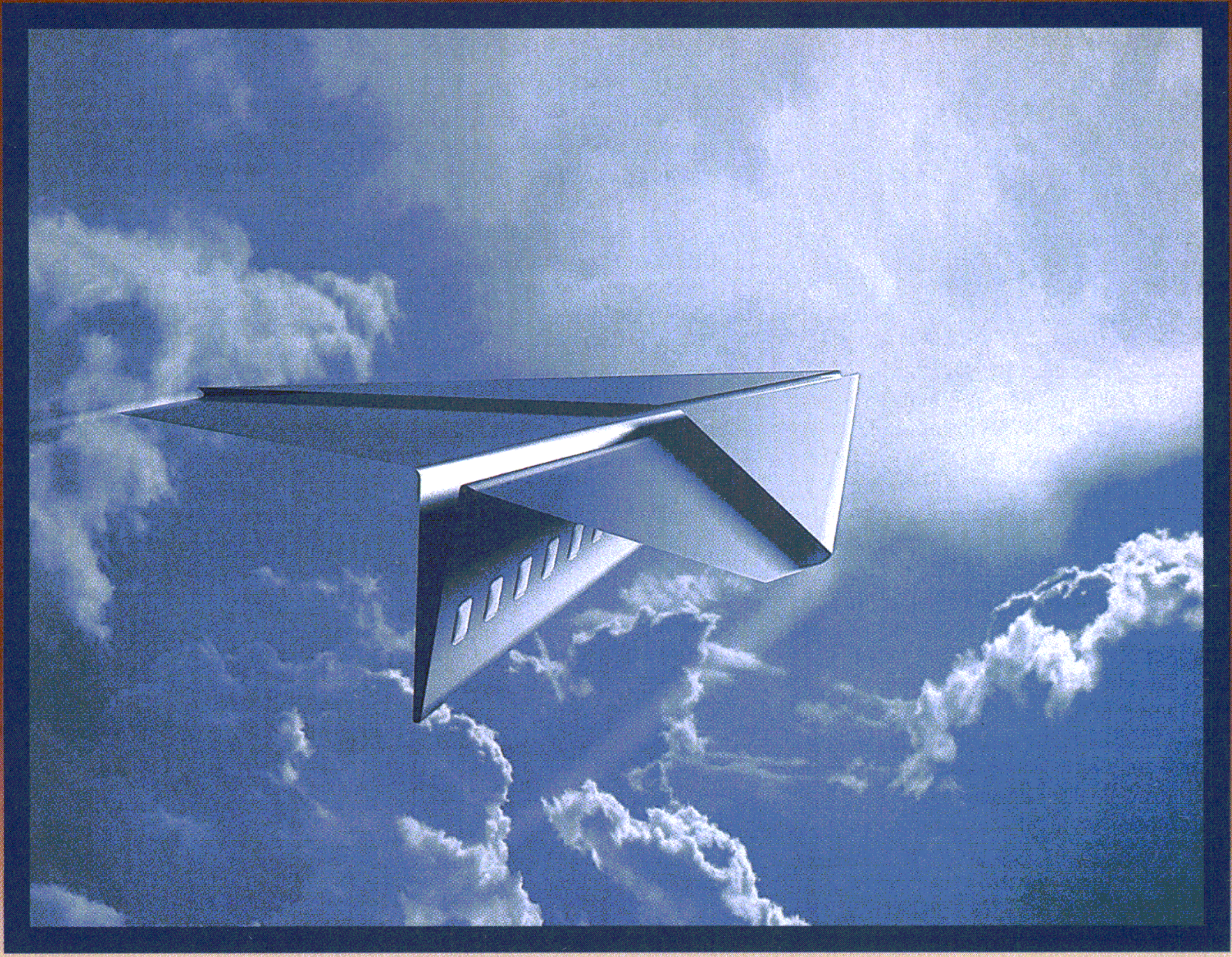

Imagine the possibilities.

Introducing our newest NGA InGaP HBT amplifier family with low thermal resistance for higher reliability and improved linearity with broader bandwidth.

Stanford Microdevices introduces the NGA-100 through 600 Series InGaP HBT amplifiers designed for today's and tomorrow's advanced communication infrastructure equipment. Design and fabricated with state-of-the-art InGaP/GaAsHBT technology for higher reliability, these devices are ideal for use as driver stages for higher power applications. Available in small-form factor plastic packages, the NGA series are biased with a single voltage and provide wide bandwidth, high gain and exceptional linearity.

For more information on these new InGaP amplifiers, visit our website today. Imagine the possibilities with RF innovation from Stanford Microdevices.

NGA - InGaP MMIC 50 Ohm Gain Block Amplifiers

Model	Freq Range (GHz)	Vd (V)	Id (mA)	Gain (dB)	PldB (dBm)	IP_3 (dBm)	Thermal Resistance (°C/W)
NGA-186	0.1-6.0	4.1	50.0	12.5	14.6	32.9	120
NGA-286	0.1-6.0	4.0	50.0	15.5	15.2	32.0	120
NGA-386	0.1-5.0	4.0	35.0	20.8	14.5	25.8	144
NGA-486	0.1-6.0	5.0	80.0	14.8	18.3	39.5	118
NGA-586	0.1-6.0	5.0	80.0	19.9	18.9	39.6	121
NGA-686	0.1-6.0	5.9	80.0	11.8	19.5	37.5	121

Data at 1 GHz and is typical of device performance.

STANFORD MICRODEVICES

www.stanfordmicro.com • 800-764-6642

CIRCLE NO. 250

Biasing N-Channel GaAs MESFETs

This tutorial discusses the problems and solutions associated with DC-current stabilization in n-channel MESFETs.

Fred Bonn
Principal Staff Engineer
Wireless Infrastructure Systems Division, Motorola SPS, 2100 E. Elliot Rd., MD EL536, Tempe, AZ 85284; (480) 413-6534, FAX: (480) 413-8690, e-mail: r19982@email.sps.mot.com.

THIS article discusses the basic problem of DC-current stabilization in n-channel, metal-semiconductor field-effect transistors (MESFETs) due to device-threshold variations. It introduces basic methods of V_{th} compensation through gate- and source-voltage control, analyzes several methods of compensation, and discusses their relative merits.

There are two basic methods of biasing n-channel, gallium-arsenide (GaAs) MESFETs for threshold-voltage (V_T) compensation. The first requires that the gate-source voltage tracks V_T changes directly. This can be accomplished by making the gate voltage, source voltage, or both, a function of V_T. Current feedback is the most straightforward method of doing this, but it has the disadvantage of placing the current-sense resistor in the bias and signal paths.

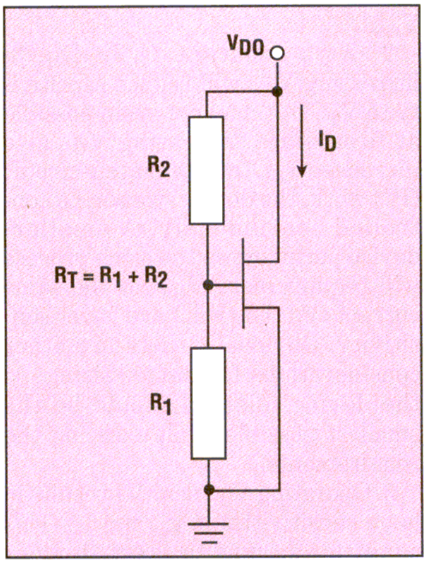

1. This schematic shows the reference bias circuit.

The second method involves using a current mirror to cancel V_T variations. This method is only as accurate as the current source for the mirror. And since this current source is constructed from another n-channel device, the mirror is affected by V_T variations.

An alternative is to combine both methods by placing the current-sense resistors in a much-lower-current "dummy" path and then mirroring this current to the device to be biased. The disadvantage is that current errors in the dummy device are multiplied by the beta ratio. Still, certain "dummy" methods offer improved control. And some implementations can achieve a compensation that is greater than one to one, which can be advantageous in certain applications.

Equation 1 shows the simple DC Curtice model for a GaAs MESFET.

$$v = (1/a) * \sqrt{(c * t)^2 - z^2} \qquad (1)$$

Equation 1 does not have the accuracy required for general analysis, but it is suitable for gaining a basic understanding of the operation of MESFET, metal-oxide-semiconductor-FET (MOSFET), and junction-FET (JFET) bias circuits. More-complex models offer greater accuracy for general analysis, but they do not offer much insight into basic FET operation. They are also too unwieldy for pencil-and-paper analysis and require simulators. When complex models and simulator are available, they should be reserved for fine-tuning.

If one assumes that the device is operating in the saturation region, Eq. 1 can be simplified further by omitting the α parameter. But if biasing must occur in the linear or triode region, say for a dual-gate mixer, this assumption obviously fails and Eq. 1 must be employed. The channel-length-modulation parameter is generally retained because its impact on bias point can be significant. If V_{DS} is constant or has negligible change, or if λ is very small, the effect can be lumped into β. The λterm describes the apparent increase in β due to increasing V_{DS}. The channel length is effectively shortened by the increasing electric field between drain and source, raising the apparent g_m. This effect is more pronounced with shorter-gate-length devices. The simplified formulation appears in Eq. 2.

$$I_D = \beta(V_{GS} - V_T)^Q(1+\lambda V_{DS}) \qquad (2)$$

The Q parameter is required because the exponent is generally not exactly 2. Most of the analyses that follow assume a Q value of 2 because it is easier to deal with when performing pencil-and-paper analysis.

The first-order-biasing problem in GaAs MESFETs is related to V_T variations due to process and temperature. If V_{GS} is fixed, the sensitivity of I_D to changes in V_T is given by Eq. 3.

$$\frac{\partial I_D}{\partial V_T} = -\beta Q(V_{GS} - V_T)^{Q-1}(1+\lambda V_{DS})$$
$$= -\frac{QI_D}{V_{GS} - V_T} \qquad (3)$$

Equation 4 includes the sensitivity of I_D to changes in V_{GS} (transconductance).

$$\frac{\partial I_D}{\partial V_{GS}} = g_m = \beta Q(V_{GS} - V_t)^{Q-1}$$
$$(1+\lambda V_{DS})$$

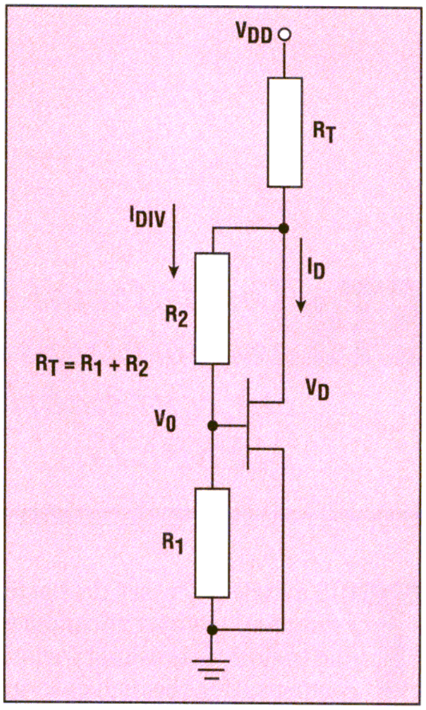

2. In this schematic, the gate voltage depends on the current.

$$g_m = \frac{QI_D}{V_{GS} - V_T} \qquad (4)$$

It is interesting to note that the sensitivity to V_T is equal but opposite in sign to the transconductance parameter g_m, and thus counters the effect of V_{GS}. Some other things should also be noted:

1. To maintain a constant bias current in Eq. 2, any changes in V_T must be countered by an equal change in V_{GS}.
2. At a constant I_D in Eq. 3, increasing V_{GS} will reduce sensitivity to V_T. This may not seem possible at first, since increasing V_{GS} also increases I_D. In integrated-circuit (IC) work, the device size can be controlled continuously. A smaller-device periphery in the same process will require more V_{GS} for the same current and thus will have lower sensitivity. Obviously, there are other considerations for device sizing, so the device selected should be the smallest possible while meeting the requirements.
3. Operating V_{GS} near V_T results in huge sensitivities in g_m and I_D. This condition occurs in large devices operated at low currents, such as low-noise amplifiers (LNAs) operating at lower frequencies. In these cases, large devices are chosen to lower the impedance and reduce the gate resistance, but the operating current is usually fixed at some low value.

If V_{GS} can be made to track changes in V_T in Eqs. 2 and 4, then I_D and g_m will be constant. In reality, there may be some higher-order effects that need to be taken into account for more precise compensation.

The circuit in Fig. 1 shows an uncompensated bias circuit consisting of a simple resistive divider. The supply voltage V_{DD} is assumed to be invariant in this case, so V_G is fixed and determined by the divider. The source voltage V_S is fixed at 0 VDC. One may not be able to track V_T perfectly, but anything that reduces variation is an improvement. A quality factor for improvement relative to this uncompensated reference is thus established. Another quality factor is the sensitivity to changes in V_{DD}. Equation 5a evaluates the sensitivity to V_T and V_{DD}.

$$I_D = \beta\left(V_{DD}\frac{R_1}{R_T} - V_T\right)^Q(1+\lambda V_{DD})$$

$$\frac{\partial I_D}{\partial V_T} = -\frac{QI_D}{\left(V_{DD}\frac{R_1}{R_T} - V_T\right)}$$

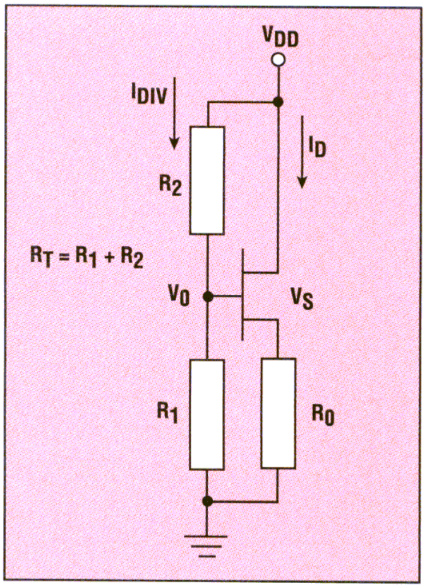

3. This schematic depicts the drain-current feedback to the source voltage.

BUILD YOUR 45MHz TO 650MHz OSCILLATOR IN 5 MINUTES

STEP 1: Choose the appropriate Maxim part from table below and calculate the inductance using the formula in the data sheet.

STEP 2: Insert inductor into EVKIT.

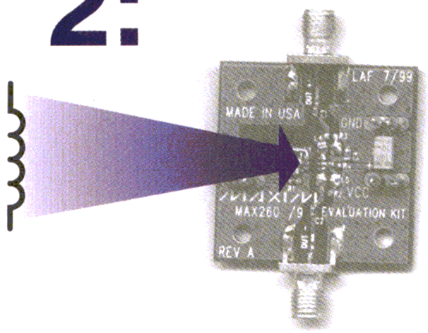

STEP 3: Test oscillation frequency. Done.

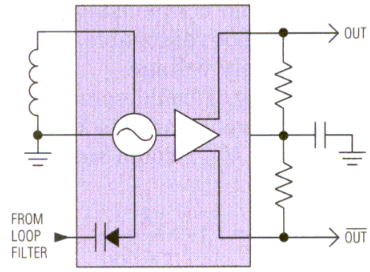

- Easy to Use
- 2.7V to 5.5V Supply
- On-Chip Temperature Compensated Bias
- Differential or Single-Ended Output
- Up to -8dBm Output Power
- Ultra-Small Implementation Size
- Low Supply Current

The MAX2605-MAX2609 series of oscillators contain varactors, core transistors, bias circuity, coupling capacitors, and a differential output buffer in a miniature SOT23-6 package. The internal varactor's tuning range is factory tested so that startup and proper operation over temperature are guaranteed.

PART	FREQUENCY RANGE (MHz)	SUPPLY CURRENT (mA)	PHASE NOISE @ 100kHz OFFSET (dBc/Hz)
MAX2605	45 to 70	1.9	-117
MAX2606	70 to 150	2.1	-112
MAX2607	150 to 300	2.1	-107
MAX2608	300 to 500	2.7	-100
MAX2609	500 to 650	3.6	-93

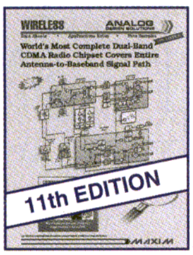

FREE* Wireless Design Guide—*Sent Within 24 Hours!

Includes: Reply Cards for Free Samples and Data Sheets

CALL TOLL-FREE 1-800-998-8800 for a Design Guide or Free Sample
6:00 a.m. – 6:00 p.m. Pacific Time

MAXIM

www.maxim-ic.com

2000 EDITION!
FREE FULL-LINE DATA CATALOG ON CD-ROM

ISO 9001

NEW! Get Price, Delivery, and Place Orders Online at www.maxim-ic.com

Maxim Integrated Products, 120 San Gabriel Drive, Sunnyvale, CA 94086, (408) 737-7600, FAX (408) 737-7194.
Distributed by Maxim Distribution, Arrow, Avnet Electronics Marketing, CAM RPC, Digi-Key, Elmo, Nu Horizons, and Zeus.
Distributed in Canada by Arrow and Avnet Electronics Marketing.

CIRCLE NO. 242

$$\frac{\partial I_D}{\partial V_{DD}} = I_D \left(\frac{R_I}{R_T} \frac{Q}{\left(V_{DD}\frac{R_I}{R_T} - V_T \right)} + \frac{\lambda}{1+\lambda V_{DD}} \right) \quad (5a)$$

If the supply voltage does not change, the gate voltage is constant and there is no compensation. It is possible, but not reasonable, to modulate the supply voltage.

If V_G in Fig. 1 could somehow be fixed and not referenced to V_{DD}, the sensitivity to V_{DD} would simplify to that of Eq. 5b.

$$\frac{\partial I_D}{\partial V_{DD}} = I_D \frac{\lambda}{1+\lambda V_{DD}} \quad (5b)$$

The drain voltage can be made a function of drain current (and, therefore, V_T) by using a current-sensing resistor in the drain path, as shown in Fig. 2.

To make the analysis manageable, Q is set to 2 and V_{DS} is assumed to be constant (although this is not quite true). This will introduce a small error, but the salient features will remain. The drain current is derived in Eq. 6, which is rather complex, despite the assumed simplifications. I_{DIV} can be made negligible by using a large V_T.

$$I_D = \beta(V_G - V_T)^2(1+\lambda V_{DS}) =$$

$$\beta'\left(V_{DD}\frac{R_1}{R_T} - V_T - I_D \frac{R_f R_1}{R_T} \right)^2$$

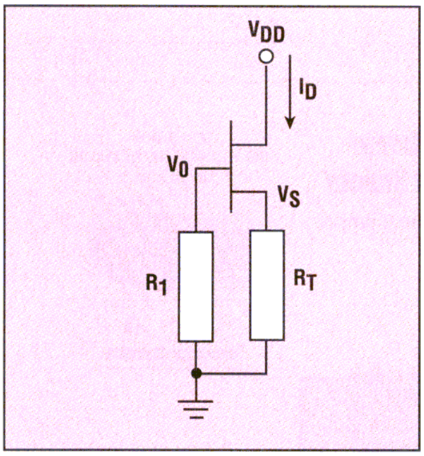

4. This schematic shows the drain-current feedback to the source voltage for depletion-mode devices.

$$I_D^2\left(\frac{R_f R_1}{R_T}\right)^2 -$$

$$I_D\left[2\frac{R_f R_I}{R_T}\left(V_{DD}\frac{R_I}{R_T} - V_T\right) + \frac{1}{\beta'}\right] +$$

$$\left(V_{DD}\frac{R_1}{R_T} - V_T\right)^2 = 0$$

$$I_D = \frac{R_T}{R_f R_1}$$

$$\left[V_{DD}\frac{R_I}{R_T} - V_T + \frac{R_T}{2R_f R_1 \beta'} \left(1 - \sqrt{1 + \frac{4R_f R_1 \beta'}{R_T}\left(V_{DD}\frac{R_I}{R_T} - V_T \right)} \right) \right]$$

$$set\ \frac{R_I}{R_T} = divider\ ratio = D$$

$$I_D = \frac{1}{R_F D}$$

$$\left[V_{DD}D - V_T + \frac{1}{2R_f D\beta'} \left(1 - \sqrt{1 + 4DR_f\beta'(V_{DD}D - V_T)} \right) \right] \quad (6)$$

The sensitivity to threshold and supply voltage is given in Eq. 7a.

$$\frac{\partial I_D}{\partial V_T} = \frac{1}{R_f D} \left[-1 + \frac{1}{\sqrt{1 + 4DR_f\beta'(V_{DD}D - V_T)}} \right]$$

$$\frac{\partial I_D}{\partial V_{DD}} = \frac{1}{R_f} \left[1 - \frac{1}{\sqrt{1 + 4DR_f\beta'(V_{DD}D - V_T)}} \right] \quad (7a)$$

In Eqs. 6 and 7a, it appears that there should be an improvement due to the division by the feedback resistor. As in the uncompensated case, the slope depends on the actual value of V_T.

It is difficult to tell by inspection how much improvement drain feedback really offers. It is probably best in this case to set up a specific design example with the reference circuit and then compare the two.

Example 1

Since the circuits of interest are low-voltage, low-current circuits, a

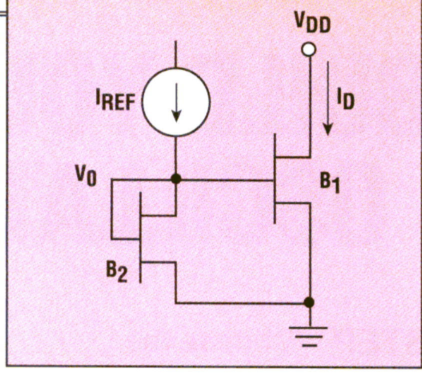

5. This schematic illustrates a basic current mirror.

supply voltage of +2.8 VDC and a drain current of 2 mA are selected. A relatively large device is generally required for reasonable matching, so the size is chosen to be 400 µm. This also places the V_{GS} closer to threshold, which is a more challenging operating point.

The device characteristics, $\beta = 0.075\ V/A^2$, $V_T = +0.225$ VDC, and Q = 2, are based on extracted model data from a 400-µm, E-mode device. Channel-length modulation is ignored, since it will not be a constant in all of the derivations that follow. It also results in third-order polynomials, which are more difficult to deal with. The uncompensated design of Fig. 1 serves as a reference, and the results appear below.

$$\frac{\partial I_D}{\partial V_T} = -\beta Q(V_{DD}D - V_T)^{Q-1}$$

$$= -24.5^{uA}\!/_{mV}$$

$$\frac{\partial I_D}{\partial V_{DD}} = DQ\beta(V_{DD}D - V_T)^{Q-1}$$

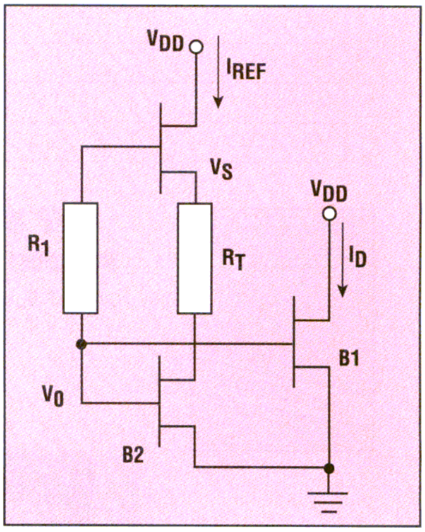

6. This schematic shows a current mirror that has a depletion-mode source.

$$= 3.40 ^{uA}\!/_{mV} \qquad (7b)$$

For the drain-feedback design of Fig. 2, a 250-Ω feedback resistor is chosen. Note that this will reduce the drain voltage.

$$V_D = V_{DD} - I_D R_f \quad = 2.3V$$

$$V_{GS} \quad = 388.3mV$$

$$D \quad = 0.1688$$

$$\frac{\partial I_D}{\partial V_T} = \frac{1}{R_f D}$$

$$\left[-1 + \frac{1}{\sqrt{1 + 4DR_f\beta'(V_{DD}D - V_T)}}\right]$$

$$= -12.0 ^{uA}\!/_{mV}$$

$$\frac{\partial I_D}{\partial V_{DD}} = \frac{1}{R_f}$$

$$\left[1 - \frac{1}{\sqrt{1 + 4DR_f\beta'(V_{DD}D - V_T)}}\right]$$

$$= 2.03 ^{uA}\!/_{mV}. \qquad (7c)$$

With a +0.5-VDC penalty, there is approximately a 200-percent improvement in both parameters. Further improvement could be made at the expense of voltage headroom by increasing the value of the feedback resistor.

In most cases, the voltage drop in the drain path is not tolerable because it wastes power and may prevent device stacking. One alternative is to scale down the circuit of Fig. 2 and use it as a reference for a larger device (Fig. 7). Although some power is used in this biasing approach, it supports more headroom in the biased device. Due to scaling, the added power may be minimal. The series resistor in Example 1 consumes 1 mW. For an equivalent power consumption at V_{DD} = +2.8 VDC, current flow can reach 357 μA. If a compensated reference for >357 μA is used, then more power can be conserved as well. The general approach to this technique is described in the Dummy Bias Circuit section. In that section, one needs to know the compensation characteristics of various candidates. For the circuit of Fig. 2, the change in V_G versus V_T is derived in Eq. 8.

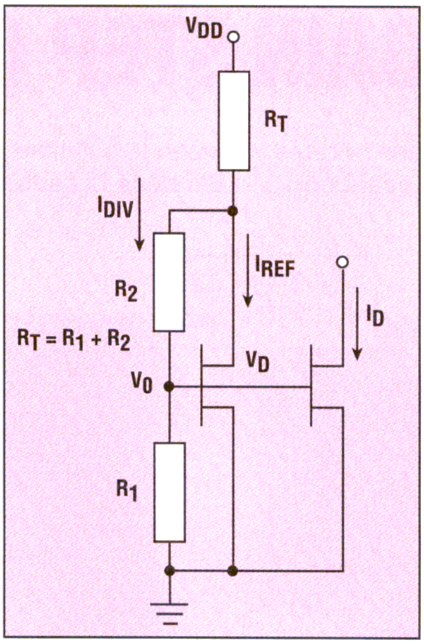

7. This schematic illustrates mirroring to a dummy device.

$$V_{GS} = D\left(V_{DD} - I_D R_f\right)$$

$$= V_T - \frac{1}{2R_f D\beta'}$$

$$\left(1 - \sqrt{1 + 4DR_f\beta'(V_{DD}D - V_T)}\right)$$

$$\frac{\partial V_G}{\partial V_T} = 1 -$$

$$\frac{1}{\sqrt{1 + 4DR_f\beta'(V_{DD}D - V_T)}} \qquad (8)$$

The ideal result in Eq. 8 would be +1. This would imply that V_{GS} tracks changes in V_T perfectly. For the reference case, the result is zero because V_{GS} is fixed. The result in Eq. 8 can be made closer to the ideal by increasing the value of the feedback resistor. Using the circuit as a V_G reference permits operating the device at lower drain voltages because there is no varying signal voltage.

Just as the gate voltage can be made V_T dependent, so can the source voltage. If the gate voltage is held fixed, then V_{GS} follows the source. Figure 3 shows the circuit employing current feedback in the source.

$$I_D = \beta'\left(V_{DD}D - I_D R_f - V_T\right)^2$$

$$I_D = \frac{1}{R_f}$$

$$\left[V_{DD}D - V_T + \frac{1}{2R_F\beta'}\left(1 - \sqrt{1 + 4R_f\beta'(V_{DD}D - V_T)}\right)\right]$$

$$\frac{\partial I_D}{\partial V_T} = \frac{1}{R_f}$$

$$\left(-1 + \frac{1}{\sqrt{1 + 4R_f\beta'(V_{DD}D - V_T)}}\right)$$

$$\frac{\partial I_D}{\partial V_{DD}} = \frac{D}{R_f}$$

$$\left(1 - \frac{1}{\sqrt{1 + 4R_f\beta'(V_{DD}D - V_T)}}\right) \qquad (9a)$$

Equation 9a would appear to have an advantage over that for the previous circuit because, for the same voltage drop in the current path, there is more feedback. This is because the voltage divider ratio, D, does not reduce the effectiveness of R_f. Voltage sensitivity should be reduced also since D appears in the numerator. Remember that D < 1.

Example 2 (using the same values as in Example 1)

$$V_S \quad = 500mV, \quad V_{GS} \quad = 388.3mV$$

$$D \quad = 0.3173$$

$$\frac{\partial I_D}{\partial V_T} \quad = -3.44uA/mV$$

$$\frac{\partial I_D}{\partial V_{DD}} \quad = 1.10uA/mV \qquad (9b)$$

For the same voltage drop in the device path, the circuit of Fig. 3 performs much better. As in Example 1, the sensitivity to V_{DD} is worse than predicted in Example 2 due to channel-length modulation. The decrease in V_T sensitivity is directly attributable to the fact that the current-sense (feedback) voltage is not divided. This is not a linear relationship, however.

$$V_{GS} = V_{DD}D - I_D R_f$$

$$= V_T - \frac{1}{2R_F\beta'}$$

$$\left(1 - \sqrt{1 + 4R_f\beta'(V_{DD}D - V_T)}\right)$$

$$\frac{\partial V_{GS}}{\partial V_T} =$$

4mm² TDMA PA SELLS FOR $1*

First TDMA Cellular Band PA in Chip-Scale Package

The MAX2251 has been designed for use at 824MHz to 849MHz in single-band or dual-band TDMA phone applications. The die-level chip-scale package allows for both very compact implementation size and inherently lower cost than devices in conventional packages.

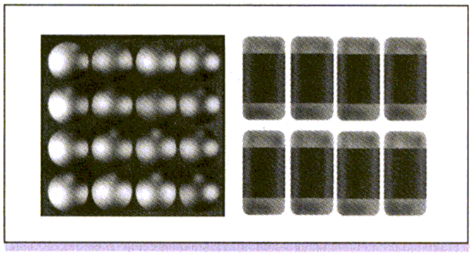

Measuring only 2mm x 2mm, the MAX2251 occupies less space than eight 0402 components.

ACPR/ALT. vs. OUTPUT POWER
V_{CC} = 3.3V

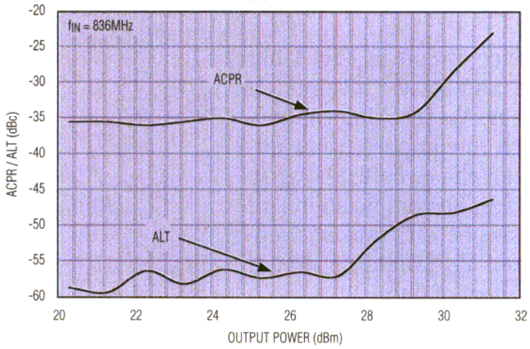

- **>30dBm TDMA Output Power**
- **>32dBm AMPS Output Power**
- **On-Chip Power Detector with 29dB Dynamic Range**
- **41% TDMA Efficiency**
- **51% AMPS Efficiency**

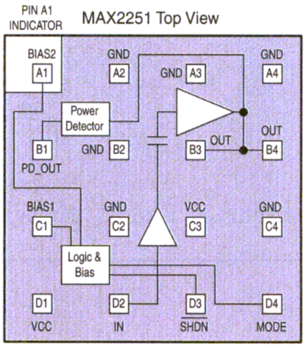

The two-stage PA MAX2251 also includes an on-chip power detector.

*1M units per month/FOB USA.

FREE* Cellular/PCS Phones Design Guide—*Sent Within 24 Hours!
Includes: Reply Cards for Free Samples and Data Sheets

CALL TOLL-FREE 1-800-998-8800 for a Design Guide or Free Sample
6:00 a.m. – 6:00 p.m. Pacific Time

MAXIM
www.maxim-ic.com

2000 EDITION!
FREE FULL-LINE DATA CATALOG ON CD-ROM

ISO 9001

NEW! Get Price, Delivery, and Place Orders Online at www.maxim-ic.com

Maxim Integrated Products, 120 San Gabriel Drive, Sunnyvale, CA 94086, (408) 737-7600, FAX (408) 737-7194.
Distributed by Maxim Distribution, Arrow, Avnet Electronics Marketing, CAM RPC, Digi-Key, Elmo, Nu Horizons, and Zeus.
Distributed in Canada by Arrow and Avnet Electronics Marketing.

CIRCLE NO. 244

$$\left(1-\frac{1}{\sqrt{1+4R_f\beta'\left(V_{DD}D-V_T\right)}}\right) \qquad (10a)$$

Source feedback should also improve the tracking of V_{gs}. Equation 10a shows this, but the problem with using this as a separate reference is that V_G is not referenced to 0 VDC, and V_G and V_S must be extracted. Perhaps a bigger problem is the fact that considerable current must be sourced into the low-impedance source of the controlled device.

Example 3

The reference circuit in Fig. 1 has fixed source and gate voltages. It therefore has no V_T tracking capability with which to compare other circuits. However, the circuits shown in Figs. 2 and 3 can be compared in this respect. As expected, source feedback produces V_T tracking that is closer to the ideal of one.

For drain feedback,

$$\frac{\partial V_{GS}}{\partial V_T} = 0.3914$$

For source feedback

$$\frac{\partial V_{GS}}{\partial V_T} = 0.8596 \qquad (10b)$$

A variant of the circuit in Fig. 3 that can be used for depletion-mode devices is shown in Fig. 4. This circuit has the advantage of referencing the gate voltage to 0 VDC. It also is not influenced by the supply voltage, if channel-length modulation is ignored. The circuit in Fig. 4 works well in stabilizing current but is still difficult to use as a reference circuit. The feedback resistor in the source is also not independently controllable because it determines drain current and the amount of feedback.

$$V_{GS} = -I_D R_F$$

$$I_D = \beta'\left(I_D R_f + V_T\right)^2$$

$$I_D = \frac{1}{R_f}$$

$$\left[-V_T + \frac{1}{2R_F\beta'}\left(1+\sqrt{1-4R_f\beta'V_T}\right)\right]$$

$$\frac{\partial I_D}{\partial V_T} = -\frac{1}{R_f}\left(1+\frac{1}{\sqrt{1-4R_f\beta'V_T}}\right)$$

$$\frac{\partial I_D}{\partial V_{DD}} = 0$$

$$V_{GSs} = -I_D R_f$$

$$\frac{\partial V_{GS}}{\partial V_T} = 1+\frac{1}{\sqrt{1-4R_f\beta'V_T}} \qquad (11)$$

According to Eq. 11, the V_T sensitivity of the circuit shown in Fig. 4 is not as good as that in Fig. 3. Equation 11 shows that the terms in the parenthesis have the same sign, so there is no partial cancellation. Remember that V_T is actually negative. This is because depletion-mode devices are normally on. A source voltage has to be developed to turn the device off.

An alternative to the previously mentioned methods is the current mirror shown in Fig. 5. The relationship between I_D and I_{REF} is rather simple and is derived in equation 12. The function of the circuit relies on the fact that B2 and B1 have the same V_T and that they track. If they are not equal or they do not track, the mirror will not work correctly. Note that the greater the difference between V_G and V_T, the less the sensitivity to V_T mismatch.

$$I_D = \beta_1\left(V_{GS}-V_T\right)^2$$

$$I_{REF} = \beta_2\left(V_G-\left(V_T+\Delta V_T\right)\right)^2$$

$$\frac{I_D}{I_{REF}} = \frac{\beta_1\left(V_{GS}-V_T\right)^2}{\beta_2\left(V_G-\left(V_T+\Delta V_T\right)\right)^2} =$$

$$\frac{\beta_1}{\beta_2}\left(1+\frac{\Delta V_T}{V_G-V_T-\Delta V_T}\right)^2$$

if there is no mismatch, $\Delta V_T = 0$ *and*

$$I_D = I_{REF}\frac{\beta_1}{\beta_2} = \text{current mirror} \qquad (12)$$

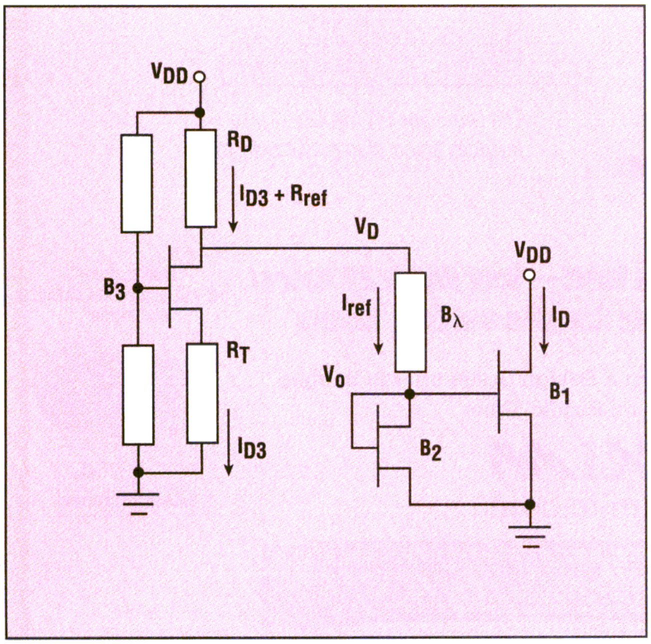

8. This schematic depicts threshold-voltage feedback through drain voltage.

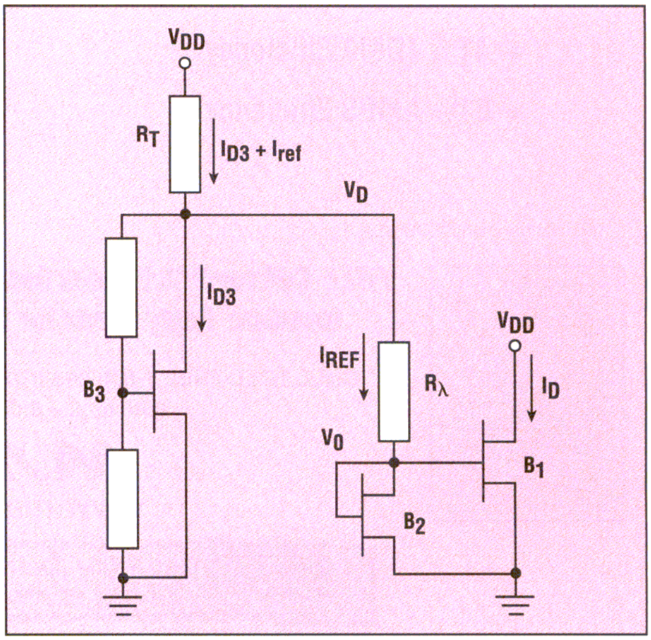

9. This schematic shows an alternative method of threshold-voltage feedback through drain voltage.

LOWEST DISTORTION
SINGLE +5V 300MHz ADC DRIVERS

LOW DISTORTION

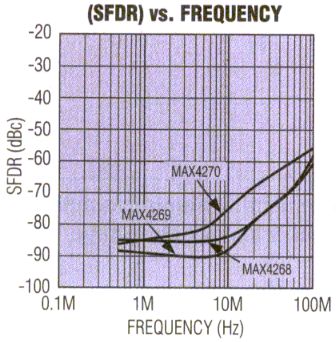

SINGLE SUPPLY

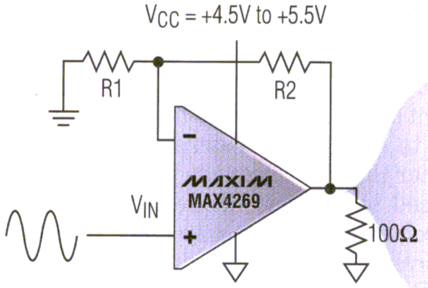

HIGH SPEED

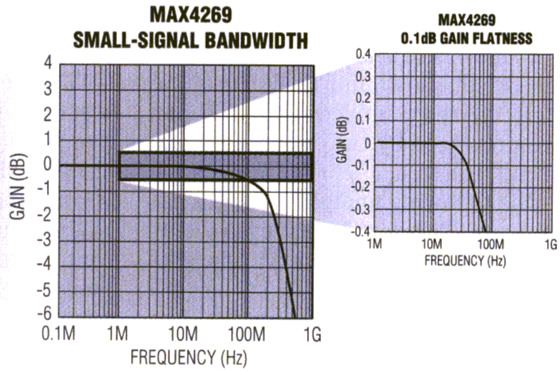

- Single +4.5V to +5.5V Supplies
- 900V/µs Slew Rate
- -90dBc SFDR (MAX4269)
- ±45mA Output Drive Current
- Low Noise: 8nV/√Hz
- 350MHz -3dB Bandwidth (MAX4269)

PART	NO. OF OP AMPS	MINIMUM STABLE GAIN (V/V)	BANDWIDTH (MHz)	0.1% SETTLING TIME (ns)	SFDR @ f_C = 5MHz (dBc)	PACKAGE
MAX4265*	1	1	300	15	85	8-SO, 8-µMAX
MAX4266*	1	2	350	15	90	8-SO, 8-µMAX
MAX4267*	1	5	200	15	82	8-SO, 8-µMAX
MAX4268	2	1	300	15	85	14-SO, 16-QSOP
MAX4269	2	2	350	15	90	14-SO, 16-QSOP
MAX4270	2	5	200	15	82	14-SO, 16-QSOP

*Future product.

FREE* Video Design Guide—*Sent Within 24 Hours!
Includes: Reply Cards for Free Samples and Data Sheets

CALL TOLL-FREE 1-800-998-8800 for a Design Guide or Free Sample
6:00 a.m. – 6:00 p.m. Pacific Time

MAXIM
www.maxim-ic.com

2000 EDITION!
FREE FULL-LINE DATA CATALOG
ON CD-ROM

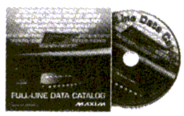

ISO 9001

NEW! Get Price, Delivery, and Place Orders Online at www.maxim-ic.com

Maxim Integrated Products, 120 San Gabriel Drive, Sunnyvale, CA 94086, (408) 737-7600, FAX (408) 737-7194.
Distributed by Maxim Distribution, Arrow, Avnet Electronics Marketing, CAM RPC, Digi-Key, Elmo, Nu Horizons, and Zeus.
Distributed in Canada by Arrow and Avnet Electronics Marketing.

The problem with the circuit of Fig. 5 is that it depends on a stable current source to make it work. Since the difficulty in stabilizing the current has been shown already, the mirror really does not accomplish much here. In fact, variations in I_{REF} are multiplied by the β ratio. This ratio is usually made rather high in order to limit the current consumption in the bias circuit.

To illustrate this problem, consider the circuit shown in Fig. 6. Here, the ideal current source of Fig. 5 has been replaced by the depletion-mode circuit of Fig. 4.

The following analysis shows what happens. The sensitivity of the current source to V_T variations was given in Eq. 11.

$$I_{REF} = \frac{1}{R_f}\left[-V_T + \frac{1}{2R_f\beta_2}\left(1+\sqrt{1-4R_f\beta_2 V_T}\right)\right]$$

$$I_D = I_{REF}\frac{\beta_1}{\beta_2}$$

$$\frac{\partial I_D}{\partial V_T} = -\frac{1}{R_f}\frac{\beta_1}{\beta_2}\left(1+\frac{1}{\sqrt{1-4R_f\beta_2 V_T}}\right) \quad (13)$$

As clearly shown in Eq. 13, the β ratio reduces the beneficial effect of R_f in the current source. The device is also tracking depletion-mode-threshold changes, which tend to be wider than enhancement-mode variations. Finally, due to the depletion-mode current source there is no partial cancellation (Eq. 11).

The circuits shown in Figs. 2 and 3 have reasonable performance, but they require the use of a resistor in the current path. There are several basic ways these circuits can be used. The simplest way is using the gate voltage of the circuit of Fig. 2 directly to control a larger device. This is shown in Fig. 8. The required control equations are given in Eqs. 6, 7, and 8. The "dummy" bias circuit is set to operate at a much-lower current than the biased device. This effectively establishes a current mirror. Variations in the reference current are multiplied by the β ratio (Eq. 14).

using (7)

$$\frac{\partial I_D}{\partial V_T} = \frac{\beta_1}{\beta_2}\frac{1}{R_F D}\left[-1+\frac{1}{\sqrt{1+4DR_f\beta'(V_{DD}D-V_T)}}\right] \quad (14)$$

The type of current source in this circuit offers some cancellation, and therefore has an advantage over that of Fig. 6.

The circuit shown in Fig. 3 has the best current control and would therefore seem to be a better reference. Since neither the source nor the gate is referenced to ground, extracting V_{GS} is a problem. One way to circumvent this problem is to use the circuit shown in Fig. 8. An analysis of this circuit becomes somewhat complex unless some simplifications are made. One would like to assume that $I_{REF}<I_{D3}$. This is unlikely, since B3 and B2 are small and approximately equal in size to minimize current. Since the goal is to keep I_{REF} constant, a good approximation is that the voltage change at V_D is due almost entirely to changes in the current I_{D3}.

In Eq. 15, the drain voltage of B3 is a positive function of V_T. This now offers the potential for compensation.

from (9)

$$I_{D3} = \frac{1}{R_f}\left[V_{DD}D - V_T + \frac{1}{2R_f\beta_3}\left(1-\sqrt{1+4R_f\beta_3(V_{DD}D-V_T)}\right)\right]$$

$$V_D = V_{DD} - I_D R_D$$

$$V_D = V_{DD}\left(1-D\frac{R_D}{R_f}\right)+\frac{R_D}{R_f}\left[V_T - \frac{1}{2R_f\beta_3}\left(1-\sqrt{1+4R_f\beta_3(V_{DD}D-V_T)}\right)\right] \quad (15)$$

The current I_{REF} is given in Eq. 16. The goal is to keep this current constant so that it is mirrored properly to I_D. In the current mirror, V_G is not constant and should track V_T precisely. If V_D tracks V_T, then I_{REF} should be constant.

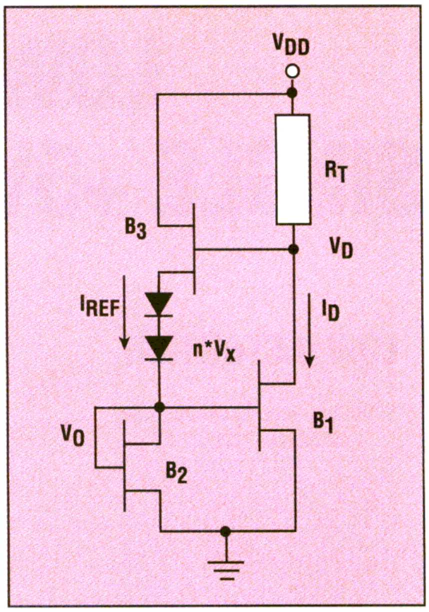

10. This schematic illustrates active feedback of drain-sense voltage

$$I_{REF} = \frac{V_D - V_G}{R_A}$$

$$\frac{\partial V_D}{\partial V_T} = \frac{R_D}{R_f}\left(1-\frac{1}{\sqrt{1+4R_f\beta_3(V_{DD}D-V_T)}}\right) = 1$$

$$\frac{R_f}{R_D} = 1-\frac{1}{\sqrt{1+4R_f\beta_3(V_{DD}D-V_T)}} \quad (16)$$

Equation 16 shows that it is possible to stabilize the current with respect to V_T changes, at least about V_T. Not all variables are ratios, however, so there will be some drift. Sensitivity is reduced by increasing R_a and V_D. In the absence of perfect cancellation, the change in I_D versus V_T is derived in Eq. 17.

$$\frac{\partial I_{REF}}{\partial V_T} = \frac{1}{R_A}\left(\frac{\partial V_D}{\partial V_T} - \frac{\partial V_G}{\partial V_T}\right) = \frac{1}{R_A}\left(\frac{\partial V_D}{\partial V_T} - 1\right)$$

$$\frac{\partial I_D}{\partial V_T} = \frac{\beta_1}{\beta_2 R_A}\left(\frac{R_D}{R_f}\left(1-\frac{1}{\sqrt{1+4R_f\beta_3(V_{DD}D-V_T)}}\right)-1\right) \quad (17)$$

bring your
design team
together with
SystemView
BY ELANIX
The program manager gets a complete view of the project at hand, including the immediate effects of changes.
The DSP designer gets bit-true simulation and a direct path to TI C5x/C6x DSP implementation.
The systems architect can build his working simulation with easy to use functional blocks—then hand off to DSP and RF designers.
The RF designer can design with distortion-true system blocks, then move directly to Xpedion simulation tools.

The sensitivity to supply variations of the circuit shown in Fig. 8 is given in Eq. 18.

While it appears that sensitivity to supply variations can be minimized, it cannot be controlled independently of V_T sensitivity.

$$\frac{\partial V_D}{\partial V_{DD}} = 1 + D\frac{R_D}{R_f}\left(\frac{1}{\sqrt{1+4R_f\beta_3(V_{DD}D - V_T)}} - 1\right)$$

for condition of (16)

$$\frac{\partial V_D}{\partial V_{DD}} = 1 - D$$

$$\frac{\partial I_{REF}}{\partial V_{DD}} = \frac{1}{R_A}\frac{\partial V_D}{\partial V_{DD}}$$

$$\frac{\partial I_D}{\partial V_{DD}} = \frac{\beta_1}{\beta_2 R_A}\frac{\partial V_D}{\partial V_{DD}} \qquad (18)$$

If one replaces the portion of the circuit that is shown in Fig. 8 represented by Fig. 3 with that of Fig. 2, some interesting results can be obtained. The new circuit is illustrated in Fig. 9. For practical values, the circuit will overcompensate for V_T changes. This is the result of the "V_G multiplier" effect at V_D, and it is seen directly in Eq. 19 where the 1/D term is in front. Supply sensitivity is less with this circuit than that of Fig. 8.

from (6)

$$I_{D3} = \frac{1}{R_f D}\left[V_{DD}D - V_T + \frac{1}{2R_f D\beta_3}\left(1 - \sqrt{1+4DR_f\beta_3(V_{DD}D - V_T)}\right)\right]$$

$$V_D = V_{DD} - I_d R_f$$

$$V_D = \frac{1}{D}\left[V_T - \frac{1}{2R_f D\beta_3}\left(1 - \sqrt{1+4DR_f\beta_3(V_{DD}D - V_T)}\right)\right]$$

$$\frac{\partial V_D}{\partial V_T} = \frac{1}{D}\left[1 - \frac{1}{\sqrt{1+4DR_f\beta_3(V_{DD}D - V_T)}}\right]$$

$$\frac{\partial V_D}{\partial V_{DD}} = \frac{1}{\sqrt{1+4DR_f\beta_3\left(V_{DD}D-V_T\right)}} \qquad (19)$$

When reflected to the drain current of the biased device, the sensitivity is given in Eq. 20.

$$\frac{\partial I_D}{\partial V_T} = \frac{\beta_1}{\beta_2 R_A}\left(\frac{\partial V_D}{\partial V_T}-1\right)$$

$$\frac{\partial I_D}{\partial V_T} = \frac{\beta_1}{\beta_2 R_A}\left(\frac{1}{D}\left[1-\frac{1}{\sqrt{1+4DR_f\beta_3\left(V_{DD}D-V_T\right)}}\right]-1\right)$$

$$\frac{\partial I_D}{\partial V_{DD}} = \frac{\beta_1}{\beta_2 R_A}\left(\frac{1}{\sqrt{1+4DR_f\beta_3\left(V_{DD}D-V_T\right)}}\right) \qquad (20)$$

In the circuit shown in Fig. 2, a resistive divider was used to feed drain-voltage changes back to the gate for V_T compensation. A variation of this circuit uses active feedback and is shown in Fig. 10. It eliminates the divider current and the divider ratio, but it introduces another V_T component. Still, under certain circumstances, it can deliver slightly better performance than the circuit of Fig. 2. The diodes in Fig. 10 are used for level shifting. The number required depends on the implementation. To understand the requirement for the diodes, consider V_D. This voltage is set by V_{DD} and the voltage drop across R V_f. The drain-gate voltage of B_1 is then $V_D - V_G$. This is also the V_{GS} of B_3 if no steps are taken to raise the source voltage of B_3.

By equating I_{REF} and I_D, and by using Eq. 12, the analysis in Eq. 20 proceeds to Eq. 21.

$$\sqrt{\frac{I_{REF}}{\beta_3}} = V_D - V_S - V_T =$$

$$V_{DD} - I_D R_f - \left(V_D + n * V_X\right) - V_T$$

$$\sqrt{\frac{I_D\beta_2}{\beta_3\beta_1}} = V_{DD} - n*V_X - 2V_T - \sqrt{\frac{I_D}{\beta_1}} - I_D R_f$$

$$\sqrt{\frac{I_D}{\beta_1}}\left(1+\sqrt{\frac{\beta_2}{\beta_3}}\right) = V_{DD} - n*V_X - 2V_T - I_D R_f$$

$$I_D = \frac{1}{R_f}\left(\left(V_{DD}-n*V_X-2V_T\right)+\frac{\left(1+\sqrt{\frac{\beta_2}{\beta_3}}\right)^2}{2\beta_1 R_f}\left(1-\sqrt{1+\frac{4\beta_1 R_f\left(V_{DD}-n*V_X-2V_T\right)}{\left(1+\sqrt{\frac{\beta_2}{\beta_3}}\right)^2}}\right)\right) \tag{21}$$

Equation 21 simplifies somewhat if B_1 and B_2 have the same beta, as shown in Eq. 22.

$$\text{for } \beta_2 = \beta_3$$

$$I_D = \frac{1}{R_f}\left(\left(V_{DD}-n*V_X-2V_T\right)+\frac{2}{\beta_1 R_f}\left(1-\sqrt{1+\beta_1 R_f\left(V_{DD}-n*V_X-2V_T\right)}\right)\right) \tag{22}$$

The sensitivity to V_T now has a factor of 2, as shown in Eq. 23a.

$$\frac{\partial I_D}{\partial V_T} = \frac{2}{R_f}\left(-1+\frac{1}{\sqrt{1+\beta_1 R_f\left(V_{DD}-n*V_X-2V_T\right)}}\right)$$

$$\frac{\partial I_D}{\partial V_{DD}} = \frac{1}{R_f}\left(1-\frac{1}{\sqrt{1+\beta_1 R_f\left(V_{DD}-n*V_X-2V_T\right)}}\right)$$

$$\frac{\partial I_D}{\partial V_X} = \frac{n}{R_f}\left(-1+\frac{1}{\sqrt{1+\beta_1 R_f\left(V_{DD}-n*V_X-2V_T\right)}}\right) \tag{23a}$$

Example 4

Consider what would happen if one decided to use active feedback instead of a divider for the circuit in Fig. 1. For the same V_{DS} of +2.3 VDC, three diodes would be required in order to shift the level. This assumes B_{T2} and B_3 are sized equally and that the voltage V_X is approximately 550 mV.

$$\frac{\partial I_D}{\partial V_T} = -5.87uA/mV \tag{23b}$$

This is a 200-percent improvement in V_T sensitivity over the circuit in Example 1. The sensitivity to V_{DD} is slightly worse.

$$\frac{\partial I_D}{\partial V_{DD}} = \frac{1}{250}\left(1-\frac{1}{\sqrt{1+0.075*250(2.8-3*0.55-2*0.225)}}\right) = 2.90uA/mV \tag{23c}$$

A new sensitivity is introduced in terms of the level-shifting diodes. While the absolute value of the drops are not too critical, temperature variation could be significant.

$$\frac{\partial I_D}{\partial V_X} = \frac{3}{250}\left(-1+\frac{1}{\sqrt{1+0.075*250*(2.8-3*0.55-2*0.225)}}\right) = -8.81uA/mV \tag{23d}$$

The sensitivity to diode voltage is a direct function of the number of diodes.

None of these circuits is designed to be independent of the power supply. The sensitivity of each circuit to power-supply variations is given on the assumption that channel-length modulation can be ignored. This is not realistic, but long-gate-length devices in the non-RF components can be used to reduce these effects. ••

Design Regular-And Irregular-Print Coupled Lines

This article explores the basics of coupled lines and offers practical designs for lowpass filters and phase shifters.

Leo Maloratsky
Principal Engineer
Rockwell Collins, 2100 Hibiscus Blvd., Melbourne, FL 32901; (407) 953-1729, FAX: (407) 953-1646, e-mail: lgmalora@mbnotes.collins.rockwell.com.

COUPLED lines are useful and widely applied structures that provide the basis for many types of components, including directional couplers, power splitters and combiners, duplexers, filters, phase shifters, transformers, baluns, etc.[1,2]

Coupled lines can be classified by several different characteristics:

- The strength of the coupling.
- The characteristic impedances of the coupled lines [i.e., whether they are equal (symmetrical lines) or nonequal (asymmetrical lines)].
- The type of transmission lines[3] [i.e., striplines, microstrip lines, etc. (Table 1 on p. 100)].
- The structure of the coupled lines (i.e., whether they are homogeneous or inhomogeneous).
- The type of output ports (i.e., whether they are terminated, open circuited, short circuited, or if they are otherwise loaded).
- The regularity or irregularity of the lines [i.e., whether or not the coupling mechanism is dominated by the time-varying electromagnetic (EM) fields or magnetic fields].

This article considers regular as well as irregular coupled lines that are due to their interesting applications.

Figures 1 and 2 of Table 1 (on p. 100) illustrate the general configuration of coupled pairs of regular striplines and microstrip lines. The two views of this configuration illustrate some general properties of the electric field under two different modes of excitation—the so-called even and odd modes. All combinations of excitation of the two lines can be expressed as a combination of the even and odd modes.

In the even mode, fundamentally, both transmission lines are identically excited by EM fields that are equal in amplitude and phase. In the odd mode, fundamentally, both transmission lines are identically excited by EM fields which are equal in amplitude but are 180 deg. out of phase. The characteristic impedances and the wave velocities are different for the even and odd modes. The characteristic impedances for the even and odd modes are denoted by Z_{0e} and Z_{0o}, respectively.

Since coupled striplines contain a homogeneous dielectric between conductors, the dominant mode of propagation is a pure transverse-electromagnetic (TEM) mode. The even and odd modes are both TEM, and the effective dielectric constant is equal to the material's dielectric constant. Thus, the wave velocities associated with the even and odd modes are

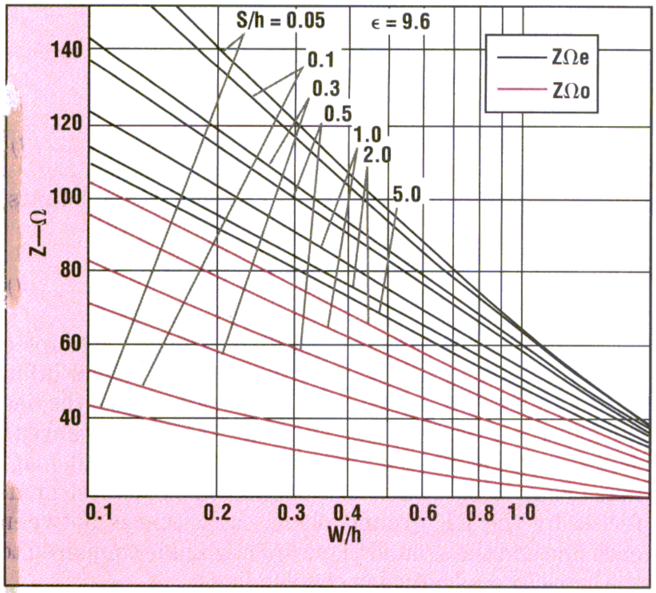

1. This graph illustrates the even- and odd-mode impedances for regular microstrip coupled lines.

equal to each other and to that in the uncoupled, individual lines.

Conceptually and pictorially, the even and odd modes in the microstrip coupled lines (Fig. 1 of Table 1) exhibit the same general field distributions as there are in the coupled striplines. But the similarities end there. The dielectric does not fill the microstrip structure homogeneously, so there is instead an effective dielectric constant that is equivalent to a weighted average of the dielectric constants of the material and the air space that is above the center conductors. With different field distributions associated with the even and odd modes, not only is there an effective dielectric constant, there are also considerably different effective dielectric constants and phase velocities associated with the even and odd modes.

The large imbalance that is between the effective dielectric constants and the related phase velocities can lead to some limitations in the application of microstrip lines. Some of these relationships between the even- and odd-mode impedances and physical dimensions of the microstrip-coupled lines are shown in Fig. 1.[4]

The plots of effective dielectric constant versus physical dimensions for microstrip coupled lines are shown in Fig. 2.[4] As S/h approaches infinity, these characteristics become identical to the characteristics of a single microstrip line.

Table 2 (p. 106) shows different regular coupled-lines networks, scattering matrix elements, and possible applications, where:

$$\Theta = \frac{2\pi l}{\Lambda} \qquad (1)$$

is the electrical length of the coupled lines; l is the physical length,

$$\Lambda = \frac{\lambda}{\sqrt{\varepsilon_{eff}}} \qquad (2)$$

is the coupled-lines guide wavelength,

$$\sqrt{\varepsilon_{eff}} = \frac{\sqrt{\varepsilon_{eff\,e}} + \sqrt{\varepsilon_{eff\,o}}}{2}, \quad \varepsilon_{eff\,e}, \varepsilon_{eff\,o} \qquad (3)$$

are even- and odd-mode effective dielectric constants, and

$$\rho = \frac{Z_{0e} + Z_{0o}}{2}, \; r = \frac{Z_{0e} - Z_{0o}}{2} \qquad (4)$$

The term "irregular coupled lines" refers to coupled lines with strong magnetic coupling and minimal influence of the RF ground plane on the parameters of the line (ideally, the absence of ground plane in the coupling area). The strong magnetic coupling is realized without magnets or ferrites.[5-7] Since an irregular line is almost unaffected by the RF ground plane, capacitances between each line and the ground plane are negligible compared to the capacitances between coupled lines.

Strong magnetic coupling between lines supports miniature dimensions and an increased bandwidth. This

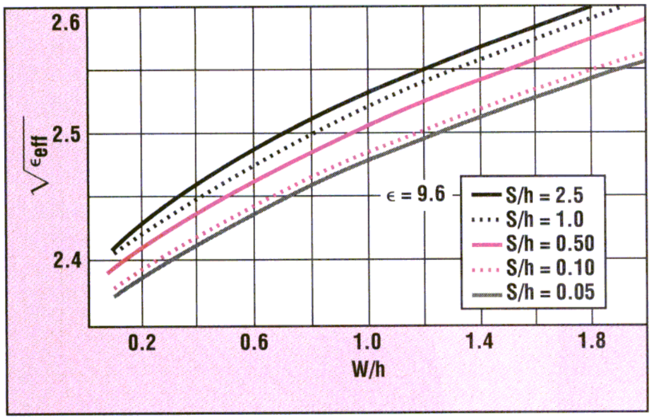

2. This graph depicts the relationship between the effective dielectric constant and the physical dimensions of regular microstrip coupled lines.

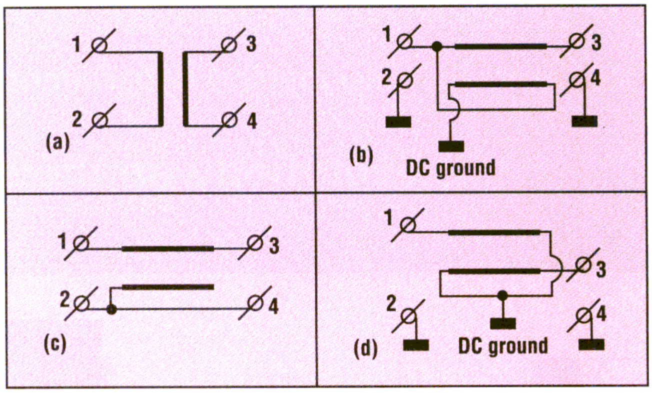

3. These diagrams describe irregular coupled lines in four configurations: vertical configuration (a), diagonal connection with one DC-grounded port (b), one port isolated (c), and diagonal connection (d).

coupling is characterized by the coefficient of magnetic coupling, k_m. In many cases, iron (Fe) or ferrite cores with large permeabilities are used to maximize k_m (k_m1). However, this approach has some disadvantages, including diminished temperature stability, high cost, and larger component dimensions. Additionally, the permeability (μ) and dielectric constant (ϵ) of ferrites may vary dramatically with frequency. The high-frequency limitations of these devices arise from core losses, winding lengths, and parasitic elements which become dominant above 1 GHz.[8]

In irregular lines, magnetic-cou-

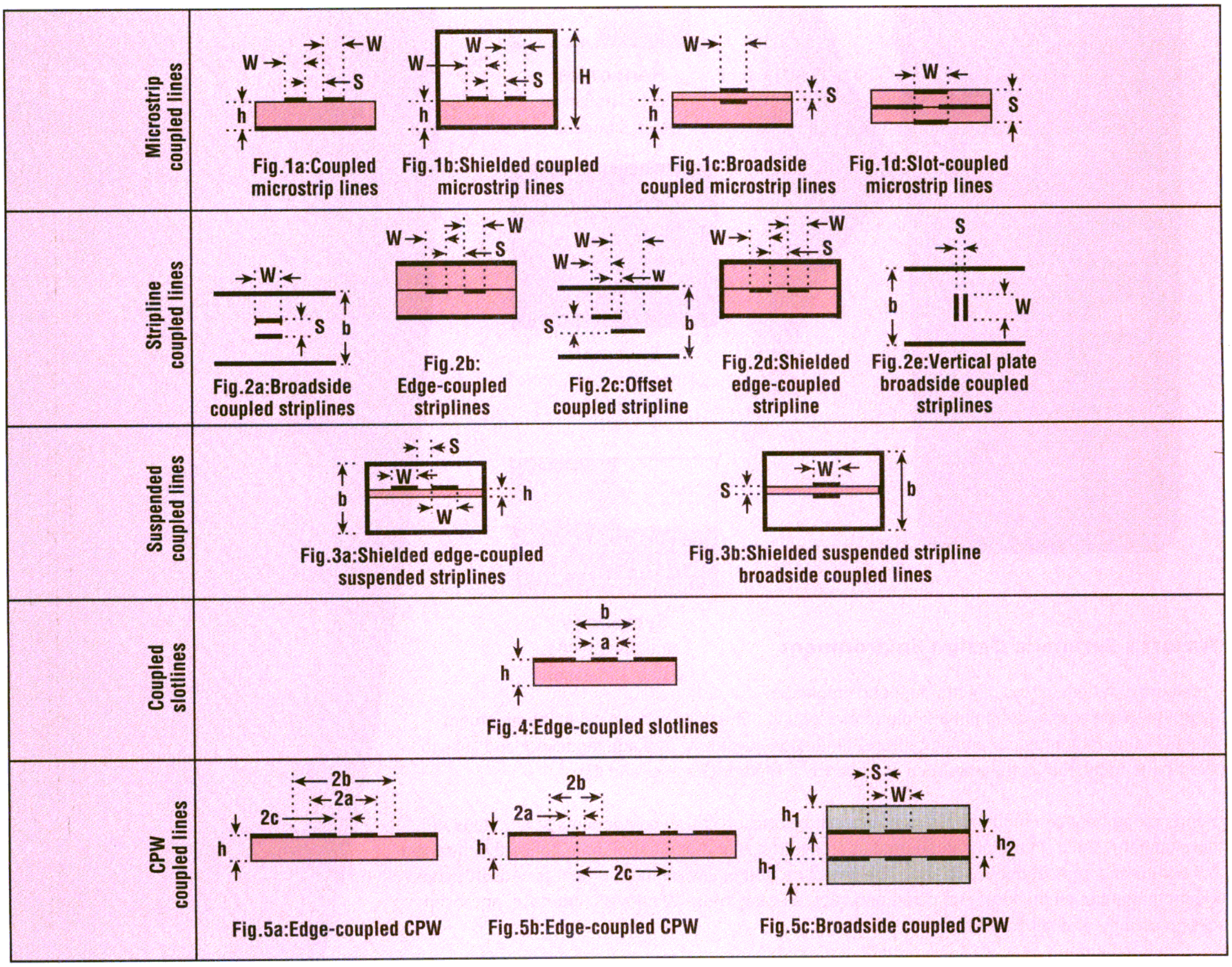

pling activation can be achieved without any cores by bringing the lines close to each other. The inductance per unit length of irregular coupled lines is given by:[5]

$$L = 2(L_0 - M) = 2L_o \left(1 - \frac{M}{L_0}\right) = 2L_o(1 - k_m), \qquad (5)$$

where:

L_0 = self-inductance per unit length of one conductor (which can be determined by isolating this line from all other parts, including the second line)

M = the mutual inductance per unit length of the two conductors, and

$$k_m = {}^{M}\!/_{L_0} \qquad (6)$$

is the coefficient of magnetic coupling between the lines

$$\left(0 < k_m \le 1\right) \qquad (7)$$

Irregular coupled lines are used in transformers, filters, phase shifters, and matching networks. Figure 3 illustrates various methods of irregular-line connections.

The vertical irregular-coupled-lines network depicted in Fig. 3a can be used for transformers, baluns, and other applications. In this case, the broadside coupled-lines length is less than the guide wavelength. A clearance is made between the ground plane and the coupled lines to increase self-inductance and to minimize parasitic capacitance to ground.[6] These irregular lines contribute the most to the magnetic-coupling factor k_m.

The circuit depicted in Fig. 3b is the well-known Ruthroff 1:4 transformer.[6] This circuit has a high-frequency limitation due to transmission-line lengths and parasitic inductance. A transformer with short irregular-coupled lines:

$$\left(l < {}^{\Lambda}\!/_{8}\right) \qquad (8)$$

and an optimum characteristic impedance provides low loss (less than 0.1 dB) and a wide operating bandwidth. With this type of transformer, it is possible to get good performance to 2 or 4 GHz.[7] Compared to a conventional transformer, a transmission-line transformer with broadside irregular-coupled lines offers higher efficiency, greater bandwidth, and simpler construction.[9]

In ultra-high-frequency (UHF) and L frequency ranges, lowpass filters with irregular lines (Fig. 3c) have small physical dimensions and low cost. One cascade of this filter is illustrated in Fig. 4a. The electrical length Θ of this cascade is small, therefore:

$$\tan\left({}^{\Theta}\!/_{2}\right) \approx {}^{\Theta}\!/_{2} \qquad (9)$$

The Marketing Guy Said No.
The Test People Said No.
The Applications Engineer Said No.
The Designers Said Maybe.

But Shep Said Yes.

It doesn't always make sense to give customers more than they think they need. After all, if testing for PCS and wireless happens right now at 0.8 to 1.9 GHz, it makes sense to do an amp that tests there. No unwanted extras. No stress on anyone's budget. At least that's what the experts say.

But here's wisdom: things are changing so fast in the wireless world, there's little logic in manufacturing or buying anything that meets only immediate needs. Only a brain donor would bank on an amp with a really narrow band. A more righteous approach gives you room at the top— extra band you're gonna be glad you have in the test room, where performance counts. And tomorrow, when the rules are rewritten.

Shep knows this. He knew it all along. That's why he insisted AR "S" Series amplifiers each offer bandwidth from 0.8 to 4.2 GHz and power from 1 to 200 watts, in increments just right for your application. With low harmonics. And other extras, like IEEE 488 and RS 232 interface for remote operation.

For frequency response to 40 GHz, ask about our other brainchild –"T" Series amplifiers 0.8 to 40 GHz, 15 to 2000 watts.

Don "Shep" Shepherd. Visionaire. President, Amplifier Research.

www.amplifiers.com/@/mrf-shep

ISO 9001
Certified

AMPLIFIER® RESEARCH

CIRCLE NO. 217

USA 215-723-8181 or 800-933-8181 for an applications engineer.
In Europe, call EMV– Munich: 89-614-1710 • London: 01908-566556 • Paris: 1-64-61-63-29 • Amsterdam: 31-172-423-000

The Force Behind The Field.


SONNET® EM® SUITE
+ CST MICROWAVE STUDIO™
DESIGN SUCCESS

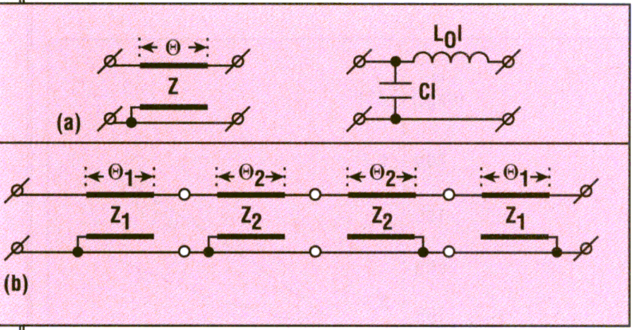

4. These diagrams show two lowpass filters using irregular coupled lines: isolation of one port (a) and lowpass-filter ladder network (b) .

(when $k_m > 0.8$).

The relationships between filter parameters are:[5]

$$Z\Theta = \omega Ll = 2\omega L_o l(1 - k_m),$$
$$\frac{\Theta}{Z} = \omega Cl, \qquad (10)$$

where:

C and L = the capacitance and inductance per unit length, and
Z = the impedance of the irregular-coupled lines.

A lowpass filter based on irregular lines can be realized by a cascade connection (Fig. 4b), with parameters chosen to meet the required characteristics of the prototype.[2]

Figure 5a illustrates a 180-deg. phase shifter[10] that uses diagonally connected irregular lines. Each part of the phase shifter is indicated by a number or letter. The phase shifter includes a single transmission line (1), and irregular-coupled lines (2), and is represented in the structure shown in Fig. 3d.

In Fig. 3d, the output port of the first coupled line, 1-3, is electrically connected with the diagonal end of the second coupled line, 2-4, and DC coupled to ground. The segment providing the diagonal connection should be as short as possible. This can be accomplished by bending the line into a ring or a rectangular frame. The RF ground must be distant from the irregular lines and close to the appropriate input/output (I/O) lines.

In Fig. 5a, the irregular lines (2) contain two parallel broadside-coupled lines—one of them (3) is located on top of the relatively thin dielectric substrate (5), and the other (4) is located on the underside of the substrate. Strong magnetic coupling supports the small length of the irregular lines. This effect is intensified by the elimination of the ground plane from the area (6) directly below the coupled lines.

The coupled lines have a short-circuit connection that is between the end of line (3) and the end of line (4), which is located at (7) and (8), respectively. The connection that completes this short circuit (19) is also DC con-

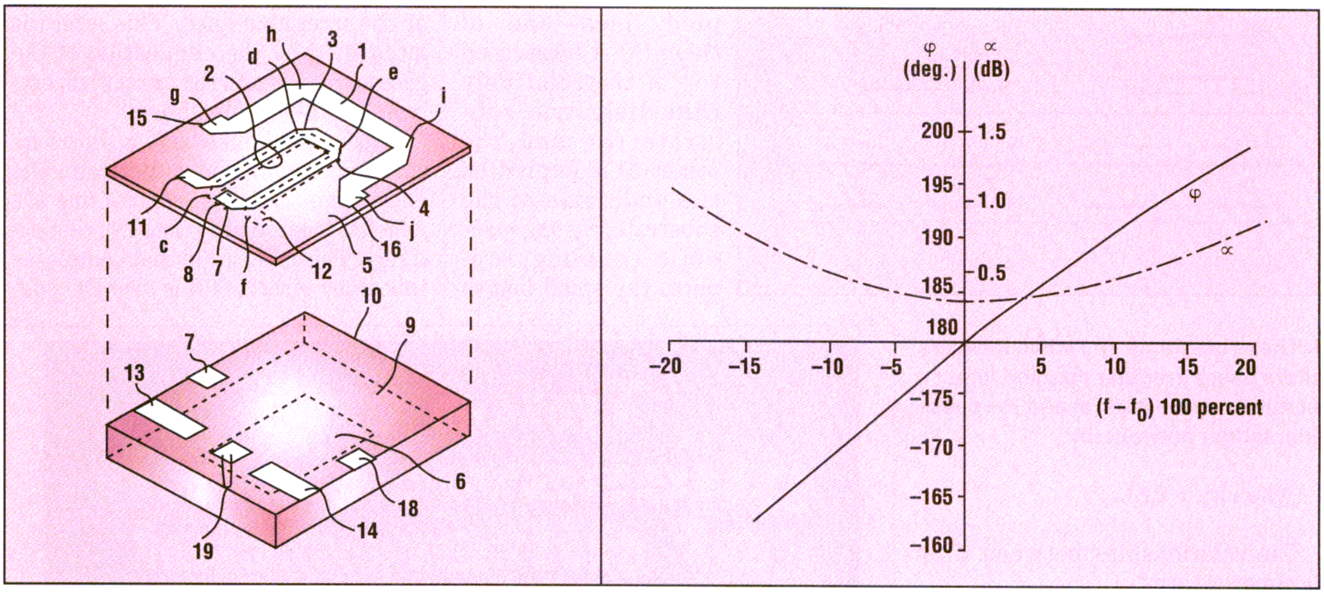

5. This is an isometric view of a printed 180-deg. differential phase shifter with irregular coupled lines (left). This graph depicts the phase shift (in degrees) and the loss (in decibels) depending on relative tuning (in percent) [right].

nected to ground plane (9) of the single line (1). The ground plane (9) is located on the base (10) of the dielectric substrate.

The input (11) and output (12) of the coupled lines are electrically interconnected by a corresponding input (13) and output (14) on the base dielectric substrate. The single-line (1) input (15) and output (16) are electrically interconnected by a corresponding input (17) and output (18).

The electrical length Θ_i of the irregular lines is equal to the electrical length Θ_S of the single line:

$$\Theta_i = \Theta_s \qquad (11)$$

where:

$$\Theta_i = \frac{2\pi l_i}{\Lambda_i} \qquad (12)$$

and

$$\Theta_s = \frac{2\pi l_s}{\Lambda_s} \qquad (13)$$

Λ_i and Λ_5 are wavelengths in the irregular and single lines. The physical length of the irregular line (cdef) l_I = (0.02—0.08) Λ_i depends on the coefficient of magnetic coupling k_m. For example, for k_m = 0.9, the physical length of the irregular coupled lines is 0.027 Λ_n.

Figure 5b shows that phase shift (in degrees) and loss (in decibels) depend on the relative detuning (in percent) for the 180-deg. differential phase (with the length of the irregular coupled lines $l_I = 0.055\Lambda_i$). The lines were designed on a Kapton™ dielectric 0.003-in. (0.008-cm)-thick (center frequency = 120 MHz). ●●

#	Regular coupled-line schematic	Scattering matrix parameters	Application
1	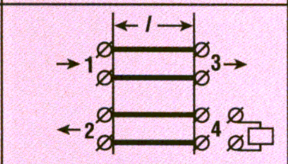	$S_{13} = S_{24} = S_{31} = S_{42} = \frac{1}{\cos\Theta + i\rho \sin \theta}$ $S_{12} = S_{21} = S_{34} = S_{43} = \frac{ir \sin\Theta}{\cos\Theta + i\rho \sin \theta}$	Directional coupler, Power divider and combiner
2	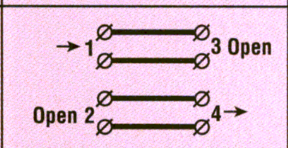	$S_{11} = S_{22} = \frac{1 - r^2 \sin^2 \Theta}{\cos\Theta + i\rho \sin \Theta}$ $S_{12} = S_{21} = \frac{-i2r \sin \Theta}{\cos\Theta + i\rho \sin \Theta}$	Bandpass filter, Transformer, DC block
3	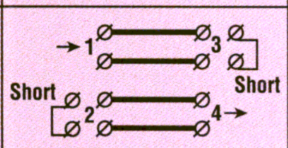	$S_{11} = S_{22} = \frac{1 - r^2 \sin^2 \Theta}{\cos\Theta + i\rho \sin \Theta}$ $S_{12} = S_{21} = \frac{i2r \sin \Theta}{\cos\Theta + i\rho \sin \Theta}$	Bandpass filter
4	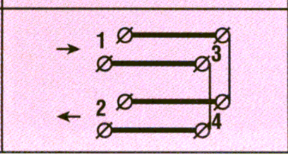	$S_{11} = S_{22} = -i\frac{(r^2 - \rho^2 + 1) \sin 2\Theta}{2(\rho\cos 2\Theta + r) + i \sin 2\Theta(1 - r^2 + \rho^2)}$ $S_{12} = S_{21} = \frac{2(r\cos 2\Theta + \rho)}{2(\rho\cos 2\Theta + r) + i \sin 2\Theta(1 - r^2 + \rho^2)}$	Schiffman phase shifter

References

1. R. Mongia, I. Bahl, and P. Bhartia, *RF and Microwave Coupled-Line Circuits*, Artech House, Norwood, MA, 1999.
2. G.L. Matthaei, L. Young, and E.M. Jones, *Microwave Filters, Impedance-Matching Networks, and Coupling Structures*, McGraw-Hill, New York, 1964.
3. L.G. Maloratsky, "Reviewing the Basic of Microstrip Lines," *Microwaves & RF*, March 2000, pp. 79-88.
4. L.G. Maloratsky, *Microminiaturization of Microwave Elements and Devices*, Soviet Radio, Moscow, 1976.
5. E. Zelyah, A. Feldstein, L. Yavich, and V. Brilon, *Miniature Devices On Base Segments of Transmission Lines At VHF and UHF Frequency Range*, Radio and Svyaz, Moscow, 1989.
6. D. Jaisson, "A Planar Impedance Transformer," *Microwave Journal*, October 1998, pp. 108-120.
7. C.L. Ruthroff, "Some Broadband Transformers," *Proceedings of the IRE.*, Vol. 47, August 1959, pp. 1337-1342.
8. M. MacDonald, "Design Broadband Passive Components with Ferrites," *Microwaves & RF*, October 1993, pp. 81, 82, 84, 86, 132.
9. J. Sevick, *Transmission Line Transformers*, NOBLE Publishing, 1996.
10. L. Maloratsky, J. Ide, *Printed 180 Degree Differential Phase Shifter.*

Create Transmission-Line Matching Circuits For Power Amplifiers

A simplified approach to the design of transmission-line matching circuits uses analytical equations to calculate the circuits elements for L, π, and T transformers.

Andrei V. Grebennikov

Institute of Microelectronics, 11 Science Park Rd., Singapore Science Park II, Singapore 117685; (65) 770 5494, FAX: (65) 773 1915, e-mail: andrei@ime.org.sg.

MATCHING circuits allow power amplifiers (PAs) to attain high gain, high linearity, high efficiency, and high stability over a narrow or wide frequency band. The techniques for designing PA-matching circuits are especially important for circuits that use transmission lines, where determining circuit parameters is more complicated than for lumped-element matching circuits. An effective approach is to use a theoretical analysis to define the appropriate matching circuit, then calculate the matching-circuit parameters to minimize final tuning and attain a stable operation mode. This article presents a transmission-line matching-circuit design based on analytical equations to calculate the circuits elements for L, π, and T transformers. The introduction of a principle of equal quality factors for multisection L transformers simplifies the calculation procedure and requires only one Q circle on the Smith chart. The article demonstrates these matching principles—analytically and by Smith chart—using two examples: a narrowband, microwave, bipolar PA and a broadband, ultra-high-frequency (UHF), laterally-diffused-metal-oxide-semiconductor-field-effect-transistor (LDMOSFET), high-power amplifier.

Figure 1 shows an impedance-matching circuit in the form of a transmission-line transformer between source impedance Z_S and load impedance Z_L. Equation 1a provides the input impedance as a function of a length of transmission line with arbitrary load impedance:

$$Z_{in} = Z_0 \frac{Z_L + jZ_0 \tan\theta}{Z_0 + jZ_L \tan\theta} \qquad (1a)$$

where:

Z_O = the characteristic impedance

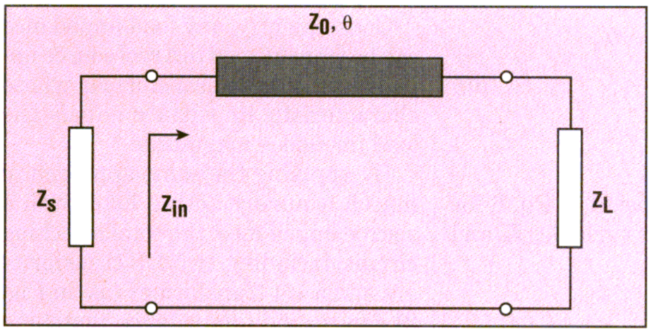

1. This schematic shows a matching circuit in the form of a transmission-line transformer.

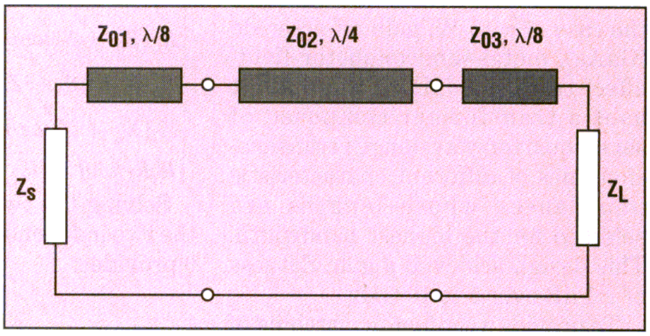

2. This schematic illustrates a matching circuit using two λ/8 transformers and one λ/4 transformer.

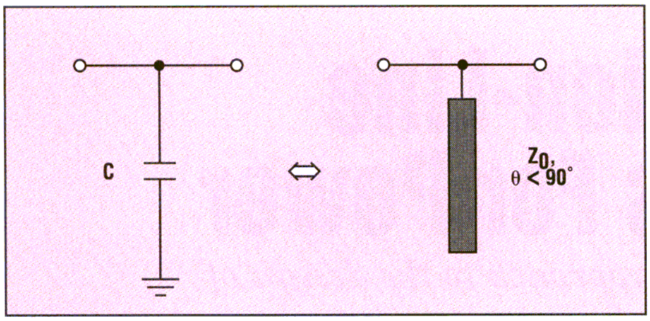

3. These are the lumped elements and transmission line for single-frequency equivalence.

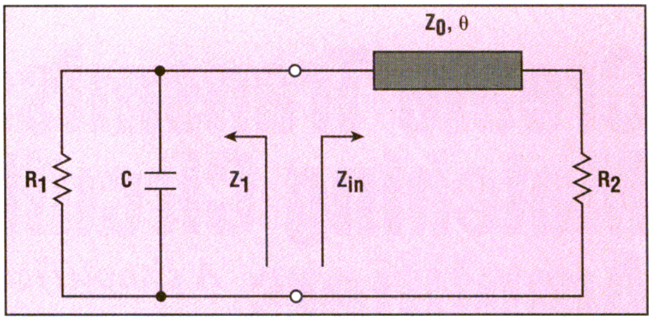

4. This schematic shows a basic L transformer with a series transmission line.

$$\theta = \beta l \qquad (1b)$$

= the electrical length of transmission line

$$\beta = \frac{\omega}{c}\sqrt{\mu_r \varepsilon_r} \qquad (1c)$$

= the phase constant,
c = the speed of light in free space,
μ_I = the substrate permeability,
ϵ_I = the substrate permittivity,
ω = the operating frequency, and
l = the length of the transmission line.[1]

It follows directly from Eq. 1a that, for a quarter-wavelength transmission line with:

$$\theta = \pi / 2 \qquad (1d)$$

the expression for Z_{in} simplifies to:

$$Z_{in} = Z_0^2 / Z_L \qquad (2)$$

Usually, this quarter-wavelength impedance transformer is used for impedance matching in a narrow bandwidth of 10 to 20 percent, and its length is chosen at the band's center frequency. However, using a multisection quarter-wave transformer widens the bandwidth and expands the choice of the substrate to include materials with high dielectric permittivity, which reduces the transformer's size. For example, consider the case of a 15-W, gallium-arsenide (GaAs), metal-semiconductor-field-effect-transistor (MESFET) PA.[2] It uses a transformer composed of seven quarter-wavelength transmission lines of different characteristic impedances whose lengths are selected for the highest bandwidth. This design achieved a gain flatness of ±1 dB over 5 to 10 GHz.

To provide a conjugate matching of input transmission-line impedance Z_{in} with a source impedance $Z_S = R_S + jX_S$ when $R_S = R_e Z_{in}$ and $X_S = -I_m Z_{in}$, Eq. 1a can be rewritten as:

$$R_S - jX_S = Z_0 \frac{R_L + j(X_L + Z_0 \tan\theta)}{Z_0 - X_L \tan\theta + jR_L \tan\theta} \qquad (3)$$

For a quarter-wavelength transformer, Eq. 3 can be divided easily into two equations representing the real and imaginary parts of source impedance Z_S:

$$R_S = Z_0^2 \frac{R_L}{R_L^2 + X_L^2}, \quad X_S = -Z_0^2 \frac{X_L}{R_L^2 + X_L^2} \qquad (4)$$

It follows from Eq. 4 that, for a purely active load with $X_L = 0$, a quarter-wavelength transmission line with characteristic impedance Z_0 can provide impedance matching for a purely active source in accordance with Eq. 5:

$$Z_0 = \sqrt{R_S R_L} \qquad (5)$$

For any values of load and source impedance, Eq. 3 can be divided in two equations representing the real and imaginary parts as follows:

$$\begin{cases} R_S(Z_0 - X_L \tan\theta) - R_L(Z_0 - X_S \tan\theta) = 0, \\ X_S(X_L \tan\theta - Z_0) - Z_0(X_L + Z_0 \tan\theta) + R_S R_L \tan\theta = 0. \end{cases} \qquad (6)$$

Solving the two parts of Eq. 6 for the two independent variables Z_0 and θ provides:

$$Z_0 = \sqrt{\frac{R_S\left(R_L^2 + X_L^2\right) - R_L\left(R_S^2 + X_S^2\right)}{R_L - R_S}} \qquad (7)$$

$$\theta = \tan^{-1}\left(Z_0 \frac{R_S - R_L}{R_S X_L - X_S R_L}\right) \qquad (8)$$

As a result, the transmission line with characteristic impedance Z_0 and electrical length θ, determined by Eqs. 7 and 8, respectively, can match any source and load impedance when the impedance ratio provides a positive value under the square-root expression in Eq. 7.

For a purely active source when $Z_S = R_S$, the ratio between the parameters of load and transmission line derived from Eq. 6 can be expressed by:

$$X_L Z_0\left(1 - \tan^2\theta\right) + \left(Z_0^2 - X_L^2 - R_L^2\right)\tan\theta = 0 \qquad (9a)$$

Then, for the electrical length of a transmission line having:

$$\theta = \pi / 4 \qquad (9b)$$

$$Z_0 = \left|Z_L\right| = \sqrt{R_L^2 + X_L^2} \qquad (10)$$

Consequently, any load impedance can be transformed to a real source impedance by a λ/8 transformer whose characteristic impedance equals the load imedance magnitude.[3]

By applying the same approach to match a purely active load with a source impedance, the total matching circuit, including two λ/8 transformers and a λ/4 transformer (as in Fig. 2) can provide impedance matching between any source impedance Z_S and load impedance Z_L.

Designed for Ultimate Quality

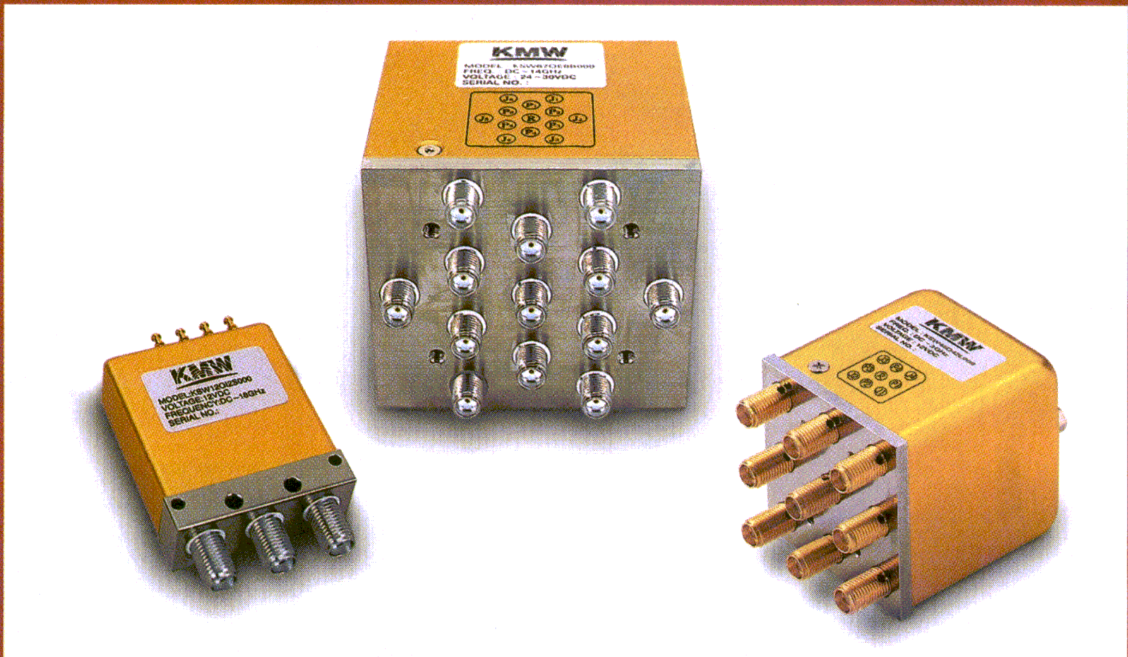

Your Complete Switching Solution from KMW

6P7T switch is designed for IMT2000 (6-sector Redundancy)

Product Code No.	KSW12OI2S000	KSW67O4AB001	KSW45O48L000
Switch Type	SPDT	6P7T	4P5T
Frequency Range	DC ~ 18GHz	DC ~ 3GHz	DC ~ 3GHz
Insertion Loss (Max.)	0.2 ~ 0.5dB	0.2dB	0.2dB
VSWR (Max.)	1.15:1 ~ 1.5:1	1.15:1	1.15:1
Isolation (Min.)	80 ~ 60dB	80dB	80dB
Operating Mode	TTL Latching with IND.	Latching with IND.	Latching
Actuating Voltage /Current (Max.)	12Vdc ± 10% /240mA (@12Vdc, 25°C)	20 ~ 30Vdc /95mA (@24Vdc, 25°C)	24 ~ 30Vdc /85mA (@26Vdc, 25°C)
I/O Port Connector	SMA(F) / SMA(F)	SMA(F) / SMA(F)	SMA(F) / SMA(F)
RF Power Handling	100W CW (@1GHz)	200W CW (@1GHz)	250W CW (@1GHz)
Dimension (inch)	1.339*1.575*0.528	2.441*2.043*2.177	1.626*1.874*1.626

Higher Frequency available on Multi-Pole Multi-Throw, up to 18GHz
Power Handling capability of 4P5T Switch, up to 250W CW & 4Kw Peak @1GHz
Slim type 6P7T Switch, 2.409*1.417*2.216 (inch), also available.

Available Options

Internal Termination, Indicator Circuitry, Suppression Diode, TTL Logic,
Self De-Energizing Circuitry, Various I/O Connector type, Other Operating Voltage

5 million life cycle SPDT switch is available now.

13131 East 166th Street, Cerritos, CA 90703-2202
1-800-8320-KMW • www.kmwinc.com
tel: 562-926-2033 • fax: 562-926-6133
CIRCLE NO. 276

KMW
RF & Microwave Products

In some simple cases, the input impedance of a transmission line at a particular frequency can be expressed as that of a lumped element, as shown in Fig. 3. So, when $Z_L = 0$, it follows directly from Eq. 1a that:

$$Z_{in} = jZ_0 \tan\theta \qquad (11a)$$

which corresponds to the inductive input impedance for:

$$\theta < \pi/2 \qquad (11b)$$

The equivalent inductance at the operating frequency ω is:

$$L = \frac{Z_{in}}{\omega} = \frac{Z_0 \tan\theta}{\omega} \qquad (12)$$

Similarly, when $Z_L = \infty$,

$$Z_{in} = -jZ_0 \cot\theta \qquad (13a)$$

which corresponds to the capacitive input impedance for:

$$\theta < \pi/2 \qquad (13b)$$

The equivalent capacitance at the operating frequency ω is:

$$C = -\frac{1}{\omega Z_{in}} = \frac{\tan\theta}{\omega Z_0} \qquad (14a)$$

To calculate the parameters of parallel open-circuited or short-circuited stubs, it is therefore advisable to use the matching-circuit technique with lumped elements. The Smith chart is particularly useful for graphical admittance solutions.[4] When the appropriate parallel capacitance or inductance is determined analytically or by Smith chart, Eqs. 12 and 14a can be used to calculate the parameters of parallel open-circuited or short-circuited stubs, the characteristic impedance Z_0, and the electrical length θ.

Microwave PA design often employs a simple matching circuit in the form of an L transformer with a series transmission line as the basic matching section. It is convenient to analyze the transforming properties of this circuit by substituting the equivalent transformation of the parallel Rx circuit into the series one. R_1 and

$$X_1 = -1/\omega C \qquad (14b)$$

are the real and imaginary components of the impedance,

$$Z_1 = jR_1X_1/(R_1 + jX_1) \qquad (14c)$$

is for parallel capacitive circuits, and

$$R_{in} = \mathrm{Re} Z_{in} \qquad (14d)$$

and

$$X_{in} = \mathrm{Im} Z_{in} \qquad (14e)$$

are the real and imaginary parts of the impedance

$$Z_{in} = R_{in} + jX_{in} \qquad (14f)$$

for the series circuit presented in Fig. 4. As a result, these two circuits are equivalent at some frequency where:

$$Z_1 = Z_{in} \qquad (14g)$$

that is, where:

$$R_{in} + jX_{in} = \frac{R_1 X_1^2}{R_1^2 + X_1^2} + j\frac{R_1^2 X_1}{R_1^2 + X_1^2} \qquad (15)$$

The solution for Eq. 15 can be written as two expressions:

$$R_1 = R_{in}\left(1 + Q^2\right) \qquad (16)$$

$$X_1 = X_{in}\left(1 + Q^{-2}\right) \qquad (17a)$$

where:

$$Q = R_1/|X_1| = X_{in}/R_{in} \qquad (17b)$$

is a quality factor equal for parallel-capacitive and series-transmission-line circuits. From Eq. 1a, the real and imaginary parts of the input impedance Z_{in} can be written as:

$$R_{in} = Z_0^2 R_2 \frac{1 + \tan^2\theta}{Z_0^2 + (R_2 \tan\theta)^2} \qquad (18)$$

$$X_{in} = Z_0 \tan\theta \frac{Z_0^2 - R_2^2}{Z_0^2 + (R_2 \tan\theta)^2} \qquad (19a)$$

From Eq. 19a, it follows that an inductive input impedance, which is necessary to compensate for the capacitive-parallel component, is realized when:

$$Z_0 > R_2 \qquad (19b)$$

for

$$\theta < \pi/2 \qquad (19c)$$

and

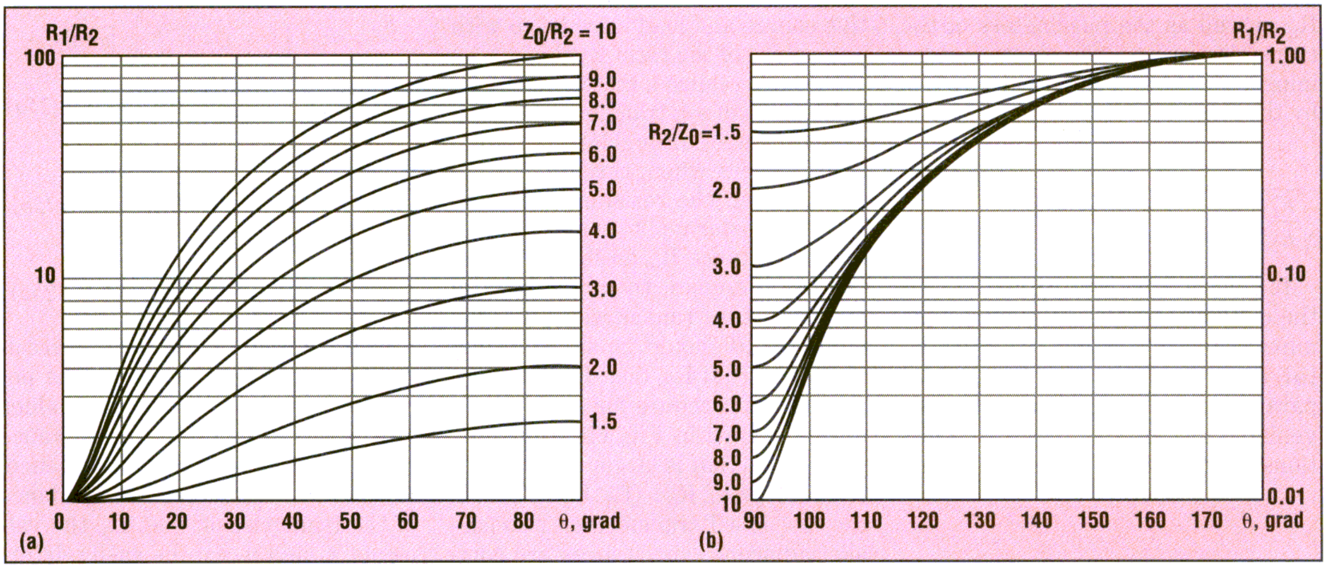

5. These two nomographs can be used to calculate L transformer parameters (a) for $Z_0/R_2 > 0$ and (b) for $Z_0/R_2 < 0$.

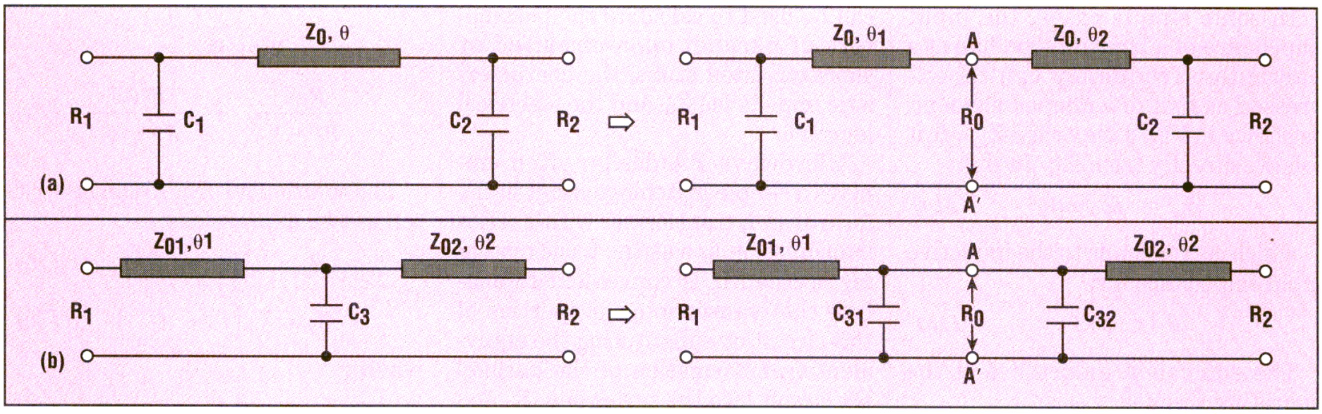

6. These schematics represent the equivalent representation of (a) a π transformer and (b) a T transformer.

$$Z_0 < R_2 \qquad (19d)$$

for

$$\pi / 2 < \theta < \pi \qquad (19e)$$

As a result, to transform resistance R_1 into another resistance R_2 at the given frequency, one must connect a two-port L transformer (including a parallel capacitance and a series transmission line) between them. When one parameter (usually the characteristic impedance Z_0), is decided beforehand, the matching-circuit parameters can be calculated from the following two equations:

$$C = Q / \omega R_1 \qquad (20)$$

$$\sin 2\theta = 2Q / \left(\frac{Z_0}{R_2} - \frac{R_2}{Z_0} \right) \qquad (21)$$

where:

Q = a function of resistances R_1 and R_2 as well as the parameters of the transmission line, the characteristic impedance Z_0, and electrical length θ, by the following equation:

$$Q = \sqrt{\frac{R_1}{R_2}\left[\cos^2\theta + (R_2/Z_0)^2 \sin^2\theta\right] - 1} \qquad (22)$$

It follows from Eqs. 21 and 22 that the calculation of θ is a result of the numerical solution of a transcendental equation with one unknown parameter. However, it is more convenient to combine these two equations and to rewrite them in the form:

$$\frac{R_1}{R_2} = \frac{1 + \left(\frac{Z_0}{R_2} - \frac{R_2}{Z_0} \right)^2 \sin^2\theta \cos^2\theta}{\cos^2\theta + (R_2/Z_0)^2 \sin^2\theta} \qquad (23)$$

Figure 5 shows the resistance ratio R_1/R_2 as a function of the parameter Z_0/R_2 and electrical length θ in the form of two nomographs—one for the case of $Z_0/R_2 > 0$, and another for the case of $Z_0/R_2 < 0$. Thus, when input resistance R_1 and output resistance R_2 are known in advance and when the value of transmission-line characteristic impedance Z_0 is chosen, evaluating the required value of θ is easy using these nomographs. These graphical results show that, in contrast to a lumped L transformer, a simple L transformer with a transmission line can match a purely resistive source and load impedance with any values of the ratio R_1/R_2.

One can realize a matching circuit in the form of a π transformer by the appropriate connection of two L transformers when, through each L transformer, the resistances R_1 and R_2 are transformed to some intermediate resistance R_0, as shown in Fig. 6a. In this case, to minimize the length of the transmission line, the value of R0 should be smaller than that of R_1 and R_2, (i.e., $R_0 < R_1, R_2$). The same procedure for the T transformer shown in Fig. 6b provides a value of R_0 that is larger than that of R_1 and R_2 (i.e., $R_0 > (R_1, R_2)$. Then, in the case of a T transformer, two parallel adjacent capacitances are combined. For a π transformer, two adjacent series transmission lines are combined into one transmission line.

For a π transformer, the lengths of each part of the combined transmission line can be calculated by equalizing the imaginary parts of the impedances from both sides at the reference plane A-A′ to zero, which means that the intermediate impedance, R_0, is real. This leads to two quadratic equations for each electrical length of the combined series transmission lines:

$$\tan^2\theta_1 - \frac{R_1}{Z_0 Q_1}\left[1 - \left(1 + Q_1^2\right)\left(\frac{Z_0}{R_1}\right)^2\right]\tan\theta_1 - 1 = 0 \qquad (24)$$

$$\tan^2\theta_2 - \frac{R_2}{Z_0 Q_2}\left[1 - \left(1 + Q_2^2\right)\left(\frac{Z_0}{R_2}\right)^2\right]\tan\theta_2 - 1 = 0 \qquad (25a)$$

where:

$$Q_1 = \omega C_1 R_1 \qquad (25b)$$

$$Q_2 = \omega C_2 R_2 \qquad (25c)$$

One can simplify this analytical calculation procedure by using the nomographs in Fig. 5. So, if the values of R_1 and R_2 are selected in advance to set the intermediate resistance, R_0, and the characteristic impedance of the transmission line, Z_0, the values of θ_1 and θ_2 can be easily determined from one of these nomographs.

More power equals more freedom.

Introducing the SXT-289. A new wideband GaAsHBT power amplifier.

Stanford Microdevices introduces the SXT-289 — the perfect driver amplifier for today's and tomorrow's advanced communication infrastructure equipment.

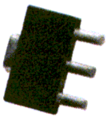

With power to spare, giving you freedom from design constraints, this amplifier was designed and manufactured using state-of-the-art Gallium Arsenide heterojunction bipolar transistor (GaAs HBT) process technology. These devices are ideal for use as a driver stage for power amplifiers installed in cellular PCS infrastructure equipment and conform to TDMA, CDMA and PCS 1900 modulation standards. The SXT-289 operates from a single 5VDC supply and offers exceptional linearity performance in a small form-factor plastic SOT-89 with backside ground.

For more information on the SXT-289 or any of our other products, visit our website today and experience RF Innovation from Stanford Microdevices.

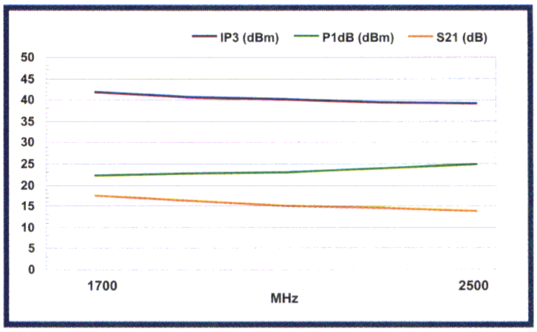

Typical device performance. Bias =5V @ 110mA typ.

STANFORD MICRODEVICES

www.stanfordmicro.com • 800-764-6642

CIRCLE NO. 207

Figure 7 shows the most-common two-port π-transformer design, along with its formulas. This type of transformer is widely used in the output-matching circuits of high-power amplifiers in Class B operation, where it is necessary to isolate the fundamental drain or collector waveform by suppressing the appropriate harmonic(s). Additionally, it is convenient to use this transformer as an input-matching circuit in high-power balanced amplifiers where capacitances can be connected between series transmission lines. And finally, the use of π transformers can be very important for high-efficiency, Class E operation where a capacitive output load provides the appropriate transistor impedance.

Figure 8 shows some of the matching-circuit configurations of two-port T transformers, along with the analytical formulas to calculate the parameters of each transformer. Here, it is assumed that the electrical lengths of the transmission lines are smaller than a quarter wavelength. That is:

$$(\theta_1,\ \theta_2,\ \theta_3) < \pi/2 \qquad (25d)$$

T transformers are usually used in the high-power amplifiers as input-, interstage-, and output-matching circuits, especially in matching circuits with two capacitances and a series transmission line. By using this type of circuit as an output matching circuit for a PA, it is possible to realize a high-efficiency, Class F operation. This is possible because the series transmission line that is adjacent to the active device's drain or collector creates the appropriate impedance through open- or short-circuit harmonic conditions.[5]

The first of two practical illustrations of transmission-line matching-circuit techniques can be seen in the design of an output matching circuit for a 5-W, 1.6-GHz bipolar amplifier that operates from a 24-VDC supply voltage and provides a gain of approximately 10 dB. The mentioned requirements can be provided with an NPN silicon transistor in Class AB operation that is intended for microwave-transmitter applications over the frequency range of 1.5 to 1.7 GHz. The manufacturer usually states the values of the complex input and output impedances or admittances at the nominal operation point on the data sheet for the device. At the operating frequency of 1.5 GHz, let

$$Z_{out} = (5.5 - j6.5)\ \Omega \qquad (25e)$$

correspond to a series combination of transistor output resistance and capacitance. To match this capacitive impedance to the standard 50-Ω load resistance, it is advisable to use a matching circuit in the form of a T transformer shown in Figure 8b. Figure 9 shows the complete network, including output-device impedance and matching circuit.

First, the circuit should compensate for the series capacitance inherent in output impedance. For a small electrical length where:

$$\tan\theta \cong \theta \qquad (25f)$$

and characteristic impedance $Z_1 > R_{out}$, one can deduce from Eqs. 18 and 19a that:

$$\begin{cases} R_{out} \cong R_2 \\ \theta_2 \cong -X_{out}/Z_0 = 1/\omega C_{out} Z_0 \end{cases} \qquad (26)$$

where:

θ_2 = a part of the total transmission line required to compensate for the output capacitance reactance. If one selects the value Z_0 to be 50 Ω, then θ_2 = 6.5/50 = 0.13 radian, which is equal to approximately 7.5 deg. of electrical length. Then, the value of quality factor Q_2, which one must choose to calculate the parameters of the matching circuit, is defined by:

$$Q_2 > \sqrt{R_1/R_2 - 1} = 2.84 \qquad (27)$$

Consequently, the value of Q_2 must be larger than 2.84. For example, a value of Q_2 = 3 can be chosen to yield a 3-dB bandwidth of 1.6 GHz/3 = 533 MHz. As a result, the values of the output-matching-circuit parameters are as follows:

$$\theta_1 = \frac{1}{2}\sin^{-1}\left[2Q_2 / \left(\frac{Z_0}{R_2} - \frac{R_2}{Z_0}\right)\right] = 21° \qquad (28)$$

$$Q_1 = \sqrt{\frac{R_2}{R_1}\frac{1 + Q_2^2}{\cos^2\theta_1 + (R_2/Z_0)^2\sin^2\theta_1} - 1} = 0.5 \qquad (29)$$

$$C_1 = 1/(\omega Q_1 R_1) = 4\ pF \qquad (30)$$

$$C_2 = (Q_2 - Q_1)/\omega R_1(1 + Q_1^2) = 4\ pF \qquad (31a)$$

Figure 10 shows the function of each element traced on the Smith chart. The easiest and most convenient way to plot the traces of the matching-circuit elements is to first plot the traces of Q_1 and Q_2. Then plot the trace of the series transmission line as far as the intersection point with the Q_2 circle, and plot the trace of capacitance C_2 as far as the intersection point with the Q_1 circle.

The second practical illustration of transmission-line matching-circuit techniques can be seen in the design of a 150-W amplifier that operates over a frequency band of 470 to 860 MHz, uses a +28-VDC supply voltage, and provides a gain of more than 10 dB. A typical application for this type of circuit is a high-power balanced LDMOS transistor in an ultra-high-frequency (UHF) TV transmitter. The center bandwidth frequency f_c is determined as:

$$f_c = \sqrt{470 \cdot 860} = 635\ MHz \qquad (31b)$$

For this operating frequency, assume that the manufacturer's stated value of input impedance for each transistor is:

$$Z_{in} = (1.7 + j1.3)\ \Omega \qquad (31c)$$

In this case, Z_{in} is expressed as a series combination of input resistance and inductive reactance. To realize the required bandwidth, low-Q matching circuits should be used to reduce in-band amplitude ripple and to improve input VSWR. To achieve a 3-dB bandwidth, the value of the quality factor must be less than Q = 635/(860−470) = 1.63. Since the device input quality factor is smaller (i.e., Q_{in} = 1.3/1.7 = 0.76), it is possible to cover the entire frequency range using a multistage matching circuit. It is very convenient to design the input matching circuit as well as the output-matching circuit by using simple L transformers in the form of series transmission lines and parallel capacitances with a constant value of Q for the balanced portion of each device. Then, the two matching circuits are combined by inserting capacitances whose values are reduced two times between the two series transmission lines. Although the requirement of a constant Q is not strictly necessary, it provides a convenient guide for the analytical calculation of the matching circuit parameters and the Smith chart.

To match the series-input inductive impedance to the standard 50-Ω input source impedance, it is necessary to use three L transformers, as shown in Fig. 11. At the center frequency of 635 MHz, the input inductance is equal to approximately 0.3 nH. To take this inductance into account, it is necessary to subtract the appropriate value of electrical length θ_{in} from total electrical length θ_3. Due to the short size of this transmission line, a value of θ_{in} can be easily calculated in accordance with:

$$\theta_{in} \cong X_{in}/Z_0 = \omega L_{in}/Z_0 \quad (32)$$

In this case, the input resistance R_{in} can be assumed to be constant.

According to Eq. 22, there are two simple ways to provide matching using equal quality factors of L transformers. One way is to use the same characteristic impedance values for all transmission lines. The other is to use the same electrical lengths for all transmission lines. Consider the first approach, which also allows direct use of the Smith chart, and choose the value of the characteristic impedance $Z_0 = Z_{01} = Z_{02} = Z_{03} = 50\ \Omega$. It is convenient to express the ratio of input and output resistances by:

$$\frac{R_1}{R_2} = \frac{R_2}{R_3} = \frac{R_3}{R_{in}} \quad (33a)$$

This provides the values of $R_2 = 16.2\ \Omega$ and $R_3 = 5.25\ \Omega$ for $R_{source} = R_1 = 50\ \Omega$ and $R_{in} = 1.7\ \Omega$. Then, the values of electrical lengths are determined from Fig. 5a as:

$$\theta_1 = 30°, \theta_2 = 7.5°, \theta_3 = 2.4°.$$

Actually, it is enough to determine an electrical length θ_1 of the first L transformer and to calculate the quality factor Q from Eq. 22. In this case, the remaining two electrical lengths can be directly obtained from Eq. 21. As a result, the quality factor of each L transformer is equal to a value of Q = 1.2. The values of the parallel capacitances are as follows:

$$C_1 = 6\text{ pF}, C_2 = 19\text{ pF}, C_3 = 57\text{ pF}$$

In the case of a constant Q, one can simplify the design of the matching circuit significantly by using a standard Smith chart. After calculating the value of Q, one must plot a constant-Q circle on the Smith chart. Figure 12 shows an input-matching-circuit design using a standard Smith chart with a constant-Q circle.

Another approach assumes the same values of electrical lengths

$$\theta = \theta_1 = \theta_2 = \theta_3 \quad (33b)$$

and calculates the characteristic impedances of transmission lines from Eq. 22 at equal ratios of the input and output resistances according to Eq. 33a. This approach is more convenient in practical designs, because, when using the transmission lines with standard characteristic-impedance $Z_0 = 50\ \Omega$, the electrical length of the transmission line adjacent to the active device's input terminal is too short. In this case, it is advisable to set the characteristic impedance of the first series-transmission line to $Z_{01} = 50\ \Omega$. Then, a value of θ should be evaluated directly from the nomograph shown in Fig. 5a. Subsequent calculation of Q from Eq. 22 provides θ = 30° and Q = 1.2. The characteristic impedances of the remaining two transmission lines are calculated easily from Eqs. 21 or 22:

$$Z_{02} = 15.7\ \Omega, Z_{03} = 5.1\ \Omega$$

References

1. D.M. Pozar, *Microwave Engineering*, John Wiley & Sons, New York, 1998.
2. Y. Ito, M. Mochizuki, M. Kohno, H. Masuno, T. Takagi, and Y. Mitsui, "A 5-10 GHz 15-W GaAs MESFET Amplifier With Flat Gain and Power Responses," *IEEE Microwave and Guided Wave Letters*, Vol. 5, pp. 454-456, December 1995.
3. D.H. Steinbrecher, "An Interesting Impedance Matching Network", IEEE Transactions Microwave Theory & Techniques, Vol. MTT-22, June 1967, p. 382.
4. A.V. Grebennikov, "Matching With Lumped Elements: Analytic Approach To Simplify Computer-Aided Design," *RF Design*, June 2000, pp. 22-38.
5. A.V. Grebennikov, "Circuit Design Technique for High Efficiency Class F Amplifiers," *2000 IEEE MTT-S International Microwave Symposium Digest*, Vol. 2, pp. 771-774.

Control Circuit Compensates Error Loop In Feedforward Amplifiers

A novel control circuit compensates for the nonlinear characteristics of high-power amplifiers used in communications systems.

Ung Hee Park

ETRI Radio Technology Department, 161 Kajong-Dong, Yusong-Gu, Taejon, 305-350 Korea; 82-42-860-6987, FAX: 82-42-860-5199, e-mail: uhpark@etri.re.kr.

WORLDWIDE progress in wireless communication systems has created requirements for high-power amplifiers (HPAs) with high efficiency and linearity. To obtain maximum efficiency in an HPA, its operating point must be located near the saturation region where the highly nonlinear characteristic occurs. When multiple carriers are injected simultaneously into an HPA, it generates intermodulation (IM) signals. Since IM signals represent noise for adjacent channels, a linearizer is needed to reduce IM signals in an HPA system. The most popular and effective scheme is known as a feedforward linearizer. Even though several linearizing schemes have been used in practical linear PAs, their effectiveness and compactness need to be improved.[1-4]

In this article, a novel control circuit that can be easily adapted to the error-sensor loop of a feedforward linearizer is proposed. It can compensate the nonlinear characteristics of an HPA, canceling the main carrier very effectively. For a power range of 11 dB, the main carrier is rejected by more than 40 dB, which implies an amplitude error between 0.05 and 0.12 dB, while the phase error is less than 0.016 deg.

The error sensor loop consists of a linear and nonlinear path. The linear path contains only power dividers, while the nonlinear path has an HPA, a phase shifter, and an attenuator. The power dividers in both paths operate as amplitude controls and as phase-control elements with detectors. Therefore, the characteristics in the nonlinear path can be controlled more efficiently. The effective control mechanism is discussed theoretically and experimental results are also presented.

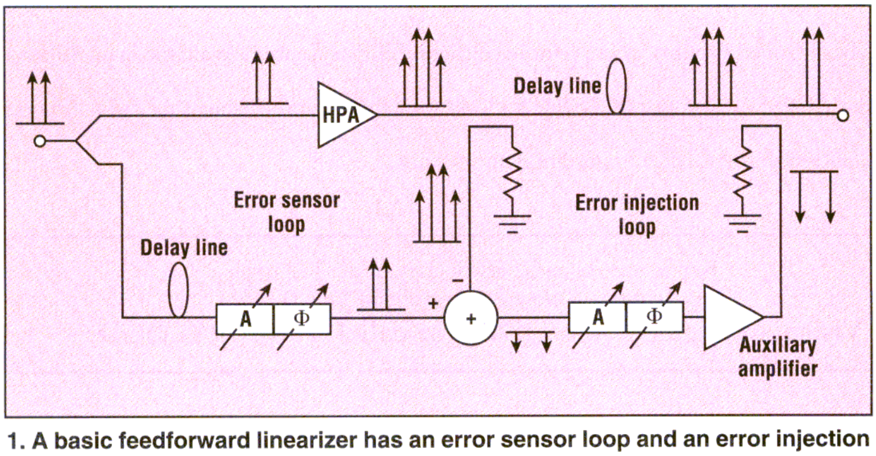

1. A basic feedforward linearizer has an error sensor loop and an error injection loop.

COMBINE AND CANCEL

The typical feedforward linearizer is shown in Fig. 1. The error sensor loop extracts only IM signals from the HPA output, which are amplified in the injection loop and coupled back to the main path to remove IM signals.

Consider the case where a signal is added through a Wilkinson combiner to another signal that has arbitrary amplitude (magnitude of RF power) and phase. The output power from the combiner is changed depending

on the phase as well as amplitude differences between two combining signals. Let two signal voltages—V_1 and V_2—whose frequencies are the same, but with different amplitudes and phases, be represented as:

$$V_1 = A_1\cos(\omega_c t) \quad (1a)$$

$$V_2 = A_2\cos(\omega_c t + \theta) \quad (1b)$$

The power of each signal in decibels is expressed by:

$$P_1 = 10\log\left(\frac{A_1^2}{2Z_0}\right) \quad (2a)$$

$$P_2 = 10\log\left(\frac{A_2^2}{2Z_0}\right) \quad (2b)$$

respectively. The combined output voltage V_3 is given as:

$$V_3 = V_1 + V_2 = A_1\cos(\omega_c t) + A_2\cos(\omega_c t + \theta) \quad (3)$$

The power of V_3 in dB is derived as:

$$P_3 = 10\log\left(\frac{A_1^2 + A_1^2 + 2A_1A_2\cos(\theta)}{2Z_0}\right) \quad (4)$$

Using Eqs. 2a and b, Eq. 4 is modified as follows:

$$P_3 = 10\log[10^{P1/10} + 10^{P2/10} + 2\times 10^{(P1+P2)/20}\times\cos(\theta)] \quad (5)$$

It is obvious in Eq. 5 that two signals are canceled completely when P_1 and P_2 have the same amplitudes and the phase difference, θ between them is π(180 deg.). Due to the amplitude imbalance and the phase offset from 180-deg. difference between two signals, the limit of the cancellation would exist. Let δP(decibels) be the amplitude difference of two signals and $\delta\theta$(deg.) be the phase difference of two signals. Then P_2 and θ are expressed by:

$$P_2 = P_1 + \delta P \quad (6a)$$

$$\theta = \pi + \delta\theta \quad (6b)$$

In the Wilkinson combiner, the difference between the output power P_3 and the input power P_1 determines the amount of the cancellation according to δP(decibels) and $\delta\theta$(deg.). This cancellation power (CP) is derived from Eq. 5 as:

$$CP(\delta P, \delta\theta) = 10\log[1 + 10^{\delta P/10} - 2\times 10^{\delta P/20}\times\cos(\delta\theta)] - 3(dB) \quad (7)$$

Figure 2 represents the power cancellation versus the amplitude and the phase errors for the power combiner based on Eq. 7. In Eq. 7, the last term is introduced by the characteristics of the Wilkinson combiner.

CONTROL CIRCUITS

Figure 3 shows the block diagram of the error sensor loop block which includes the amplitude- and phase-control circuits. Path 1 in the figure—the main path—consists of an HPA

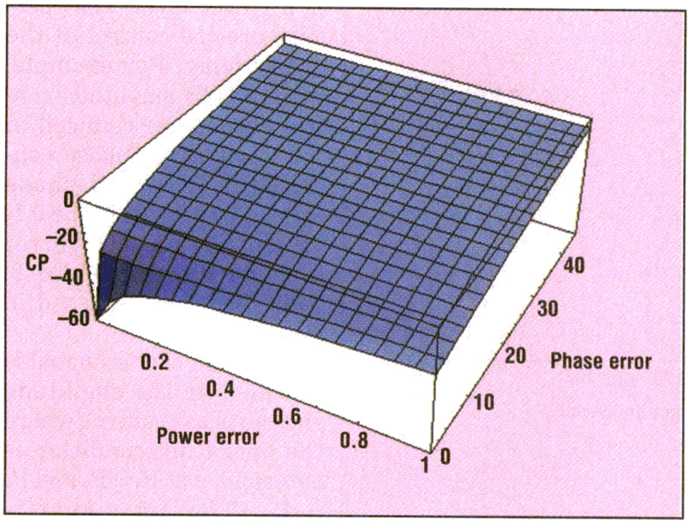

2. This three-dimensional (3D) graph shows the cancellation power (CP) with respect to the amplitude and phase errors of the power combiner.

HPA output with and without a control circuit

Output (dBm/tone)	Characteristic of HPA (without control)		P_5 (dB) (with control)
	Gain (dB)	Phase Deg.	
37	27.73	−4.33	−45.40
36	28.12	−1.57	−47.07
35	28.26	−0.03	−43.12
34	28.52	1.16	−44.82
33	28.49	1.84	−44.75
32	28.46	2.03	−44.97
31	28.47	1.93	−44.27
30	28.47	1.67	−42.65
29	28.32	1.19	−43.57
28	28.23	0.23	−42.87
27	28.22	0	−40.62

and a variable attenuator as well as a phase shifter located in front of the HPA for compensation of the amplitude and phase errors. The other path (Path 2) works as the reference for the amplitude control as well as the phase control in the main path. The amplitude and the phase of Path 1 are changed so that the amplitudes are equal and the phase difference is 180 deg. when compared with Path 2. The Wilkinson combiner C is used only for obtaining the IM signals. Therefore, the IM signals are obtained efficiently as an error signal output of the cancellation circuit.

The amplitude-control circuit operates as follows: The reference power P_1 is coupled from Path 2 which is converted to the reference voltage V_1 through the amplitude detection circuit. P_2 is coupled from the output of the HPA and converted to voltage V_2 representing the level of the power P_2 at Path 3. If Schottky-diode detectors are employed in each path, the detector output voltages could be different from each other for the same applied power due to the unequal nonlinear characteristics of the diodes. To overcome this problem, a single detector is switched to P_1 and P_2 (Fig. 3). Therefore, when the same powers P_1 and P_2 are applied to the detector, the same voltages V_1 and V_2 are generated. The auto-level-control (ALC) circuit is composed of several operational amplifiers, which adjust V_2 to be equal to V_1 by increasing or decreasing the output voltage V_A which controls the variable attenuator.[5,6]

The phase-control circuit operates as follows. The circuit is implemented in two blocks. One block is the amplitude-control circuit that was described, while the other block, composed of Wilkinson combiners and dividers, detects the phase difference between the signals through Path 2 and Path 3 in Fig. 3. To obtain the phase difference as a power level, the latter block is designed so that the electrical length of each path to

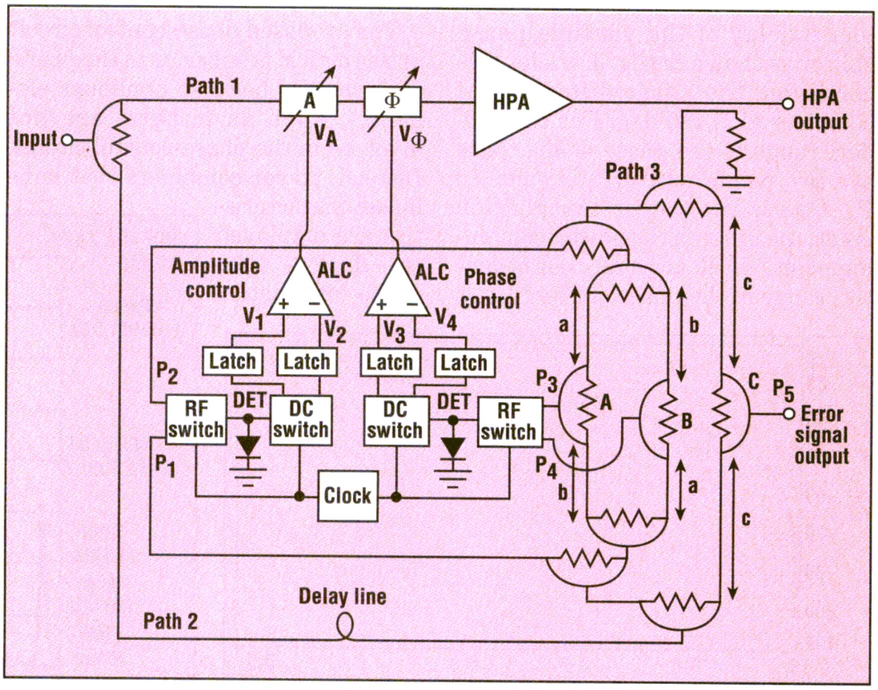

3. The block diagram of the error sensor loop includes amplitude- and phase-control circuits. Path 1 is the main path while path 2 is the reference for the amplitude and phase controls in the main path.

the power combiners A, B, and C are different from each other. In power combiner A and B, the electrical length of 'b' is longer than that of 'a' by 2 deg. However, the paths to power combiner C have the same electrical lengths as 'c.' Figure 4 represents output power P_3, P_4, and P_5 from each power combiner versus the signal-phase delays.

The main signals through the two paths 'c' in Fig. 3 are canceled at the output of the power combiner C, when the phase difference between them is 180 deg. Since the electrical lengths of path 'a' and 'b' are different from each other by 2 deg., the output power P_3 of combiner A has minimal value at a phase difference of 178 deg., while the output power P_4 of combiner B reaches its minimum value at a phase difference of 182 deg. The power P_3 and P_4 are applied to the input of the amplitude-control circuit. Therefore, the ALC maintains the level of P_3 and P_4 equally by controlling the phase delay of the variable phase shifter as shown in Fig. 3. Under this condition, the phase difference of combiner C is 180 deg. For the 360-deg. range of the phase delay, there are two points where P_3 is equal to P_4. One is the power-cancellation point, the other is the power-combining point, which is usually out of control range of the phase shifter.[7]

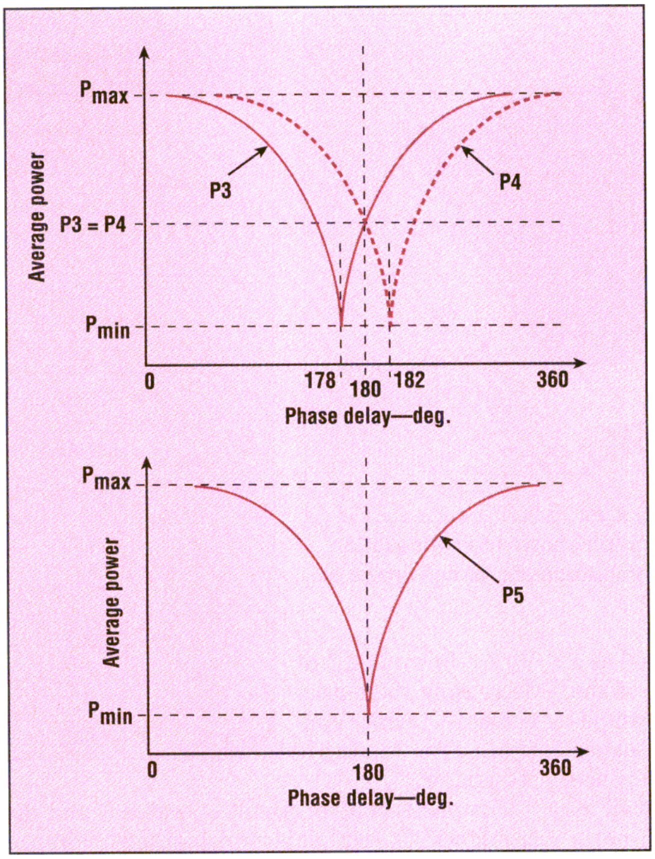

4. Output power levels P_3, P_4, and P_5 versus the phase delays of the signals illustrate the minimum values of each power level caused by the different electrical lengths of their paths.

The proposed phase-control circuit in this article is superior to the previous schemes because nonlinear elements, such as mixers, are not involved in the phase-control circuit. Instead, power combiners that have linear characteristics are employed to derive the phase information as a power level. That permits precise control of the phase delay. For example, when 0.1-dB amplitude-control error is introduced in the ALC of the phase control, the practical phase error resulting from the 0.1-dB amplitude control error is only 0.0127 deg. by Eq. 9, which will be discussed in detail.

The main carrier signal is canceled by the amplitude and the phase control, where the operating condition is determined at $P_1 = P_2$ and $P_3 = P_4$. The IM signal is obtained from the output of the combiner C as in Fig. 3. Since the amplitude and phase are controlled by amplitude detection and ALCs, the amplitude error between two signals at path 2 and path 3 primarily determines the limit of cancellation. Since the phase-error $\delta\theta$ is converted to the amplitude-error δP as seen in Eq. 7, the cancellation of the main signals is determined only by the amplitude-control errors. The cancellation outputs CP_3 and CP_4 of combiners A and B occur with amplitude-control error δP in the phase-control circuit. Assume that the phase error in power combiner C is $\delta\theta$, the following equation is derived:

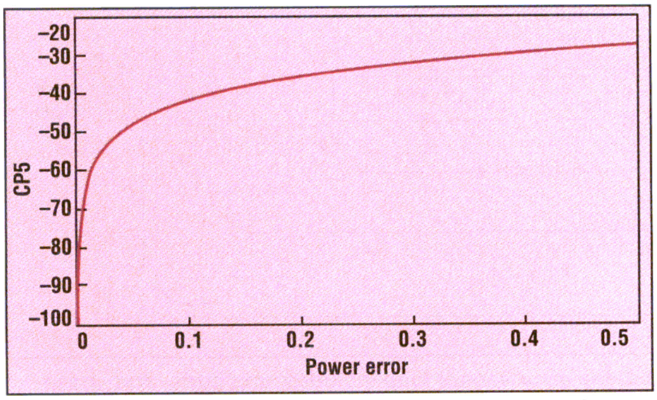

5. This curve shows the cancellation of the main carrier versus the power error in power combiner C.

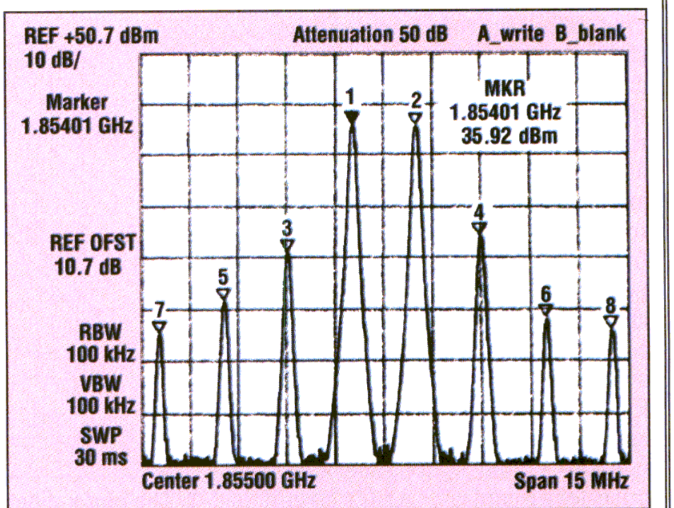

6. The spectrum of the 10-W HPA is shown here at +37-dBm/tone output.

Application Profile

How Do I Make Bluetooth Wireless Products Small and Inexpensive?? Use the Integrated ASIC LTCC Modules from National Semiconductor Using DuPont Green Tape™ and Fine-Line Technology.

An integrated ASIC? Inexpensive?? Tell me more!!!

National Semiconductor leads the way in Bluetooth, Cell Phone and other wireless applications in applying LTCC to integrated wireless modules. National's latest advances in LTCC manufacturing technology, combined with DuPont's advances in Green Tape™, Fodel® Compositions and thick film conductor materials, have established a new low-cost standard for wireless modules.

LOW-COST LTCC

LTCC is the least expensive alternative for your RF wireless design. Consider that the LTCC raw material is inorganic (earth oxides) versus the alternatives — organic (oil). Also, the process is scalable in panel size as the manufacturing volume increases, thereby drastically reducing cost per square inch.

LTCC has the highest passive integration capability of any active/passive component board-level system. More passive components in the LTCC and not on top of the module, resulting in less space utilized and

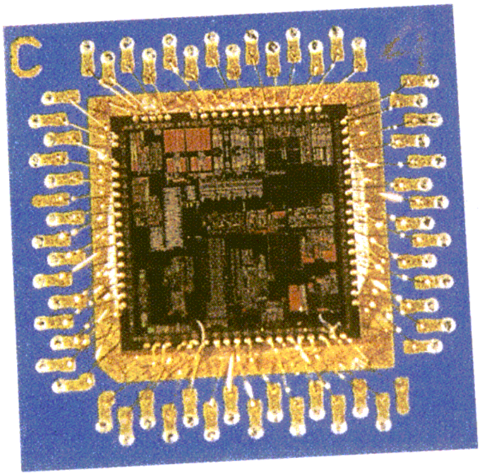

the lowest system cost solution.

THE INTEGRATED ASIC

With the capability of DuPont's Fodel® fine-line technology, active components can be flip-chip mounted to the LTCC module. The high frequency characteristics of the entire vertical structure can be modeled, and performance optimized. Also, results have shown higher-yielding DC interconnects, improved Q on edge-coupled, edge-sensitive structures, and more consistent electromagnetic results in RF structures. The resultant module performance is optimized, space minimized, and the resultant cost 25% to 50% below competing technologies.

LTCC has come to lead the wireless revolution, and offers the lowest-cost, smallest-size, and highest-performance solution to your wireless design. National's LTCC foundry technology offers you the fastest design-to-volume format. Proto cycle times in less than seven days, flexible manufacturing lines accommodating design and capacity changes without delivery interruption, 30-day ramp to volume — all this plus complete assembly and test services that support the full line of DuPont Green Tape™ products.

National: Doing what we do best — prototype turns in 7 days; state-of-the-art technology; and low-cost/high-volume QS9000 manufacturing.

For more information, call National at (949) 380-2054 or visit the National LTCC website at http://www.national.com/ltcc.

National Semiconductor®

DUPONT®

GREEN TAPE™ FODEL® BIROX® DIFFUSION PATTERNING™ LUXPRINT®

CIRCLE NO. 223

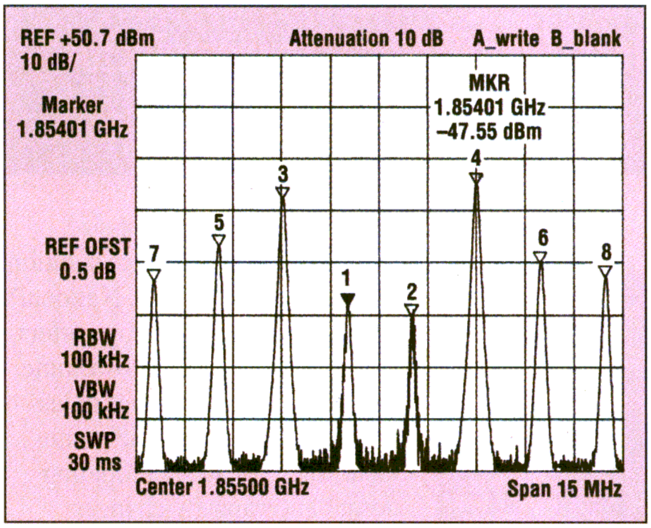

7. The output response of the error sensor loop with the HPA operating at +37-dBm/tone output is shown in Fig. 6.

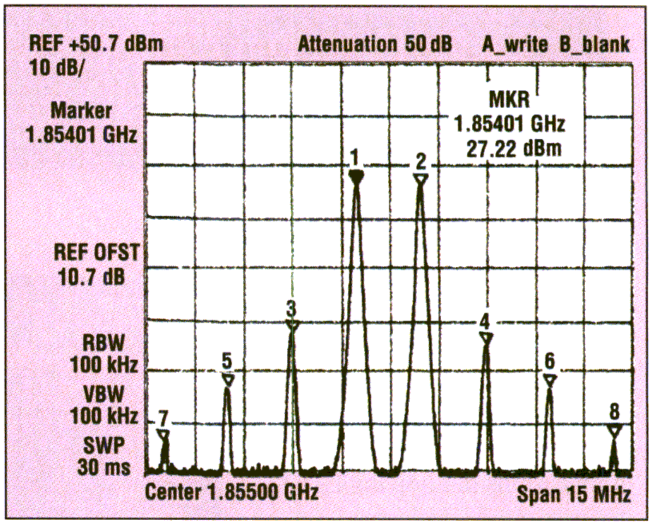

8. This spectrum of the HPA is similar to the one in Fig. 6, except at +27-dBm/tone output.

$$CP_{3\ or\ 4}(\delta P,2)-\delta P = CP_{3\ or\ 4}(\delta P,2-2\delta\theta) \qquad (8)$$

The phase error is derived by solving Eq. 8 as:

$$\delta\theta(deg) = 1-\frac{1}{2}\cos^{-1}\left[\frac{-10^{(CP_{3or4}(\delta P,2)-\delta P+3)/10}+1+10^{\delta P/10}}{2\times 10^{\delta P/20}}\right] \qquad (9)$$

The cancellation of the output of the power combiner C is finally expressed as follows:

$$CP_5 = 10\log\{1+10^{\delta P/10}-2\times 10^{\delta P/20} \times\cos[1-\frac{1}{2}\cos^{-1}\left(\frac{-10^{(CP_{3or4}(\delta P,2)-\delta P+3)/10}+1+10^{\delta P/10}}{2\times 10^{\delta P/20}}\right)]\} -3 \qquad (10)$$

In Fig. 5, CP_5 is plotted as a function of amplitude error using Eq. 10.

It is important to reduce the amplitude-control error in the proposed control circuit, because the limit of the cancellation is affected more strongly by the amplitude error than by the phase offset.

The proposed control circuit and the error sensor loop block are implemented and tested at the frequency range of the Korea personal-communications-services (PCS) band (f_c = 1855 MHz). A reflection-type variable attenuator is used for controlling the amplitude of the main carrier.[4] Its attenuation range varies from 1.64 to 9.05 dB with a control voltage between 0 and approximately +10 VDC, whereas the phase variation is less than 1 deg. The reflection-type variable phase shifter provides approximately 0 to 35.8 deg. of phase shift for the control voltage from 0 to +10 VDC, whereas the amplitude variation is less than 0.2 dB.[5] The control circuits are combined with an HPA, providing 10-W output power at the center frequency of 1855 MHz. The implemented circuits are tested with two-tone signals at 1854 and 1856 MHz.

The table shows the performance of the control circuit. Without control, the gain and phase of an HPA vary with changes of input power. With control, the main carrier is canceled by more than 40 dB from the output P_5 of the error sensor loop. For the cancellation range of approximately 40 to 47 dB, the circuits operate with an amplitude error of approximately 0.05 to 0.12 dB, which can be predicted from Eq. 10. Under this condition, the phase-control error is calculated at less than 0.016 deg. from Eq. 9. Figure 6 shows the output spectra of the 10-W HPA at +37-dBm/tone output, and Fig. 7 shows the output spectra from the error sensor loop when the HPA is operating at +37-dBm/tone output. Figures 8 and 9 show the output spectra of the HPA and the error-sensor loop, respectively, at 27-dBm/tone output. ••

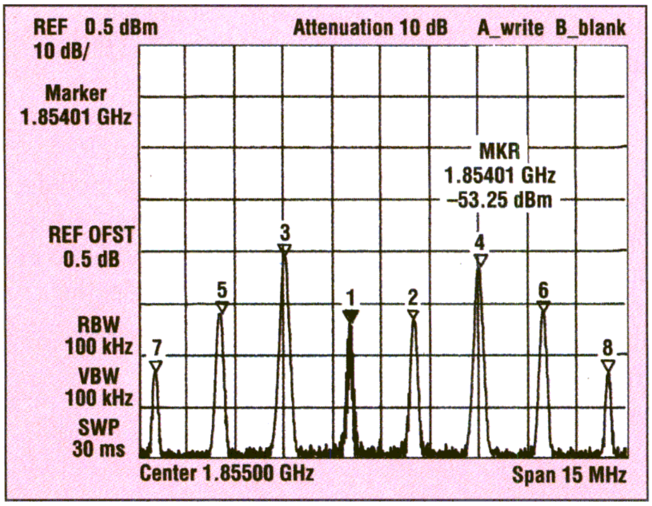

9. This spectrum of the error sensor loop is similar to that of Fig. 7, except at +27-dBm/tone output.

References

1. H. Seidel, "A Microwave Feed-Forward Experiment," *The Bell System Technical Journal*, Vol. 50, No. 9, pp. 2879-2916, November 1971.
2. In-ho Kang, Ik-soo Chang, Youg-chae Jeong, and Sang-won Yun, "The Design of Automatic Gain and Phase Controlled Amplifier," *APMC Proceedings*, Vol. 1, pp. 18-20, October 1995.
3. James Frank Long, "Feedforward Amplifier," Motorola, US Patent 5,831,478, November 1998.
4. Robert E. Myer, "Feed Forward Linear Amplifier," AT&T, US Patent 4,885,551., December 1989.
5. David A. Bell, *Operational Amplifier*, Prentice Hall, 1990.
6. Won-tae Kang, Ik-soo Chang, and Min-soo Kang, "Reflection Type Low-Phase Shifter Attenuator," *IEEE Trans. Microwave Theory and Techniques*, Vol. 46, No. 7, pp. 1019-1021, July 1998.
7. Shiban K. Koul, Bharathi Bhat, *Microwave and Millimeter Wave Phase Shifter*, Artech House, pp. 527-540, 1991.

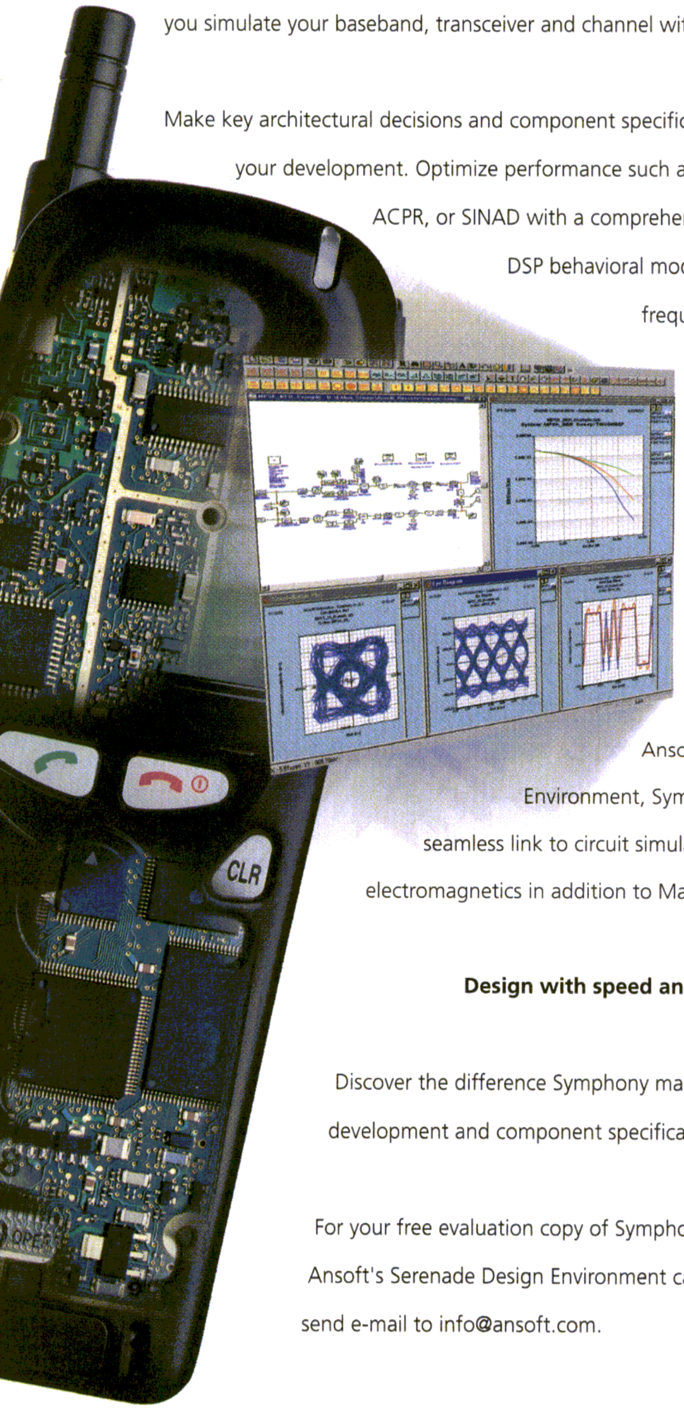

CLR

Applying RFID to electronic commerce

RF identification (RFID) refers to a wide range of data-carrying technologies by which the transfer of data from a carrier to a reader is accomplished through radio waves. An article in the July issue of the Low Power Radio Association's *LPRA News*, "RFID For Rapid Response," details how the technology can be used for rapid response in growing electronic-commerce (e-commerce) and mobile-commerce (m-commerce) markets.

Both chip-based and chip-less RFID technologies are in common use, although the former is more predominant worldwide. Chip-based RFID devices operate in a variety of different frequency bands, including 125 kHz, 13.56 MHz, 862 to 869 MHz (in Europe), 902 to 928 MHz (in the US), 2.45 GHz, and 5.8 GHz. An RFID system comprises one or more data-carrying tags, a reader or interrogator, and a programming device to accommodate the need for read/write devices (in some cases, the interrogator may support read and write operations). The tags are distinguished by their frequencies and modes of operation: using inductive coupling at the lower (125-kHz and 13.56-MHz) frequencies and propagation coupling at the higher frequencies. The tags may be passive (relying on power from the interrogator) or active (employing a battery).

The article reviews some of the additional advantages of RFID systems for e-commerce and m-commerce applications, and provides a breakdown of expected prices for different RFID systems in the US and in the UK. Copies of the July issue of *LPRA News* are available from the **Low Power Radio Association, Brearley Hall, Luddenden Foot, Halifax HX2 6HS, United Kingdom; (44) 0-1422-886463, FAX: (44) 0-1422-886950, e-mail: info@lpra.org, Internet: http://www.lpra.org.**

CIRCLE NO. 194 or visit www.mwrf.com

Testing high-speed DWDM systems

Hunger for information and data is driving communications systems designers and operators to seek more bandwidth. And while fiber-optic communications systems offer enormous potential bandwidth, designers are realizing that bandwidth poses practical problems in real-world systems. Dense-wavelength-division multiplexing (DWDM), however, offers tremendous promise for fulfilling present and future needs for information bandwidth. An eight-page application note from Tektronix (Beaverton, OR), "Testing High-Rate DWDM Systems," provides a clear introduction to DWDM technology, reviews the challenges for testing these systems, and provides practical solutions in terms of test-equipment and measurement techniques. DWDM transfers multiple colors of light simultaneously over a single optical fiber, vastly increasing the amount of information that the fiber is capable of carrying.

Despite its higher efficiency and flexibility compared to other fiber-optic formats, DWDM transmission systems are still subject to many high-rate testing issues. In high-rate DWDM testing, there are three chief areas of concern—the physical layer, the timing and synchronization, and the bit-error-rate (BER) performance. Physical-layer measurements, which are typically performed with oscilloscopes, optical spectrum analyzers and reference receivers (Rxs), wavelength meters, and optical power meters, provide the ability to verify interface specifications, and comply with industry standards. Typical measurements include analysis of mean optical-launch power, laser chirp (variations in the wavelength of the optical laser), extinction ratio, gain tilt, attenuation, and dispersion. Typical analysis tools include eye diagrams.

Timing and synchronization measurements are performed with the help of specialized test sets, such as Synchronous Optical Network (SONET) testers, while BER testing is performed with stable clock sources and BER testers. A trend in BER testing is to perform accelerated BER testing. That is, rather than check systems for less than one error in 10^{14}, which can be time-consuming, the system is evaluated at higher error rates to produce faster test results. The low BERs are then extrapolated from the results of these higher-BER tests.

For more on testing DWDM systems and optical links at speeds beyond 10 Gb/s, obtain a copy of the application note. Copies of "Testing High-Rate DWDM Systems" are available for free download from the company's website. **Tektronix, Inc., Measurement Business Division, Howard Vollum Industrial Park, P.O. Box 500, M/S 50216, Beaverton, OR 97077-0001; (800) 426-2200, FAX: (503) 222-1542, Internet: http://www.tektronix.com.**

CIRCLE NO. 195 or visit www.mwrf.com

Aluminum Nitride Forges High-Power Resistive Components

By refining the use of special thick-film pastes and AlN ceramic substrates, a line of resistive passive components has been developed as an alternative to BeO in high-power applications.

Thomas J. Dowling

Director of Engineering

RF Power Components, Inc., 125 Wilbur Pl., Bohemia, NY 11716; (516) 563-5050, FAX: (516) 563-4747, e-mail: info@rf-power.com, Internet: http://www.rf-power.com.

RESISTORS and terminations for high-power applications have traditionally used beryllium oxide (BeO) as the ceramic substrate material. While BeO has proven to be a reliable performer in terms of power dissipation per unit volume, alternatives are often sought in many international markets. Fortunately, RF Power Components (Bohemia, NY), a subsidiary of Anaren Microwave (East Syracuse, NY), has developed a line of high-power resistive components based on aluminum nitride (AlN), a more ecologically "friendly" substrate material for sensitive overseas markets. The resistive components include resistors and terminations for applications through 150 W at cellular and personal-communications-services (PCS) frequencies.

Any fear of BeO is related to its handling rather than its use. Although BeO is harmless in solid form, it can be harmful in dust or powder forms if inhaled in sufficient quantities. The US Occupational Safety and Health Administration (OSHA) lists BeO dust as a hazardous substance and a probable carcinogen in humans. OSHA states legal permissible exposure limits (PEL) for airborne particles in the work environment as 0.002 mg/m^3 averaged over an eight-hour shift. Ceramic AlN material has emerged as a leading alternative to BeO due to its lack of toxicity and its high power-handling capabilities for resistive components.

When compared to BeO ceramic, AlN comes close in many aspects (Table 1), with the primary parameter of interest being thermal conductivity due to the high-power nature of the applications where the materials are used. Electrically, AlN has a higher dielectric constant than BeO, which leads to a somewhat higher-capacitance part. When using AlN, careful layout and film design must be employed to mitigate this difference.

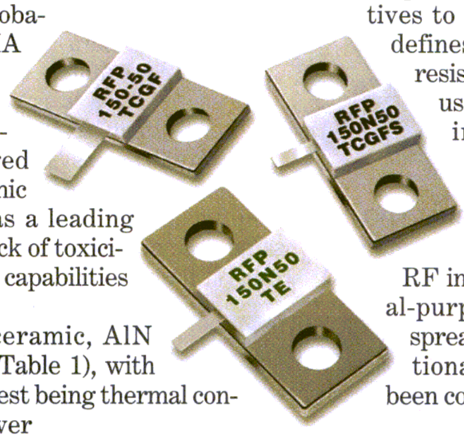

1. Representative samples of the thin- and thick-film AlN and BeO resistive components were tested to compare electrical and mechanical characteristics.

As part of a year-long development program, AlN resistors and terminations were designed at the RF Power Components subsidiary as drop-in alternatives to existing BeO product lines. This defines a general class of non-BeO RF resistive power products which can be used in a wide range of applications, including in absorptive filters, antenna feeds, isolators, power combiners, and RF power amplifiers (PAs).

AlN ceramic has been used in the RF industry for many years as a general-purpose electrically insulating heat spreader and thin-film substrate. Traditionally, AlN resistive devices have been constructed using thin-film technology, although the high cost of this approach has limited the use of these devices in some applications. With the continuing growth of the wireless industry and the subsequent need for a cost-effec-

Table 1: Comparing BeO and AlN

Parameter	BeO	AlN
Dielectric constant (ϵ_r)	6.7	8.5
Temperature coefficient (W/m-K)		
(at +25°C)	280	170
(at +100°C)	200	150
(at +200°C)	150	130
Coefficient of thermal expansion (PPM/°C)	6.4	4.6

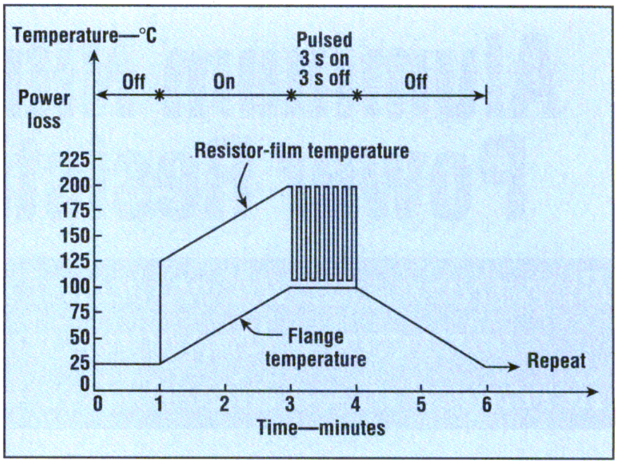

2. These temperature-cycling curves were applied to the thin- and thick-film BeO and AlN resistive components for accelerated life testing.

tive and safe BeO alternative, it was thought that lower-cost thick-film fabrication processes could be applied to AlN materials in order to produce an inexpensive line of resistive high-power passive components.

Thick-film systems for alumina (Al_2O_3 or aluminum oxide) and BeO were developed years ago and have been the workhorse of the RF power-resistive industry. Al_2O_3 is well-suited and often used for power levels to approximately 5 W. For higher power levels to approximately 800 W, BeO resistive components are used. However, the transfer of thick-film technology to AlN ceramic substrates is not a simple matter. Thick-film resistor and conductor systems that were developed for Al_2O_3 and BeO do not work on AlN ceramic materials. This is because the lead-oxide (PbO_2) glass-bonding system that takes place between the thick-film pastes and the Al_2O_3 or BeO ceramic material, when fired, is reducible by AlN ceramic. Applying thick-film pastes designed for Al_2O_3 or BeO on AlN ceramic materials will achieve inconsistent adhesion of the resistor and metal films to the AlN ceramic; this erratic adhesion has often been attributed to inconsistencies in the AlN ceramic material.

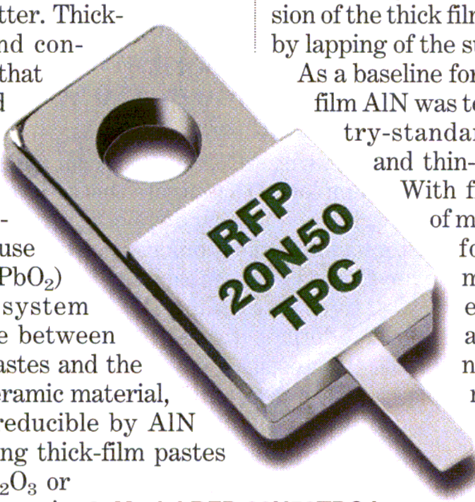

3. Model RFP-20N50TPC is a flange-mount component designed for 50-Ω systems.

Adhesion of the thick films to the ceramic is key to the long-term reliability of the component. Due to the recent demand for a cost-effective and safe BeO alternative by the wireless industry, thick-film paste manufacturers have recently developed thick-film AlN paste systems. Using these paste systems along with properly prepared AlN ceramic substrates has resulted in a new product offering of thick-film resistive components on AlN ceramic substrates. Another key to adhesion of the thick film is the proper preparation of the AlN ceramic material. During the AlN sintering process, Al_3O_3 + Y_2O_3 is driven to the surface of the ceramic. This unwanted material layer, which impedes adhesion of the thick film, must be removed by lapping of the substrate.

As a baseline for comparison, thick-film AlN was tested against industry-standard thick-film BeO and thin-film AlN products. With film adhesion being of main concern, testing focused on experiments which would exacerbate film-adhesion weaknesses or nonuniformities. For consistency, tests for all three systems were conducted on the same type of device, a 150-W, flange-mounted, 50-Ω termination. The device is a 0.250 × 0.375-in. (0.64 × 0.95-cm) ceramic chip mounted onto a nickel (Ni)-plated copper (Cu) flange with 96-percent-tin (SN96) solder. (Figure 1 illustrates the test parts.) Multiple parts of each system type were tested for lead pull, shear test, thermal cycling, film temperature, and resistor satiability.

Silver (Ag) ribbon leads measuring 0.050 × 0.006 in. (0.13 × 0.15 cm) were soldered to the same-sized conductor pad on the three types of devices and then pulled to destruction. The averaged results are listed in Table 2. The horizontal pull strength of all three systems was excellent, while the vertical pull tests appeared to show more robustness for the thin-film AlN and thick-film BeO devices.

Each type of part was soldered to a Ni-plated flange with SN96 solder and destructively sheared off the flange. The averaged results are listed in Table 3. Shear testing showed excellent initial adhesion for all systems with the BeO force being expectantly better and the thick-film AlN slightly better than the thin-film AlN system.

Table 2: Comparing thin- and thick-film systems during pull tests

Part number	System type	Substrate	Vertical pull	Horizontal pull
RFP-150N50TCGFS	Thin film	AlN	2.8 lbs.	10.9 lbs.
RFP-150-50TCGF	Thick film	BeO	2.8 lbs.	10.2 lbs.
RFP-150N50TE	Thick film	AlN	1.4 lbs.	9.4 lbs.

ACE YOUR TEST
WITH A TOTAL INTEGRATED SYSTEM SOLUTION
FROM DOW-KEY
Dow-Key Microwave has expanded its Switch Matrix product line to include integrated modular assemblies targeted specifically for the Automatic Test Equipment market.
Designed for Microwave, RF, video, and audio test applications in the DC to 18 GHz range, these customized, integrated assemblies provide the perfect interface between your test equipment and complex, sophisticated systems with multiple inputs and outputs that need to be tested.
The Dow-Key Switch Matrix technology is the basis of the integrated assembly. A variety of passive components and amplifiers are added, depending on your schematic, to provide customization and increased functionality to your testing process. Its modular design adds flexibility by allowing removal of sections from this complex assembly for easy maintenance and service.
For uniquely and superbly engineered designs that meet and exceed market demands, for unprecedented customer service and on-time delivery, for the highest quality product with unsurpassed reliability at the right price,
Dow-Key Microwave is your solution.
ISO 9001 CERTIFIED
VSWR
ISOLATION
INSERTION LOSS
FREQUENCY
Dow-Key® Microwave
CORPORATION
4822 McGrath Street, Ventura, Ca 93003
Tel: (805) 650-0260 • Fax: (805) 650-1734
Visit us at www.dowkey.com
A DOVER TECHNOLOGIES COMPANY
CIRCLE NO. 211

Table 3: Comparing thin- and thick-film systems during sheer-force testing

Part number	System type	Substrate	Shear force
RFP-150N50TCGFS	Thin film	AlN	218 lbs.
RFP-150-50TCGF	Thick film	BeO	314 lbs.
RFP-150N50TE	Thick film	AlN	234 lbs.

Table 4: Comparing thin- and thick-film systems during accelerated life testing

Part number	System type	Substrate	Cycles to failure
RFP-150N50TCGFS	Thin film	AlN	300 to 378
RFP-150-50TCGF	Thick film	BeO	300 to 378
RFP-150N50TE	Thick film	AlN	300 to 378

While shear testing is a good measure of the initial adhesion of the paste to the ceramic substrate, thermal cycling provides a good measure of the long-term reliability for a device. Differences in thermal expansion coefficients (TCE) between the AlN ceramic and the Cu flange create stress in the material that must be absorbed by the solder/thick-film-paste interfaces. For all three types of resistive components, thermal cycling acts as an excellent accelerated-life test. Simply dissipating power in a resistive component at a near-constant temperature does not provide an indication of the component's long-term reliability nor does it represent the worst-case working conditions. The adhesion layer must be repeatedly stressed from hot to cold in order to truly get a useful measure of how long the adhesion layer will absorb the stress without failure. This test is equivalent to a metal-fatigue test of repeatedly bending a metal bar back and forth until the bar breaks. The Cu-flange material and SN96 solder were chosen to provide a comparative accelerated measure of the long-term adhesion of the thick films to the ceramic substrates. The TCE of the Cu is 3.6 times the TCE of the AlN, and the SN96 solder has a tensile strength close to 6000 lbs. per square inch (psi). All three component versions were bolted to a microprocessor-controlled chill plate with a small amount of thermal grease under the flange. The parts were cycled at 100 percent of rated power (DC) and maximum flange temperature. The cycling profile (Fig. 2) was designed to provide an accelerated and harsh environment to expedite failures. The results of this testing are shown in Table 4.

All three parts failed between the 300th and 378th thermal cycle. Failure occurs due to the formation of micro cracks in the solder and/or thick film that propagates with each additional thermal cycle, thus increasing the thermal resistance between the ceramic and the flange. When the thermal resistance increases to the point where the thermal gradient across the system becomes large enough, a thermal runaway condition is set up and the part fails. From the test data, it can be seen that all three system types failed in the same range.

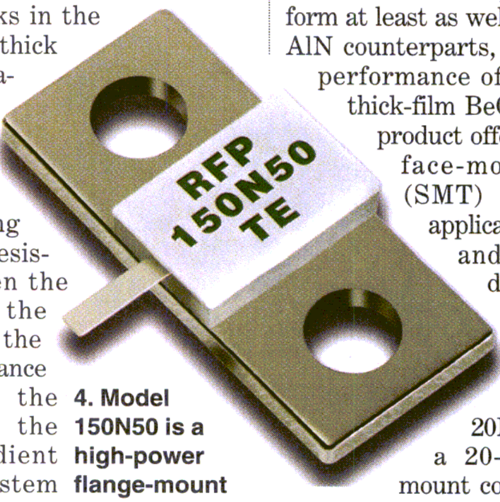

4. Model 150N50 is a high-power flange-mount termination capable of handling 150-W RF power in 50-Ω systems.

Parts from each system were mounted to a controlled heatsink at +100°C and 150 W of dissipation. Film-temperature measurements provide a good idea of the thermal resistance of each type of termination. Film-temperature measurements were performed using an infrared (IR) thermal probe. The results are detailed in Table 5. As expected, the BeO part exhibited a lower film temperature due to the lower thermal resistance of the BeO ceramic material. The thin- and thick-film AlN parts were within a few degrees of each other.

These tests validate the usefulness of the thick-film AlN ceramic resistive components as alternatives to widely used BeO products. The components are fabricated with a reliable and repeatable AlN process, made so by proper preparation of the AlN ceramic material and the use of pastes developed specifically for AlN. These special thick-film pastes contribute to a line of AlN resistive components that perform at least as well as their thin-film AlN counterparts, and approach the performance of more-expensive thick-film BeO products. Initial product offerings include surface-mount-technology (SMT) components for applications through 5 W, and flange-mount devices for applications through 150 W at PCS frequencies. As examples, model 20N50TPC (Fig. 3) is a 20-W AlN flange-mount component for 50-Ω systems while model 150N50 (Fig. 4) is a flange-mount termination for RF power levels to 150 W. For engineers interested in incorporating these AlN passive components into their newest designs, the firm plans on making S-parameter files freely available on their website. **RF Power Components, Inc., a subsidiary of Anaren Microwave, 125 Wilbur Pl., Bohemia, NY 11716; (516) 563-5050, FAX: (516) 563-4747, e-mail: info@rf-pow er.com, Internet: http://www.rf-power.com.**

CIRCLE NO. 51 or visit www.mwrf.com

Table 5: Comparing thermal characteristics of thin- and thick-film systems

Part number	System	Substrate	Film temperature	Theta film flange
RFP-150N50TCGFS	Thin film	AlN	+192°C	0.61°C/W
RFP-150-50TCGF	Thick film	BeO	+168°C	0.45°C/W
RFP-150N50TE	Thick film	AlN	+200°C	0.67°C/W


CapCadv3
Cap Cad V3 is the latest capacitor modeling software from Dielectric Laboratories. You'll work faster and smarter.
Quality
Choice
Reliability
Performance
CapCadv3
DLI DIELECTRIC LABORATORIES
A DOVER TECHNOLOGIES COMPANY
Now easier to use!
New Features:
Spice models
Smith chart plotting
S2P file exports
Compare 2 parts on the same graph
Modeling by part number input
Device1 Multilayer Capacitors
Multilayer Capacitors Part Number
Dielectric Laboratories
Visit us on the web...
www.dilabs.com
DLI DIELECTRIC LABORATORIES
A DOVER TECHNOLOGIES COMPANY
CIRCLE NO. 222
Call The Solutions Experts
At Dielectric Labs
2777 Route 20 East, Cazenovia, NY 13035
Ph: 315-655-8710 • Fax: 315-655-8179

VNAs Set New Marks For Noise, Speed, And Automation

Mixer-based receivers, a high-speed data-acquisition engine, and the Windows 2000 operating system arm these RF VNAs with considerably more power than their predecessors.

Steve Westerman and Mohamed Sayed

Agilent Technologies, 1400 Fountaingrove Pkwy., Santa Rosa, CA 95403; (800) 452-4844, Internet: http://www.agilent.com.

SPEED, accuracy, and ease of use: These three characteristics are among the many benefits to be gained from a new line of vector-network analyzers (VNAs) from Agilent Technologies (Santa Rosa, CA). The PNA series of analyzers, with models having top frequencies of 3, 6, and 9 GHz, leverage advances in high-speed microprocessors, digital-signal processors (DSPs), and software instruments to keep pace with the needs of high-volume component manufacturing. Incorporation of Microsoft's Windows 2000 operating system should ensure ease of use never before found in a high-frequency VNA.

In many cases, the overall architecture of modern VNAs remains remarkably similar to its predecessors of a decade ago, due in large measure to the enormous cost of creating a completely new instrument from start to finish. The PNA series of VNAs (Fig. 1) is an exception to this trend, however. Although created to displace the company's popular 8753 line of RF and microwave VNAs (introduced in 1981 and regularly upgraded), the PNA line is an entirely new instrument family.

To optimize RF performance, Agilent took an entirely different approach for signal processing than that employed in its other network analyzers. The instruments perform measurements faster, have lower noise and greater dynamic range, and provide more comprehensive automation and connectivity. The instruments also have four mixer-based receivers (Rxs) which facilitate through-reflect-line (TRL) and line-reflect-match (LRM) calibrations, a high-speed data-acquisition (DAQ) engine, and DSP algorithms which together increase measurement speed without exacting a penalty in noise or another instrument's performance parameters.

The validity of the new design shows in the performance. The measurement speed alone is between six and 35 times faster than its predecessor, the Agilent 8753ES (see table), and as fast as 35 μs per point. The trace noise is as low as 0.0005 dB, which is the best achievement of any VNA that Agilent (or its predecessor, Hewlett-Packard) has ever created. The normal dynamic-range performance of 128 dB, which is broad enough for most devices, can be extended to 143 dB by bypassing or reversing the transmission coupler.

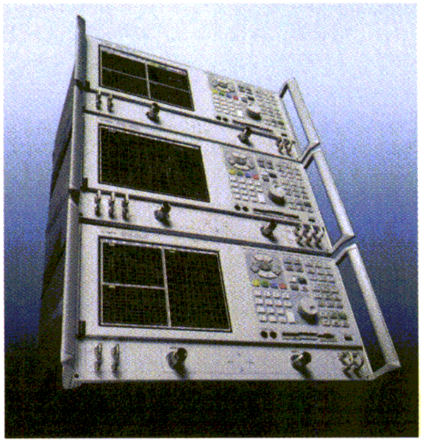

1. The PNA line of RF and microwave VNAs introduces a new approach to mixer-based vector analysis with models reaching 3, 6, and 9 GHz.

Most network analyzers, including the Agilent 8753, use samplers in their Rxs. These samplers have a host of advantages, including wide bandwidth, flat frequency response, excellent stability, and good compression. From a local-oscillator (LO) design standpoint, sampled systems are less complicated to construct, since they consist only of a low-frequency synthesizer followed by a sampling pulse generator. However, two attributes of samplers reduce their achievable performance. Noise floor and trace noise are high due to the sampler's inherently high noise figure, and phase locking is difficult in order to eliminate the possibility of locking to the wrong tooth of the sampler LO comb.

Since reducing the noise floor of the PNA series was one of its designers' primary goals, mixers rather than samplers were chosen (Fig. 2). In this design, the low-frequency pulsed LO is replaced by a high-frequency sinusoidal LO, and the conflicting requirements for greater sensitivity and higher power-handling capability are met with a configurable testset (the front-panel reference and Rx jumpers are a standard feature of the PNA series, and the source jumpers and 35-dB attenuators are optional). Rather than employing a single reference receiver, Agilent chose two. The second-reference Rx supports source leveling after

Contactless Phase Shifters:

World-First 'Contactless' Brings Better Reliability under All Conditions

Designed by KMW for low insertion loss and good stability under hard environmental conditions, these Contactless Phase Shifter (:CPS) will provide the linear characteristic of phase and low IMD performance

KPH90OSCL000

KPH90OSCL001

Standard Connectorized CPS

Product Code No.	A type : KPH90OSCL000 B type : KPH90OSCL001		
Frequency Range	~ 1GHz	1 ~ 2GHz	2 ~ 3GHz
Insertion Loss (Max.)	0.15dB	0.25dB	0.35dB
VSWR (Max.)	1.25:1	1.25:1	1.25:1
Incremental Phase Shift	90 degree min. @ 2GHz		
Electrical Delay	125 psec min.		
Nominal Impedance	50 ohm		
I/O Port Connector	SMA(F) / SMA(F)		
Average Power Handling	20W @ 2GHz		
Temperature Range	-30°C ~ +60°C		
Dimension (inch)	A type : 1.496*1.102*0.457 B type : 1.225*1.102*0.457		

KPH30OSCL000

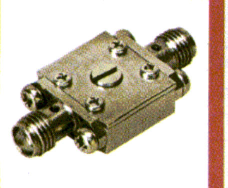

KPH35OSCL000

Miniature CPS

Product Code No.	Drop-In type (KPH30OSCL000)			Connectorized type (KPH35OSCL000)		
Frequency Range	~ 1GHz	1 ~ 2GHz	2 ~ 2.5GHz	~ 1GHz	1 ~ 2GHz	2 ~ 3GHz
Insertion Loss (Max.)	0.15dB	0.25dB	0.35dB	0.15dB	0.25dB	0.35dB
VSWR (Max.)	1.3:1	1.3:1	1.3:1	1.25:1	1.25:1	1.25:1
Incremental Phase Shift	30 degree min. @ 2GHz			35 degree min. @ 2GHz		
Electrical Delay	41.7 psec min.			48.6 psec min.		
Nominal Impedance	50 ohm			50 ohm		
I/O Port Connector	Drop-In			SMA(F) / SMA(F)		
Average Power Handling	30W @ 2GHz			30W @ 2GHz		
Temperature Range	-30°C ~ +60°C			-30°C ~ +60°C		
Dimension (inch)	0.709*0.433*0.244			0.630*0.551*0.244		

13131 East 166th Street, Cerritos, CA 90703-2202
1-800-8320-KMW • www.kmwinc.com
tel: 562-926-2033 • fax: 562-926-6133

CIRCLE NO. 374

KMW
RF & Microwave Products

Comparing the PNA analyzers with the 8753ES VNA

Parameter	8753ES	PNA series
Sweep time (201) points	73 ms, 14 updates/s (6-kHz IF bandwidth	12 ms 83 updates/s (35-kHz IF bandwidth)
Measurement time per point (1601) points	265 µs per point 423-ms sweep (6-kHz IF BW)	35 µs per point 60-ms sweep (35-kHz IF BW)
Measurement speed 100-dB dynamic range 120-dB dynamic range	 470 ms (1-kHz IF bandwidth) 42.5 s (10-Hz IF bandwidth)	 29 ms (35-kHz IF bandwidth) 1.2 s (300-Hz IF bandwidth)

the switch, which improves power-level accuracy, source match, and measurement repeatability, and also enables TRL calibration (which is useful for on-wafer device probing) to be performed.

The inherent lower noise figure of mixers directly impacts dynamic range, reducing the noise floor in the instrument by 15 to 20 dB. Fundamental mixing is employed to 3 GHz and third-harmonic mixing from 3 to 9 GHz. This contrasts with sampled systems, which can perform conversion on LO harmonics greater than 100. Low-order mixing also produces superior system spurious and residual performance which, in turn, reduces analyzer trace noise and increases usable dynamic range.

Mixers enable the instrument to make measurements faster as well, since the time required to make high-dynamic-range measurements is inversely proportional to the measurement bandwidth. That is, a sweep performed in a 10-Hz bandwidth will take 10 times as long as a sweep made in a 100-Hz bandwidth. If the system noise figure is lowered by 10 dB through the use of mixers instead of samplers, or if the source power is increased by 10 dB, the 100-Hz bandwidth will yield the same signal-to-noise ratio (SNR) as the 10-Hz bandwidth did before either improvement was made. In either case, however, the measurement speed increases tenfold. If the source power is increased by 10 dB, and the noise figure is improved by 10 dB, a 1-kHz bandwidth can be used, and the measurement speed may be increased one hundredfold.

In addition, mixers increase measurement speed because the mixing order is low, so fewer false responses enter the phase-lock circuitry. Avoiding false locking reduces the time for phase-lock acquisition. Since the LO and source have the same tuning sensitivities, open-loop frequency tracking of the LO and source are greatly improved which, in turn, lowers closed-loop frequency error, speeding up phase-lock acquisition, sweeping, and stepping.

Optimizing the mixer-based approach requires attention to one inherent characteristic—mixer bounce—which, if left unimproved, can dramatically reduce achievable instrument sensitivity. The mechanism (Fig. 3), which can be present in sampler and mixer-based systems, causes spurious responses. An insertion-loss measurement of a low-loss 3.6-GHz filter with very reflective stopband (Fig. 4a) provides a graphic illustration of the phenomena. The source frequency is in the filter's stopband, so following the dashed line from the source, energy can be reflected from the filter input. This signal enters reflection Rx A and mixes with the harmonics of the LO.

The resulting products N $\times$ LO $\pm$IF exit Rx A, pass through the filter, re-mix with LO harmonics in transmission Rx B, and create false responses. Source power is +10 dBm, and the IF bandwidth is 10 Hz with no averaging. The largest response, at 1.8 GHz, is produced by the 1LO + 1RF term from Rx A converting with the 2LO term in Rx B. Reference Rx R1 will also generate mixer bounce, but at a much lower level than Rx A, due to splitter isolation.

To rid the PNA series of mixer bounce, Agilent employs two techniques. In the first, reverse isolation from each mixer to its respective RF input is increased as much as possible, so the mixing products cannot leave the reflection Rx. If even more mixer-bounce reduction is needed, the reflection receiver can be disabled entirely when making a transmission measurement. Alternately, turning off the A or B mixers requires twice as many sweeps to gather all four S-parameters and, ultimately, residual mixer bounce from the reference Rx can limit dynamic range. The same filter measured

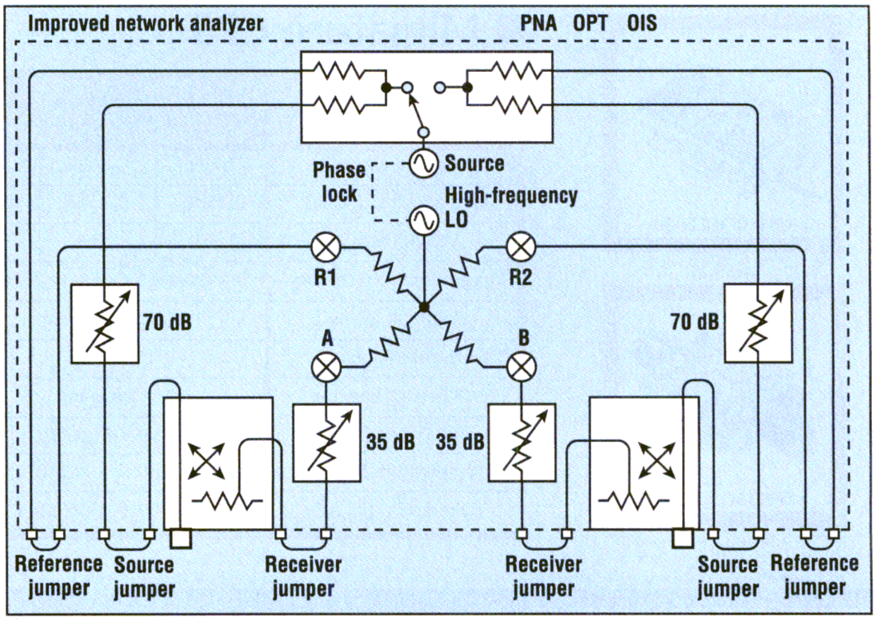

2. The PNA receivers employ mixers rather than samplers.

RIDE THE POWER CURVE

OF NONLINEAR SIMULATION PERFORMANCE

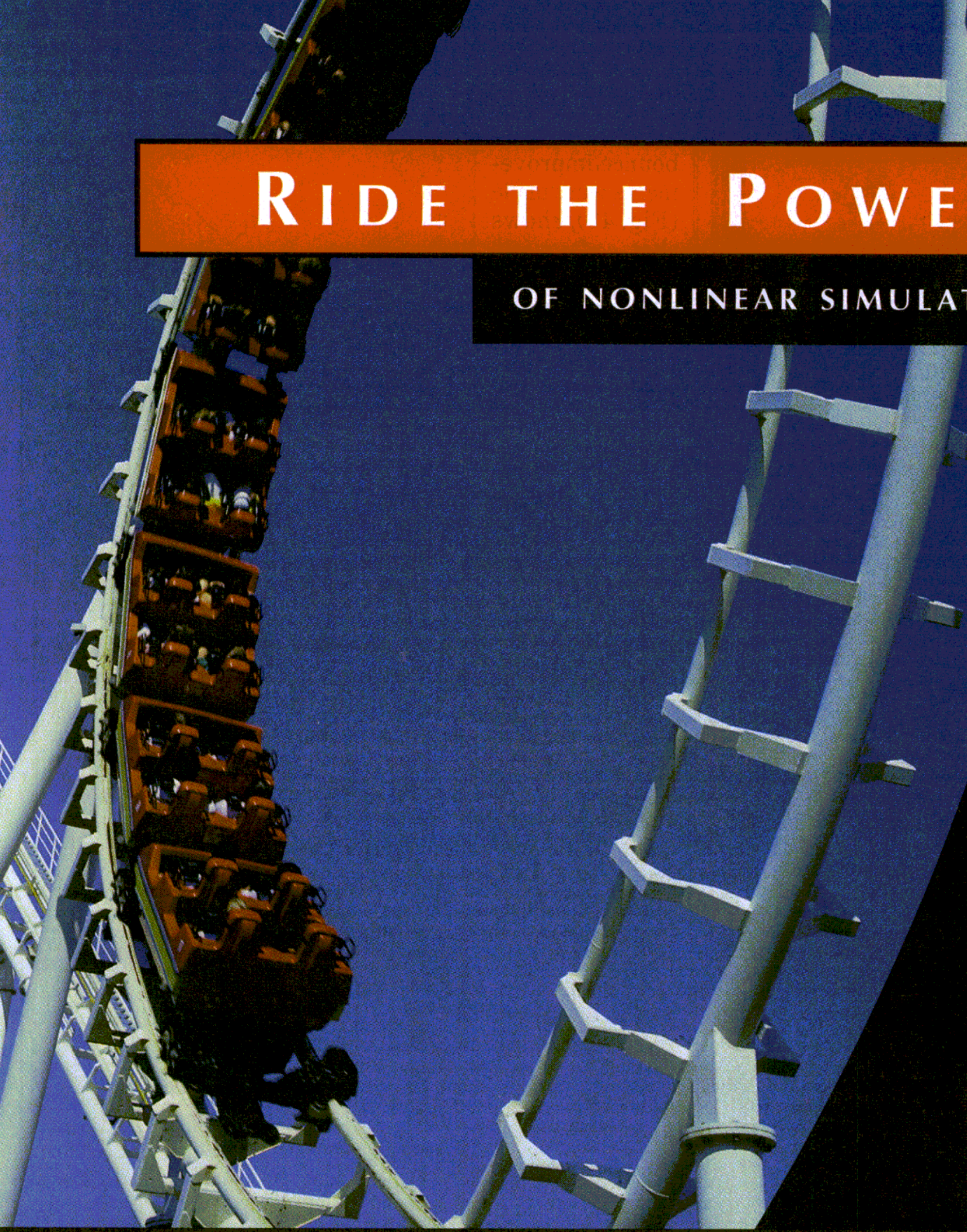

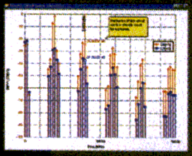

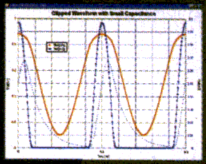

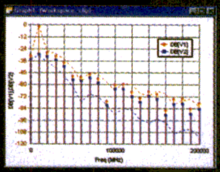

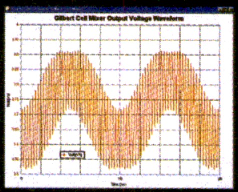

Power, Accuracy and Speed. That's what you get with Eagleware's new harmonic balance simulator, HARBEC™. From real-time tuning, to application of artificial intelligence techniques, to co-simulation with electromagnetics, HARBEC does it all ... with a powerful set of features that includes:

Robust Simulation
- unlimited, arbitrary circuit topology
- wide range of nonlinear device models (diodes, JFET, BJT, MOSFETS, MESFETS)
- wide range of sources (voltage, power, current, waveform)
- DC analysis and optimization
- unlimited tone harmonic balance analysis and optimization

EM Co-simulation

High Performance Design
- AI performance optimization
- fast tuning

Spice Model Import

Extensive Parts Library

Equations and Post Processing

And it's fully integrated into the GENESYS suite of synthesis, S-parameter, electromagnetic and physical design tools.

So Grab a Seat and Hold On! With nonlinear modules priced at $4990, they're going fast. And so will your design.

EAGLEWARE
RF and Microwave Design Software

CIRCLE NO. 225

Phone: +1 678-291-0995
sales@eagleware.com
www.eagleware.com
Fax: +1 678-291-0971

after mixer-bounce improvements were made (Fig. 4b), shows that after 10 sweeps are averaged to reduce noise floor, the problem is dramatically reduced. Mixer bounce is not coherent from sweep to sweep as in crosstalk, so it will not average-down like noise.

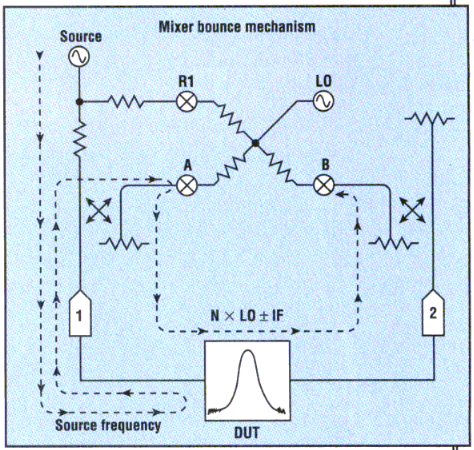

3. The mixer-bounce mechanism causes spurious responses.

The Windows 2000 Professional operating system endows the instruments with capabilities found only in the personal-computer (PC) domain. The PNA series is one of the first microwave-instrument families to be so endowed, and operates with the familiar Windows interface, rather than the more-common "Windows-like interface." As a result, the instruments require no leap of knowledge for anyone familiar with Windows and perform functions in the same way as a Windows 2000 PC.

More important, however, is the PNA's ability to integrate into any network based on Windows NT or Windows 2000 no differently than any other node on the network would. It can run from the network, can avail itself of network-attached storage, peripherals, software, off-line data-analysis capabilities, and virtually anything else connected to the network, including intranet and Internet communications through the integrated Web browser. Firmware can be downloaded from the Agilent website, and interactive remote trou-

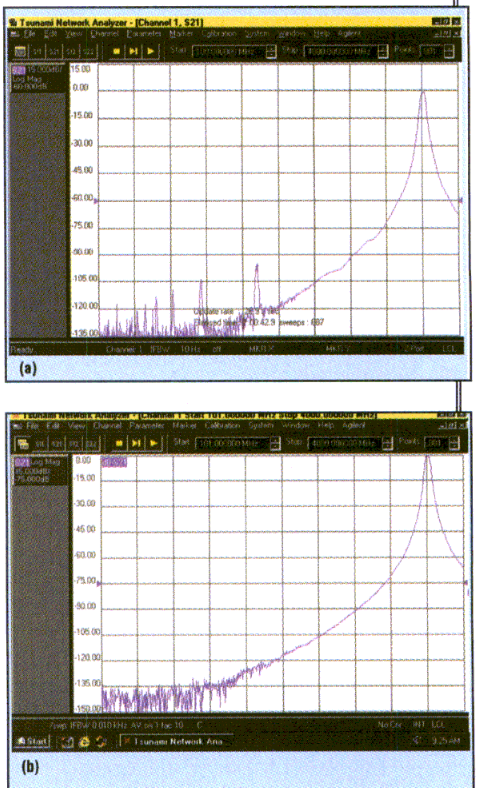

4. This insertion-loss measurement of a filter without mixer-bounce improvements (a) shows spurious responses. In (b), the problem is dramatically reduced.

In the race to get to hardware...

Ensemble gives you room to move

Opening a new world in
Analog, Digital,
Signal Integrity, RF and
Microwave Design.
Check out
http://www.ansoft.com/
No-Boundaries.html

Whether you are designing a Si RFIC for Bluetooth, a high performance GaAs power amplifier for 3G, or a multi-band planar antenna, Ensemble's advanced planar electromagnetic field solver helps you reduce die space, predict EM coupling, and calculate antenna radiation.

Use Ensemble to compute S-parameters and full wave fields for on-chip components such as spiral inductors, capacitors, thin-film resistors, and interconnects in microstrip, stripline, slotline, and coplanar waveguides. Ensemble handles realistic circuits with straight and curved traces, radiation, multiple layers, open plus closed cavities, and packaging effects.

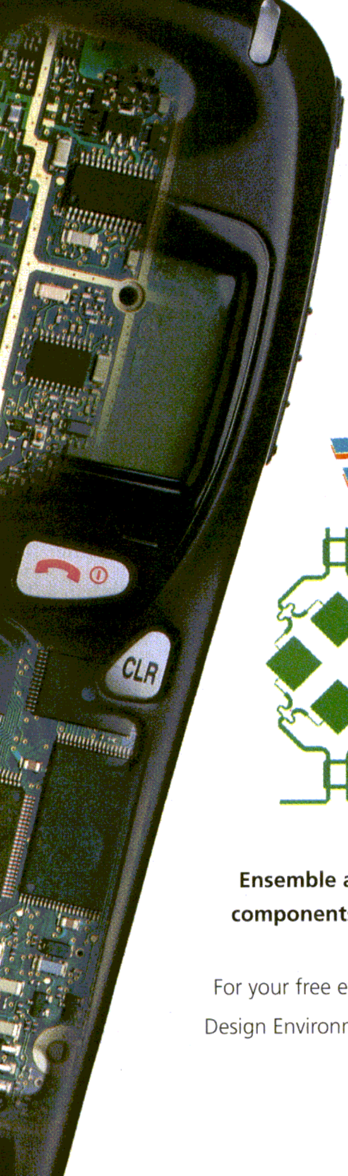

Ensemble offers an easy-to-use interface, DXF import, a graphical post-processor, optimization, parametrics, industry leading fast solver technology, and integration with other products in the Serenade Design Environment.

Design Freedom

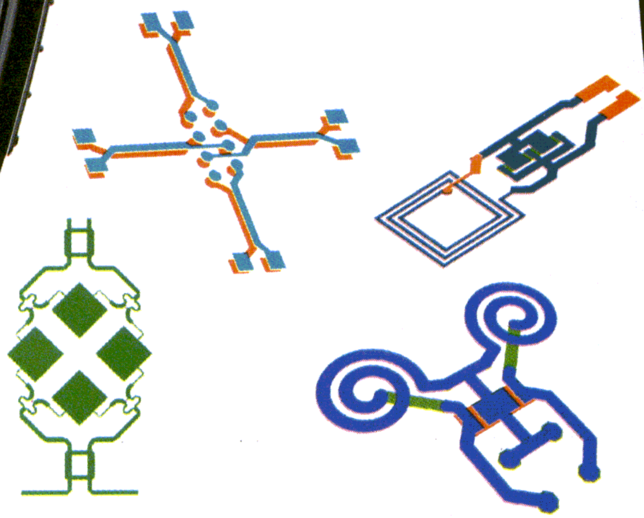

Ensemble allows you to design complex planar antennas and on-chip components like spiral inductors, vias and interconnects.

For your free evaluation copy of Ensemble, or any of the tools in Ansoft's Serenade Design Environment call 412-261-3200 or send e-mail to info@ansoft.com

ANSOFT
high performance EDA

www.ansoft.com

CIRCLE NO. 271

bleshooting through Agilent technical support can be performed online as well.

In a production environment, several analyzers can run programs independently to control their test stations, and the measurement data collected at each test station can be stored locally on the network analyzer or on a remote file server accessible through the local-area network (LAN). In addition, code can be executed directly from the analyzer or over a LAN or general-purpose interface bus (GPIB), and developed in popular programs such as LabVIEW, Visual Basic, Visual C++, or Agilent-VEE. Trace data and screen images can be imported directly into Microsoft Word or Excel for post-processing on the analyzer or a PC. The instruments feature GPIB, parallel, serial, and universal-serial-bus (USB) interfaces.

The PNA series allows measurements to be made over user-defined frequency segments, which significantly increases measurement speed by collecting data only at specific points. To optimize sensitivity, the instrument's transmitted coupler can be reversed, which is handy when characterizing filters used in transmit/receive duplexers and other applications where high-performance filters are used. The resulting reduction in system noise figure can also be employed to increase measurement speed. Greater dynamic range can also be achieved by inserting a low-noise amplifier (LNA) which has stable amplitude and phase characteristics before the instrument's Rx. The dynamic range of the PNA series can be increased to more than 143 dB by bypassing or reversing the transmission coupler, and even further with the addition of the LNA.

Increasing source power, implemented with an external power amplifier (PA), reference coupler, and reference attenuator, can also increase dynamic range. The internal port-1 coupler is used for reflection measurements and the 35-dB, five-step attenuator ensures that the power from the coupled arm of port 1 remains within the allowable input power range of the Rx. A high-power output coupler and internal 35-dB attenuator handle the high transmitted power, and a high-power isolator provides a good termination to the amplifier output, and keeps dangerous levels of power out of the analyzer.

The full range of PNA series capabilities includes full integration of Agilent's ECal electronic-calibration product, the ability to display up to 16 traces simultaneously, along with four stimulus settings, and optional time-domain filter tuning (which reduces tuning time by up to 10 percent). P&A: E8356A (3 GHz) $43,000, E8357A (6 GHz) $49,000, E8358A (9 GHz) $55,000. **Agilent Technologies, 5301 Stevens Creek Blvd., MS 54LAK, Santa Clara, CA 95052; Internet: http://www.agilent/find/pna.**

CIRCLE NO. 52 or visit www.mwrf.com

HBT Amplifiers Boast High Linearity

A family of low-cost, medium-power, InGaP/GaAs HBT amplifiers provides high reliability and linearity over broad bandwidths through 3 GHz.

DON KELLER
Senior Editor

DIGITAL wireless communications systems have pushed the limits of high-frequency technology while operating under severe price constraints. The amplifiers for these systems, for example, must be inexpensive yet provide generous gain with high linearity. The amplifiers must also be extremely reliable, since wireless customers expect no less from their services. These seemingly unrealistic requirements are met through smart design practices and controlled manufacturing processes, a combination that has led to the development of a family of medium-power, heterojunction-bipolar-transistor (HBT) amplifiers from EiC Corp. (Fremont, CA). The amplifiers provide better than 15-dB gain and more than +18-dBm output power through 3 GHz.

The amplifier family includes models EC1089, EC1019, EC1078, and EC1119 (see table). The newest member of the family, model EC1089, is designed for applications from DC to 2.5 GHz. This is not a fully matched 50-Ω device; rather, it requires some nominal input matching circuitry for use in 50-Ω systems. While it can be used without output matching circuitry, optimum performance is achieved by adding a small amount of output matching. The EC1089, which is supplied in a low-cost, plastic SOT-89 package, is a true Class A amplifier, with linearity characterized by an impressive output third-order intercept point (IP3) of +42 dBm. The HBT amplifier boasts 15-dB gain across its frequency range, and achieves +23.5-dBm output power at 1-dB compression. The amplifier includes on-chip negative feedback to guarantee stability and protect against unwanted oscillation. In fact, a load mismatch up to an equivalent VSWR of 10.0:1 creates no spurious products across the frequency band.

Model EC1019 is also a Class A amplifier, designed for +5-VDC operation. It delivers 18.5-dB gain from DC to 3 GHz, and generates +19-dBm output power at 1-dB compression. While lacking the outstanding linearity of the EC1089, the EC1019 nonetheless achieves an output IP3 of +34 dBm.

The EC1119, also a +5-VDC Class A amplifier, offers somewhat less gain than the EC1019, at 14.8 dB from DC to 3 GHz. The output power at 1-dB compression is comparable, at +18.6 dBm, but the amplifier provides approximately 2-dB more dynamic range, with an output IP3 of +36 dBm. The EC1019 and EC1119 are supplied in standard micro-X packages, although both are also available in plastic SOT-89 packages.

Model EC1078 is a +6-VDC linear HBT amplfier that is matched to 50 Ω through on-chip resistive feedback. Only DC blocking capacitors are needed at its input and output ports. The rugged amplfier achieves 19.5-dB typical small-signal gain from DC to 3 GHz with +21-dBm typical output power at 1-dB compression. The amplifier's linearity is marked by an output IP3 of +37 dBm. It is supplied in a standard plastic SOT-89 package.

The amplifiers are based on a proven indium-gallium-phosphide (InGaP)/gallium-arsenide (GaAs) HBT process developed at the company's foundry. To ensure long operating lifetimes, each of the amplifiers is subjected to a rigorous burn-in procedure. **EiC Corp., 45738 Northport Loop West, Fremont, CA 94538; (510) 979-8999, FAX: (510) 979-8902, e-mail: sales@eiccorp.com, Internet: http://www.eiccorp.com.**

CIRCLE NO. 53 or visit www.mwrf.com

Vital statistics for EiC Corp.'s family of HBTs

Model	Bandwidth (GHz)	Gain (dB)	Output power (dBm)	Third-order intercept (dBm)
EC1089	DC to 2.5	15	+23.5	+42
EC1019	DC to 3.0	18.5	+19	+34
EC1078	DC to 3.0	19.5	+21	+37
EC1119	DC to 3.0	14.8	+18.6	+36

Bluetooth Enables Line Of Remote Wireless Sensors

This line of sensors uses low-power communications within the unlicensed 2.4-GHz Bluetooth band to form remote and cost-effective wireless data-acquisition systems.

JACK BROWNE
Publisher/Editor

BLUETOOTH is commonly referred to as the "wireless personal connectivity" standard, since it is aimed primarily at wireless communications between computing devices and peripherals. But in the CrossNet architecture from Crossbow Technology (San Jose, CA), Bluetooth has been given a whole different look, since the unlicensed Bluetooth band from 2400 to 2500 MHz is the basis for cost-effective data-acquisition (DAQ) systems using personal computers (PCs) or personal digital assistants (PDAs) compliant with the Bluetooth specification.

Crossbow's CrossNet architecture gathers data from wireless Bluetooth connections, rather than from wires, simplifying the setup and modification of a DAQ network. The architecture allows computers to quickly gather data from sensors in a variety of equipment, including industrial equipment, medical systems, within vehicles, factories, and buildings. The CrossNet technology enables the use of sensors in equipment which is difficult to connect through wired sensors. Data can be moved quickly and easily through the CrossNet system to the Internet, for example, for access by one or more authorized users in remote locations.

The modular CrossNet architecture is adaptable to a variety of changing requirements. It employs compact nodes measuring only 3.5 × 2.5 × 0.75 in. (8.89 × 6.35 ×1.91 cm) which can control and monitor as many as four sensors. Each node contains a Bluetooth radio capable of transmitting and receiving data over a distance of 10 m (transmit power of 0 dBm) with a PC or PDA. Optionally, distances as far as 100 m can be handled by using a Bluetooth radio in class 1 operation, with transmit power of +20 dBm.

The architecture also features smart-input/output (S I/O) connections for linking individual sensors to a node. Based on the IEEE 1451 transducer-electronic-data-sheet (TEDS) standard, S I/O sensor-interface cables can connect with virtually any sensor. The S I/O interface cable contains the required circuitry, such as a microcontroller for node communications along with memory for the TEDS configuration information. The IEEE 1451 standards define the protocols and functions that provides the transducers with interchangeability, self-identification, and network independence.

After a sensor has been configured with S I/O, the CrossNet node can automatically detect the type of sensor that is being used, determine its usable range, and report the data in appropriate engineering units. By using the S I/O, sensors can be calibrated and reconfigured through wireless connections over the Internet.

The CrossNet architecture supports a variety of sensor manufacturers and types of sensors, including temperature, pressure, motion, flow, gas, chemical, humidity, magnetic, light, strain, and Global Positioning System (GPS) sensors. The sensors are connected to the CrossNet nodes through the S I/O connected to the node. Data collected at the CrossNet nodes are transmitted to a network hub or other Internet appliance, such as a desktop computer or PDA. The node can supply excitation to each sensor, or external sensor power can be used. Sensor signals are digitized with 16-b resolution for transmission along with the TEDS for each sensor.

A CrossNet hub can be any Bluetooth-enabled device. The hub downloads data, including the TEDS information, from multiple nodes with multiple sensors. Hubs can be as simple as a single computer or PDA to web servers communicating through transmission-control-protocol/Internet-protocol (TCP/IP) Internet communications protocols for wide-area networks (WANs). The hubs can also connect using the TCP/IP to other wired or wireless network configurations, including Ethernet networks.

CrossBow Technology provides Windows-based software to transmit commands to and gather data from the CrossNet nodes. The firm also provides ServeWare software which extends real-time access to CrossNet data to remote users. It is connected through the Internet. **Crossbow Technology, Inc., 41 E. Daggett Dr., San Jose, CA 95134; (408) 965-3300, FAX: (408) 324-4840, e-mail: info@xbow.com, Internet: http://www.xbow.com.**

CIRCLE NO. 54 or visit www.mwrf.com

Dielectric Resonators Offer Broad Tuning Ranges

Designers can now adjust the center frequency of their dielectric resonator filters and oscillators by up to 500 MHz at frequencies to 25 GHz.

JACK BROWNE
Publisher/Editor

DIELECTRIC-RESONATOR oscillators (DROs) and dielectric-resonator filters are generally assembled with great care and effort. Placement of the dielectric puck in the resonant cavity must be precise to ensure a center frequency within acceptable bounds. In the case of multistage filters, the sensitivity of placing the dielectric pucks is multiplied. Because the size of the dielectric puck determines the ultimate oscillating or resonant frequency in these designs, there has been no easy solution to manufacturing DROs and dielectric resonator filters—until now. With the PUCK-TRIM line of dielectric resonator tuners from Tekelec Components, engineers are now afforded tuning ranges of 300 to 500 MHz for operating frequencies from 8.5 to 25.0 GHz.

The use of a dielectric resonator supports frequency generation and filtering in a smaller volume than conventional metallic cavities. Essentially, a large metallic resonant cavity is replaced with the much smaller dielectric puck, comprised of a ceramic material that is extremely stable over wide temperature ranges. In Tekelec's standard lines of dielectric resonators, materials with dielectric constants ranging from 20 to 90 are used, with frequency stability in many cases as good as 0 ± 1 PPM/°C. By correctly defining the dimensions of the puck (i.e., its height and diameter), an operating frequency can be adjusted within ±0.5 percent.

The PUCK-TRIM line of dielectric-resonator tuners add a new dimension to the use of dielectric resonators. While good design practices should still be followed, the PUCK-TRIM dielectric-resonator tuners afford generous tuning ranges to fine-tune the final frequency of operation. The PUCK-TRIM tuners feature a base formed of the dielectric puck, above which is a metallic plate and tuning screw to adjust the resonance of the puck.

The PUCK-TRIM dielectric-resonator tuners can be supplied with puck diameters ranging from 5.9 mm for the lowest frequencies of operation (8.5 to 10.5 GHz) and as small as 2.2 mm for the highest frequencies of operation (22 to 25 GHz). A tuner designed for applications from 12 to 15 GHz, for example, provides a total tuning range of 400 MHz. It features a dielectric resonator puck with diameter of 4.1 mm (see table) and height of 5 mm above the mounting plate or substrate.

For those who would prefer the use conventional (fixed) dielectric-resonator pucks, the company also offers traditional dielectric resonators, as well as a free program to help designers select the right materials for their applications. Available for free download from the firm's website, the "dielpuck.exe" dielectric-resonator calculator program helps designers define the parameters of dielectric resonators. Users can calculate the dimensions of a dielectric puck by entering their desired frequencies of operation, or select from a list of suggested diameters to compute the operating frequency and height of the dielectric puck. **Temex Components, a subsidiary of the Tekelec Group, 33 avenue Faidherbe 93106, Montreuil Cedex, France; (33) (0) 149884900, FAX: (33) (0) 148581046, e-mail: componentssales@temex.fr, Internet: http://www.temex-components.com.**

CIRCLE NO. 55 or visit www.mwrf.com

The PUCK-TRIM dielectric-resonator tuners at a glance

Operating frequencies	Tuning range	Puck diameter	Height
8.5 to 10.5 GHz	300 MHz	5.9 mm	5 mm
10 to 12.5 GHz	300 MHz	4.9 mm	5 mm
12 to 15 GHz	400 MHz	4.1 mm	5 mm
14 to 18 GHz	400 MHz	3.4 mm	5 mm
18 to 22 GHz	500 MHz	3.1 mm	4 mm
22 to 25 GHz	500 MHz	2.2 mm	4 mm

Note: Height refers to the typical height of the dielectric-resonator trimmer above the substrate on which it is mounted.

Filter-Based Subsystem Switches From 1 To 18.5 GHz

This 10-channel switched-filter bank (SFB) is ideally suited for radar-warning receivers (RWRs) and electronic-intelligence (ELINT)-gathering receivers.

Floyd Parin
President
Microwave & Video Systems, Inc., 87B Sandpit Rd., Danbury, CT 06810; (203) 792-7474, FAX: (203) 792-7475, e-mail: mvsmicro@att.net, Internet: http://www.micronetics.com.

SWITCHED-FILTER banks (SFBs) serve receivers where wide frequency ranges are partitioned into more manageable portions for analysis. The model 10SF8181 SFB from Microwave & Video Systems, Inc. (Danbury, CT) divides the range from 1.0 to 18.5 GHz into 10 channels, while maintaining maximum input and output VSWR of less than 2.20:1 for all subbands.

The model 10SF8181MFA SFB exhibits maximum insertion loss of 1 dB, with minimum isolation between channels of 55 dB. The SFB incorporates a transistor-transistor-logic (TTL) decoder for band-switching control, and can shift among its different bands with maximum switching speed of 200 ns.

SFBs, such as the 10SF8181, are used in the front end of broadband superheterodyne receivers. They divide the RF band into separate channels before the separated signals are downconverted for signal analysis and processing. The band breaks are typically less than one octave to minimize signal harmonics and reduce the amplitude of second harmonics generated from the input PIN-diode switches in the presence of strong signals. Band breaks of less than one octave also reduce the probability of receiving simultaneous signals and the effects of third-order intermodulation distortion (IMD) on receiver (Rx) performance. Band breaks in the 10SF8181 include 1.0 to 1.5 GHz, 1.5 to 2.5 GHz, 2.5 to 4.5 GHz, 12.5 to 14.5 GHz, and 16.5 to 18.5 GHz.

By design, the low band (1.0 to 6.5 GHz) has a highpass filter before the single-pole, four-throw (SP4T) filter switch, to reduce interference from high-frequency and very-high-frequency (VHF) sources and emitters typically found in military environments (see figure). Another highpass filter at the outputs provides additional attenuation to signals below 1 GHz. A highpass filter preceding the single-pole, six-throw (SP6T) switch in the 6.5-to-18.5-GHz band provides attenuation of signals below 6.5 GHz, such as those used in radar systems.

The dual RF output can be used as inputs to separate frequency-converting receivers for specific applications. For example, a fast-tuning activity receiver operating with a wide intermediate-frequency (IF) bandwidth (200 to 500 MHz) can scan and record signals in selected bands of interest. Scanning in a wideband IF reduces the dwell time for each tuning step with the penalty of reduced sensitivity for a particular minimum signal-to-noise ratio (SNR).

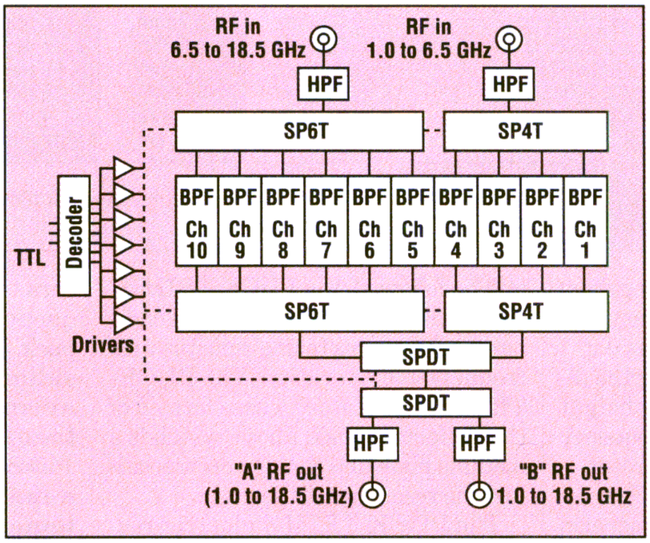

Highpass filters are used to remove unwanted harmonic signals and interfering emitters.

The 10SF8181 switched-filter bank measures 11.18 × 12.7 × 1.55 cm. Its operating temperature is –30 to +85°C. **Microwave & Video Systems, Inc., 87B Sandpit Rd., Danbury, CT 06810; (203) 792-7474, FAX: (203) 792-7475, e-mail: mvsmicro@ att.net, Internet: http://www.micronetics.com.**

CIRCLE NO. 57 or visit www.mwrf.com

ELECTRONIC PACKAGING AND INTERCONNECTION HANDBOOK

Charles A. Harper

Electronic packaging brings together a wide range of engineering and manufacturing technologies to transform an idea (an electronic circuit) into a tangible object (a manufactured assembly). Success requires project leaders to understand the fundamentals of electronics, mechanics, thermodynamics, chemistry, materials, components, computer-aided simulation and design, as well as testing and manufacturing. The challenge is made daunting by the rapid changes taking place in all of these areas.

Electronic Packaging and Interconnection Handbook provides an up-to-date review of many of the technologies involved. The third edition of the text is divided into three parts. Part 1 covers the fundamentals of electronic packaging. Part 2 focuses on interconnection technologies. Part 3 considers system-level issues related to packaging.

Chapter 1 introduces some of the materials employed in electronic packaging, highlighting the latest polymeric materials used as encapsulants, coatings, and adhesives. Much of the chapter illustrates flip-chip technologies that promise to improve the performance and density of complex, high-speed systems. The chapter also discusses a variety of ceramic, glass, and diamond materials.

Chapter 2 looks at thermal management, with a thorough tutorial on heat flow and the thermal properties of numerous materials and electronic components. Also presented are methods of measuring the temperature profiles of operating circuits. The chapter illustrates several cooling methods such as jet impingement and thermoelectric modules.

Chapter 3 describes several effects of thermal and mechanical stresses on a variety of materials and structures. Methods of simulating heat flow are also described. Chapter 4 outlines connector and interconnection technologies.

Chapter 5 introduces the details of wiring and cabling. The chapter describes important electrical characteristics such as cross-talk, bandwidth, pulse risetime, reflections, and delay. A number of useful websites are listed at the end of Chapter 5. Chapter 6 closes Part 1 of the text by discussing the soldering technologies used in a variety of applications. Topics include solder mixtures, fluxes, temperature profiles, and processing equipment.

Part 2 of the *Handbook* begins with Chapter 7, which highlights integrated circuits (ICs) and the packaging and interconnecting technologies used therein. Topics include package layout, wire bonding, tape-automated bonding, and flip-chip bonding. Chapter 8 examines surface-mount technologies, including process guidelines, methods of inspection, and reliability issues. Chapter 9 discusses the packaging of hybrid microelectronic circuits and multi-chip modules.

Chapter 10 reviews chip-scale packaging (CSP) and direct-chip-attach (DCA) technologies with a discussion of current applications and challenges. Topics relating to CSP include dimensional standards, thermal management, and encapsulation materials. Issues surrounding DCA include the need for known good die, reliable bonding processes, and compatible substrates. Chapter 11 targets both rigid and flexible printed-wiring boards, highlighting the materials and manufacturing methods employed. Microvias are discussed in detail, and dozens of industry standards are listed for materials, design guidelines, test methods, applications, reliability, and electromagnetic (EM) compatibility.

The third part of the book looks at system-level issues. Chapter 12 addresses the challenges of high-speed and microwave systems, comparing the advantages and disadvantages of various transmission lines and circuit structures. Chapter 13 deals with the unique challenges of packaging high-voltage systems.

Chapter 14 devotes 50 pages to one of the most challenging aspects of electronic packaging—electrical characterization and modeling. Due to this short length, the modeling tools provided are simplistic and do not adequately demonstrate the difficulties normally encountered when one attempts to accurately characterize electrical parameters such as crosstalk, dispersion, and parasitic resonances.

Every chapter is well-organized, with numerous references for additional information. As it packs a wealth of information into a relatively small space, the *Handbook* limits the extent of most theoretical discussions to those required to make a particular point. Most design guidelines are presented as "rules of thumb" without the necessary complex theoretical analyses to back them up. Although much of the information may be oversimplified for many applications, the text is a valuable tool for rapid development, guiding designers and managers from the initial planning stages to final production.

(2000, 1069 pp., hardcover, ISBN: 0071347453, $125.00.) **McGraw-Hill Co., 2 Penn Plaza, New York, NY 10121; (800) 262-4729, FAX: (614) 759-3641, e-mail: pbg.ecommerce_custserv@mcgraw-hill.com, Internet: http://www.books.mcgraw-hill.com.**

BWOs Tune Across Millimeter-Wave Applications

This line of rugged BWO tubes provides broad frequency ranges and fast sweep times for a wide range of millimeter-wave applications.

JACK BROWNE
Publisher/Editor

BACKWARD-WAVE oscillators (BWOs) are powerful broadband sources of millimeter-wave signals. Ideal for communications systems, test equipment, and plasma diagnostics applications, these vacuum-tube devices are now available from stock from an unexpected source: the ELVA-1 Millimeter Wave Division (St. Petersburg, Russia). The BWO tubes can be specified from 36 to 178 GHz in four bands, with output-power levels of 20 mW or more at 100 GHz.

The 36-to-178-GHz band is covered by four models: BWO-6 (36 to 55 GHz), BWO-4 (52 to 79 GHz), BWO-3 (78.2 to 119 GHz), and BWO-2 (118 to 178 GHz). The BWOs feature linear characteristics of output power versus anode current. The output frequency is determined by a high voltage applied to the tube's anode, typically in the range of +500 to +1500 VDC. Precision machining and a unique design result in power-versus-frequency curves across these bands that are relatively flat, with amplitude flatness that is typically ±2 dB (see table). The tubes support precise and independent control of frequency and output power, making possible full-band frequency sweeps in a matter of only a few microseconds and on/off power modulation in only approximately 10 ns.

Model BW03 is an example of the BWO line (see figure). It operates from 78.2 to 119 GHz with 6 to 30 mW output power and worst-case output-power variations of ±3 dB. Its tuning range is achieved by modifying the anode voltage from +500 to +1500 VDC at a cathode current range of 20 to 25 mA. The anode current is controlled through a control electrode, where a change in current of 16 to 25 mA causes a change in heater voltage of +0.96 to +1.19 VDC. Model BW03 is rated for a mean time before failure (MTBF) of 1000 h.

Model BWO-6 is another BWO example, at the lower tuning frequencies of 36 to 55 GHz. It achieves minimum output-power levels of 15 to 40 mW with worst-case output-power flatness of ±2.5 dB (see figure).

Each tube is supplied with calibration data of output power as a function of frequency and frequency as a function of voltage. Extensive data are available on the company's website, or on a compact-disc read-only memory (CD-ROM), which is available free upon request. The firm also operates a US Sales Office: (831) 335-3884 or by FAX at (831) 335-4382. **ELVA-1 Millimeter Wave Division, DOK Ltd., Nevesky 74, 23-H, 191025, St. Petersburg, Russia; 7-182-326-10-90, FAX: 7-812-325-58-56, e-mail: korneev@exch.nnz.spb.su, Internet: http://www.elva-1.spb.ru.**

CIRCLE NO. 57 or visit www.mwrf.com

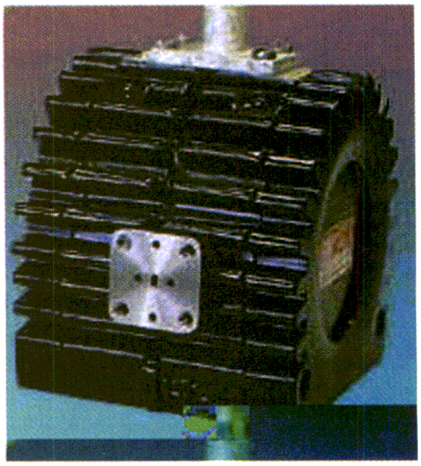

The BW03 BWO tube operates from 78.2 to 119 GHz with 6 to 30 mW output power and worst-case output-power variations of ±3 dB.

The BWOs at a glance

Parameter	BWO-6	BWO-4	BWO-3	BWO-2
Frequency range (GHz)	36 to 55	52 to 79	78.2 to 119	118 to 178
Output power (mW)	15 to 40	12 to 30	6 to 30	6 to 20
Power variations (dB)	3 to 5	3 to 5	3 to 6	3 to 6
Anode voltage (V)	400 to 1200	400 to 1200	500 to 1500	500 to 1800
Cathode current (mA)	20 to 25	20 to 25	20 to 25	20 to 25
MTBF	2000	2000	1000	1000

Call For Speakers

internet Device BUILDER

Creating Intelligent Appliances for a Networked World

MAY 14th - 16th, 2001

SANTA CLARA CONVENTION CENTER, SANTA CLARA, CA

The next Internet revolution is approaching in the form of smart, interactive devices that can be controlled over, gather information from, or distribute data via the Internet. With its open protocols, its support for compelling, Web-based graphics, and its worldwide reach, the Internet has gone far beyond the desktop. Small devices in remote locations, as well as software entities within huge systems can each leverage the inherent power of the Internet. The future of device development requires an ongoing interchange of professional expertise. Your participation helps to further that growth. It's also a great opportunity to meet your peers, showcase your ideas, and build your career. Your ideas are needed!

About the Internet Device Builder Conference

The Spring 2001 Internet Device Builder Conference, May 14-16, 2001, will feature core technologies that will make "ubiquitous computing" a reality.

Acceptance Guidelines

Sessions are selected based on content originality, quality and timeliness. We do not imitate programs found at other conferences. If you are planning to present the same topic within the next 12 months, please indicate where so your program can be adjusted appropriately. We do not accept canned topics, or overtly commercial content. Each session must be one-of-a-kind and intended to inform, not sell attendees. All submitted material becomes the property of Penton Media, Inc.

About Penton Media

Internet Device Builder Conference & Showcase is managed and produced by Penton Media, Inc., publishers of *Microwaves & RF*, *EE Product News*, *Wireless Systems Design*, *Internet World*, *Electronic Design*, *Boardwatch*, and *Embedded Systems Development*. Penton Media, Inc., 611 Route 46 West, Hasbrouck Heights, NJ 07604 Phone: 201-393-6060 Fax: 201-393-6297

Submission Guidelines

To be considered as a speaker, please submit the following information:

1. Your name, title, company or organization, address, phone, fax, and e-mail address.
2. A short professional biography (25 words maximum).
3. Proposed session title and a 50-to-100 word abstract. This material must be included or your submission will not be considered.
4. If you will be speaking elsewhere within the next 12 months, please indicate where.

We're looking for presentations by expert instructors on concise topics, case studies, "tips and tricks", or research based on an original written paper.

Submit your session proposal by December 14, 2000 to Conference Manager Betsy Tapp: btapp@penton.com.

PENTON'S EMBEDDED SYSTEMS DEVELOPMENT — ELECTRONIC DESIGN — EE Product News — Microwaves & RF — WIRELESS SYSTEMS DESIGN

SDLVAs Detect High-Speed Pulsed Signals

This line of successive-detection log-video amplifiers (SDLVAs) is ideal for processing adjacent pulses over a wide dynamic range.

DAWN PRIOR

Editorial Assistant

PROCESSING high-speed pulses calls for a detection device with rapid response time. The model 8091 successive-detection log-video amplifier (SDLVA) from Microphase, Inc. (Norwalk, CT) is such a device, capable of capturing short-pulsed signals from 2 to 6 GHz over an impressive 70-dB dynamic range of −65 to +5 dBm. The unit is one member of a series of high-performance, multi-octave assemblies designed for use in a wide range of applications including instrumentation, telecommunications and electronic-warfare (EW) receivers (Rxs).

The SDLVAs blend the latest gallium-arsenide (GaAs) active circuitry with reliable thin-film hybrid microcircuit construction to achieve high performance in compact housings. The design provides a detected-video-output voltage which is logarithmically proportional to the applied RF or intermediate-frequency (IF) input level. The SDLVAs also offer a limited IF output for use in frequency discriminator or precision direction-finding (DF) applications.

Model 8091 is a typical amplifier in the line (see figure). It operates from 2 to 6 GHz with the 70-dB dynamic range and tangential signal sensitivity (TSS) of better than −70 dBm. The logarithmic slope is typically 20 ±0.7 mV/ dB with log linearity of ±1.75 dB maximum. The log accuracy is typically ±1.9 dB at 4 GHz with frequency flatness of ±1.75 dB maximum. The output DC offset voltage is typically 100 ±30 mV at room temperature (+25°C).

One of the keys to good SDLVA performance in these applications is fast recovery time when faced with large amplitude signals. This characteristic is critical when sorting close adjacent pulses with wide amplitude variations. Amplifiers suffering long recovery times can obscure small signals which occur within the time period that the unit is recovering from a larger signal.

To demonstrate the effects of recovery time in a system, the system-level computer-aided-engineering (CAE) software SystemView from Elanix, Inc. (Westlake Village, CA) was used to model a pair of log amplifiers with close adjacent signals under different circumstances. The first amplifier was set for fast recovery time, while the second amplifier was hindered with a degraded recovery time. In the first case, the detected output of two pulses separated by 30 ns is clearly discernible. In the second case, the poor performance of the SDLVA with degraded recovery time is apparent when it is compared to the unit with fast recovery time. The slower-responding unit blends the lower amplitude signal into the fall time of the larger signal.

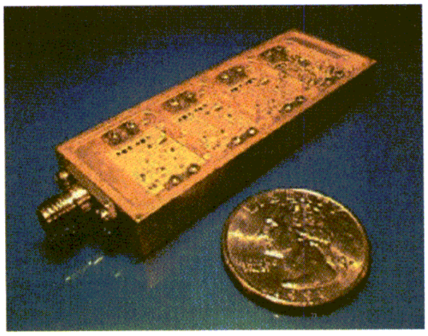

Model 8091 is a successive-detection logarithmic video amplifier with wide dynamic range and frequency coverage from 2 to 6 GHz.

The model 8091 SDLVA achieves rise and fall times of 12 and 60 ns, respectively, measured at 10- and 90-percent amplitude points. This rise/fall performance is maintained for the full 70-dB dynamic range, with maximum output overshoot of 1 dB. The output level of the limited IF port is – 3.0 to + 2.5 dBm over the operating frequency band with typical IF harmonic rejection of –10 dBc. The maximum VSWR at the RF and IF ports is 2.0:1. The video-output load impedance is 100 ±0.5 Ω.

The model 8091 SDLVA operates from +15 VDC and –15 VDC at quiescent currents of 350 and 50 mA, respectively. Model 8091 measures 2.75 × 1.0 × 0.30 in. (6.99 × 2.54 × 0.76 cm), and is rated for operating temperatures of –40 to +85°C. **Microphase, Inc., 587 Connecticut Ave., P.O. Box 960, Norwalk, CT 06854-0960; (203) 866-8000, FAX: (203) 853-3304, Internet: http://www.microphase.com.**

CIRCLE NO. 58 or visit www.mwrf.com

RF ICs Serve Handsets And Base Stations

Two new chips include an upconverter for dual-band, tri-mode handsets, and an LNA that aids base-station reception.

DON KELLER
Senior Editor

WIRELESS industry growth in the US has led to a proliferation of providers, each of which offers its services on one of two different frequency bands—900 MHz or 1900 MHz—and one of two different modulation schemes—frequency modulation (FM) for Advanced Mobile Phone Service (AMPS), or code-division multiple access (CDMA) for cellular and personal communications services (PCS). This has resulted in incompatibility among services, and confusion for handset users. To remedy this situation, some providers are establishing an overarching organization that combines several services under one "banner." This consolidation allows the banner provider to offer its users access to all three wireless modes available in the US—900-MHz AMPS, 900-MHz cellular, and 1900-MHz PCS. It also creates a demand for handsets that can operate in these three modes. To help handset manufacturers meet this demand, Agilent Technologies (Santa Clara, CA), has developed an upconverter/driver amplifier chip for dual-band, tri-mode handsets.

The model HPMX-7202 monolithic microwave integrated circuit (MMIC), introduced at the IEEE MTT-S Symposium last June in Boston, operates in two frequency bands—900 MHz and 1900 MHz, and three modes—AMPS, 900-MHz cellular, and 1900-MHz PCS. The chip's cellular- and PCS-circuitry chains contain an upconverter and an RF variable-gain driver. In the AMPS-circuitry chain, the chip contains an upconverter and a driver amplifier. The drivers are adaptively biased to reduce current draw. When less gain is required, the current draw is significantly reduced. This increases the chip's overall efficiency, and extends the battery life of the handset. The chip also includes circuitry to switch from one mode to another (see figure).

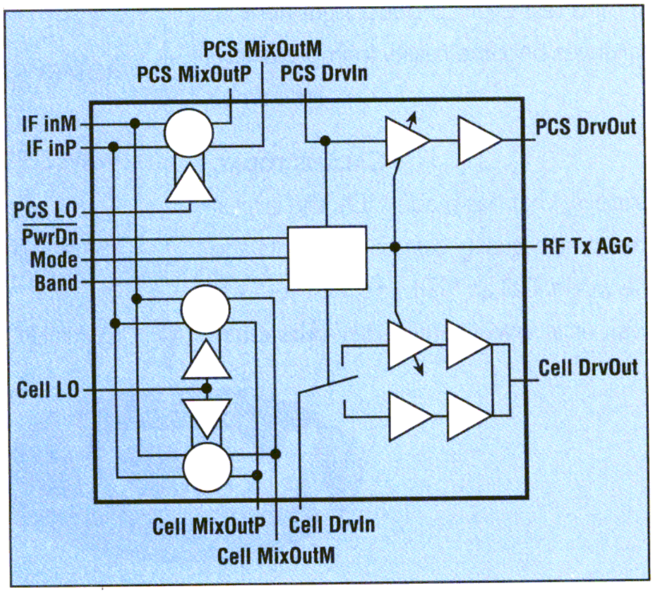

This block diagram shows the functional components of the HPMX-7202 upconverter/driver.

The cellular upconverter's typical power output is –8 dBm, and the PCS upconverter's typical power output is –7 dBm. The output of each upconverter is then boosted by its own variable-gain amplifier. These drivers can deliver power levels to +10 dBm—enough to interface directly with CDMA power amplifiers (PAs). When operating in the 900-MHz cellular mode at an output power of +7 dBm, the chip provides a typical adjacent-channel power ratio (ACPR) of –55 dBc/30 kHz. When operating in the 1900-MHz PCS mode at an output power of +9 dBm, the chip provides a typical ACPR of –58 dBc/30 kHz.

The AMPS upconverter's typical output power is –5 dBm. The AMPS driver typically boosts this signal to +9.5 dBm. The AMPS upconverter's typical FM noise level is –148 dBm/Hz.

The HPMX-7202 is a silicon (Si) bipolar chip that can be powered at voltages from +2.7 to +3.6 VDC and draws an average current of 56 mA. The power-down functionality reduces current draw to 1 μA. These features make it ideal for use with a single lithium-ion battery. It has a measured mean time to failure in excess of 75 years at a junction temperature of 100°C. The chip is housed in an industry-standard TQFP-32 package. **Agilent Technologies, Inc., 5301 Stevens Creek Blvd., MS 54 LAK, Santa Clara, CA 95052; (800) 452-4844, Internet: http://www.agilent.com.**

CIRCLE NO. 59 or visit www.mwrf.com

LNA BOOSTS BASE-STATION RECEPTION

For the other end of the cellular/personal-communications-services (PCS) link—the base station—Agilent has developed a low-noise amplifier (LNA) chip for receivers. The model MGA-52543 gallium-arsenide (GaAs) monolithic microwave integrated circuit (MMIC) can operate at frequencies from 0.4 to 6.0 GHz, but its main focus is 900-MHz cellular and 1900-MHz PCS base-station receivers.

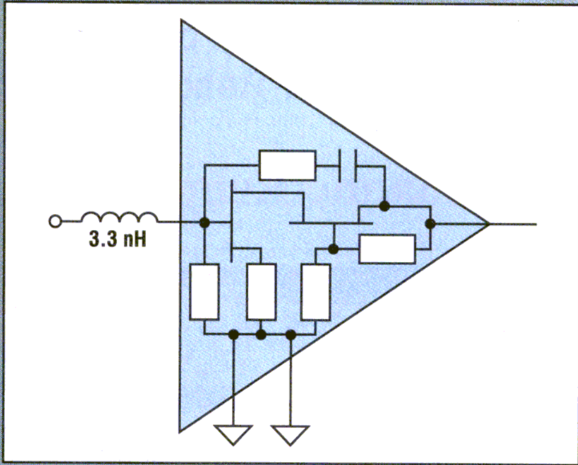

Typically, at 900 MHz, the amplifier offers a gain of 15 dB and a noise figure of 1.8 dB. Input third-order intercept point (IP3) is +18 dBm, output IP3 is +33 dBm, and output power at the 1-dB compression point is +18 dBm. Input return loss is 15 dB, output return loss is 22 dB, and isolation is –25 dB.

At 1900 MHz, its typical gain is 14.2 dB and its typical noise figure is 1.9 dB. Input IP3 is +17.5 dBm, output IP3 is 31.7 dBm, and output power at the 1-dB compression point is +17.4 dBm. Input return loss is 11 dB, output return loss is 20 dB, and isolation is –25 dB.

The chip can be powered by a single +5-VDC supply, and it typically draws 53 mA. It is housed in an SOT-343/four-lead SC-70 package and measures 1.2 × 2.0 mm.

Microwaves & RF

New and Current Products Presented By The Manufacturer

DIRECT CONNECTION ADS

For futher information circle the appropriate number on the Reader Service Card.

To Advertise Call Joanne Reppas (201) 666-6698

For Best Performance in a Supporting Role, the Winner is...

Sector Microwave

Go With the Winner.....
Use Sector Switches!!

smi

999 Grand Blvd.,
Deer Park, L.I., N.Y. 11729
(631) 242-2300
FAX: (631) 242-8158

www.sectormicrowave.com

SECTOR MICROWAVE CIRCLE 566

To 40 GHz

Filters, Multiplexers & MIC's

Suspended Substrate MIC
Switched Filter Banks
Image Reject Mixers
Quadrature IF Mixers
PIN Switches
Variable PIN Attenuators
Bias Tee's

ES MICROWAVE, LLC.
8031 Cessna Ave., Gaithersburg, MD 20879
301-519-9407 • Fax: 301-519-9418
E-mail: esmllc@aol.com
Website: esmicrowave.com

ES MICROWAVE, LLC. CIRCLE 555

Rb Standards & DDS Synthesizers

"Precision You Can Afford"

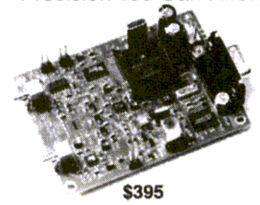

$395

- **Atomic Frequency Standards**
  - 1450A Rubidium+DDS Synthesizer (Rack)
  - 2950AR Rubidium Standard (Bench)
- **Modular and PC-based Synthesizers**
  - DDS6m (shown) 40MHz RS232 Controlled
  - DDS5m Locks to Standards RS232 & Switch
  - DDS3pc & DDS4pc PC ISA-bus to 34 MHz
- **Bench Top Synthesizers**
  - 2910A Series 1μHz steps to 48MHz

Novatech Instruments, Inc.
206-301-8986 (v) , 206-363-4367 (fax)
Specs & prices: www.eskimo.com/~ntsales

NOVATECH INSTRUMENTS CIRCLE 561

Coupled Line Filter Design Software Windows™ 95/98/NT

***NEW* APERTURE COUPLED RODS**

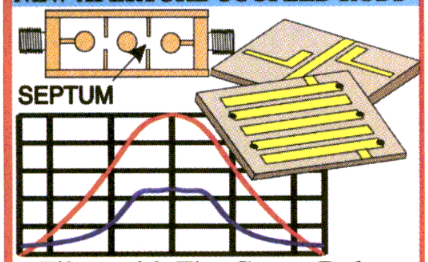

Filter with Flat Group Delay

WAVECON
P.O. Box 2697, Escondido, CA 92033
Tel: (760) 747-6922 Fax: (760) 747-5270
Website: www.waveconsoft.com

WAVECON CIRCLE 568

"Instant RF" building blocks generate, receive, and attenuate from 100 KHz to 1 GHz

- Design RF into your next project, even without RF Expertise
- Three modules available:
  - ✔ SGM-1000 RF Generator, 100 KHz to 1 GHz
  - ✔ FRM-1000 FM Receiver with SPI Port for programming, -110 dbm sensitivity
  - ✔ ATN-1000 attenuator module is serially programmed from 0 to 135 db
- Optional software and "exerciser" boards allow easy test and evaulation.

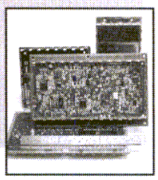

RAMSEY

RAMSEY ELECTRONICS, INC. • 793 Canning Parkway • Victor, NY 14564
800 446-2295 www.ramseytest.com

RAMSEY ELECTRONICS CIRCLE 563

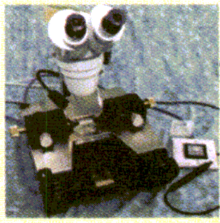

Microwave Test Fixture

Easily Configurable High Thru-put

A compact, full featured, user configurable, manually operated test fixture with rapid load unload capability. Useful for production measurements of thin film and packaged microwave components with NIST traceability.

• BenchtopSize(<1ft^2) • Vacuum chuck • X-Y-Z probe positioners • Top Plate Z-lift • Locking Stage • Integral Vacuum Accessory Manifold • 7X-40X Stereo Zoom Microscope • Adjustable Halogen Illuminator • Vacuum Accessories • Compatible with 40GHz+ probes •

Standard and custom chuck plates for testing

MICROSTRIP PACKAGES

J microTechnology
3744 NW Bluegrass Pl
Portland, OR 97229
(503) 614-9509
(503) 531-9325 [FAX]
www.jmicrotechnology.com

J micro Technology

The Standard for Test Correlation

J MICROTECHNOLOGY CIRCLE 559

40MHz TO 18GHz
HIGH ISOLATION, RADIAL
SP6T & SP7T, PIN DIODE SWITCHES

- HIGH ISOLATION
- ULTRA-BROADBAND
- LOW INSERTION LOSS
- LOW PROFILE RADIAL DESIGN

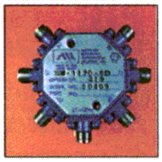

AMC MODEL Nos:
SWN-1170-6DT-00418 & SWN-1170-7DT-00418

SPECIFICATIONS:

• FREQUENCY RANGE	:	0.04 TO 18.0 GHz MIN. (10 MHz TO 18.0 GHz AVAILABLE)
• INSERTION LOSS	:	4.0 dB MAX. (ABSORPTIVE) (≤0.5dB LESS LOSS FOR REFLECTIVE MODELS)
• ISOLATION	:	65 dB MIN. (75dB TYPICAL)
• VSWR	:	2.0:1
• SWITCHING SPEED	:	≤ 25 nS RISE/FALL MAX.
	:	≤ 250 nS ON/OFF MAX. (FASTER SWITCHING SPEEDS AVAILABLE)
• CONTROL	:	TTL COMPATIBLE STANDARD (OTHER CONTROL OPTIONS AVAILABLE)
• DC POWER SUPPLY	:	± 5VDC @ +200mA, -35mA MAX. (OTHER VOLTAGES AVAILABLE)
• SIZE	:	1.25" (diameter) X 0.70" (height)
• WEIGHT	:	< 3.0 oz.

OTHER MODELS AVAILABLE FROM SPST TO SP16T, BOTH ABSORPTIVE AND REFLECTIVE.

"In Pursuit of Excellence Through Engineering"
AMERICAN MICROWAVE CORPORATION
7311-G GROVE ROAD
FREDERICK, MD 21704
TEL: 301-662-4700, FAX: 301-662-4938

AMERICAN MICROWAVE CORP. CIRCLE 551

New and Current Products Presented By The Manufacturer

Microwaves & RF DIRECT CONNECTION ADS

For further information, circle the appropriate number on the Reader Service Card.

To advertise, Call Joanne Reppas at (201) 666-6698, Fax (201) 666-0557

Call For Speakers

Wireless Symposium
Portable by Design

February 12-16, 2001
San Jose Convention Center
San Jose, CA
www.WirelessPortable.com

Take a position as a leader in one of the fastest-growing forums for professional dialogue in electronics engineering and design. We're looking for industry experts to propose a session for the upcoming Wireless Symposium/Portable by Design Spring 2001 Conference. Much of the rapid growth of the wireless and portable industry has been due to the ongoing interchange of professional expertise. Your participation helps to further that growth. It's also a great opportunity to meet your peers, showcase your ideas, and build your career. Your ideas are needed!

About the Wireless Symposium/ Portable by Design Conference

The conference will take place February 12-16, 2001 at the San Jose Convention Center, San Jose, CA. For over eight years the Wireless Symposium/Portable by Design Conference has been a place for engineers to investigate new technologies and techniques. It has become the preeminent technical conference for designers and engineers of portable and wireless products.

Acceptance Guidelines

Sessions are selected based on content originality, quality, and timeliness. We do not imitate programs found at other conferences. If you are planning to present the same topic within the next 12 months, please indicate where so your program can be adjusted appropriately. We do not accept canned topics, or overtly commercial content. Each session must be one-of-a-kind and intended to inform, not sell, attendees. All submitted material becomes the property of Penton Media, Inc.

About Penton Media

Wireless Symposium/Portable by Design Conference and Exhibition is managed and produced by Penton Media, Inc., publishers of Microwaves & RF, EE Product News, Wireless Systems Design, Internet World, Electronic Design, Boardwatch, and Embedded Systems Development. Penton Media, Inc., 611 Route 46 West, Hasbrouck Heights, NJ 07604
Phone: 201-393-6060 Fax: 201-393-6297.

Submission Guidelines

To be considered as a speaker, please submit the following information:

1. Your name, title, company or organization, address, phone, fax, and e-mail address.
2. A short professional biography (50 words maximum).
3. Proposed session title and a 150-word abstract. This material must be included or your submission will not be considered.

   Please indicate what type of session you are proposing. We offer three types of sessions at the Wireless Symposium/Portable by Design Conference:

   - Paper Presentation Session: Led by a "Session Chair" and includes a number of papers on a general theme. Each speaker/author makes a 20-to-30 minute presentation based on their paper.
   - Mini-Tutorial "Expert" Session: Presented by an expert instructor on one concise topic, a case study, a narrow discipline, or "tips and tricks". 1 to 1.5 hours in length.
   - Full-Day Workshop Tutorial Session: 1-or-2 day session presented by an expert instructor.
4. If you will be speaking elsewhere within the next 12 months, please indicate where.

Submit your session proposal by September 8, 2000 to Betsy Tapp, Conference Manager, via fax 201-393-6297

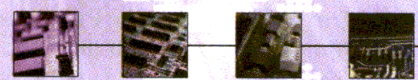

PENTON'S EMBEDDED SYSTEMS DEVELOPMENT
ELECTRONIC DESIGN
EE Product News
Microwaves & RF
WIRELESS SYSTEMS DESIGN

Attenuators span DC to 3 GHz

A series of miniature 50-Ω coaxial attenuators for use from DC to 3 GHz is now available with SMA, SMB, BNC, and TNC connectors in 1-dB steps from 1 to 10 dB and 2-dB steps to 20 dB. The attenuators provide 0.5-dB accuracy to 2.5 GHz and 1-dB accuracy to 3 GHz. VSWR is 1.2:1 nominal and 1.35:1 maximum. The units feature gold (Au)-plated connectors, and resistor networks are mounted in military-specified plated housings. **Elcom Systems, Inc., PMB 255, 20423 State Rd. 7 No. F6, Boca Raton, FL 33498; (561) 883-1945, FAX: (561) 883-1945, e-mail: sales@elcomsystems.com, Internet: http://www.elcomsystems.com.**

CIRCLE NO. 60 or visit www.mwrf.com

Generator boasts fast PCI card

Model AWG1000 is a 1-GSamples/s arbitrary-waveform generator that boasts a fast digital-to-audio (DA) card housed on a PCI-compliant board. It features 12-b vertical resolution from one normal output and one complementary output. The board is capable of generating a completely arbitrary waveform from 60 MSamples/s to 1 GSamples/s. The analog outputs are unfiltered and have typical rise/fall times of 260 per second. Spurious-free dynamic range (SFDR) is less than −50 dB at 100 MHz. The integrated clock synthesizer features 1-Hz resolution. Digital outputs include eight high-speed, TTL marker outputs and a dual-complementary optional positive-emitter-coupled-logic (PECL) buffered-clock output. **Chase Scientific Co., 7960-B Soquel Dr., No. 191, Aptos, CA 95003; (831) 464-2584, FAX: (831) 479-8572, e-mail: sales@chase2000.com, Internet: http://www.chase2000.com.**

CIRCLE NO. 61 or visit www.mwrf.com

Crosspoint switch serves OC-12 data rates

Model MAX3640 is a +3.3-VDC dual-path, crosspoint switch for use at OC-12 data rates to receive and transmit 622-Mb/s low-voltage differential signals (LVDS) across a backplane with minimum jitter accumulation and it operates from a +3.3-VDC supply over a temperature range of 0 to +85°C. The device boasts signal-path redundancy for critical data streams, making it ideal for Synchronous Optical Network/synchronous-digital-hierarchy (SONET/SDH) backplanes, digital cross-connects, and high-speed parallel links. Each path of the switch incorporates input buffers, multiplexers, a 2 × 2 crosspoint switch, and output drivers. The four output channels have redundant outputs for test or fanning purposes. **Maxim Integrated Products, 120 San Gabriel Dr., Sunnyvale, CA 94086; (800) 998-8800, (408) 737-7600, Internet: http://www.maxim-ic.com.**

CIRCLE NO. 62 or visit www.mwrf.com

Capacitors suit high-Q applications

The 1500 series of Eco-Trim® variable capacitors boasts a capacitance range of 1 to 10 pF with a rated voltage of +250 VDC and an operating temperature range of −65 to +125°C. The units are low-cost, high-performance air capacitors for applications where high quality factor (Q) and cost are design concerns. Applications include impedance matching, filter tuning, interstage coupling, and antenna tuning. The units are available in five mounting styles for PC and surface-mount applications. **Johanson, Rockaway Valley Rd., Boonton, NJ 07005; (973) 334-2676, FAX: (973) 334-2954, e-mail: jmcsales@johansonmfg.com, Internet: http://www.johansonmfg.com.**

CIRCLE NO. 63 or visit www.mwrf.com

Chip resistors offer low VCR

The HVC series of chip resistors provides voltage-coefficient-of-resistance (VCR) ratings of less than 1 PPM/V. The resistors have a temperature coefficient of resistance (TCR) that is less than 25 PPM/°C, with a +2500-VDC rating in air (+7500 VDC potted). Packages range from 0.250 × 0.125 in. (0.635 × 0.318 cm) to 0.020 × 0.020 in. (0.051 × 0.051 cm). The resistors can be used in any applications that require extreme voltage stability, such as power supplies and instrumentation. **OhmCraft, 93 Paper Mill St., Honeoye Falls, NY 14472; (716) 624-2610, FAX: (716) 624-2692, e-mail: sales@ohmcraft.com, Internet: http://www.ohmcraft.com.**

CIRCLE NO. 64 or visit www.mwrf.com

Splitter/combiner supports cable communications

Model CX4002 is a next-generation, two-way RF splitter/combiner supporting interactive broadband cable communications. The unit boasts a VSWR of 1.1:1 over the full frequency range and typical isolation of 30 dB to 400 MHz, and 21 dB to 1000 MHz. Its compact size [0.310 × 0.255 in. (0.787 × 0.648 cm)], ceramic base, cover for pick-and-place compatibility, and capacity to withstand 235°C during infrared (IR) solder reflow make the CX4002 splitter/combiner suitable for applications such as cable-network amplifiers and nodes. **Pulse, 12220 World Trade Dr., San Diego, CA 92128; (858) 674-8100, FAX: (858) 674-8262, Internet: http://www.pulseeng.com.**

CIRCLE NO. 65 or visit www.mwrf.com

Antenna targets portable GPS applications

The DAX dielectric patch antenna is a low-profile ceramic antenna element for use in portable Global Positioning System (GPS) receivers and navigation systems. The antenna offers an impedance of 50 Ω and a maximum temperature coefficient of 20 PPM/°C. Designed specifically for l1575.42-MHz L1 reception, the antenna is packaged with an 18 × 18-mm footprint and a low profile of 4.5 mm. The antenna incorporates a rectangular microstrip design for GPS righthand circular polarization reception. The DAX ceramic antenna features ceramic materials that are well-suited for GPS applications. **Toko America, Inc., 1250 Feehanville Dr., Mt. Prospect, IL 60056; (847) 297-0070, FAX: (847) 699-7864, e-mail: info@tokoam.com, Internet: http://tokoam.com.**

CIRCLE NO. 66 or visit www.mwrf.com

Filters provide group-delay response

Fourth-order absorptive Besel filters boast superior group-delay while maintaining impedance matching far into the stopband. The filters are available with −3-dB cutoff frequencies from 10 to 3000 MHz, attenuation from −0.1 to −21.5 dB, and attenuation accuracy from ±0.2 to ±1.0. The filters have a power rating of 0.5 W average, and an impedance of 50 Ω. VSWR is 1.5:1 from DC to 2 × 3-dB cutoff frequency. They can operate over a temperature range of −55 to +85°C. Lossy elements are designed into these filters to produce a response that closely mimics the classic Bessel in amplitude and phase. Applications include designs of digital systems where accurate reproduction of waveforms is important. The filters can also be used to reduce the impact of high-order distortion and noise in lightwave receivers. **RLC Electronics, Inc., 83 Radio Circle, Mt. Kisco, NY 10549; (914) 241-1334, FAX: (914) 241-1753, e-mail: sales@ricelec tronics.com, Internet: http:// www.ricelectronics.com.**

CIRCLE NO. 67 or visit www.mwrf.com

Antennas suit outdoor router system

Three antennas for the ORINOCO outdoor router system include the 24-dBi directional parabolic grid, the 12-dBi directional wide angle, and the 10-dBi omnidirectional. These antennas enable enterprises and ISPs to provide high-speed, wireless networking and Internet access with ranges up to 26 km (point to point). They are available in point-to-point and multipoint configurations. **Lucent Technologies, 2 Oak Way, Room 5 SD 32, Berkley Heights, NJ 07922; (908) 508-8225, FAX: (908) 508-8192, Internet: http://www.lucent.com.**

CIRCLE NO. 68 or visit www.mwrf.com

Contacts serve space applications

The PkZ® series is a blindmate, size-12 contact that boasts high-frequency performance, lightweight construction, and dense packaging due to its tight 0.2-in. (0.51-cm) center-to-center spacing. Designed for easy assembly and flexible use, these components are ideal for satellite and aerospace applications. The PkZ design supports a Z-axis mating tolerance of up to 0.070 in. (0.178 cm) without compromising electrical performance while maintaining constant impedance. High-frequency designs are available to 40 GHz with radial- and axial-float capabilities for misalignment in board-to-board applications. **The Phoenix Co. of Chicago, Inc., 555 Pond Dr., Wood Dale, IL 60191; (630) 595-2300, FAX: (630) 595-6579, e-mail: sales@phoenixofchicago.com, Internet: http://www.phoenixof chicago.com.**

CIRCLE NO. 69 or visit www.mwrf.com

Ultra-thin antenna boasts broad bandwidth

A line of antennas is 0.10-in. (0.25 cm) thick. The antennas feature 3-dBi gain and a maximum VSWR of 1.5:1. The ultra-thin form factor supports practically invisible mounting on ceiling tiles, and the antennas can be built with a pigtail assembly for remote mounting or embedded applications. The omnidirectional pattern of this antenna suits a variety of applications, including handheld devices, in-building systems, as well as Global System for Mobile Communications (GSM), personal-communications-network (PCN), and specialized-mobile-radio (SMR) markets. **Xertex Technologies, Inc., 452 Burbank St., Broomfield, CO 80020; (303) 635-2000, FAX: (303) 635-2003, Internet: http://www. xertex.com.**

CIRCLE NO. 70 or visit www.mwrf.com

Adapters designed for long life

The Quick Test QT3.5 mm™ 8006 adapter series are push-on/pull-off units designed for long life and excellent repeatability. The in-series adapters adapt from standard 3.5 mm (female) to one of four optional QT3.5 mm connector configurations—the "No Nut" design, the 3/8-in. (0.97-cm) nut design, the 9/16-in. (1.42-cm) nut design, and the guide-sleeve design. The 3/8- and 9/16-in. designs are quick connect, while 1-1/2-turn connectors support the push-on/pull-off capability and a threaded connection when necessary. The guide-sleeve design is for connector alignment in automated applications. **Maury Microwave Corp., 2900 Inland Empire Blvd., Ontario, CA 91764-4804; (909) 987-4715, FAX: (909) 987-1112, Internet: http:// www.maurymw.com.**

CIRCLE NO. 71 or visit www.mwrf.com

Controller monitors fiber channel servers

Model SSC200 is an integrated single-chip enclosure-management controller used to monitor and control the physical environment within a fiber-channel server or storage enclosure. The unit supports 2-Gb/s fiber-channel disc drives through the enclosure-services interface (ESI) of the SFF-8067 specification. The SSC200 also complies with the initiated mode of the enclosure-initiated-ESI (EIE) specification, supporting information transfers to and from the enclosure controller. The SSC200 supports two fully independent, enclosure-service interfaces, configured by the software-developers-kit (SDK) firmware which is provided. **Vitesse Semiconductor Corp., 741 Calle Plano, Camarillo, CA 93012; (805) 388-3700, FAX: (805) 987-5896, Internet: http://www. vitesse.com.**

CIRCLE NO. 72 or visit www.mwrf.com

Antenna meets broadband applications

The model DB794 is a ceiling-mounted, single-monopole, corner-reflector antenna. It features high-directional gain with reliable coverage of up to three bands, including GSM-1800, PCS-1900, and Universal Mobile Telecommunication System (UMTS) frequencies that span the 1710-to-2000-MHz frequency range. The unit is suitable for high-capacity pedestrian venues requiring reliable mass voice and/or data communications. **Decibel Products, 8635 Stemmons Freeway, Dallas, TX 75247-3701; (214) 631-0310, FAX: (214) 631-4706, Internet: http://www.decibelprod ucts.com.**

CIRCLE NO. 73 or visit www.mwrf.com

Machinable ceramic targets electrical insulators

The model Aremcolox™ 502-1400-BF is a bisque-fired, machinable ceramic available in various rod and plate sizes for use in high-temperature industrial applications to 2600°F (1430°C). Typical properties include a compressive strength of 9000 psi, flexural strength of 4000 psi, dielectric strength of 80 V/M, and thermal conductivity of 30 (4.3) BTU-in/hr-ft²°F (W/M-°K. The ceramic is a low-density, 96-percent purity, alumina ceramic which is easily machined using conventional high-speed-hardened steel tools. This product enables end users to produce prototype electrical insulators. **Aremco Products, Inc., P.O. Box 517, 707B Executive Blvd., Valley Cottage, NY 10989; (914) 268-0039, FAX: (914) 268-0041, e-mail: aremco@aremco.com, Internet: http://www.aremco.com.**

CIRCLE NO. 74 or visit www.mwrf.com

Synthesizers provide superior phase noise

The CFS HP series of synthesizers features superior phase noise (−100 dBc/Hz at 10-kHz offset at C-Band), tunable C-band or Ku-band, and a fixed L-band. This unit is built with a low-profile construction and can be fitted with a parallel or serial interface. Applications include use in dual-conversion upconverters and downconverters. **MITEQ, Inc., 100 Davids Dr., Hauppauge, NY 11788; (516) 436-7400, FAX: (516) 436-7430, e-mail: sales@miteq.com, Internet: http://www.miteq.com.**

CIRCLE NO. 75 or visit www.mwrf.com

Antenna offers low-gain performance

The OGB6-915 low-gain omni antenna is suitable for carriers, utilities, and trunking providers who need low-gain, high-power performance. The antenna is available with an N or 7/16 DIN female input. The antenna is designed to provide long-service life in all types of adverse environmental conditions. The antenna features a one-piece mounting system for easy installation. **Kathrein, Inc., Scala Division, P.O. Box 4580, Medford, OR 97501; (541) 779-6500, FAX: (541) 779-3991, e-mail: mail@kathrein.com, Internet: http://www.kathrein.com.**

CIRCLE NO. 76 or visit www.mwrf.com

Capacitor achieves higher voltage rating

The JZ and JR series of miniature chip-trimmer capacitors now provides a DC working voltage of 100, with a DC withstanding voltage of 220. The JZ and JR series boast ranges from 1.5 to 3.0 pF and 8 to 40 pF. These series are ideal solutions for tuning problems. They feature ±1-percent long-term capacitance stability. Package sizes are either 4.50 × 3.20 × 1.45 mm or 3.50 × 3.10 × 1.15 mm. **Voltronics Corp., 100 Ford Rd., Denville, NJ 07834; (973) 586-8585, FAX: (973) 586-3404, e-mail: info@voltronicscorp.com.**

CIRCLE NO. 77 or visit www.mwrf.com

Adhesive suits temporary bonding

The MB600 model adhesive is a single-component, storage-stable inorganic compound boasting heat resistance and excellent adhesion to metals, ceramics, glass, most plastics, and rubbers. The adhesive cures readily at ambient and more quickly at moderately elevated temperatures. The adhesive is completely odorless, nontoxic, and nonflammable. **Master Bond, Inc., 154 Hobart St., Hackensack, NJ 07601-3922; (201) 343-8983, FAX: (201) 343-2132, Internet: http://www.Masterbond.com.**

CIRCLE NO. 78 or visit www.mwrf.com

Laser system supports calibrations

LIMTEK is a compact, high-performance laser-measurement system for position, velocity, acceleration, straightness, squareness, parallelism, angles, and flatness measurements. It provides dimensional metrology calibrations, internal multi-axis measurements, and high-speed dynamic analysis. This personal-computer (PC)-controlled modular system is small, lightweight, and easy to operate. It features certified laser wavelength, synchronous measurements in up to three axes, an automatic environmental compensation unit, and miniature optics for X/Y table positioning. The system uses a CCD camera for accurate straightness, squareness, as well as parallelism measurements, and straightness deviations in two directions are measured simultaneously with position. **Davidson Optronics, 2223 Ramona Blvd., West Covina, CA 91790; (626) 962-5181, FAX: (626) 962-5188, e-mail: sales@davidsonoptronics.com.**

CIRCLE NO. 79 or visit www.mwrf.com

Epoxy works at absolute zero

SUPERTHERM 816HH01 is a two-component epoxy for use at extremely low temperatures, approaching absolute zero. The epoxy is available in custom BIPAX packaging, enabling use in small quantities on an as-needed basis, or for use in mass production. The epoxy develops strong, durable, high-impact bonds with metals, silica, alumina, sapphire, as well as other ceramics, glass, and plastics. **Tra-Con, Inc., 45 Wiggans Ave., Bedford, MA 01730; (800) TRA-CON1, FAX: (781) 275-9249, Internet: http://www.tra-con.com.**

CIRCLE NO. 80 or visit www.mwrf.com

Station equipped with hand tools

Model MBT 250-SDPT is an advanced multifunction rework station equipped with hand tools for soldering, desoldering, tweezing, and vacuuming. For soldering, the PS-80 iron is rugged and versatile. For desoldering, the SX-80 SODR-X-TRACTOR is a handpiece with a disposable solder chamber. For tweezing, the Thermo-Tweez is a flexible handpiece which can remove anything from the smallest two-sided components to the largest four-sided quad flat packs. **Pace, Inc., 9893 Brewers Ct., Laurel, MD 20723-1990; (301) 490-9860, FAX: (301) 498-3252, Internet: http://www.paceusa.com.**

CIRCLE NO. 81 or visit www.mwrf.com

Touchscreen computer suits OEM needs

The GenTouch™ series of industrial touchscreen computer systems is available for industrial computer or embedded original-equipment-manufacturer (OEM) needs. They can be ordered as totally enclosed and sealed systems. This factory-hardened series is ideal for operation where dirt, grease, grime, oil, water, dust, and heat are present. The series supports disk-on-a-chip to 72 Mb. The series-standard offering is 15-, 14-, and 12.1-in. (38.10-, 35.56-, and 30.73-cm) TFT infrared (IR) touchscreen liquid-crystal displays (LCDs) at resolutions up to 1024 × 768, with wide viewing angles of 160 (H) and 145 (V). The standard package comes with 64-Mb static random-access memory (SRAM), a 500-MHz central-processing unit (CPU), a 6.4-Gb hard disk, floppy disk, mouse, an IR touchscreen, and industrial keyboard. The modularity of the series allows the touchscreen LCD portion of the unit to be purchased separately as a display for the user's industrial computer system, since it supports direct connections to any standard video-graphics-array (VGA) connector port. The series operates on Windows 95/98, NT, DOS, UNIX, or OS/2 operating systems. **H3 Technologies, Inc., 2050 Woodrun SE, Unit B, Lowell, MI 49331; (616) 897-8544, FAX: (616) 897-0306, Internet: http://www.h3tech.com.**

CIRCLE NO. 82 or visit www.mwrf.com

Satellite seeker finds strongest signal

A digital satellite seeker connects to any satellite antenna and finds the strongest satellite signal with no adjustments necessary. It features a numerical liquid-crystal display (LCD) with dual-high and low readings. Its input frequency range is 900 to 2000 MHz. The maximum voltage input is +30 VDC, while resolution is 1/10 dB. With its compact size of 2.25 × 3.75 × 0.50 in. (5.72 × 9.53 × 1.27 cm), the digital satellite seeker fits easily into small spaces. **Jensen Tools, Inc., 7815 S. 46th St., Phoenix, AZ 85044-5399; (800) 426-1194, (602) 453-3169, FAX: (800) 366-9662, (602) 438-1690, Internet: http://www.jensentools.com.**

CIRCLE NO. 83 or visit www.mwrf.com

Termination ensures even-heat distribution

The model 150-WT-FN is a high-powered termination using thermal imaging photography in order to ensure even-heat distribution. The unit offers a power rating of 150 W average at 25°C and 50-Ω nominal impedance. Frequency range and VSWR are DC to 1 GHz at 1.10:1 maximum, and 1 to 2.4 GHz at 1.25:1. The unit is equipped with N female connectors, a horizontal or vertical operating position, and a 2.5-lb. package measuring 4.85 × 5.40 × 4.30 in. (12.32 × 13.72 × 10.92 cm). **Bird Component Products, 10950 72nd St. N., Suite 107, Largo, FL 33777-1527; (727) 547-8826, FAX: (727) 547-0806, e-mail: sales@birdfla.com, Internet: http://www.birdfla.com.**

CIRCLE NO. 84 or visit www.mwrf.com

Kit simplifies EMI shielding-material selection

A comprehensive electromagnetic-interference (EMI) test-lab sample kit is designed to simplify the selection and specification of EMI shielding materials. The kit materials include wire mesh, conductive elastomers, beryllium-copper (BeCu) fingerstock, foil tapes, conductive fabric over soft-foam gaskets, and oriented wire in silicone. **Tecknit, 129 Dermody St., Cranford, NJ 07016; (908) 272-5500, FAX: (908) 272-2741.**

CIRCLE NO. 85 or visit www.mwrf.com

Varactors support WCDMA/UMTS applications

Models SMV1232-079, SMV1263-079, and SMV1405-079 are low-capacitance silicon (Si) varactor diodes for voltage-controlled-oscillator (VCO) designs in IMT-2000 wide-band code-division-multiple-access/Universal Mobile Telecommunications System (WCDMA/UMTS) applications. These varactors have low series resistance for low phase noise and low capacitance which makes them suitable for applications ranging up to 2.5 GHz. Manufactured in the ultra-small SC-79 package for reduced parasitics, the devices are available in tape and reel for high-volume, low-cost applications. **Alpha Industries, 20 Sylvan Rd., Woburn, MA 01801; (781) 935-5150, FAX: (617) 824-4564, Internet: www.alphaind.com.**

CIRCLE NO. 86 or visit www.mwrf.com

Microwave switch houses building blocks

The model SM7001A is a modular microwave switch which can house up to four microwave building blocks. They range from terminated 1 × 4 and 1 × 6 26.5- and 40-GHz relays. Each microwave building block can be mixed and matched to form the final configuration, and/or combined with other microwave, optical, or general-purpose switch modules within the same system. The final switch solution can be controlled through general-purpose-interface-bus (GPIB), PCI, RS-232, FireWire, or other interface mechanisms. **VXI Technology, 17912 Mitchell, Irvine, CA 92614; (949) 955-1894, FAX: (949) 955-3041, Internet: http:// www.vxitech.com.**

CIRCLE NO. 87 or visit www.mwrf.com

Connector series targets automatic control systems

The Han®R23 industrial/electrical connector series is suitable for measurement and automatic control systems, as well as in field-bus systems. The connector series features up to 19 contacts 25 V~/+60 VDC at 7.5 A; screw, solder, or printed-circuit-board (PCB) solder termination; Internet-protocol (IP)-67-rated, corrosion-resistant housings; an outer diameter of 26 mm; a vibration-proof screw-locking system; and excellent electromagnetic-compatibility (EMC) characteristics. The industrial/electrical connectors can be assembled from a wide range of inserts and housings in order to meet different application requirements. Mateability with other circular R23 types can also be achieved. **Harting, Inc., 1370 Bowes Rd., Elgin, IL 60123-5538; e-mail: more.info@harting-usa.com.**

CIRCLE NO. 88 or visit www.mwrf.com

(continued from p. 68)

polymer coatings. With proper cleaning, thin-film depositions adhere well to the AlN surfaces. Thick-film formulations frequently rely on chemical reactions with surface oxides to aid in film adhesion. Since the AlN surface should be oxide-free, thick-film mater ials for AlN must rely entirely on frit-based systems for adhesion.

There has been a good deal of debate about the performance of high-power components fabricated using thick- and thin-film materials. EMC has produced thick-film, thin-film, and combined thick- and thin-film technology devices. Frit-based thick-film conductors are available which have quite good adhesion to AlN. Thick-film ink manufacturers have developed a variety of conductor materials. However, they have been less inclined to invest in the development of resistors and dielectrics due to the lower demand. In power tests conducted at EMC, high-power components built using thick-film resistors had approximately 10-percent-higher power-handling capability than comparable parts built using thin-film resistor films.

MANUFACTURERS OF AlN SUBSTRATES HAVE STRUGGLED FOR YEARS TO PRODUCE CONSISTENT MATERIAL. VARIATIONS IN THE AlN FABRICATION PROCESS SUCH AS TEMPERATURE, GRAIN SIZE, AND FIRING ATMOSPHERE CAN AFFECT THE PROPERTIES OF THE FINISHED PRODUCT.

An important step in the process of depositing materials on AlN is the preparation and cleaning of the surface. Care must be used when introducing water into any AlN processing. Water will react with the AlN to produce aluminum hydroxide (AlH_2), and later, aluminum oxide (AlO_2) on the surface of the substrate. The presence of AlO_2 on a completed component will have no effect on either the electrical performance or the reliability of the part. During the deposition process, the contamination will interfere with the adhesion of materials to the surface of the AlN if it is not removed prior to the material deposition. Inadequate adhesion can affect the power capability of the part, as well as the long-term reliability. Care must be taken to assure that the substrate surface is cleaned prior to film deposition, and that the films are deposited on nearly pure AlN.

With proper mechanical, high frequency, and process design, it is possible to replace many BeO-based components with AlN. Evidence for this claim may be taken from the years of successful production and installation of more than one million EMC, high-power AlN resistors in RF and microwave equipment worldwide. The widespread use of these parts has provided some of the best evidence for the reliability and utility of AlN-based, high-power components. Reducing the use of toxic materials not only helps make the environment cleaner and safer for all people, but it also makes good business sense to offer customers a better, lower-risk product. ••

Acknowledgement

I would like to offer special thanks to Dr. Martin Helfand and Rajendra Shah of EMC Technology for their technical advice and review of this paper.

References

1. Center for Disease Control website.
2. Agency for Toxic Substances and Disease Registry website.
3. Occupational Safety and Health Administration (OSHA) Unified Agenda Proceeding 2042: *Occupational Exposure to Beryllium.*
4. Nancy L. Sprince, NIOSH Report on Occupational Respiratory Diseases.
5. Toxicological Profile for Beryllium, US DHHS TP-92/04.
6. Ceramic Industry, July 1991.
7. Carborondum Hi-Therm Data Sheet.

For more information on this topic, visit us at **www.mwrf.com**

Reaction injection

A four-page brochure details a company's capabilities. Single-source capabilities for injection and reaction-injection services are detailed in a four-page catalog. The telecommunications and electronics industries applications are discussed. **GI Plastek;** *(440) 250-0006, FAX: (440) 250-0007, Internet: http://www.giplastek.com.*

CIRCLE NO. 90 or visit www.mwrf.com

Integrated assemblies

A five-page brochure details a company's capabilities, facility, an engineering laboratory, and manufacturing floor. Products include integrated assemblies, converter assemblies, log components, detector-log-video amplifiers (DLVAs), log intermediate frequencies (IFs), filter banks, and switch-filter banks. **AKON;** *(408) 432-8039, FAX: (408) 432-1089, e-mail: sales@akoninc.com, Internet: http://www.akoninc.com.*

CIRCLE NO. 91 or visit www.mwrf.com

SAW products

Frequency sources, surface-acoustic-wave (SAW) products, bulk-acoustic-wave (BAW) delay-line products, data-conversion products, and custom microelectronics are offered in a 24-page catalog. Fixed-frequency oscillators, voltage-controlled oscillators (VCOs), bandpass filters, compressive intermediate-frequency (IF) receivers, delay lines, and oscillators are presented. Packing information is included. **Micro Networks Corp.;** *(508) 852-5400, FAX: (508) 852-8456, Internet: http://www.micronetworks.com.*

CIRCLE NO. 92 or visit www.mwrf.com

Test solutions

Telecom networks, enterprise networks, and wireless and multimedia applications are featured in a 528-page catalog. Test solutions for development, manufacture, installation, maintenance, and repair of systems, as well as networks for transmitting speech, data, and images are discussed. Specifications, application information, and descriptions are provided. A keyword index is included. **Wandel & Goltermann GmbH & Co. Marketing International;** *+49 7121 86-1616, FAX: +49 7121 86-1333, e-mail: info@wwgsolutions.com, Internet: http://www.wwgsolutions.com.*

CIRCLE NO. 93 or visit www.mwrf.com

RF components

Precision RF and microwave components are featured in a 40-page catalog. Instrumentation-grade adapters, precision attenuators, high return-loss connectors, and precision terminations are offered. **Anritsu Co., Microwave Measurements Division;** *(800) ANRITSU, Internet: http://www.anritsu.com.*

CIRCLE NO. 94 or visit www.mwrf.com

Power switching

Universal front-end modules (UFMs) are discussed in an application note (No. 46). A complete schematic with an input filter, input fuse, transient protection, and appropriate hold-up capacitors are described. Detailed configuration drawings and output (EN)-control specifications are provided. **Powercube;** *(800) 866-3590, FAX: (800) 866-3589, Internet: http://www.powercube.com.*

CIRCLE NO. 95 or visit www.mwrf.com

PCB drilling

Printed-circuit-board (PCB) drilling and routing are covered in a four-page monthly newsletter. Laser-drilling machine innovations, mechanical blind via drilling with depth-control accuracy to 0.0002 in. (0.0005 cm), and large back-plane drilling are discussed. A question-and-answer section is provided. **Excellon Automation Co.;** *(310) 534-6300, FAX: (310) 534-6777, e-mail: subscriptions@via-news.com, Internet: http://www.excellon.com.*

CIRCLE NO. 96 or visit www.mwrf.com

Magnetic components

Magnetic components are covered in a 100-page catalog. Inductors, coils, chokes, and transformers for surface-mount and through-hole requirements are presented. Engineering assistance, product samples, and custom designs are available. **J.W. Miller Magnetics;** *(310) 515-1720, FAX: (310) 515-1962, e-mail: lpalmer@bellind.com, Internet: http://www.jwmiller.com.*

CIRCLE NO. 97 or visit www.mwrf.com

Epoxy preforms

Uni-form™ epoxy preforms are the subject of an eight-page foldout brochure. Mechanical specifications, cure requirements, cure schedules, liquid problems, solid solutions, application information, as well as quality and testing are discussed. **multi-seals, Inc.;** *(860) 643-7188, FAX: (860) 643-5669, e-mail: sales@multi-seals.com, Internet: http://www.multi-seals. com.*

CIRCLE NO. 98 or visit www.mwrf.com

Coaxial connectors

RF coaxial connectors are featured in a 12-page catalog. Quick-disconnect connectors that correspond to LC, C, SC, BNC, and TNC types; quick designs for sputtering, wafer processing, and high-power applications; and quick-change types for use with wattmeters and other high-power testing and monitoring equipment are listed. A line of adapters and custom-designed cable assemblies is included. **Tru-Connector Corp.;** *(800) COAXTRU, (978) 532-0775, FAX: (978) 531-6993, e-mail: trusales@tru-con.com, Internet: http://www.tru-con.com.*

CIRCLE NO. 99 or visit www.mwrf.com

Coaxial cables

A 752-page catalog (No. 38) describes broadband antenna products, base-station antennas, industrial-scientific-medical (ISM), multichannel-multipoint-distribution-services (MMDS), and UNII-band passive products, coaxial cables, as well as terrestrial microwave products. Specifications, planning guides, technical data, and system-planning software information are provided. **Andrew Corp.;** *(800) 255-1479, (708) 349-3300, Internet: http://www.andrew.com.*

CIRCLE NO. 100 or visit www.mwrf.com

RF switches

A 650-page catalog covers RF and microwave telecommunications systems. Wireless products, electromechanical RF switches, passive components, active components, RF radiation safety products, and power meters/monitors are offered. Application notes, conversion tables, and indexes are provided. **Link Microtek Ltd.;** *01256 355771, FAX: 01256 355118, e-mail: sales@linkmicrotek.com, Internet: http://www.linkmicrotek.com.*

CIRCLE NO. 101 or visit www.mwrf.com

Tuner system

An automated tuner system (ATS) is the subject of a 16-page brochure (No. 4T-050E). Application information, power characterization, dynamic prematching, harmonic tuning, intermodulation-distortion (IMD) and adjacent- channel-power (ACP) applications, noise characterization, software features and options, and calibration accuracy are discussed. Specifications include frequency range, matching range, along with noise and power. **Maury Microwave Corp.;** *(909) 987-4715, FAX: (909) 987-1112, e-mail: maury@maurymw.com, Internet: http://www.maurymw.com.*

CIRCLE NO. 102 or visit www.mwrf.com

Controllers and software

PXI™ and CompactPCI solutions for measurement and automation are discussed in a 224-page catalog. PXI and CompactPCI-compliant chassis, controllers, software, and modules are featured. A tutorial on PXI and CompactPCI specifications, information on the PXI Systems Alliance, and a PXI systems configurations guide are provided. **National Instruments;** *(800) 258-7022, FAX: (512) 683-9300, e-mail: info@ni.com, Internet: http://www.ni.com.*

CIRCLE NO. 103 or visit www.mwrf.com

Cable products

A 288-page catalog/technical handbook focuses on wire, cable, and heat-shrinkable products. Complete military specifications, as well as commercial, coaxial, and fiber-optic wire and cable sections with UL/CSA specifications are discussed. In-depth formulas, conversion tables, and comparison charts are provided. **Standard Wire & Cable Co.;** *(800) 326-0006, FAX: (310) 609-1862, e-mail: sales@std-wire.com, Internet: http://www.std-wire.com.*

CIRCLE NO. 104 or visit www.mwrf.com

Dielectric capacitors

Air dielectric-trimmer capacitors are the subject of a four-page engineering bulletin (No. SG-660B). Features, specifications, outline drawings, and application notes are provided. Models in the 2-to-16°F range are also detailed. Sprague-Goodman **Electronics, Inc.;** *(516) 334-8700, FAX: (516) 334-8771, e-mail: info@sprague-goodman.com.*

CIRCLE NO. 105 or visit www.mwrf.com

RFI shielding

A 44-page catalog discusses RF electromagnetic-interference (RFI/EMI) products for doors, panels, covers, connectors, enclosures, and cabinets. Omni contacts, panel gaskets, strip gaskets, reverse bend, cylindrical and spherical contacts, contact rings, "D" connector gaskets, and board-level shielding are offered. Material specifications, compatibility charts, installation information, and technical drawings are provided. **Tech-Etch, Inc.;** *(508) 747-0300, FAX: (508) 746-9639, e-mail: sales@tech-etch.com, Internet: http://www.tech-etch.com.*

CIRCLE NO. 106 or visit www.mwrf.com

Microwave amplifiers

A 112-page catalog details the products and capabilities of a microwave amplifier manufacturer. Ultra-low noise amplifiers, octave-band amplifiers, ultra-broadband amplifiers from 0.5 to 20 GHz, multioctave electronic-warfare (EW) and electronic-counter-measures (ECM) amplifiers, and extended radar-band field-effect-transistor (FET) amplifiers are presented. Ka-band amplifiers from 26 GHz and above, limiting amplifiers, triband amplifiers, and narrowband power amplifiers (PAs) are also specified. **JCA Technology, Inc.;** *(805) 445-9888, FAX: (805) 987-6990, e-mail: jca@jcatech.com, Internet: http://www.jcatech.com.*

CIRCLE NO. 107 or visit www.mwrf.com

Coaxial cables

High-performance coaxial cables are the subject of a catalog (No. TL-14). Connectors and cable assemblies for a broad range of RF transmission applications are offered. Specifications, applications notes, reference data, attenuation tables, and power tables are included. **Times Microwave Systems;** *(203) 949-8489, FAX: (203) 949-8423, e-mail: lcaruso@timesmicrowave.com, Internet: http://www.timesmicrowave.com.*

CIRCLE NO. 108 or visit www.mwrf.com

Fiber optics

A 170-page catalog details coaxial and fiber optic products. Adapters, attentuators, breakouts, circulators, coaxial cables and assemblies, coaxial connectors, and DC blocks are offered. Detectors, directional couplers, fiber-optic cable assemblies, fuse holders, isolators, limiters, matching pads, mounting holes, patch cords, phase trimmers, power dividers, shorts, switches, terminations, and twinax cables are included. **Pasternack Enterprises;** *(949) 261-1920, FAX: (949) 261-7451, e-mail: sales@pasternack.com, Internet: http://www.pasternack.com.*

CIRCLE NO. 109 or visit www.mwrf.com

Coaxial connectors

A 120-page catalog features a range of standard and RF custom coaxial connectors. BNC, TNC, ultra-high-frequency (UHF), mini-UHF, MB, MHV, SMB, SMA, MCX, MMCX, 7/16 DIN, FME, LMR series, corrugated cable connectors are included. **RF Connectors;** *(800) 233-1728, (858) 549-6340, FAX: (858) 549-6345, e-mail: rfi@rfindustries.com, Internet: http://www.rfindustries.com.*

CIRCLE NO. 110 or visit www.mwrf.com

Integrated circuits

A 160-page catalog features integrated circuits (ICs) and other electronic components. Tools, test equipment, computer products for original-equipment-manufacturer (OEM) applications, input/output (I/O) cards, transformers, power supplies, and switches are listed. **Jameco;** *(800) 831-4242, (650) 592-8097, FAX: (800) 237-6948, (650) 592-2503, e-mail: info@jameco.com, Internet: http://www.jameco.com.*

CIRCLE NO. 111 or visit www.mwrf.com

Carbon fiber

A six-page brochure highlights pitch-based carbon (C) fiber. The brochure outlines important carbon-fiber properties, target markets, and applications. A comparison of pitch versus pan-based carbon-fiber is presented and the cost-effective benefits of carbon-fiber technology are also discussed. **Conoco Carbon Fibers;** *e-mail: ahm@ahminc.com, Internet: http://www.carbonfiber.conoco.com.*

CIRCLE NO. 112 or visit www.mwrf.com

MICROWAVES & RF ENGINEERING CAREERS

RATES

Effective January 1, 2000
$205 per column inch
Commissionable to agencies

DEADLINES

Space reservation: 5th of month preceding issue date
Ad material to: Penton Media Inc., Classified Dept.,611 Route 46 West, Hasbrouck Heights, NJ 07604

SALES STAFF

Call Customer Service Department
(201) 393-6083
Fax(201) 393-0410

All The Connections You Need

When you have the freedom to fly, the motivation to be the best, and you're backed by an all-pro team – you have all the connections you need. Experience it at Nokia. Nokia is a global company whose key growth areas are wireless and wireline telecommunications. We are a pioneer in mobile telephony, and the world's leading mobile phone supplier. Nokia was named to Fortune magazine's "100 Best Companies to Work for in America" list for 1999. This honor is the culmination of an employee-focused assessment of work-life issues and human resources programs throughout the U.S. There are positions currently available at our state-of-the-art facility for individuals who thrive in a culture where setting new standards is all in a day's work. We are seeking individuals with a Bachelor's, Masters, or Ph.D. for the following opportunities:

RF ENGINEERS

Designs and characterizes RF circuits/subsystems (LNA, mixer, filter, oscillator) at the printed circuit board level. Knowledge of impedance matching, distortion, noise figure and RF measurements a must. Familiarity with RF simulation tool and PCB layout necessary. BSEE and 1+ years of experience required.

RF EDA SPECIALIST

Support the ESG EDA group including RF, RFIC, ASIC and PCB. Analyzes technical lines and project/program needs; plans and establishes priorities for design, development, implementation or modification of the R&D EDA methodologies; installs, upgrades, and licenses software; tracks and administers software versions/OS Systems; and system administration. Strong HW/SW computer skills and intermediate scripting skills. Computer memory/workstation capacity, etc., and knowledge of UNIX. Experience with L.S.F. Agilen ADS in PC environment and Mentor/Cadence in UNIX environment.

SENIOR RF IC DEVELOPMENT MANAGER

Plans, coordinates and executes activities of the RFIC design and RF lines; allocate resources to projects, budget analysis, develop training plans and mentorships; and hires and evaluates personnel. Minimum BSEE, MSEE/Ph.D. EE preferred, with 5 + years of experience in the wireless IC industry. Deep knowledge of silicon IC processes and tools. Proven management ability and demonstrated detailed technical ability with RF System, RFHW and RFIC.

Nokia offers a culture rich in diversity, personal and professional growth, generous compensation, and exceptional benefits that only a leader in its field could provide. Interested candidates should forward a resume to: Nokia Mobile Phones, 12278 Scripps Summit Dr., San Diego, CA 92131; E-mail: sandiego.resumes@nokia.com Fax: 858-831-6502. EOE.

100 Best Companies to Work For FORTUNE 2000

NOKIA
CONNECTING PEOPLE

www.nokia.com

RF Job Network™
Jobs for RF/Wireless/Microwave Engineers
www.rfjn.com
Free to Job-Seekers / $100 for Employers

WENZEL ASSOCIATES, INC.
www.wenzel.com
AUSTIN, TEXAS

Wenzel is centrally located in beautiful Austin, Texas, known as the Live Music Capital of the World and often chosen as one of the best cities to live in the U.S. Austin has just over 1 million residents and is home to beautiful lakes, rolling hills, great restaurants, and the University of Texas.

Senior RF Design Engineers

Design state-of-the-art oven controlled crystal oscillators, RF components, and multiple frequency synthesizers for wireless communications and military systems. Involves some modifications of existing designs to meet customer requirements. Requires BSEE or equivalent experience in RF Design.

Entry-Level Engineers

Work with Senior RF engineers to develop and construct new RF products for wireless and aerospace markets. Requires BSEE or equivalent experience in electronics.

Electronic Technicians

Work with RF engineers to construct and test RF products for wireless and aerospace markets. Requires familiarity with electronic schematics, ability to troubleshoot to component level, proficiency in soldering and in the use of oscilloscopes, frequency counters, and spectrum analyzers.

Please send resumes to:
Wenzel Associates, Inc., Dept. M
1005 La Posada Drive
Austin, TX 78752
Fax: 512-450-1490
E-mail: Liz@wenzel.com
Equal Opportunity Employer

ENGINEERS & MANAGERS

ASTeX is a global leader in the design & manufacture of reactive gas modules and power supplies used in semiconductor manufacturing and medical markets, as well as etch and deposition systems for semiconductor advanced packaging, telecomms, and magnetic sensors. With facilities in Wilmington, MA, Santa Clara, CA, Austin, TX, and Colorado Springs, CO, Microwave and RF jobs are mainly Colorado and Massachusetts based.

MICROWAVE ENGINEERS
BS/MSEE; 5 + years microwave experience.

POWER SUPPLY DESIGN MANAGER/ENGINEERS
BS/MSEE; 5+ years in high voltage power supplies, switching power devices, analog, digital and/or high power electronics. Manager position requires related experience as a manager/team leader.

SR. RF DESIGN ENGINEERS
BSEE; 7+ years high power solid-state experience in RF Design.

HYBRID/PACKAGING DESIGN ENGINEERS
BS in Engineering; 5+ years experience in hybrid, microelectronics, or device packaging.

They also seek SOFTWARE ENGINEERS, RELIABILITY ENGINEERS, MANUFACTURING PROCESS/TEST ENGINEERS, APPLICATIONS ENGINEERS, FIELD SERVICE ENGINEERS, a MATERIALS MANAGER, PRODUCTION MANAGER, and a DIRECTOR OF MANUFACTURING.

For more information about ASTeX, these positions, or our service, visit www.aztechjobs.com or send your resume to:

AzTECH Recruitment Co.

AzTech Recruitment Co,
4131 N.24th St, Phoenix, AZ 85016
email: resumes@aztechjobs.com.
Call 800.790.8710 • Fax 602.955.9639

www.aztechjobs.com

High-Speed Innovation Starts Here

At GTRAN, a rapidly-growing pre-IPO technology firm, our world-class team is driving our innovative products to the pinnacle of the wireless markets. We produce mobile wireless data products for next-generation communication systems.

SYSTEM TEST ENGINEER

Requires 8 years of well-rounded experience, including knowledge of wireless standards and working knowledge of HP RF communications test sets. Electrical Engineering degree preferred.

SR. SOFTWARE ENGINEER

Requires a degree in Computer Science or Electrical Engineering and 8 years' experience with 2 years in wireless handset software design. Fluent in real-time imbedded C.

RF ENGINEER

You will perform impedance matching, RF circuit design, component evaluation and troubleshooting. Requires a BSEE, 5+ years' related experience, understanding of RX Line-up selection, knowledge of power amplifier requirements, and experience with HP RF lab equipment.

Our excellent salary/benefits package includes 100% paid medical, pre-IPO stock options, and a 401(k) with 100% company match to maximum limit. If you're looking for new challenges, growth and a bright future, send your resume in confidence, to: **GTRAN, HR Dept., 5701 Lindero Canyon Road, Ste. I-204, Westlake Village, CA 91362; Fax: 818-889-3798; E-mail: kelly@gtran.com.**

GTRAN™
EOE

www.gtran.com

BAE SYSTEMS

BAE SYSTEMS is pushing the envelope on Microwave and Antenna Products with an exciting new array of projects. Get on the fast track and leverage your antenna design and measurement background with our growing Microwave and Antenna Products team. Join us and give your career a jump-start!

Greenlawn, NY Facility

Antenna Engineer Advanced Development Center
Job Code: H00039

Lansdale, PA Facility

Antenna Engineer
Job Code: 400293

Radar ECM Systems Principal Engineer
Job Code: 400337

Radar ECM Systems Engineer
Job Code: 400187

Missile Seeker Lead Engineer
Job Code: 400349

Program Manager
Job Code: 400243

Quality Engineer IV
Job Code: 400362

We offer exceptional opportunities for growth and advancement as well as a solid compensation package. All positions require security clearance. Please send your resume and salary requirements, indicating position of interest and Job Code:, to: **BAE SYSTEMS, Aerospace Electronics, Attn: Human Resources, 305 Richardson Rd., Lansdale, PA 19446.**

Equal Opportunity Employer.

Visit our web site at: www.jobs@aes.tracor.com

In most cases, advertisements contained in Microwaves &RF employment section indicate that the companies are equal opportunity employers. The Federal Civil Rights Act of 1964, and other laws, prohibit discrimination in employment based on race, color, religion, national origin, sex or for any reason other than lack of professional qualification for the position being offered. It should be noted that employment advertisements in Microwaves & RF are published for the readers convenience and in no way, to the best of our knowledge, promote unlawful discrimination.

*Domestic Edition only
**International Edition only

This index is provided as an additional service by the publisher, who assumes no responsibility for errors or omissions.

MARKETING AND ADVERTISING STAFF

GROUP PUBLISHER
Craig Roth
(201) 393-6225
e-mail:croth@penton.com

DIRECT CONNECTION ADS
Joanne Reppas
(201) 666-6698
e-mail: jrepfran@aol.com

DIRECTOR, ELECTRONICS EVENTS
Bill Rutledge
(201) 393-6259, FAX: (201) 393-6297
e-mail: brutledge@penton.com

RECRUITMENT ADVERTISING
Call Customer Service Dept.
(201) 393-6083
FAX: (201) 393-0410

NORTHERN CA, NORTHWEST
Gene Roberts
Regional Sales Manager
Penton Media, Inc.
San Jose Gateway
2025 Gateway Place, Suite 354
San Jose, CA 95110
(408) 441-0550
e-mail: groberts@penton.com

NEW YORK, NEW ENGLAND, MIDWEST, MID-ATLANTIC, CANADA
Paul Barkman
Regional Sales Manager
Penton Media, Inc.
611 Route #46 West
Hasbrouck Heights, NJ 07604
(908) 704-2460
FAX: (908) 704-2496
e-mail: pbarkman@penton.com

SOUTHWEST, SOUTHEAST, SOUTHERN CA
Mary Bandfield
Regional Sales Manager
Penton Media, Inc.
501 N. Orlando Avenue
Winter Park, FL 32789
(407) 629-8745
FAX: (407) 629-8715
e-mail: mbandfield@penton.com

MIDWEST, MID-ATLANTIC
Paul Barkman
Regional Sales Manager
Penton Media, Inc.
611 Route #46 West
Hasbrouck Heights, NJ 07604
(908)391-8735
FAX: (201) 393-6297
e-mail: pbarkman@penton.com

PRODUCTION
Robert D. Scofield
(201) 393-6253
e-mail: rscofield@penton.com

ISRAEL
Igal Elan, General Manager
Elan Marketing Group
2 Habonim Street
Ramat Gan, Israel 52462
Phone: 011-972-3-6122466
011-972-3-6122467
011-972-3-6122468
FAX: 011-972-3-6122469

TAIWAN, R.O.C.
Charles C.Y. Liu, President
Two-Way Communications Co., Ltd.
11F/1, No. 421
Sung Shan Road
Taipei 110, Taiwan, R.O.C.
Phone: 886-2-727-7799
FAX: 886-2-728-3686

INDIA
Shivaji Bhattacharjee
Information & Education Services
1st Floor, 30-B, Ber Sarai Village,
Near I.I.T. Hauz Khas, Behind
South Indian Temple
New Delhi, 110016 India
FAX: 001-91-11-6876615

ITALY
Cesare Casiraghi
Via Napo Torriani 19/c
1-22100 Como - Italy
Phone: 39-31-261407
FAX: 39-31-261380

FRANCE
Emmanual Archambeauld
Defense & Communication
10 Rue St. Jean, 75017 Paris,
France
Phone: 33-4294-0244
FAX: 33-4387-2729

SPAIN
Luis Andrade, Miguel Esteban
Espana
Publicidad Internacional
Sepulveda, 143-38
08011 Barcelona, Spain
Phone: 011-34-93-323-3031
FAX: 011-34-93-453-2977

SCANDINAVIA
Paul Barrett
I.M.P. Hartswood
Hallmark House
25 Downham Road
Ramsden Heath
Billericay, Essex
CM 11 1PV
United Kingdom
Phone: 44-1268-711-560
FAX: 44-1268-711-567

GERMANY, AUSTRIA, SWITZERLAND
Friedrich K. Anacker
Managing Director
InterMedia Partners GmbH (IMP)
Deutscher Ring 40
42327 Wuppertal
Germany
Phone: 011-49-202-271-690
FAX: 011-49-202-271-6920

HOLLAND, BELGIUM
William J.M. Sanders, S.I.P.A.S.
Rechtestraat 58
1483 Be De Ryp, Holland
Phone: 31-299-671303
FAX: 31-299-671500

JAPAN
Hiro Morita
Japan Advertising
Communications, Inc.
Three Star Building
3-10-3 Kanda Jimbocho
Chiyoda-ku, Tokyo 101,
Japan
Phone: 81-3-3261-4591
FAX: 81-3-3261-6126

PORTUGAL
Paulo Andrade
Ilimitada-Publicidade
Internacional. LDA
Av. Eng. Duarte Pacheco
Empreedimento das
Amoreiras-Torre 2
Piso 11-Sala 11
1070 Lisboa, Portugal
Phone: 351-1-3883176
FAX: 351-1-3883283

EUROPEAN OPERATIONS
Paul Barrett, Mark Whiteacre,
David Moore
Phone: 44-1268-711-560
FAX: 44-1268-711-567
John Maycock
Phone: 44-1142-302-728
FAX: 44-1142-308-335
Hartswood, Maycock Media
Hallmark House
25 Downham Road
Ramsden Heath
Billericay, Essex
CM 11 PV. U.K.

CZECH REPUBLIC
Robert Bilek
Production International
Slezska 61, 13000 Praha 3
Czech Republic
Phone: 011-42-2-730-346
FAX: 011-42-2-730-346

KOREA
BISCOM
Jo Young Sang
Rm. 521 Midopa Bldg. 145
Dan Ju-Dong
Chongno-Gu
Seoul 110-071 Korea
Phone: 027397840
FAX: 027323662

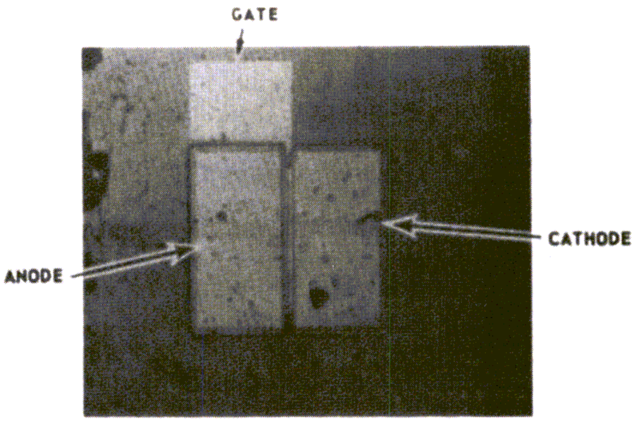

A news story in the bicentennial year of 1976 reported on the need for high-speed logic devices for electronic-warfare (EW) systems. The report highlighted a transferred-electron logic device (TELD) developed by RCA's Microwave Technology Center (Princeton, NJ) which combined a gallium-arsenide (GaAs) Gunn diode with a Schottky barrier gate. The device could process pulses as narrow as 80 ps with device delays of only 80 ps.

Microwaves & RF October Editorial Preview

Issue Theme: Integrated Circuits

News

Silicon germanium (SiGe) has been heralded as the best thing since gallium arsenide (GaAs), and many manufacturers have been quick to develop small-signal integrated circuits (ICs) based on the process. But how is the high-frequency design community warming to these new semiconductors? Don't miss this special report on SiGe ICs.

Design Features

October offers a strong lineup of contributed technical articles, including details on the design of a pseudomorphic-high-electron-mobility-transistor (PHEMT) mixer integrated circuit (IC) for millimeter-wave applications. Additional features include the use of software to analyze high-frequency signal-integrity problems and the design of a Gaussian-minimum-shift-keying (GMSK) modulator based on digital-signal-processing (DSP) techniques.

Product Technology

October features a close-up look at a novel bus architecture for multipole switches and switch matrices. The architecture is simple to program and offers reliable operation, even given the demands of high-throughout test systems. Additional Product Technology stories will examine microwave integrated circuits (ICs) which support high-data-rate wireless local-area networks (WLANs), as well as several new power transistors based on silicon-carbide (SiC) semiconductor materials.